Betonarme Yapılarda, Sürtünmeli V veya X Çapraz Çelik Elemanları Kullanarak Yapılacak Desteklerle Sismik Analiz Modelli

Lida Afsari

YÜKSEK LİSANS TEZİ

İnşaat Mühendisliği Anabilim Dalı

Haziran 2019

Seismic Analysis Model of V or X Braced Frames Using Friction Damper on Concrete Buildings

Lida Afsari

MASTER OF SCIENCE THESIS

Department of Civil Engineering

June 2019

Seismic Analysis Model of V or X Braced Frames Using Friction Damper on Concrete Buildings

A thesis submitted to the Eskişehir Osmangazi University

Graduate School of Natural and Applied Sciences in partial

fulfillment of the requirements for the degree of Master of Science

in Discipline of Structural Design of the Department of the Civil Engineering

by

Lida Afsari

Supervisor: Assist. Prof. Dr. Hande Gökdemir

June 2019

APPROVAL OF THE THESIS

The thesis titled “Seismic Analysis Model of V or X Braced Frames Using Friction Damper on Concrete Buildings” and submitted by Lida Afsari has been accepted as satisfactory in partial fulfillment of the requirements for the degree of Master of Science in Department of Civil Engineering.

Supervisor **:** Assist. Prof. Dr. Hande Gökdemir

Co-Supervisor **: -**

Examining Committee Members:

Member : Assist. Prof. Dr. Hande Gökdemir

Member : Prof. Dr. Mizan Doğan

Member : Prof.Dr. Gülgün Yilmaz

Graduation of Lida Afsari was approved by the Graduate School Board Decision on ..... with the decision number .....

Prof. Dr. Hürriyet ERŞAHAN

Director of the Institute

ETHICAL STATEMENT

I hereby declare that this thesis study titled “Seismic Analysis Model of V or X Braced Frames Using Friction Damper on Concrete Buildings” has been prepared in accordance with the thesis writing rules of Eskişehir Osmangazi University Graduate School of Natural and Applied Sciences under academic consultancy of my supervisor Assist. Prof. Dr. Hande Gökdemir. I hereby declare that the work presented in this thesis is original. I also declare that, I have respected scientific ethical principles and rules in all stages of my thesis study, all information and data presented in this thesis have been obtained within the scope of scientific and academic ethical principles and rules, all materials used in this thesis which are not original to this work have been fully cited and referenced, and all knowledge, documents, and results have been presented in accordance with scientific ethical principles and rules.
24/06/2019

Lida Afsari

Signature

ÖZET

Ansızın ortaya çıkan depremler tasarım kriterleri açısından yapı mühendislerini daima zorlamaktadır. Meydana gelen bu depremler yalnızca şehirleri, yolları ve binaları değil, aynı zamanda insan hayatını da olumsuz etkilemektedir. Deprem kaynaklı ortaya çıkan problemler, çözüm yolu bulmada yeni tekniklerin keşfi açısından yapı mühendislerini teşvik etmektedir. Bu problemlerin başında ise "yapı titreşimi" gelmektedir. Depremlerin aniden ortaya çıkması ve beraberinde büyük hasarlar bırakması bu duruma karşı bir çözüm bulunması gerekliliğini de arttırmaktadır. Pasif enerjinin dağıtılması için istifade edilen sistemler, depremin ortaya çıkardığı zararları azaltmak için tüm dünyada sıkça başvurulan yöntemlerdendir. Sistem üzerindeki sönümleme etkisi herhangi bir harici yükleme olmadan elde edilir ve bunların performansı deprem uyarımı ile sağlanır. Sürtünme damperi, tediklenen enerjiyi yer değiştirme kontrol mekanizması ile dağıtan bir tür pasif damperdir. Bu çalışmada ani direnç çerçeveli 7 katlı beton bir yapı SAP2000'de dampersiz, X ve ters V damperli olmak üzere üç farklı şekilde tasarlanmış ve modellenmiştir. Maskimum deplasman ve taban kesme kuvveti sonuçları lineer olmayan zaman tanım alanında yöntemi analizlerinden çıkarılır. Sonuçlar, X konfigürasyonlu binanın tüm depremlerde en iyi performansa sahip olduğunu göstermektedir.

Anahtar Kelimeler: Sürtünme damperi, Betonarme çerçeve, Zaman Tanım Alanında Yöntemi Analizi, Kat deplasman, Taban kesme kuvvetileri.

SUMMARY

Earthquakes as a sudden rupture phenomenon have always been one of the most challenging design criteria for structural engineers around the globe. The disaster caused by an earthquake does not only ruin the buildings, cities, roads and but also leaves a big financial loss, and put human life at serious risk. The collapse of structures due to earthquake motions amplified concerns of structural engineers in finding more accomplished techniques for dissolving the released energy of earthquakes by structures. Structure vibration is the main concern of structural engineers. The inevitable occurrence of earthquakes and imposing plenty of damages lead to finding a proper and trustworthy solution to encounter this natural phenomenon. Using passive energy dissipating systems are utilized all around the world to mitigate the substantial damages. The damping effect on the system is obtained without any external loading and the performance of these is achieved by the earthquake excitation. Friction damper is a kind of passive damper which dissipates the induced energy by the displacement control mechanism. At this dissertation, a concrete 7-story-building with moment resisting frame is designed and modeled in SAP2000 at three different cases including without damper and with X and inverted V damper. The results of maximum story drifts and base shear are extracted from the nonlinear time history analyses. The results indicated that building with X configuration showed excellent performance under all the earthquakes.

Keywords: Friction damper, Concrete frame, Time history analysis, Story drift, Base shear.

DEDICATION

This dissertation is dedicated to my respected thesis advisor Assoc. Prof. Dr. HANDE GÖKDEMİR, who has been a constant source of knowledge and inspiration.

Additionally, I would like to dedicate this dissertation to my amazing husband SAYED MANSOOR KAZEMI. For all your support, encouragement, understanding, and enthusiasm during this incredibly long process. I also dedicate this thesis to my wonderful parents, YAHYA AFSARI and FARZANA AFSARI, for your everlasting love and support of my dreams. You always pushed me to be my best, knowing that I could accomplish all I set out to do.

TABLE OF CONTENTS

Page

ÖZET vi

SUMMARY vii

DEDICATION viii

TABLE OF CONTENTS ix

FIGURES xi

TABLES xvii

SYMBOLS AND ABBREVIATIONS xx

1. INTRODUCTION AND PURPOSE 1

2. LITERATURE REVIEW 4

3. MODEL APPLICATIONS 25

3.1. Introduction 25

3.2. Dynamic Response of Simple Structural Models 25

3.2.1. General Formulation 25

3.2.1.1. Time Dependent Force 25

3.2.1.2. Earthquake Ground Motion 28

3.3. Friction Damper 30

3.3.1. Basic Principles 30

3.3.2. Solid Friction 30

3.4. Analyses Methods 31

3.5. Features of Models 32

3.5.1. Gravity Loadings 33

3.5.2. Lateral Seismic Load 34

3.5.3. Load Combinations 37

3.5.4. Structure's Views 38

3.6. Design Considerations 49

3.6.1. Design of Friction Damper 54

3.7. Modelling of Pall Friction Dampers 59

TABLE OF CONTENTS (continued)

Page

3.7.1. Inverted V (Chervon) Pall Friction Damper Modelling…….59
3.7.2. Tension Only Cross Brace with pall Friction Damper (Figure C)…….60
3.8. Verification Modelling and Design Method…….63
4. FINDING AND DISCUSSIONS……..…….68
4.1. Introduction……...68
4.1.1. Scalling Procedure……..76
4.2. Nonlinear Time History Analyses (NTHA) Results…….81
4.2.1. Evidence About Northridge Earthquake……81
4.2.2. Evidence About Kobe Earthquake……85
4.2.3. Evidence About Imperial Vally (El Centro) Earthquake……...89
4.2.4. Evidence About Bam Earthquack……..93
4.2.5. Evidence About Southern California Earthquake……..97
4.2.6. Evidence About Parkfield Earthquake……101
4.2.7. Evidence About Düzce Earthquake……..105
4.3. Elimination of Dampers……..110
4.4. Further Comparison……132
4.4.1. Beams Maximum Bending Moments At 1st, 2nd, And 7th Story Under 6 Different Earthquakes…….…..133
4.4.2. Beams Maximum Shear Forces Bending At 1st,2nd, And 7th Story Under 6 Different Earthquakes…….……..155
4.4.3. Columns Lables Characterizations……...177
4.4.4. Columns Maximum Axial Force……..179
4.4.5. The Maximum Axial Forces Under Kobe Earthquake at the 1st,2nd and 7th Stories……..180
4.4.6. The Maximum Axial Forces Under Düzce Earthquake at the 1st,2nd and 7th Stories……..195
5. RESULTS AND SUGGESTIONS……..……211
5.1. Suggestions…….214
REFERENCES……..215

FIGURES

Figure **Page**

2.1. Components of FDD……6
2.2. Friction damper used as Knee Element ……8
2.3.(a) Modeled X-Shaped Metallic Damper……..12
2.3.(b) Application X-Shaped Metallic Damper in a School Building…….....12
2.4.(a) Model of Viscoelastic Damper…… 13
2.4.(b) Application of Viscoelastic Damper in a Structure……..... 13
2.5.(a) Model of Viscoelastic Damper……..…….. 14
2.5.(b) Application of Viscoelastic Damper in a Structure in the Inverted V Form….14
2.6.(a) Tuned Mass Damper……..……..15
2.6.(b) Application of Tuned Mass Damper in Taipei 101 Structure…… 15
2.7. Application of Tuned Liquid Mass in One Rincon Hill Structure…….....16
2.8.(a) Boeing Commercial Airplane Factory at Everett, WA, USA…… 18
2.8.(b) Pall Friction Dampers Used for Boeing Commercial Airplane Factory at Everette, WA, USA……..19
2.9.(a) View of Moscone West Convention Center, San Francisco, USA…… 19
2.9.(b) Pall Friction Dampers Used for Moscone West Convention Center, San Francisco, USA……20
2.10.(a) Friction Damper in Tension-Only Cross Brace……22
2.10.(b) Friction Damper Chevron Bracing……22
2.10(C) Single Diagonal Tension Compression Bracing..……22
2.11. Response Versus Slip Load……23
3.1.(a) Single Degree of Freedom Structure…….……27
3.1.(b) Time Dependent Force SDOF Structure……..……27
3.1.(c) The Summation of Forces Acting on the SDOF Structure……28
3.2.(a) Earthquake Ground Motion on SDOF…….……29
3.2.(b) The Summation of Forces Acting on the SDOF Structure……29
3.3. Turkey Earthquake Hazard Map…..……35
3.4. Reading SS475 from Turkish Seismic Map AFAD Website for Düzce……. 36
3.5. Reading S1 475 from Turkish Seismic Map AFAD Website for Düzce……36
3.6. Seismic Load Definition in SAP2000 Software…..……37
3.7. Three-Dimensional Model of the 7-Story Building Without Friction Damper……39
3.8. X-direction Plan View of the 7-Story Building Without Friction Damper…..39
3.9. Y-direction Plan View the 7-Story Building Without Friction Damper……40
3.10. Three-Dimensional Model of the 7-Story Building with X Friction Bracing (Arr 1)……40
3.11. X-Direction Plan View of the 7-Story Building with X Friction Bracing (Arr 1)…….....41
3.12. Y-Direction Plan View of the 7-Story Building with X Friction Bracing (Arr 1)…….....41
3.13. Three-Dimensional Model of the 7-Story Building with Inverted V Friction Bracing (Arr1)…….....42

FIGURES (continued)

Figure **Page**

3.14. X-Direction Plan View of the 7-Story Building with Inverted V Friction Bracing (Arr1)……42
3.15. Y-Direction Plan View the 7-Story Building with Inverted V Friction Bracin (Arr 1)……43
3.16. Three-Dimensional Model of the 7-Story Building with X Friction Bracing (Arr 2)……43
3.17. X-Direction Plan View of the 7-Story Building with X Friction Bracing (Arr 2)……44
3.18. Y-Direction Plan View the 7-Story Building with X Friction Bracing (Arr 2)……44
3.19. Three-Dimensional Model of the 7-Story Building with Inverted V Friction Bracing (Arr 2)……45
3.20. X-Direction Plan View of the 7-Story Building with Inverted V Friction Bracing (Arr 2)……45
3.21. Y-Direction Plan View the 7-Story Building with Inverted V Friction Bracing (Arr 2)……46
3.22. Three-Dimensional Model of the 7-Story Building without X Friction Bracing at the 1st Story……46
3.23. X-Direction Plan View of the 7-Story Building without X Friction Bracing at the 1st Story……47
3.24. Y-Direction Plan View the 7-Story Building without X Friction Bracing at the 1st Story……47
3.25. Three-Dimensional Model of the 7-Story Building without Inverted V Friction Bracing at the 1st Story……48
3.26. X-Direction Plan View of the 7-Story Building without Inverted V Friction Bracing at the 1st story……48
3.27. Y-Direction Plan View the 7-Story Building without Inverted V Friction Bracing at the 1st Story……49
3.28. Construction of Design Slip-Load Spectrum……51
3.29. Design Slip-Load Spectrum for Y-Direction……56
3.30. Design Slip-Load Spectrum for X-Direction……56
3.31. Friction Damped Inverted V Brace Frame……60
3.32. Friction Damped X Brace Frame……61
3.33. Friction Damped Single Diagonal Brace Frame……61
3.34. Definition of Friction Damper in SAP2000…… 62
3.35. Definition of Friction Damper in SAP2000……62
3.36. Low-Rise Steel Industrial Building…… 63
3.37. The Result of Verification by SAP2000……64
3.38. Damper Configuration in SAP2000 (X Bracing)…… 64
3.39. The Arrangement (1) for Dampers……67
3.40. The Arrangement (2) for Dampers……67
4.1. Northridge Horizontal Acceleration Time Histories……69

FIGURES (continued)

Figure **Page**

4.2. Kobe Horizontal Acceleration Time Histories…… 70
4.3. Imperial Valley Horizontal Acceleration Time Histories……71
4.4. Bam Horizontal Acceleration Time Histories……..72
4.5. Southern Calif Horizontal Acceleration Time Histories…..……73
4.6. Southern Calif Horizontal Acceleration Time Histories…….……74
4.7. Düzce Horizontal Acceleration Time Histories……75
4.8. Spectrum Accelerations of Northridge Ground Motions for Normalized Records.....77
4.9. Spectrum Accelerations of Kobe Ground Motions for Normalized Records…… 77
4.10. Spectrum Accelerations of Imperial Valley Ground Motions for Normalized Records…….....78
4.11. Spectrum Accelerations of Bam Ground Motions for Normalized Records…… 78
4.12. Spectrum Accelerations of Southern Calif Ground Motions for Normalized Records…… 79
4.13. Spectrum Accelerations of Parkfield Ground Motions for Normalized Records…….....79
4.14. Spectrum Accelerations of Düzce Ground Motions for Normalized Records……..80
4.15. The Comparison Between the Mean Value of Calculated Spectrum with ASCE7-16 Design Spectrum at Sa(T1)…… 80
4.16. The Results of Drift Ratio for Northridge 1 Earthquake at X-Direction…… 82
4.17. The Results of Drift Ratio for Northridge 1 Earthquake at Y-Direction…… 83
4.18. The Results of Drift Ratio for Northridge 2 Earthquake at X-Direction…… 84
4.19. The Results of Drift Ratio for Northridge 2 Earthquake at Y-Direction…… 85
4.20. The Results of Drift Ratio for Kobe 1 Earthquake at X-Direction……. 86
4.21. The Results of Drift Ratio for Kobe 1 Earthquake at Y-Direction…….. 87
4.22. The Results of Drift Ratio for Kobe 2 Earthquake at X-Direction…….. 88
4.23. The Results of Drift Ratio for Kobe 2 Earthquake at Y-Direction…….. 89
4.24. The Results of Drift Ratio for Imperial Valley 1 Earthquake at X-Direction..90
4.25. The Results of Drift Ratio for Imperial Valley 1 Earthquake at Y-Direction..91
4.26. The Results of Drift Ratio for Imperial Valley 2 Earthquake at X-Direction..92
4.27. The Results of Drift Ratio for Imperial Valley 2 Earthquake at Y-Direction..93
4.28. The Results of Drift Ratio for Bam 1 Earthquake at X-Direction……94
4.29. The Results of Drift Ratio for Bam 1 Earthquake at Y-Direction……95
4.30. The Results of Drift Ratio for Bam 2 Earthquakes at X-Direction……. 96
4.31. The Results of Drift Ratio for Bam 2 Earthquake at Y-Direction……97
4.32. The Results of Drift Ratio for Southern Calif 1 Earthquake at X-Direction…98
4.33. The Results of Drift Ratio for Southern Calif 1 Earthquake at Y-Direction…99
4.34. The Results of Drift Ratio for Southern Calif 2 Earthquake at X-Direction…100
4.35. The Results of Drift Ratio for Southern Calif 2 Earthquake at Y-Direction…101

FIGURES (continued)

Figure **Page**

4.36. The Results of Drift Ratio for Parkfield 1 Earthquake at X-Direction…… 102
4.37. The Results of Drift Ratio for Parkfield 1 Earthquake at Y-Direction…… 103
4.38. The Results of Drift Ratio for Parkfield 2 Earthquake at X-Direction…… 104
4.39. The Results of Drift Ratio for Parkfield 2 Earthquake at Y-Direction……104
4.40. The Results of Drift Ratio for Düzce 1 Earthquake at X-Direction…….. 106
4.41. The Results of Drift Ratio for Düzce 1 Earthquake at Y-Direction…… 106
4.42. The Results of Drift Ratio for Düzce 2 Earthquake at X-Direction…… 107
4.43. The Results of Drift Ratio for Düzce 2 Earthquake at Y-Direction…… 108
4.44. The Results of Maximum Base Shear Under Different Ground Motions…… 109
4.45. The Results of Drift Ratio for Northridge 1 Earthquake at X Direction……111
4.46. The Results of Drift Ratio for Northridge 1 Earthquake at Y Direction……111
4.47. The Results of Drift Ratio for Northridge Earthquake 2 at X Direction……113
4.48. The Results of Drift Ratio for Northridge 2 Earthquake at Y Direction……113
4.49. The Results of Drift Ratio for Kobe 1 Earthquake at X Direction……114
4.50. The Results of Drift Ratio for Kobe 1 Earthquake at Y Direction……115
4.51. The Results of Drift Ratio for Kobe 2 Earthquake at X Direction……116
4.52. The Results of Drift Ratio for Kobe 2 Earthquake at Y Direction……116
4.53. The Results of Drift Ratio for Imperial Valley 1 Earthquake at X Direction..117
4.54. The Results of Drift Ratio for Imperial Valley 1 Earthquake at Y Direction..118
4.55. The Results of Drift Ratio for Imperial Valley 2 Earthquake at X Direction..119
4.56. The Results of Drift Ratio for Imperial Valley 2 Earthquake at Y Direction..119
4.57. The Results of Drift Ratio for Bam 1 Earthquake at X Direction…… 120
4.58. The Results of Drift Ratio for Bam 1 Earthquake at Y Direction…… 121
4.59. The Results of Drift Ratio for Bam 2 Earthquake at X Direction…… 122
4.60. The Results of Drift Ratio for Bam 2 Earthquake at Y Direction…… 122
4.61. The Results of Drift Ratio for Southern Calif 1 Earthquake at X Direction… 123
4.62. The Results of Drift Ratio for Southern Calif 1 Earthquake at Y Direction… 124
4.63. The Results of Drift Ratio for Southern Calif 2 Earthquake at X Direction… 125
4.64. The Results of Drift Ratio for Southern Calif 2 Earthquake at Y Direction… 125
4.65. The Results of Drift Ratio for Parkfield 1 Earthquake at X Direction……..126
4.66. The Results of Drift Ratio for Parkfield 1 Earthquake at Y Direction……127
4.67. The Results of Drift Ratio for Parkfield 2 Earthquake at X Direction……128
4.68. The Results of Drift Ratio for Parkfield 2 Earthquake at Y Direction……128
4.69. The Results of Drift Ratio for Düzce 1 Earthquake at X Direction……129
4.70. The Results of Drift Ratio for Düzce 1 Earthquake at Y Direction……130
4.71. The Results of Drift Ratio for Düzce 2 Earthquake at X Direction……131
4.72. The Results of Drift Ratio for Düzce 2 Earthquake at Y Direction……..131
4.73. Beams Labels at the 1st Story – Top View……133
4.74. Beams Labels at the 2nd Story – Top View……...134
4.75. Beams Labels at the 7th Story – Top View……134
4.76. Beams and Columns Labels View Section 1-1…… 135
4.77. Beams and Columns Labels View Section 2-2…… 135

FIGURES (continued)

Figure **Page**

4.78. Beams and Columns Labels View Section 3-3…… 136
4.79. Beams and Columns Labels View Section 4-4…… 136
4.80. Beams Labels at the 1st Story – Top View……155
4.81. Beams Labels at the 2nd Story – Top View……156
4.82. Beams Labels at the 7th Story – Top View……156
4.83. Beams and Columns Labels View Section 1-1…… 157
4.84. Beams and Columns Labels View Section 2-2…… 157
4.85. Beams and Columns Labels View Section 3-3…… 158
4.86. Beams and Columns Labels View Section 4-4…… 158
4.87. Beams and Columns Labels View Section 1-1…… 177
4.88. Beams and Columns Labels View Section 2-2…… 177
4.89. Beams and Columns Labels View Section 3-3…… 178
4.90. Beams and Columns Labels View Section 4-4…… 178
4.91. Maximum Columns Axial Forces on 1st, 2nd, and 7th Stories under Kobe Earthquake Without Damper X-Z Axis……180
4.92. Maximum Columns Axial Forces on 1st, 2nd, and 7th Stories under Kobe Earthquake Without Damper Y -Z Axis……182
4.93. Maximum Columns Axial Forces on 1st, 2nd, and 7th Stories under Kobe Earthquake X-Damper Arrangement 1 X -Z Axis.....183
4.94. Maximum Columns Axial Forces on 1st, 2nd, and 7th Stories under Kobe Earthquake X-Damper Arrangement 1 Y -Z Axis……185
4.95. Maximum Columns Axial Forces on 1st, 2nd, and 7th Stories under Kobe Earthquake V-Damper Arrangement 1 X -Z Axis……186
4.96. Maximum Columns Axial Forces on 1st, 2nd, and 7th Stories under Kobe Earthquake V-Damper Arrangement 1 Y -Z Axis……188
4.97. Maximum Columns Axial Forces on 1st, 2nd, and 7th Stories under Kobe Earthquake X-Damper Arrangement 2 X-Z Axis……189
4.98. Maximum Columns Axial Forces on 1st, 2nd, and 7th Stories under Kobe Earthquake X-Damper Arrangement 2Y-Z Axis……..191
4.99. Maximum Columns Axial Forces on 1st, 2nd, and 7th Stories under Kobe Earthquake V-Damper Arrangement 2X-Z Axis…… 192
4.100. Maximum Columns Axial Forces on 1st, 2nd, and 7th Stories under Kobe Earthquake V-Damper Arrangement 2 Y-Z Axis……194
4.101. Maximum Columns Axial Forces on 1st, 2nd, and 7th Stories under Düzce Earthquake Without Damper X-Z Axis……195
4.102. Maximum Columns Axial Forces on 1st, 2nd, and 7th Stories under Düzce Earthquake Without Damper Y-Z Axis……197
4.103. Maximum Columns Axial Forces on 1st, 2nd, and 7th Stories under Düzce Earthquake X-Damper Arrangement X-Z Axis……198
4.104. Maximum Columns Axial Forces on 1st, 2nd, and 7th Stories under Düzce Earthquake X-Damper Arrangement 1 Y-Z Axis……200
4.105. Maximum Columns Axial Forces on 1st, 2nd, and 7th Stories under Düzce Earthquake V-Damper Arrangement 1 X-Z Axis……201

FIGURES (continued)

Figure **Page**

4.106. Maximum Columns Axial Forces on 1st, 2nd, and 7th Stories under Düzce Earthquake V-Damper Arrangement 1 Y-Z Axis……203
4.107. Maximum Columns Axial Forces on 1st, 2nd, and 7th Stories under Düzce Earthquake X-Damper Arrangement 2 X-Z Axis……204
4.108. Maximum Columns Axial Forces on 1st, 2nd, and 7th Stories under Düzce Earthquake X-Damper Arrangement 2 Y-Z Axis……206
4.109. Maximum Columns Axial Forces on 1st, 2nd, and 7th Stories under Düzce Earthquake V-Damper Arrangement 2 X-Z Axis……207
4.110. Maximum Columns Axial Forces on 1st, 2nd, and 7th Stories under Düzce Earthquake V-Damper Arrangement 2 Y-Z Axis……209

TABLES

Table **Page**

1.1. Structural Protective Systems……..... 3
3.1. Turkey's Earthquake Regulation on Buildings TBDY-201…….. 34
3.2. Summary of the Structure Properties……. 38
3.3. The Characteristics of Damper with X Configuration for Arrangement (1)……... 65
3.4. The Characteristics of Damper with Inverted V Configuration Arrangement (1)……. 65
3.5. The Characteristics of Damper with X Configuration for Arrangement (2)…66
3.6. The Characteristics of Damper with Inverted V Configuration Arrangement (2)……. 66
4.1. Ground Motions Properties…….....68
4.2. The Maximum Values of Story Drift Ratios for Northridge (1) Earthquake…….....82
4.3. The Maximum Values of Story Drift Ratios for Northridge (2) Earthquake……83
4.4. The Values of Maximum Story Drift Ratios for Kobe (1) Earthquake……....86
4.5. The Values of Maximum Story Drift Ratios for Kobe (2) Earthquake……....87
4.6. The Values of Maximum Story Drift Ratios for Imperial Valley (1) Earthquake……90
4.7. The Values of Maximum Story Drift Ratios for Imperial Valley (2) Earthquake……92
4.8. The Values of Maximum Story Drift Ratios for Bam (1) Earthquake……94
4.9. The Values of Maximum Story Drift Ratios for Bam (2) Earthquake…….95
4.10. The Values of Maximum Story Drift Ratios for Southern Calif (1) Earthquake……98
4.11. The Values of Maximum Story Drift Ratios for Southern Calif (2) Earthquake……99
4.12. The Values of Maximum Story Drift Ratios for Parkfield (1) Earthquake…..101
4.13. The Values of Maximum Story Drift Ratios for Parkfield (2) Earthquake…..103
4.14. The Values of Maximum Story Drift Ratios for Düzce (1) Earthquake……...105
4.15. The Values of Maximum Story Drift Ratios for Düzce (2) Earthquake…….. 107
4.16. The Values of Maximum Base Shear Under Different Earthquakes……109
4.17. The Maximum of Story Drifts Values Under Northridge 1 Earthquake with Elimination of Dampers from At The 1st Story…… 110
4.18. The Maximum of Story Drifts Values Under Northridge 2 Earthquake with Elimination of Dampers at the 1st Story…….112
4.19. The Maximum of Story Drifts Values Under Kobe 1 Earthquake with Elimination of Dampers from Story 1……..114
4.20. The Maximum of Story Drifts Values Under Kobe 2 Earthquake with Elimination of Dampers from Story 1……..115

TABLES (continued)

Table **Page**

4.21. The Maximum of Story Drifts Values Under Imperial Valley 1 Earthquake with Elimination of Dampers from Story 1……..117
4.22. The Maximum of Story Drifts Values Under Imperial Valley 2 Earthquake with Elimination of Dampers from Story 1……..118
4.23. The Maximum of Story Drifts Values Under Bam 1 Earthquake with Elimination of Dampers from Story 1……..120
4.24. The Maximum of Story Drifts Values Under Bam 2 Earthquake with Elimination of Dampers from Story 1……..121
4.25. The Maximum of Story Drifts Values Under Southern Calif 1 Earthquake with Elimination of Dampers from Story 1……..123
4.26. The Maximum of Story Drifts Values Under Southern Calif 2 Earthquake with Elimination of Dampers from Story 1……..124
4.27. The Maximum of Story Drifts Values Under Parkfield 1 Earthquake with Elimination of Dampers from Story 1……..126
4.28. The Maximum of Story Drifts Values Under Parkfield 2 Earthquake with Elimination of Dampers from Story 1……..127
4.29. The Maximum of Story Drifts Values Under Düzce 1 Earthquake with Elimination of Dampers from Story 1……129
4.30. The Maximum of Story Drifts Values Under Düzce 2 Earthquake with Elimination of Dampers from Story1……130
4.31. The Maximum Values of Base Shears with Elimination of Dampers Story1..132
4.32. Fundamental Period of the Buildings……133
4.33. Maximum and Minimum Bending Moment on Beams under Northridge Earthquake……137
4.34. Maximum and Minimum Bending Moment on Beams under Kobe Earthquake……140
4.35. Maximum and Minimum Bending Moment on Beams under Imperial Valley Earthquake……....143
4.36. Maximum and Minimum Bending Moment on Beams under Bam Earthquake……146
4.37. Maximum and Minimum Bending Moment on Beams under Parkfield Earthquake……149
4.38. Maximum and Minimum Bending Moment on Beams under Düzce Earthquake……152
4.39. Maximum and Minimum Shear Forces on Beams under Northridge Earthquake……159
4.40. Maximum and Minimum Shear Forces on Beams under Kobe Earthquake…162
4.41. Maximum and Minimum Shear Forces on Beams under Imperial Valley Earthquake……165
4.42. Maximum and Minimum Shear Forces on Beams under Bam Earthquake…..168
4.43. Maximum and Minimum Shear Forces on Beams under Parkfield Earthquake……....171
4.44. Maximum and Minimum Shear Forces on Beams under Düzce Earthquake...174

TABLES (continued)

Table **Page**

4.45. Column Labels Characterization……..179
4.46. Columns Maximum Axial Forces Under Kobe Earthquake 1st, 2nd and 7th Story, X-Z Axis……181
4.47. Columns Maximum Axial Forces Under Kobe Earthquake 1st, 2nd and 7th Story, Y-Z Axis……182
4.48. Columns Maximum Axial Forces Under Kobe Earthquake 1st, 2nd and 7th Story, X-Z Axis…… 184
4.49. Columns Maximum Axial Forces Under Kobe Earthquake 1st, 2nd and 7th Story, Y-Z Axis…… 185
4.50. Columns Maximum Axial Forces Under Kobe Earthquake 1st, 2nd and 7th Story, X-Z Axis……187
4.51. Columns Maximum Axial Forces Under Kobe Earthquake 1st, 2nd and 7th Story, Y-Z Axis……188
4.52. Columns Maximum Axial Forces Under Kobe Earthquake 1st, 2nd and 7th Story, X-Z Axis…… 190
4.53. Columns Maximum Axial Forces Under Kobe Earthquake 1st, 2nd and 7th Story, Y-Z Axis 191
4.54. Columns Maximum Axial Forces Under Kobe Earthquake 1st, 2nd and 7th Story, X-Z Axis……193
4.55. Columns Maximum Axial Forces Under Kobe Earthquake 1st, 2nd and 7th Story, Y-Z Axis……194
4.56. Columns Maximum Axial Forces Under Düzce Earthquake 1st, 2nd and 7th Story, X-Z Axis……196
4.57. Columns Maximum Axial Forces Under Düzce Earthquake 1st, 2nd and 7th Story, Y-Z Axis…… 197
4.58. Columns Maximum Axial Forces Under Düzce Earthquake 1st, 2nd and 7th Story, X-Z Axis ……199
4.59. Columns Maximum Axial Forces Under Düzce Earthquake 1st, 2nd and 7th Story, Y-Z Axis ……200
4.60. Columns Maximum Axial Forces Under Düzce Earthquake 1st, 2nd and 7th Story, X-Z Axis…… 202
4.61. Columns Maximum Axial Forces Under Düzce Earthquake 1st, 2nd and 7th Story, Y-Z Axis…… 203
4.62. Columns Maximum Axial Forces Under Düzce Earthquake 1st, 2nd and 7th Story, X-Z Axis…… 205
4.63. Columns Maximum Axial Forces Under Düzce Earthquake 1st, 2nd and 7th Story, Y-Z Axis…… 206
4.64. Columns Maximum Axial Forces Under Düzce Earthquake 1st, 2nd and 7th Story, X-Z Axis……208
4.65. Columns Maximum Axial Forces Under Düzce Earthquake 1st, 2nd and 7th Story, Y-Z Axis…… 209

SYMBOLS AND ABBERVIATIONS

Abbreviations	**Statements**
f_i	Inertia force
f_d	Damping force
f_s	Elastic restoring force
$p(t)$	Time-dependent applied force
$\ddot{u}$	Total acceleration for the mass
$\dot{v}$	Displacement of the mass relative to the base
v	Velocity of the mass relative to the base
$\ddot{v}(t)$	Acceleration of the mass relative to the base
$\ddot{g}(t)$	Acceleration of the base
$P_e(t)$	Effective time-dependent force
F	Frictional Forces
N	Normal Forces
μ	Coefficient of Friction.
NTHA	Nonlinear time history analysis
S_s	Short period spectral acceleration coefficient map
S_1	1 second period spectral acceleration coefficient map
F_s	Spectral acceleration coefficient map for short period regions
F_1	Spectral acceleration coefficient map for 1 second period
G	Dead load
E	Earthquake load
Q	Live load
T_g	Predominant ground period,
R	Epicentral Distance
M_L	Local Richter magnitude
T_b	Natural period of braced structure

SYMBOLS AND ABBERVIATIONS (continued)

Abbreviations	Statements
T_u	Natural period of unbraced structure
a_g	Peak ground acceleration
g	Acceleration of the gravity.
α and β	Ordinates to construct design slip load spectrum
NS	The number of the stories
T_b	Natural period of braced structure
T_u	Natural period of unbraced structure
$V_{s(i)}$	Slip shear in (i) story
V_0	Total optimum slip shear
NS	Number of the stories
N_{Di}	Number of friction dampers inserted in the rth floor
P_0	Optimum local slip load
cos α	Angle of inclination of diagonal braces from horizontal
I	The story number
j	The number of braces
$V_{s(i)}$	Slip shear in (i) story
A_{bij}	Cross Sectional area for the (j)th tensile brace in the (i)th floor
σ_{yij}	Tensile yield stress for the (j)th tensile brace in the (i)th floor
P_0	The optimum local slip load
$P_{(cr)}$	Critical Euler buckling load
V_s	Average Shear Wave Velocity
R	Epicentral distance
M_L	Local Richter magnitude

1. INTRODUCTION AND PURPOSE

Gravity loadings are the initial loadings which have to be noticed because of their continuous presence during the serviceability of the structure and static nature. But for earthquake loading the fact is different and the focus is on inertial loading which leads to the amplification of loading. Because of the difficulties in defining the exact value of earthquake loading, the formwork of them are completely different with gravity loading.

Despite these significant differences, there is a natural tendency to treat the environmental forces with the same methods used for gravity loads. For example, wind and earthquake forces are often idealized as lateral static loads of suitable magnitude that must be resisted by the structure.

Utilizing this approach, the lateral loads corresponding to wind and small earthquakes are designed to be resisted by elastic action only, while those associated with moderate or severe seismic events are permitted to damage but not collapse the structure. This philosophy has provided the basis for a number of building codes since the early twentieth century, and results have been reasonably successful. Even an estimated accounting for lateral effects will definitely expand building survive ability.

Although there are more differences between the gravity and earthquake loading, the trend to use a similar way (static idealization) to calculate the earthquake loading is considered for special building for example low-rise or regular buildings. But with understanding the complexity of the dynamic loading, more considerable attention could be extracted which results in new methods to calculate the earthquake loading or decrease the induced energy and the generation of new seismic dissipative energy systems. These new systems are clarified into three groups depicted in Table 1.1. The differences between the groups are in the way they dissipate the energy.

The technique of seismic isolation is now widely used in many parts of the world. A seismic isolation system is typically placed at the foundation of a structure. By means of its flexibility and energy absorption capability, the isolation system partially reflects and

partially absorbs some of the earthquake input energy before this energy can be transmitted to the structure and apply a uniform drift to the stories. A comprehensive review of this system could be found on Skinner et al. (1993).

The other systems in Table 1.1 are Semi-active and active systems which adjust themselves based on the earthquake input energy. The semi-active systems just need the nominal value of energy to set their properties and cannot add any energy to the building. Considerable attention has been paid to both semi-active and active structural control research in recent years, with particular emphasis on the alleviation of wind and seismic response.

Considerable attention has been paid to both semi-active and active structural control research in recent years, with particular emphasis on the alleviation of wind and seismic response. The technology is now at the stage where actual systems have been designed, fabricated and installed in full-scale structures. The interested reader may consult Soong (1990) and Soong and Constantinou (1994) for discussions on many theoretical and practical aspects of semi-active and active structural control.

The energy dissipation systems should be considered in somewhat broader context than isolation systems (which are not feasible in taller buildings) as a design strategy when performance goals include damage control.

Also, the construction cost is less with energy dissipation systems than base isolation systems. Seismic isolation and energy dissipation systems are relatively new and sophisticated concepts that require more extensive design and detailed nonlinear time-history dynamic analysis than most conventional schemes.

Nowadays the technology is at the stage of placing these systems on the structure with full-scale at laboratory to determine the real behavior. The interested reader may consult Soong (1990) and Soong and Constantinou (1994) for discussions on many theoretical and practical aspects of semi-active and active structural control.

It’s obvious that all of the above-mentioned technologies have a significant effect in the designing of different buildings, but the concentration of this dissertation is on passive energy dissipation systems with the type of friction dampers, displayed in the of Table 1.1.The recent studies on the generation and improvement of friction dampers have a 25-year background.

Table 1.1. Structural Protective Systems

Structural Protective Systems	
Seismic Isolation	1.Elastomeric Bearings 2.Lead Rubber Bearings 3.Sliding Friction Pendulums
Passive Energy Dissipation	1. Metallic Dampers 2. Friction Dampers 3. Viscoelastic Dampers 4.Viscose Fluid Dampers 5. Tuned Mass Dampers 6. Tuned Liquid Dampers
Semi-active and Active Control	1. Active Bracing Systems 2. Active Mass Dampers 3. Variable Stiffness or Damping Systems 4. Smart Materials

The main purpose of passive energy dissipation systems is dissipating the induced energy and reducing the internal attempts of the elements, like the base isolation method. This results in the reduction of internal forces and damages to the structural and non-structural elements.

2. LITERATURE REVIEW

The studies on friction damper from the first researches including the introducing and applications are presented. The main focus of this chapter is on the studies about passive control of induced seismic energy by adding friction dampers to the buildings.

Pall and Marsh in (1982), proposed friction damper as a novel structural system for the aseismic design of framed buildings. By providing sliding friction devices in the bracing system of the framed buildings, their earthquake resistance and damage control potential were evaluated. The results of these studies have shown that the use of inexpensive friction damper in the bracings of the steel framed buildings can significantly enhance their earthquake resistance. In brief, the concept is of particular importance for the following reasons:

1. Energy is dissipated mechanically throughout the height of the building rather than by localized inelastic action of the main structural members.
2. The frame is softened without losing its elasticity and recovers with little or no permanent set.
3. The friction device acts like a structural damper to control the amplitude and as a safety valve to limit the loads exerted.
4. The amplitude of vibrations and accelerations are considerably reduced; thus, secondary damage is minimized.
5. The resonance of the structure is difficult to establish, i.e. the device acts like an automatic gear in limiting the input energy.
6. The building can be "tuned" for optimum response without resorting to expensive devices.
7. There is no yielding of materials involved in the process of energy dissipation, thus no damage is caused, and the structure is ready to face future earthquakes with the same efficiency (Pall, A. S., and Marsh).

Pall (1985-1987), The U.S. National Science Foundation tested a 9-story frame structure on a shaking table at the University of California at Berkeley, and the National

Research Council of Canada tested 3-story frame structures on a shaking table at the University of British Columbia, Vancouver, the structures were subjected to more than 20 different major earthquake records. Even for an earthquake five times greater than the 1985 Mexico earthquake, the frames equipped with friction dampers remained damage free. (Pall, A., Vezina, S., Proulx, Pall, R., 1993).

Filiatrault and Cherry (1990), proposed a design method for Pall friction dampers. They proposed a simplified seismic design procedure for structures equipped with an innovative friction-damping system. The system has been shown experimentally to perform very well and could represent a major new development in earthquake-resistant design. This paper first presents an efficient modeling approach for the seismic analysis and design of friction-damped structures. The hysteretic properties of the friction dampers are derived theoretically and are included in a Friction Damped Braced Frame Analysis Program, which is adaptable to a microcomputer environment. FDBFAP is then used to perform a parametric study of the optimum slip-load distribution for the friction dampers. The results of the study lead to the construction of a design slip-load spectrum for the rapid evaluation of the optimum slip-load distribution. The spectrum considers the properties of the structure and of the ground motion anticipated at the construction site. The availability of this design slip-load spectrum should lead to a greater acceptance by the engineering profession of this innovative design concept (Filiatrault, A. and Chery, S. 1990).

Palls (1996), investigated the use of friction dampers in different buildings. The use of Pall friction dampers has shown to provide a practical, economical and effective new approach to design buildings against the earthquakes. Also, these can be conventionally incorporated in existing frame buildings to upgrade their seismic resistance. Some of the technical and economic advantages of Pall friction dampers observed in studied practical applications are saving in initial costs, simple construction, large rectangular hysteretic loops with negligible fade and very high energy dissipation capacity and no repair or replacement needed after an earthquake (Pall. A. S., and Pall. R. 1996).

Mualla and Belev (2002), studied the performance of steel frames with a new friction damper device Figure 2. under earthquake excitation. A study on the dynamic response of single-story steel frames equipped with a novel friction damper device (FDD) is presented.

Extensive testing was carried out for assessing the friction pad material, damper unit performance and scaled model frame response to lateral harmonic excitation. Numerical simulations based on non-linear time history analysis were used to evaluate the seismic behaviour of steel frames with inserted FDD. The governing parameters were identified, and their influence was traced and summarised along with implications for practical design. The application of the new FDD presents a feasible alternative to the conventional ductility-based earthquake-resistant design both for new construction and for upgrading existing structures (Mualla. I. H., and Belev. B., 2002).

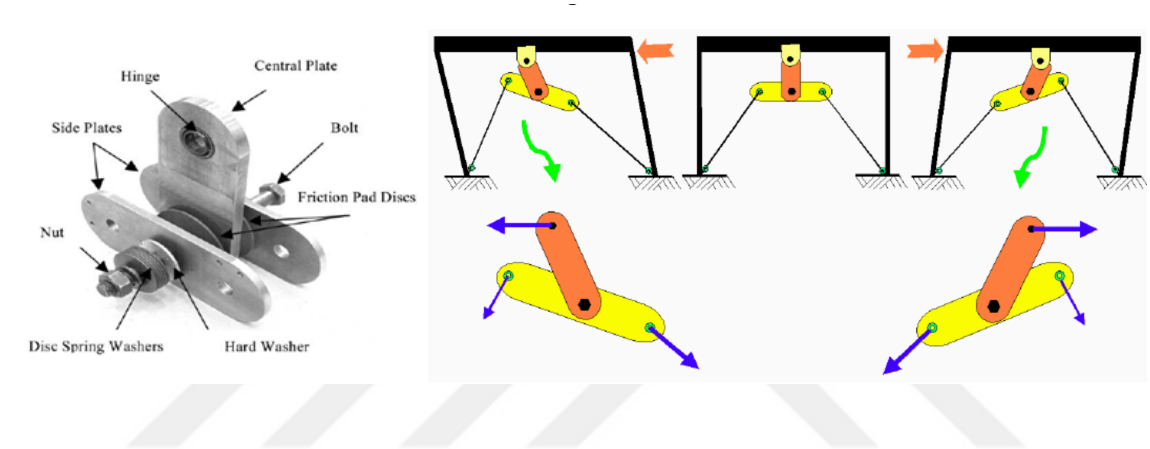


Figure 2.1 Components of FDD

Saeed Monir and Zeynali (2013), studied the dynamic behavior of a recently developed friction damper has been demonstrated. It is made from nine steel stripes and nine high strength steel bolts and is applied in the diagonal bracing of structures. This device has a square geometric shape and should be installed in the square spans. During this research work, a prototype of the modified friction damper was tested by a universal machine. Then the damper was installed inside a SDOF steel frame and tested by the shaking table under several earthquake excitations. For numerical assessment of the system, the model of SDOF frame was created in SAP2000 and analyzed under the same excitations which had been applied during the shaking table tests. By comparing the results obtained from SAP2000 to those of experimental tests, the validity of numerical modeling was proved. In order to assess the behavior of damper in multi-story buildings, the model of a four-story frame, with and without the modified damper, was created in SAP2000 and analyzed under several seismic records. The results were indicating that the lateral displacements and the base shears of the multi-story building have been significantly reduced by the installation of this modified

energy absorber and a considerable energy has been dissipated by the damping system (Habib Saeed Monir, Keyvan Zeynali 2013).

Papadopoulos and Salonikios (2013), made an experimental investigation of a new steel friction device with link element for seismic strengthening of structures. In this work a new friction device, with a set of single or double rotational friction flanges and a link element, is described and tested. The mechanism may be applied for the strengthening of existing R/C or steel buildings as well as in new constructed buildings. The device has selectable variable behavior in different levels of displacement and an interlock mechanism that is provided by the link element. The link element may be designed to lock at preselected level of displacement, offering in this way an extra safety reserve against strong earthquakes. A summary of the existing literature about other similar mechanisms is initially presented in this paper. The proposed mechanism is presented and described in detail. Laboratory experiments are presented in detail and the resulted response that proves the efficiency of the mechanism at selectable levels of strength capacity is discussed. Drawings of the mechanism attached to a R/C frame with connection details are also included. Finally, a dynamic analysis of two R/C frames, with and without the proposed mechanism attached, is performed and the resulted response is given. The main conclusion is that the proposed mechanism is a cheap and efficient devise for the improvement of the performance of new or existing framed buildings to seismic loads (Papadopoulos. P. K., Salonikios. T. N., Dimitrakis. S. A. and Papadopoulos. A. P., 2013).

Gholizad and Moghadam (2014), made a research on friction damper dynamic performance in seismically excited knee braced steel frames. High performance and reliability of refurbish able knee braced steel frames has been confirmed in previous researches trying to get an optimal design for its configuration. Buckling of diagonal member which affects the hysteretic behavior of KBF under cyclic loadings has not been foreseen in previous evaluations of this system. This deficiency can be improved by utilization of adjustable rotary friction damper device (FDD) as knee element. Diagonal element buckling can be prevented considering a suitable value for FDD sliding threshold moment Mf. Lower values of Mf Lower energy dissipation rate in FDD and this leads to an optimization problem. Nonlinear time history analyses have been performed in addition to lateral cyclic loading analyses to evaluate the response of single story KBF subjected to seismic excitation.

Optimal Mf in FDD has been chosen according to these analyses results. Roof displacement and acceleration, base shear and diagonal element's buckling status have been compared in optimally designed KBF and FDD utilized KBF with different configurations. Nonlinear dynamic analyses have been performed for one, four, eight and twelve story frames under different seismic records with several PGAs. More than 60% displacement response reduction has been earned for the FKBF without considerable increase in base shear (Gholizad A, Kamrani Moghaddam P.,2014). Figure 2.1 shows the friction damper as knee element.

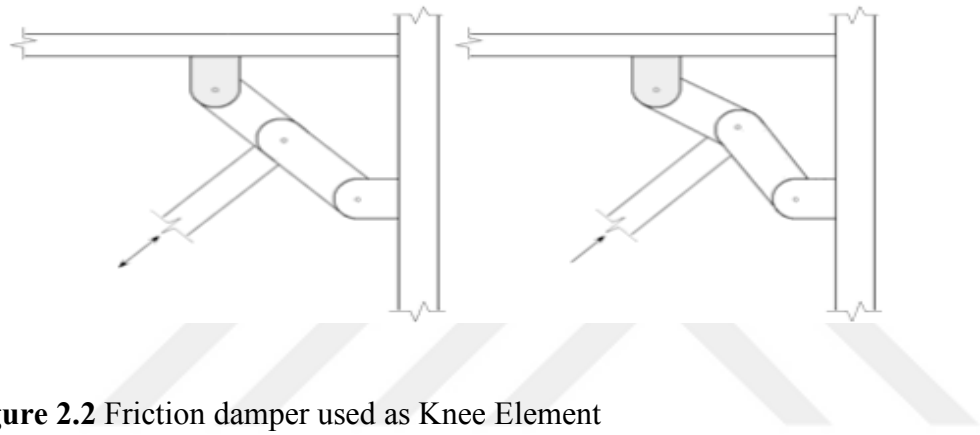


Figure 2.2 Friction damper used as Knee Element

Mirza Bagheri (2015), Performance of friction dampers with two and three units was evaluated experimentally because of a lack of research data on performance of these dampers with multi units. Results of multi-unit dampers were compared with the results of one-unit damper. Increasing trend in dissipating energy was observed. Then, the behavior of these dampers in frames of 3, 7 and 12 stories were studied by modeling the damper directly. Nonlinear time history was used. It was observed that by increasing the number of stories in the buildings, dampers with multi units should be used to perform properly against earthquake. The equivalent damping method was also investigated to consider the effects of this damper without of the damper. Effective damping of the frames equipped with this type of damper was estimated and used in nonlinear time history dynamic analysis and it was observed that the responses of these structures with dampers can be approximated by the responses of frames without damper but with damping equal to the effective damping due to rotational friction damper (S. Mirza bagheri, M. Sanati, A.A. Aghakouchak, S.E. Khadem, 2015)

Samani et al. (2015), conducted an Experimental and numerical study of a new adjustable frictional damper. In this paper, the concept of a semi active frictional damper called Adjustable Frictional Damper (AFD) is introduced. The clamping force of such damper is secured by hydraulic pressure, which not only reduces the manufacturing costs but also makes it possible to control the seismic response of the structure by changing the clamping force of the dampers. The hysteretic behavior of AFD is studied by experimental means as well as by numerical model. Experimental process involves tests with various hydraulic pressures (which cause various frictional forces) at nearly static loading as well as dynamic loading with various frequencies. The results show that the proposed damper has significant energy absorption by stable hysteretic loops, which can be used for enhancement of the performance of structures subjected to earthquake loads with various intensities. Force–displacement characteristics of AFD such as slippage load, dissipated energy, effective stiffness and equivalent viscous damping for consecutive cycles of loading is calculated. The system is qualified based on the requirements for displacement-dependent devices according to ASCE/SEI 41-06 specification. Furthermore, the hysteretic behavior of AFD is studied by numerical method and a close agreement between the experimental and numerical results is observed (Hamid Rahmani Samani, Masoud Mirtaheri, Amir Peyman Zandi, 2015).

Passive Energy Dissipation

A recent research states that the momentary shaking of the ground has been increasing and it is mentioned that; natural geomorphological phenomenon, ground water extraction, mining, nuclear explosions and cooling of the earth are the main factors of earthquake increment. These factors have direct effect on the design and construction sectors.

Hence, the design of structures has become more complex and amplified the concern of the structural engineers in discovering more accomplished design techniques for dissolving the applied energy to the structure. The traditional method of seismic design has been based upon providing a combination of strength and ductility to resist the imposed loads. Thus, the level of the structural security cannot be achieved, because the disadvantage of the designing method is lack of adjusting capability subjected to an undefined earthquake.

Seismic isolator devices and energy dissipation devices are the advanced techniques used by structural designers to protect the building under the seismic loads. (Soong and Dargush 1998)

Passive energy dissipation devices are a type of seismic protection system which are designed to absorb the amount of applied energy to the structure. Meanwhile, energy dissipation devices in a structure can be effective in reducing the dynamic reaction of the structure under the service and wind loads. (Soong and Dargush 1998)

The development of passive energy devices started with the earthquake occurred in Northridge on Jan 17, 1994 and caused 13 to 44 billion dollars damage and also the Loma Pietà Oct 17, 1989 earthquake which caused 5.6 to 6 billion dollars destruction. (P. Castaldo, 2014) And the implementation of these devices started in mid 1990s.

Generally passive energy dissipation devices are categorized as:

a) Metallic Dampers
b) Friction Dampers
c) Viscoelastic Dampers

d) Viscous Fluid Dampers
e) Tuned Mass Dampers
f) Tuned Liquid Dampers

Metallic Dampers:

The inelastic behavior of metal properties in metallic dampers are one of the most effective mechanism to dissipate the applied energy to the structure during an earthquake. (Soong and Dargush 1997)

The theoretical and experimental work of applying additional hysteretic metallic dampers in the structure to dissipate the seismic energy, was done by Kelly et al., (1972) and Skinner et al., (1975). (Soong and Dargush 1997

Over the last years, there has been different types of metallic dampers developed, among all of them; the Triangular plate dampers also known as Added Damping and Stiffness (ADAS) and X-shaped dampers shown in Figure 1.1(a) and (b) did receive significant attentions. These parallel plate devices are installed between chevron tracings and floor beams. The geometric shape of different metallics dampers does not change the dissipative mechanism result from the inelastic deformation of metal.

The applied horizontal forces related to inter-story drift deformation of the plates can be resisted by the dampers and after a certain level of force, the plate yield and thus afford an additional amount of energy dissipation.

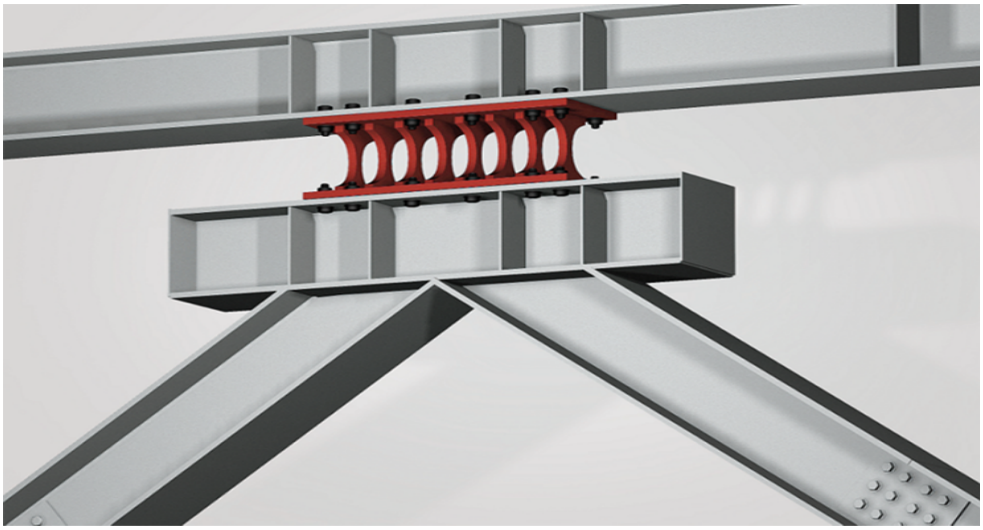


Figure 2.3. (a) Modeled X-Shaped Metallic Damper



Figure 2.3. (b) Application X-Shaped Metallic Damper in a School Building

Viscoelastic Dampers:

Back in 1950s, viscoelastic materials widely used in aerospace industry to reduce the vibration which causes fatigue in the airframes. In civil engineering industry, viscoelastic dampers firstly used in New York World Trade center in 1969 to induce wind loads. Recently, viscoelastic dampers have been used in the purpose of reducing the dynamic

response of the structure. Their low cost and minimal maintenance requirements made them one of the most highly recommended dampers. The affected factors on the behavior of viscoelastic materials when subjected to dynamic loading are the frequency of vibration, the level of strain and the temperature. Figure 1.2 (a) and (b) shows the viscoelastic damper's model and application.

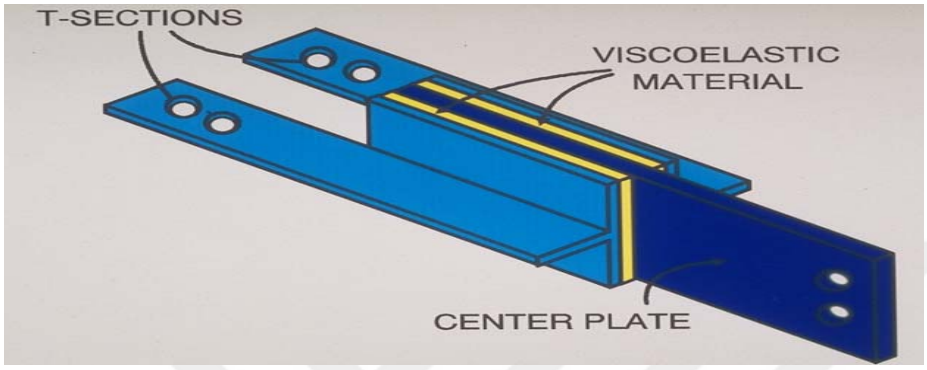


Figure 2.4 (a) Model of Viscoelastic Damper



Figure 2.4 (b) Application of Viscoelastic Damper in a Structure

Viscous Fluid Dampers

These dampers have the same history as viscoelastic dampers which used to be placed in aircrafts back in 1950s. viscoelastic fluid dampers shown in Figure 1.3 (a) and (b) are consist of a moving piston dipped in a highly viscous fluid and are widely used for the purpose of isolation in the industrial machine's equipment. As the damper piston rod and

piston head are stroked, fluid is forced to flow through openings either around or through the piston head. The resulting differential in pressure across the piston head (very high pressure on the upstream side and very low pressure on the downstream side) can produce very large forces that resist the relative motion of the damper.

The affected factors on the behavior of viscoelastic materials when subjected to dynamic loading are the frequency of vibration, the level of strain and the temperature. These dampers can be installed in the foundation floor as seismic isolation, in inverted V and diagonal braces.

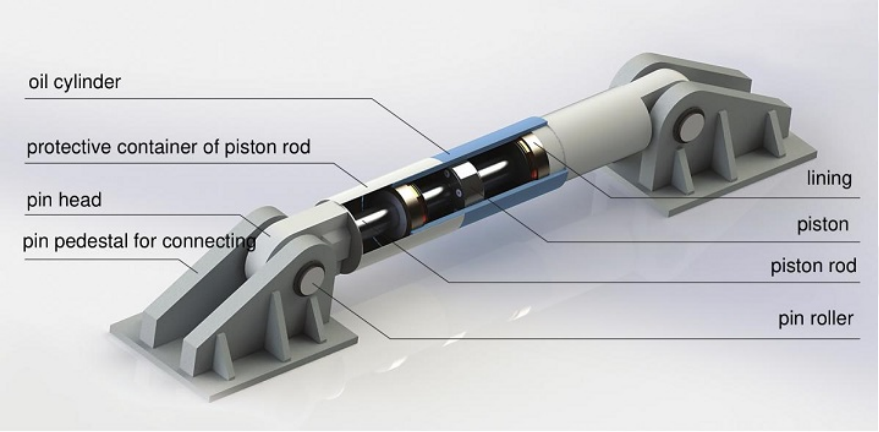


Figure 2.5 (a) Model of Viscoelastic Damper



Figure 2.5 (b) Application of Viscoelastic Damper in a Structure in the Inverted V Form

Tuned Mass Dampers

The concept of tuned mass dampers firstly applied to reduce the rolling motion and hull vibration of ships by Frahm in 1909. Later on, the usage of tuned mass dampers on a simple single degree of freedom frame was presented by Den Hartog's book on mechanical vibrations in 1940. The consistency of a mass, a spring, and a damper that is attached to a structure Tuned mass damper device is consist of a mass, a spring, and a damper which is attached to the structure to reduce the dynamic response of the structure. Lately tuned mass damper used for the Taipei 101 structure shown in Figure 1.4 (a) and (b).

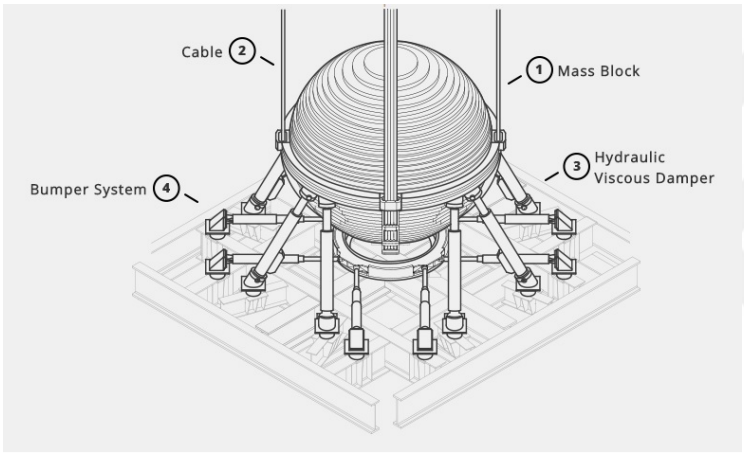


Figure 2.6 (a) Tuned Mass Damper



Figure 2.6 (b) Application of Tuned Mass Damper in Taipei 101 Structure

Tuned Liquid Damper

A tuned liquid damper is water confined in a container that uses the sloshing energy of the water to reduce the dynamic response of the system when the system is subjected to excitation. Tuned liquid dampers are also very effective in cancelling the vibration caused due to wind. The origin of these dampers is Tuned mass dampers but, tuned liquid dampers are more effective in dissipating low frequency vibrations caused by wind load, they are low in cost, there implementation is easier and doesn't require high maintenance. One Rincon hill is one of the buildings with the tuned liquid damper shown in Figure 1.5.



Figure 2.7 Application of Tuned Liquid Mass in One Rincon Hill Structure

Friction Dampers

During a major earthquake, a large amount of energy is pumped into the building. The manner in which this energy is consumed in a structure determines the level of damage. The building codes recognize that it is economically not feasible to reconcile this energy within the elastic capacity of materials. The standard specified in conventional building

codes is to design structures to resist moderate earthquakes without significant damage and avoid collapse during major earthquakes. The primary importance is on life safety. The reliance for survival is placed on ductility to dissipate energy during inelastic deformations causing bending, twisting and cracking. This assumes permanent damage, repair costs of which could be significant. Recent earthquakes have clearly demonstrated that conventional construction, even in technologically advanced countries, is not immune to destruction.

What are important to an owner is how much it will cost to build and how much it will cost to repair the damage. Early on, the structural engineers should resolve these issues with the owner and develop performance-based design criteria consistent with the performance goals. In most cases, providing good seismic performance yields good return on the investment. If the amount of energy getting into the structure can be controlled and a major portion of the energy can be dissipated mechanically independent of primary structure, the seismic response of the structure and damage control potential can be considerably improved.

These objectives can be delivered by adopting new techniques of base isolation and energy dissipation devices. With the introduction of energy dissipation devices, supplemental damping of 20-30% of critical can be easily achieved (inherent damping is merely 1-5%). Therefore, forces exerted on the structure and the amplitudes of vibrations are considerably reduced. The drifts of the structure can be reduced by a factor of about two to three and by larger factors if the devices also add stiffness to the structure, refer to Article C9.1 of FEMA-356.

The energy dissipation systems should be considered in somewhat broader context than isolation systems (which are not feasible in taller buildings) as a design strategy when performance goals include damage control. Also, the construction cost is less with energy dissipation systems than base isolation systems. Seismic isolation and energy dissipation systems are relatively new and sophisticated concepts that require more extensive design and detailed nonlinear time-history dynamic analysis than most conventional schemes. With the availability of several commercial programs and powerful desktop computers, the sophisticated analysis is no longer a daunting task and can be easily and quickly done in a small design office environment. With the emergence of Pall Friction Dampers, the

performance-based design of buildings is now economically feasible. The first building with seismic dampers in North America was built with Pall Friction Dampers.

Their low cost and maintenance free characteristics suggest wide application for new construction as well as for retrofit of existing buildings. Public sectors, private sectors and developers are using and benefiting this technology. They have been used for the seismic protection of more than 80 major building projects, including the Boeing Commercial Airplane Factory at Everett, WA – the world's largest building in volume shown in Figure 1.6 (a) and (b). This technology is credited with savings for Boeing more than US$ 30 million. The City and County of San Francisco chose Pall Friction Dampers for the seismic control of Moscone West Convention Center and saved US$2.25 million, shown in Figure1.7 (a) and (b).



Figure 2.8 (a) Boeing Commercial Airplane Factory at Everett, WA, USA.



Figure 2.8 (b) Pall Friction Dampers Used for Boeing Commercial Airplane Factory at Everette, WA, USA.



Figure 2.9 (a) View of Moscone West Convention Center, San Francisco, USA.



Figure 2.9 (b) Pall Friction Dampers Used for Moscone West Convention Center, San Francisco, USA.

Pall Friction Damper

Of all the methods so far available to extract kinetic energy from a moving body, the most widely adopted is undoubtedly the friction brake. Mechanical engineers have successfully used this concept for centuries to stop the motion of equipment, automobiles, railway trains, airplanes etc. No other mean has been able to replace the friction brake. It is the most effective, reliable and economical mean to dissipate kinetic energy. Similar to automobiles, the motion of vibrating building can be slowed down by dissipating seismic energy in friction. Inspired by the principle of friction brake in mid 1970's, Pall Friction Dampers were established for the seismic control of buildings. Pall Friction Dampers significantly reduce the initial cost of construction while dramatically increasing the earthquake resistance against damage.

Friction dampers for a building must possess a reliable and stable performance over the life of building. Developing a reliable friction is very difficult and tricky. Over a period of more than a decade of research and development, the common problems in friction were successfully overcome by using specially treated surfaces and a unique manufacturing process.

Over the years, Pall Dynamics has earned an international reputation for excellence and is a world leader in friction dampers for seismic control of buildings. Pall Friction Dampers have successfully undergone rigorous proof testing in the U.S and Canada. In 1985, the National Research Council of Canada tested three story frame structures on a shaking table at the University of British Columbia, Vancouver (Pall, A.S., Pall, R.,1993). In 1986-1987, the U.S. National Science Foundation tested a 9-story frame structure on a shaking table at the University of California at Berkeley (Pall, A., Vezina, S., Proulx, Pall, R., 1993).

The structures were subjected to more than 20 different major earthquake records. Even for an earthquake 5 times stronger than the 1985-Mexico earthquake, the frames equipped with friction dampers remained damage free. Pall Friction Dampers are well recognized and accepted by the building codes in Canada, the U.S and many other countries.

Important Features

Pall Friction Dampers are guaranteed in construction. Basically, these consist of series of steel plates, which are particularly treated to develop very dependable friction. These plates are fastened together and permitted to slip at a predetermined load. Decades of research and testing have succeeded to perfecting the art of friction. Their performance is consistent, repeatable and they own large rectangular hysteresis loops with insignificant fade. Their performance is independent of velocity and consequently applies constant force for all future earthquakes, design-based earthquake (DBE) or maximum credible earthquake (MCE). A much superior quantity of energy can be dissipated in friction than any other method involving the yielding of steel plates, viscous or viscoelastic dampers. Therefore, less Pall Friction Dampers are needed to provide the essential amount of energy dissipation. Pall Friction Dampers are passive energy dissipation devices and, therefore, need no energy source other than earthquake to operate it. They do not require any repair or replacement after the earthquake and are always ready to do their job (Pall, Avtar and Pall, R., T, 2004).

In a typical undamped structure, the inherent damping is merely 1-5% of critical. With the introduction of Pall Friction Dampers, structural damping of 20-30% of critical can be easily achieved. As the dampers dissipate a major portion of the seismic energy, forces

and deformations on the structure are significantly reduced. Pall Friction Dampers significantly reduce the initial cost of construction while dramatically increasing the earthquake resistance against damage. Pall Friction Dampers are customized to suit site conditions and allow greater adaptability than is possible with other systems. These dampers can be bolted or welded into place. Pall Friction Dampers are available for long slender tension-only cross bracing, single diagonal tension compression bracing and chevron bracing Figure 1.8 (a), (b) & (c).

The damper for cross bracing is a unique mechanism; when one of the braces in tension forces the damper to slip, the damper mechanism forces the other brace to shorten and thus avoid buckling; in this manner, the other brace is immediately ready to slip the damper on reversal of cycle. These dampers have been used in 65 feet (22 m) long slender bracing. To avoid pounding at the expansion joints, Pall Friction Connectors are custom made to accommodate bidirectional movements (Pall, Avtar and Pall, R., T, 2004).



Figure 2.10 (a) Friction Damper in Tension-Only Cross Brace



(b) Friction Damper Chevron Bracing



(C) Single Diagonal Tension Compression Bracing

Slip Load of Friction Damper

The friction dampers are designed not to slip during wind. During a major earthquake, they slip prior to yielding of structural members. In general, slip load should be equal to 75% of the shear at which the members will yield and 130% of wind shear.

As seen in Figure 1.9, if the slip load is very low or very high, the response is very high. Several parametric studies have shown that the slip load of the friction damper is the principal variable with the appropriate selection of which it is possible to tune the response of structure to an optimum value. Optimum slip load gives minimum response, and selection of slip load should also ensure that after an earthquake, the building returns to its near original alignment under the spring action of an elastic structure. Studies have also shown that variations up to (±20%- ±25%) of the optimum slip load do not affect the response significantly. Therefore, small variations in slip load (8- 10%) over life of the building do not warrant any adjustments or replacement of friction damper.

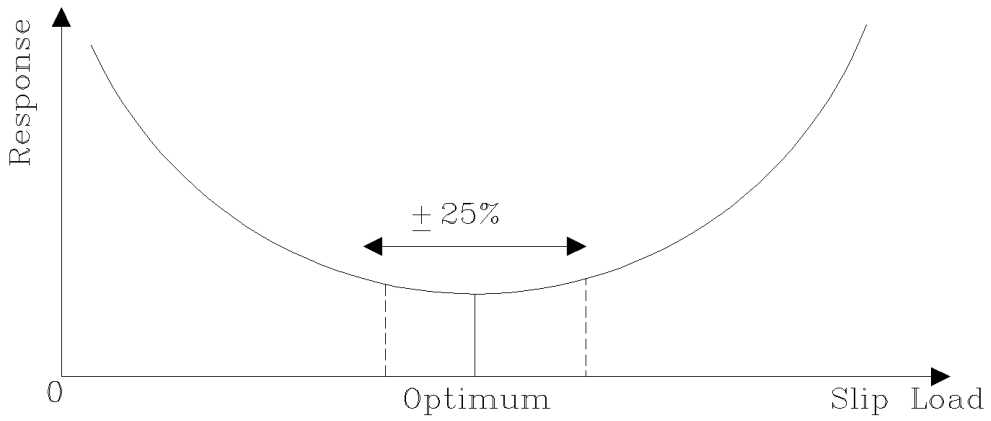


Figure 2.11 Response Versus Slip Load

The reasons that friction dampers may be favored in comparison to other systems are listed as follows:

- They are simple and guaranteed in construction.
- Offer reliable and repeatable performance at low cost.

- Possess large rectangular hysteresis loops. Greater energy dissipation for a given force. Hence, fewer Pall Friction Dampers are needed. Conversely, exert lesser force for a given damping.
- Provide supplemental damping and stiffness for added stability.
- Performance is independent of velocity and temperature.
- Constant force for all future earthquakes (DBE/MCE). Therefore, design of connections and members is economical.
- They are not active during service loads and wind. Hence, no possibility of failure due to fatigue before an earthquake
- Need no repair or replacement before and after earthquake. There is nothing to damage or leak.
- Energy dissipation is through friction and not through the damaging process of yielding.
- After an earthquake, the building returns to its near original alignment due to spring action of an elastic structure.
- Compact and narrow enough to be hidden in partitions.
- Available for all types of bracing, including tension cross bracing, and expansion joints.
- Custom made. Easily adaptable to any site condition. Can be welded or bolted

The purpose of this dissertation is to evaluate the performance of a 3d concrete moment resisting frames in the presence of friction dampers with different bracing configurations in the terms of structure total weight, base shears and story drifts. The 7-story structure location is taken in Düzce, Turkey which is designed based on the Turkish Standard (TS 500) and modeled in SAP2000.

3. MODEL APPLICATIONS

3.1 Introduction

This chapter firstly presents the basis of structural dynamics relations briefly. Then the design procedure and considerations with the structural implementations and the applicant samples are discussed.

3.2 Dynamic Response of Simple Structural Models

3.2.1 General Formulation

3.2.1.1 Time Dependent Force

A single degree of freedom model that exhibits some of the key response characteristics of a structure subjected to dynamic loading is presented. It is important to keep in mind that here we are studying the behavior of the mathematical idealization, not that of a physical structure. Much more detail is required to properly model an actual building. Our treatment was influenced by presentations included in Newmark and Rosenbluth (1971) and Hanson (1993).

However, several concepts can be most easily introduced by examining these simple models. Single degree of freedom structure as shown in Figure 3.1(a) is the most idealized and simplest structure for dynamic analysis. Three assumptions are made in this idealization which are the rigid roof system, mass concentrated at the roof and the axial deformation of columns are neglected. These assumption's result is presented in Figure 3.1(b) with a time-dependent force applied at the roof level. And, the forces acting on the mass of the structure are shown in Figure 3.1 (c)

The summation of the forces acting on the free body results as the following equation of equilibrium which must be satisfied at each instant of time (Equation 3.1):

$$f_i + f_d + f_s = p(t) \qquad (3.1)$$

Where;

f_i = Inertia force = $m\ddot{u}$

f_d = Damping force = $c\dot{v}$

f_s = Elastic restoring force = kv

$p(t)$ = Time-dependent applied force

$\ddot{u}$ is the total acceleration for the mass, $\dot{v}$ and v are the velocity and displacement of the mass relative to the base.

(Equation 3.1) Is written in terms of physical parameters results (Equation 3.2):

$$m\ddot{u} + c\dot{v} + kv = p(t) \qquad (3.2)$$

Must be noted that the forces in damping elements depend upon the relative velocity and relative displacement respectively, across the ends of these elements, whereas inertia force depends upon the total acceleration of the mass.

The total acceleration of the mass equation can be written as (Equation 3.3):

$$\ddot{u}(t) = \ddot{g}(t) + \ddot{v}(t) \qquad (3.3)$$

Where;

$\ddot{v}(t)$: acceleration of the mass relative to the base

$\ddot{g}(t)$: acceleration of the base

In this case the base is assumed to be fixed with no motion, and hence $\ddot{g}(t) = 0$ and $\ddot{u}(t) = \ddot{v}(t)$. Making this substitution for the acceleration, (Equation 3.2) For a time-dependent force becomes (Equation 3.4):

$$m\ddot{v} + c\dot{v} + kv = p(t) \qquad (3.4)$$

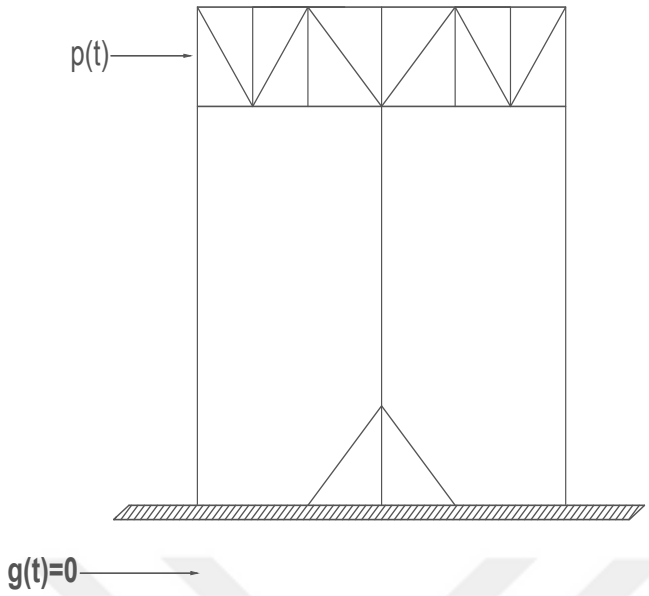


Figure 3.1(a) Single Degree of Freedom Structure

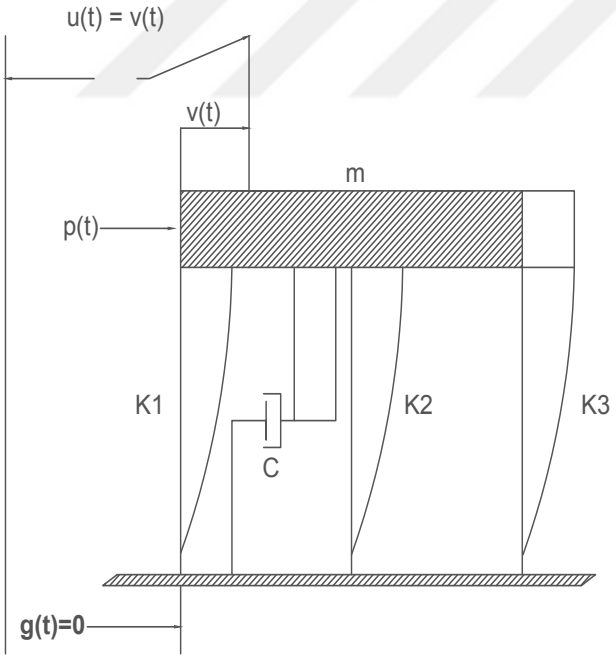


Figure 3.1 (b) Time Dependent Force SDOF Structure

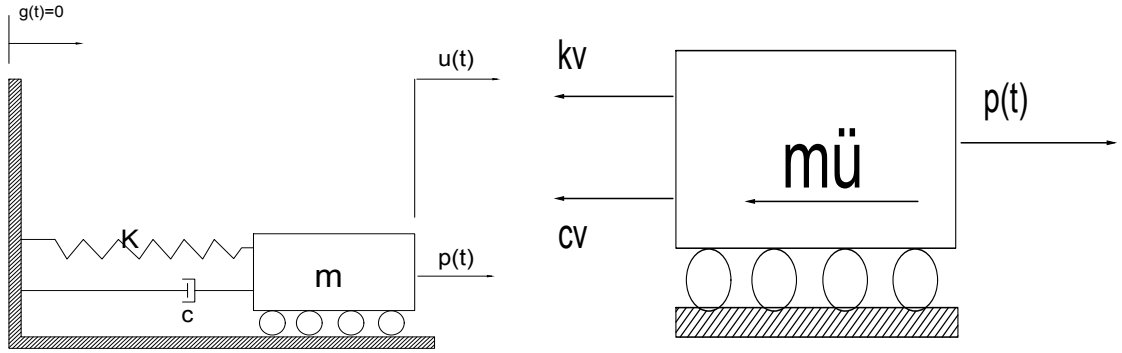


Figure 3.1(c) The Summation of Forces Acting on the SDOF Structure

3.2.1.2 Earthquake Ground Motion

For a single-story structure, no external dynamic force is applied at roof level when it is subjected to earthquake ground motions. Instead an acceleration occurs at the base of the structure. The effect of it on the single-story structure is shown in Figure 3.2 (a), and the forces summation as shown in the Figure 3.2 (b) Results as below equation of equilibrium (Equation 3.5)

$$f_i + f_d + f_s = 0 \qquad (3.5)$$

The substitution of the physical parameters of (Equation 3.5) results in an (Equation 3.6) of equilibrium:

$$m\ddot{u} + c\dot{v} + kv = 0 \qquad (3.6)$$

This equation can be written in the form of (Equation 3.4) by substituting (Equation 3.3) into (Equation 3.6) and rearranging terms to obtain (Equation 3.7)

$$m\ddot{u} + c\dot{v} + kv = P_e(t) \qquad (3.7)$$

Where;

$P_e(t)$ =effective time-dependent force = $-m\ddot{g}(t)$

Therefore;

$$m\ddot{u} + c\dot{v} + kv = -m\ddot{g}(t) \qquad (3.8)$$

Hence the equation of motion for a structure subjected to a base motion is similar to that for a structure subjected to a time-dependent force if the base motion is represented as an effective time-dependent force which is equal to the product of the mass and the ground acceleration.

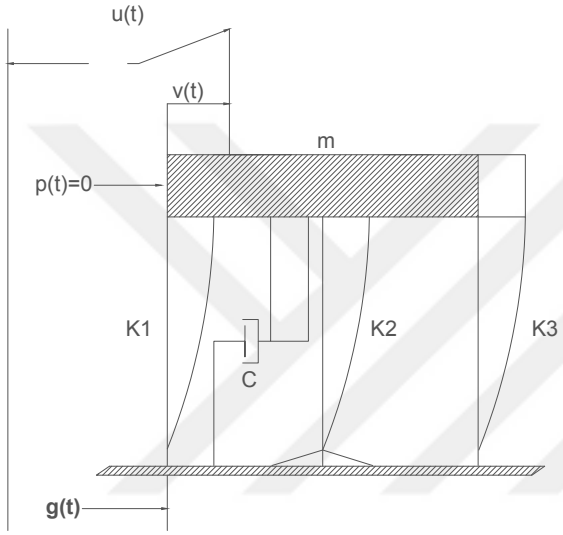


Figure 3.2 (a) Earthquake Ground Motion on SDOF

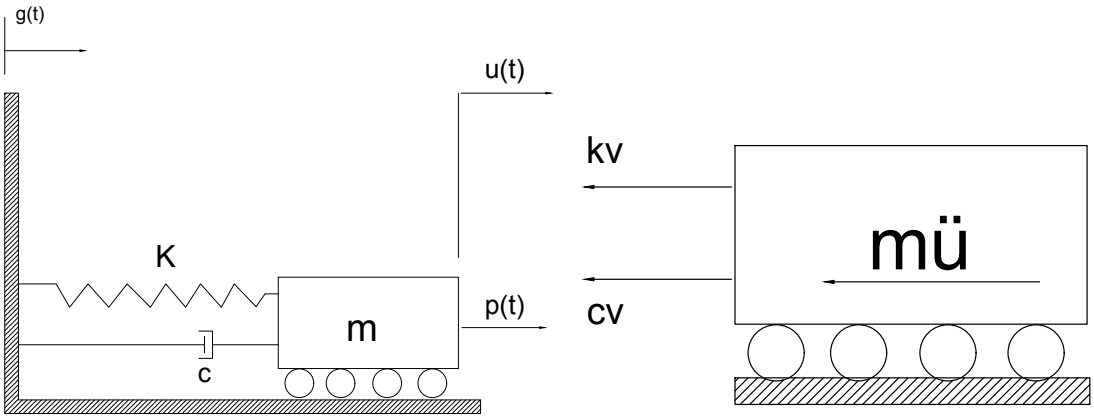


Figure 3.2 (b) The Summation of Forces Acting on the SDOF Structure

3.3 Friction Damper

3.3.1 Basic Principles

There are numerous forms of friction that can be effectively used to mitigate damage to structures during environmental disturbances. All of the devices to be discussed in the present chapter employ solid sliding friction as their basic dissipative mechanism. Thus, in friction dampers, irrecoverable work is done by the tangential force required to slide one solid body across the surface of another. One objective, Ofcourse, is to maximize the energy dissipation.

Consequently, there is no desire to introduce a hydrodynamic lubricating layer on the interface. The contacting surfaces are generally intended to remain dry during operation.

In accordance with this, our presentation of basic principles will begin with a discussion of dry, sliding, solid friction. More detailed information, along with numerous references, can be found in articles by Tabor (1981) and Larsen-Basse (1992), and in the classical textbooks by Bowden and Tabor (1950, 1964). It is naturally of paramount importance that a consistent, predictable frictional response be maintained throughout the life of the damper. However, this response depends to a considerable extent on surface conditions, which may in turn be affected by environmental factors.

3.3.2 Solid Friction

The scientific study of dry-friction has a long history dating to the illustrious work of Davinci, Amontons, and Coulomb. The basic theory is founded upon the following hypotheses, which were initially inferred from physical experiments involving planar sliding of rectilinear blocks:

1. The total frictional force that can be developed is independent of the apparent surface area of contact.
2. The total frictional force that can be developed is proportional to the total normal force acting across the interface.

3. For the case of sliding with low relative velocities, the total frictional force is independent of that velocity.

As a result of these assumptions, at the instant of impending slippage or during sliding itself, one can write (Equation 3.9):

$$F = \mu * N \qquad (3.9)$$

Where: F and N represent the frictional and normal forces, respectively, and μ is the coefficient of friction. Since it is frequently observed that the coefficient of friction is somewhat higher when slippage is pending than it is during sliding, separate static (μ_s) and kinetic (μ_k) coefficients are often introduced. In either case, the frictional force F acts tangentially within the interfacial plane in the direction opposing the motion or impending motion. The concept of Coulomb friction, as described above, provides the theoretical basis for most of the work that has appeared concerning friction dampers.

3.4 Analyses Method

Nonlinear time history analysis (NTHA) are performed on the 3D models. The inelastic time-history analysis is the most accurate method to predict the force and deformation demands at various components of the structure. The use of the inelastic time history analysis is limited because the dynamic response is very sensitive to the modeling and ground motion characteristics. It requires proper modeling of the cyclic load-deformation characteristics, and careful consideration of the weakening properties of all the important components.

The computation time, the time required for input preparation, and interpreting the capacious output, makes the use of the inelastic time history analysis difficult for seismic performance evaluation. In the present study, SAP2000 was used in performing the nonlinear dynamic time-history analysis on the three-dimensional model of the building with Direct-integration analysis method.

Direct-integration analysis is a dynamic analysis method in which the equilibrium equations of motion are fully integrated as a structure is subjected to dynamic loading. Analysis involves the integration of structural properties and behaviors at a series of time steps which are small relative to loading duration. Note that integration is performed at every time step of the input record, regardless of the output increment.

3.5 Features of Models

In this work, seven types of 7-story structures located in Düzce, are designed according to the Turkish building code and regulations. These structures are consisted of concrete moment resisting building, concrete moment resisting building with X friction bracing and concrete moment resisting building with inverted V friction bracing. The X and Inverted V dampers are arranged and analyzed in two different arrangement for both X and Y directions and also eliminated at the first story for first arrangement in different analyze. The structures are modeled in SAP2000 software and analyzed for 7 different earthquakes which are explained briefly in this chapter.

The standards and provisions used to analyze and design the buildings are:

- TS 500. Requirements for Design and Construction of Reinforced Concrete Structures (TS 500-2000)
- Turkish 498, 1997. Design Loads for Buildings. Turkish Standard Institute, Necatibet Street No. 112 Ministries, Ankara
- TSC 2018, Turkish Seismic Code, Specification for Structures to be Built in Seismic Areas, Official Gazette No. 26454 and 26511, Ministry of Public Works and Settlement, Government of Republic of Turkey
- ASCE/SEI 41-13. Seismic evaluation and retrofit of existing buildings for assigning hinge properties to structural elements

General requirements for the designing of the bare structures (BS) are material properties, flooring details, surrounding walls details and snow loads which are calculated below and entered to the SAP2000 software.

The concrete material is C20/25 with the compressive strength of 20MPa and 25MPa for cylindrical and cubic standards specimens respectively. Utilized rebars have the yielding strength equal to 413MPa.

3.5.1 Gravity Loadings

Considering the length of spans the flooring system for the structure is Two-way slab. The loadings are calculated based on the Turkish building codes and regulations as below:

Dead Load:

Covering + Plaster = 1 kN/m^2
Slab Concrete = $0.15m\ x\ 25\ kN/m^3\ =\ 3.75\ kN/m^2$

Where 0.15m is the slab thickness and $25\ kN/m^3$ is the concrete density. Therefore, the dead load for the floor is equal to $4.75\ kN/m^2$.

The walls dead loads are calculated as below; where wall height 2.8m, the thickness for the external walls 0.25m, the external plaster 0.02m and the internal plaster is considered to be 0.015m. the calculation is as below:

Concrete block = $0.25m\ x\ 7\ kN/m^3\ =\ 1.75\ kN/m^2$
External Plaster = $0.02m\ x\ 20\ kN/m^3\ =\ 0.4\ kN/m^2$
Internal Plaster = $0.015\ x\ 20\ kN/m^3\ =\ 0.3\ kN/m^2$

The sum of the load is 2.45 kN/m^2 which is applied as a linear load which is equal to $2.8m\ x\ 2.45\ kN/m^2\ =\ 6.86\ kN/m$ in the SAP2000 software.

Live Load:

Based on (TS 498), live load on slab and on the roof slab for residential buildings is taken 2 kN/m^2 and 1 kN/m^2 respectively. And the snow load is calculated as 1.2 kN/m^2 for the Düzce which is located in region III in the snow load regions table.

3.5.2 Lateral Seismic Load

The distribution of lateral load is calculated and applied automatically by SAP2000 in the Düzce region with the assumption of ZB and DD-2 for ground type and earthquake ground motion level respectively shown in Table 3.1 The summary of calculation based on the new Turkish seismic design code TBDY-2018 is presented as below:

Table 3.1 Turkey's Earthquake Regulation on Buildings TBDY-2018

Turkey's Earthquake Regulations on Buildings TBDY-2018	
Earthquake Ground Motion Levels (DD)	
DD-1	The probability of exceeding in 50 years is 2%, the repetition period is 2475 years, very rare, but the greatest possible earthquake. (Use for high-rise and special buildings).
DD-2	The probability of exceeding in 50 years is 10%, the repetition period is 475 years and infrequent earthquake, is called standard earthquake ground motion. (Except high-rise buildings and old buildings, it is for every other type).
DD-3	The probability of exceeding in 50 years is 50%, the repetition period is 72 years and it is very frequent earthquake.
DD-4	The probability of exceeding in 50 years is 68%, the repetition period is 43 years and it is a rare type earthquake

The earthquake ground motion is selected DD-2; repetition period 475. The importance factor for residential buildings which is categorized as BKS = 3 based on the structure's usage is taken 1. And the ground type is taken ZB where Vs = (760 – 1500) m/s

Turkey's Earthquake Regulations on Buildings - TBDY-2018

S_{DS} , S_{D1}: Calculation of design spectral acceleration coefficient:

$$S_{Ds} = S_s * F_s$$
$$S_{D1} = S_1 * F_1$$

Where;

S_s: Short period spectral acceleration coefficient map

S_1: 1 second period spectral acceleration coefficient map

F_s: Spectral acceleration coefficient map for short period regions

F_1: Spectral acceleration coefficient map for 1 second period

S_s 475 = 1.232 g and S_1 475 = 0.336 g are taken from the map as shown in below Figure 3.3 through Figure 3.5.

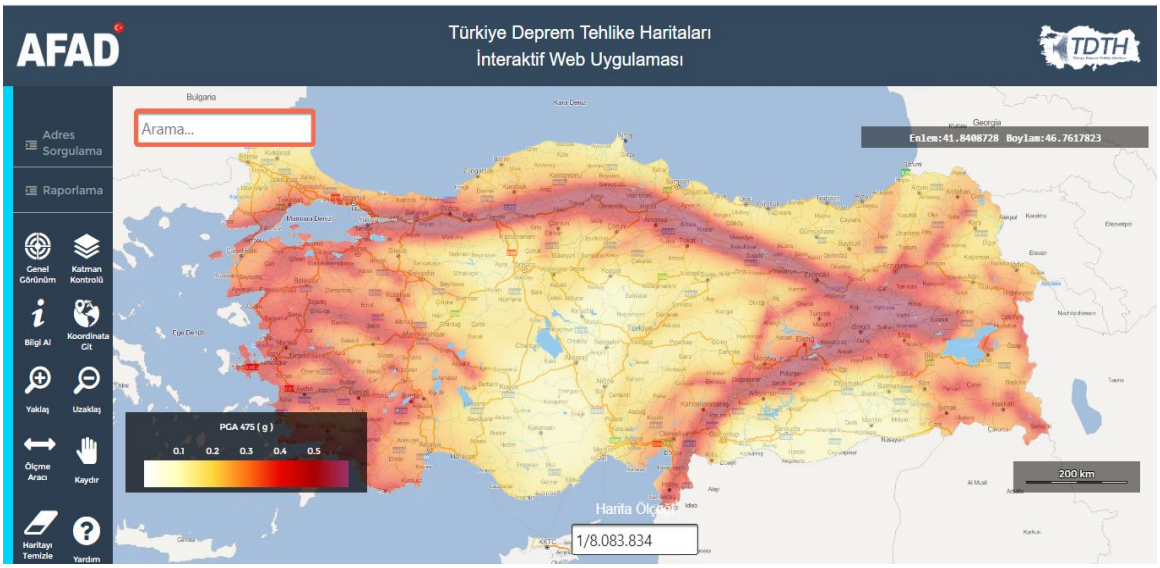


Figure 3.3. Turkey Earthquake Hazard Map

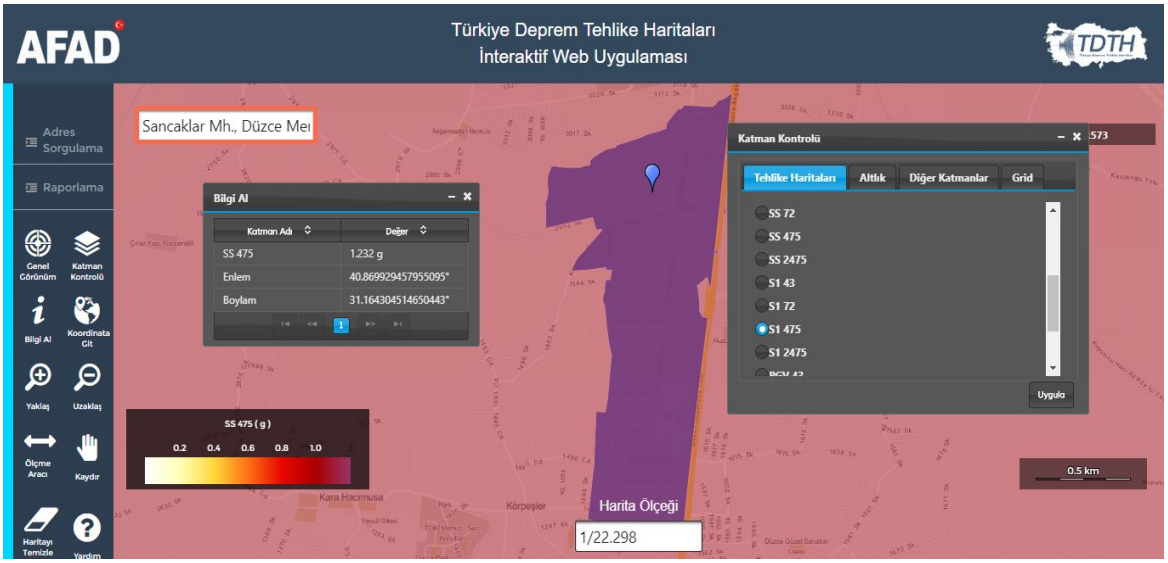


Figure 3.4 Reading SS475 from Turkish Seismic Map AFAD Website for Düzce

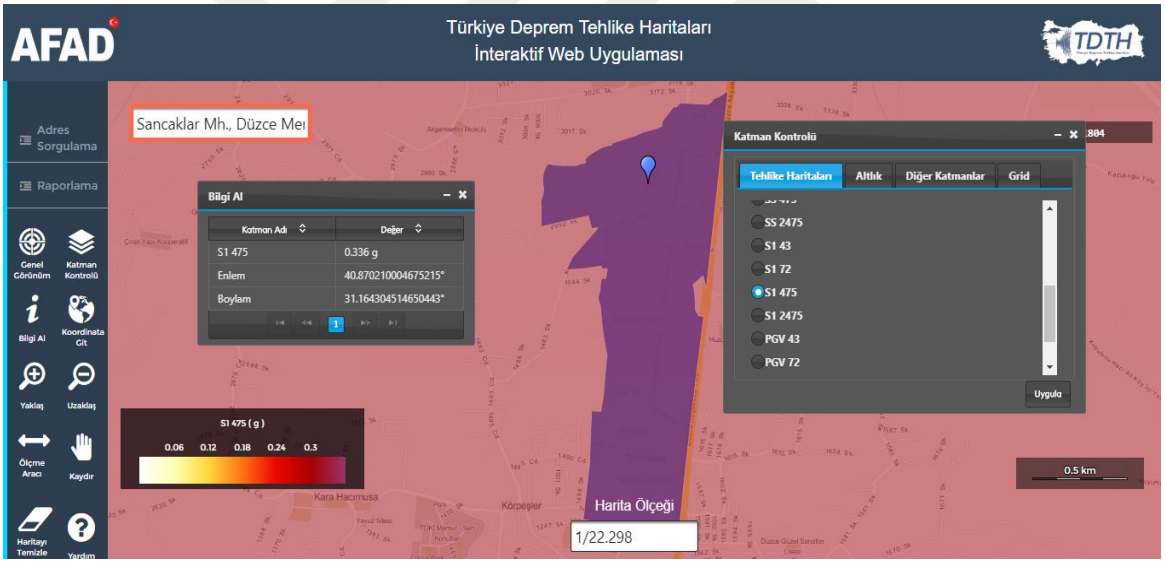


Figure 3.5 Reading S1 475 from Turkish Seismic Map AFAD Website for Düzce

R = 8 and D = 3 for the high-rise concrete buildings according to the carrier system behavior for building bearing systems.

The data selected for the seismic design of the structure is entered to the SAP2000 is shown in Figure 3.6.

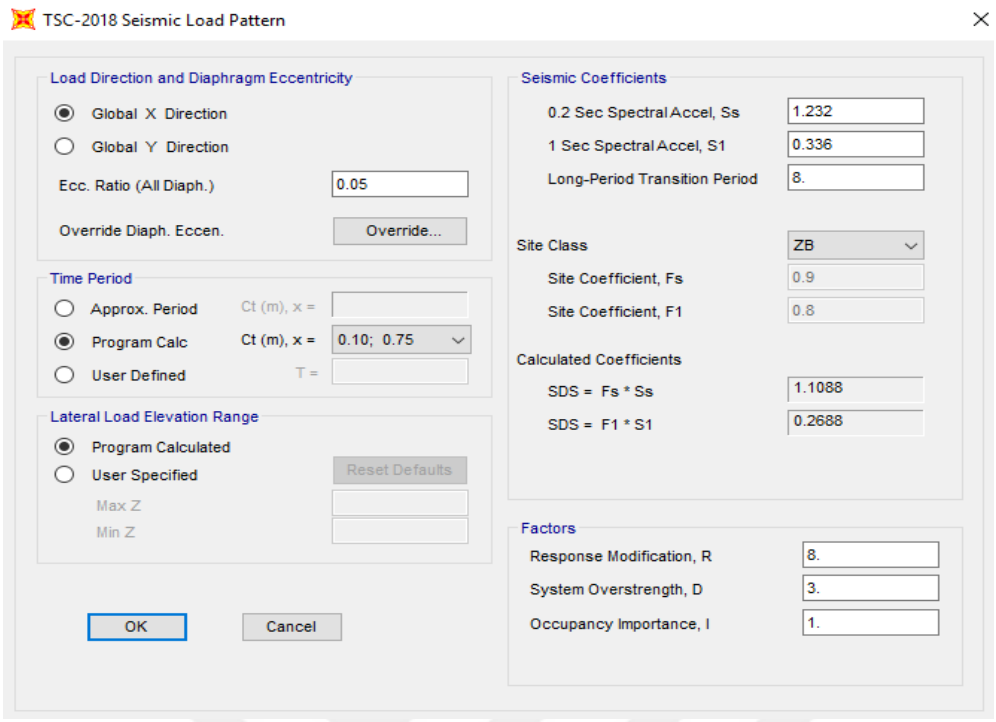


Figure 3.6 Seismic Load Definition in SAP2000 Software

3.5.3 Load Combinations

According to the TSC 5000-2000 the load combination for the strength design of the structures is:

1) $1.4G + 1.6Q$
2) $G + Q \pm E_x \pm 0.3\ E_y$
3) $G + Q \pm E_y \pm 0.3\ E_x$
4) $0.9G \pm E_x \pm 0.3\ E_y$
5) $0.9G \pm E_y \pm 0.3\ E_x$

Which is automatically generated by the SAP2000 Software. The symbols in load combinations are indicated as below:

G: Dead load;
E: Earthquake load;
Q: live load;

The summary of the above-mentioned requirements has been summarized in Table 3.2. Also, the 3D model is illustrated in Figure 3.7.

Table 3.2 Summary of the Structure Properties

Properties	**Values**
Column Section	800mmX800mm for 1st story interior columns 700mmX700mm for 2nd story interior columns 600mmX600mm for others
Beam Section	250mmX500mm
Slab Thickness	150mm
External Wall's height	2.80m
Concrete	C20/25
Rebars	Yield Strength = 413Mpa
Live Load on Roof Slab	1 kN/m2
Roof Dead Load	3.75 kN/m2
Live Load on Slab	2 kN/m2
Slab Dead Load	4.75 kN/m2
Snow Load on Roof	1.20 kN/m2
External Wall's Dead Load	6.86 kN/m2
Parapet Dead Load	1.92 kN/m2
Slab Type	Two way
Earthquake ground motion level	DD-2
Ground Type	ZB

3.5.4 Structure's Views:

The damped braces are arranged in three different types for X braced damped frames and Inverted V damped frames. the arrangements are shown in Figure 3.7 through Figure 3.27.

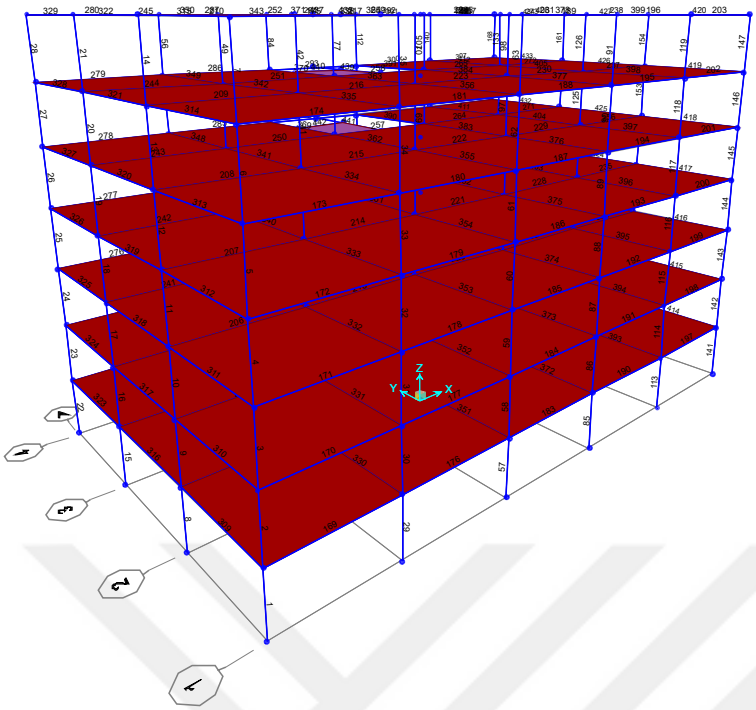


Figure 3.7. Three-Dimensional Model of the 7-Story Building Without Friction Damper

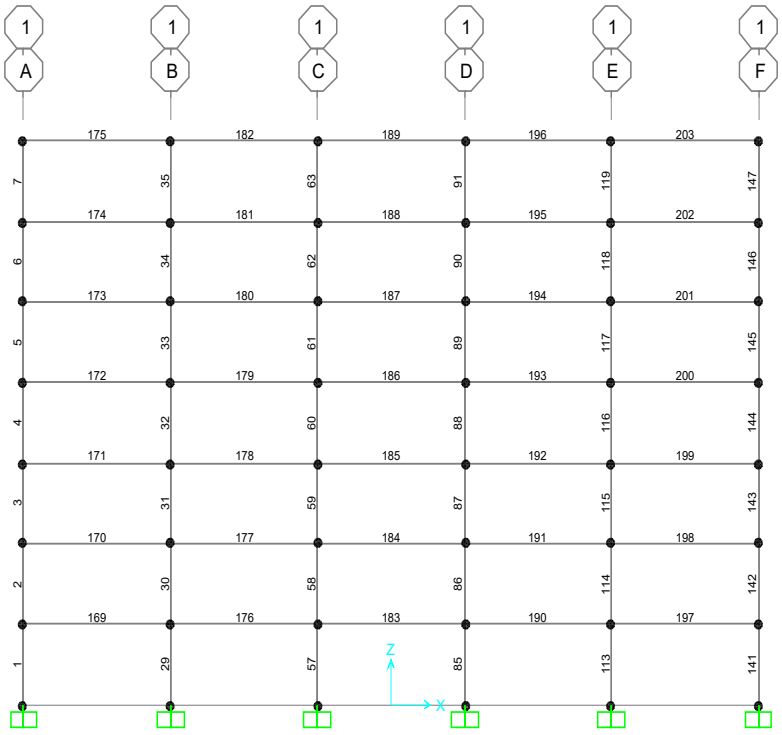


Figure 3.8. X-direction Plan View of the 7-Story Building Without Friction Damper

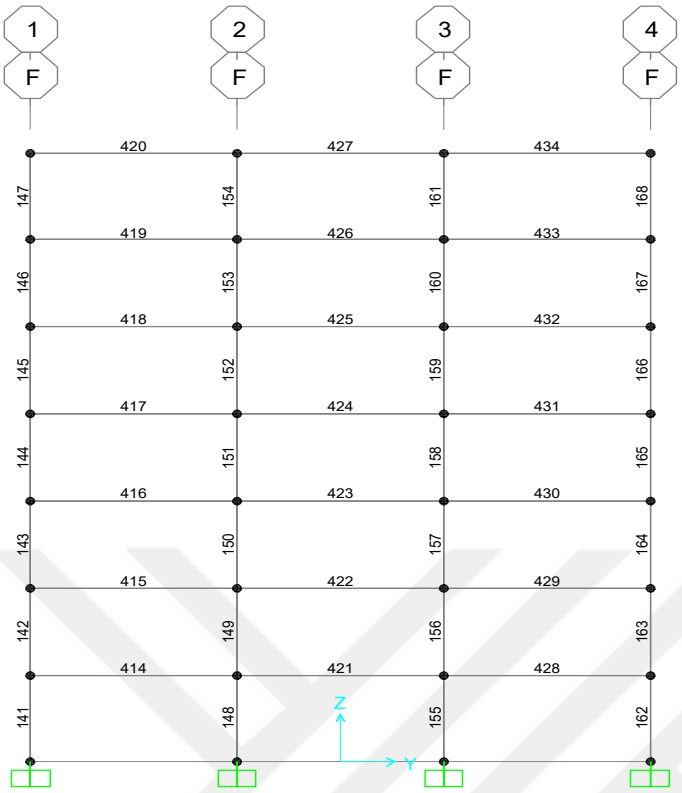


Figure 3.9. Y-direction Plan View the 7-Story Building Without Friction Damper

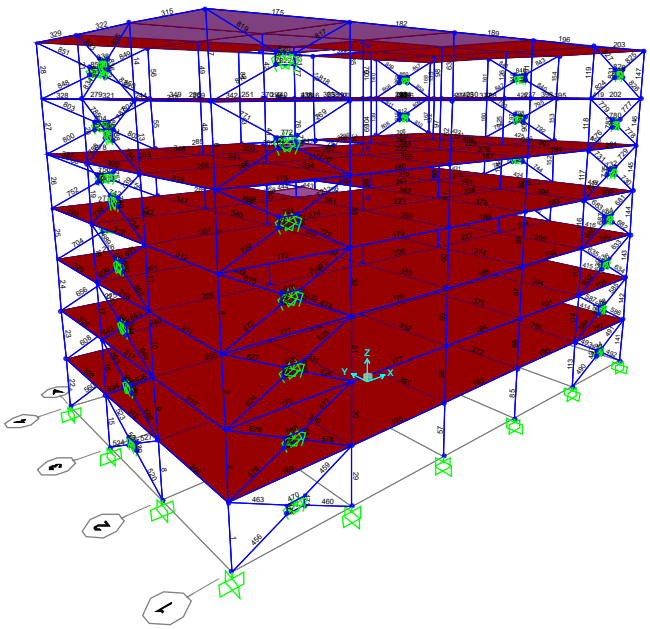


Figure 3.10. Three-Dimensional Model of the 7-Story Building with X Friction Bracing (Arr 1)

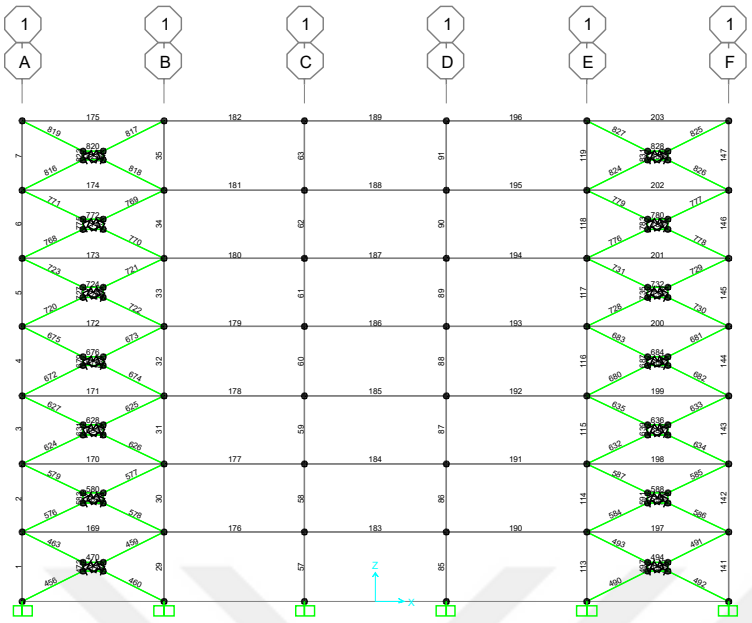


Figure 3.11. X-Direction Plan View of the 7-Story Building with X Friction Bracing (Arr 1)

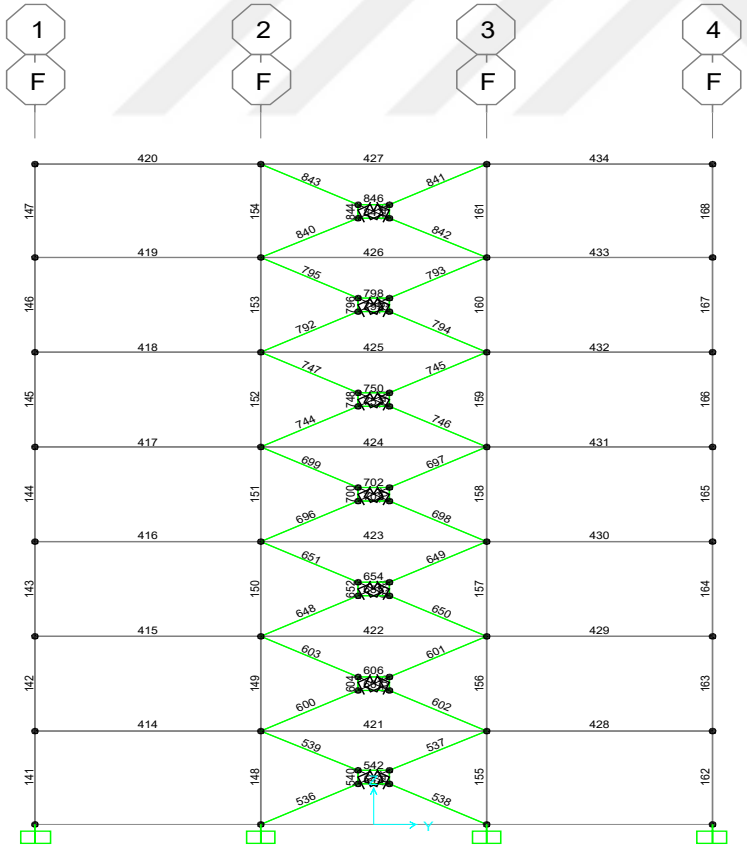


Figure 3.12. Y-Direction Plan View of the 7-Story Building with X Friction Bracing (Arr 1)

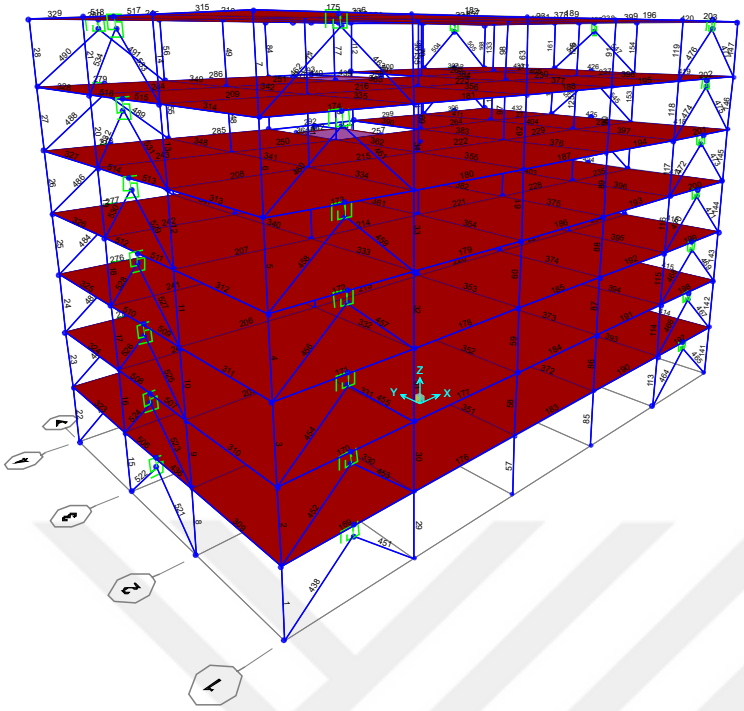


Figure 3.13. Three-Dimensional Model of the 7-Story Building with Inverted V Friction Bracing (Arr 1)

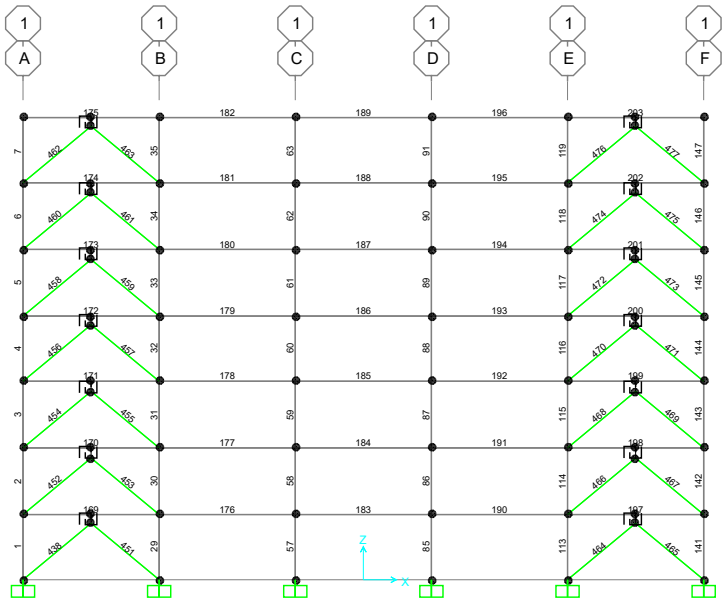


Figure 3.14. X-Direction Plan View of the 7-Story Building with Inverted V Friction Bracing (Arr1)

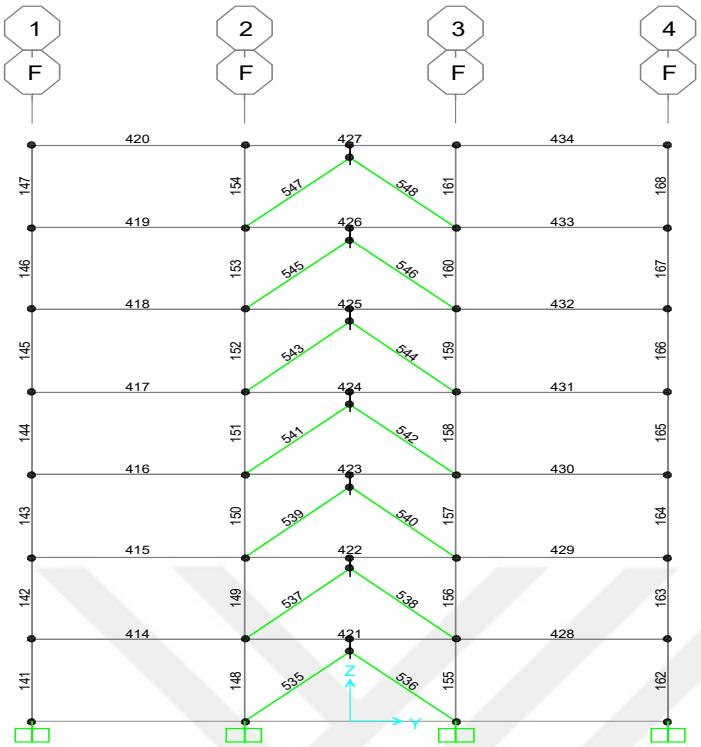


Figure 3.15. Y-Direction Plan View the 7-Story Building with Inverted V Friction Bracing (Arr 1)

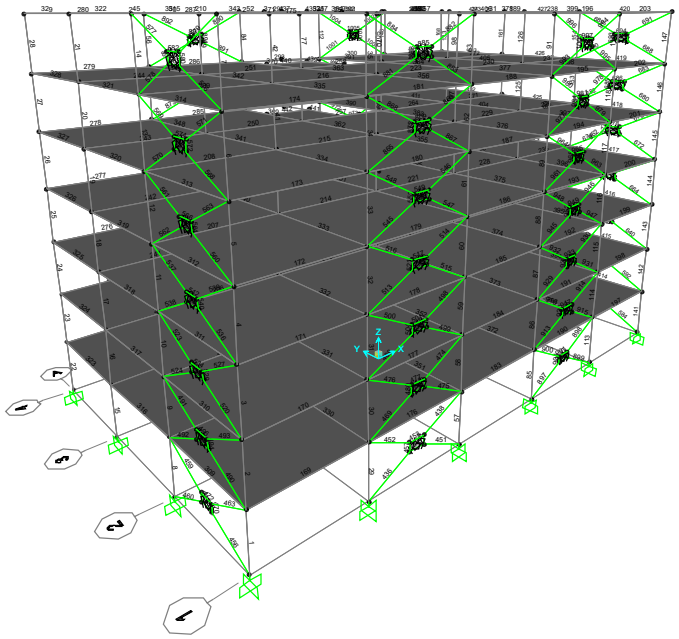


Figure 3.16. Three-Dimensional Model of the 7-Story Building with X Friction Bracing (Arr 2)

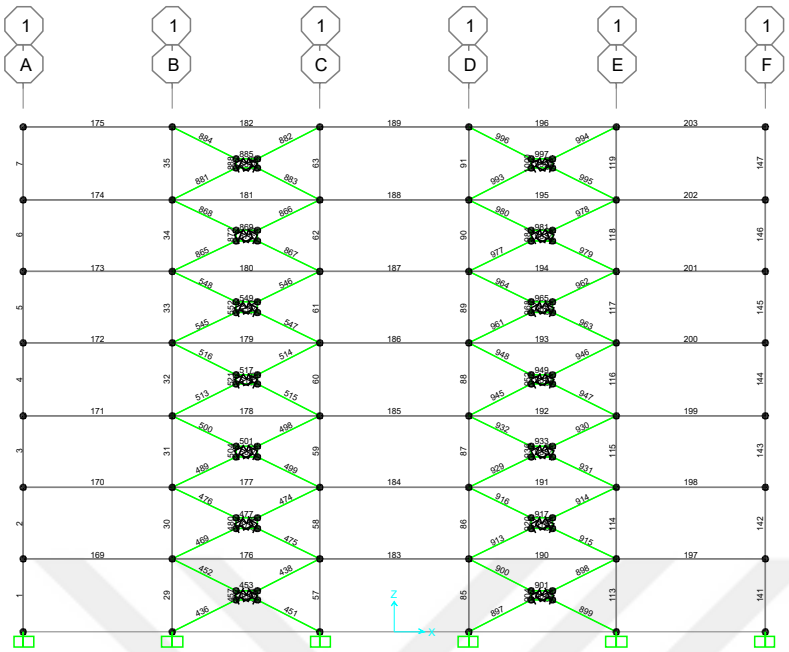


Figure 3.17. X-Direction Plan View of the 7-Story Building with X Friction Bracing (Arr 2)

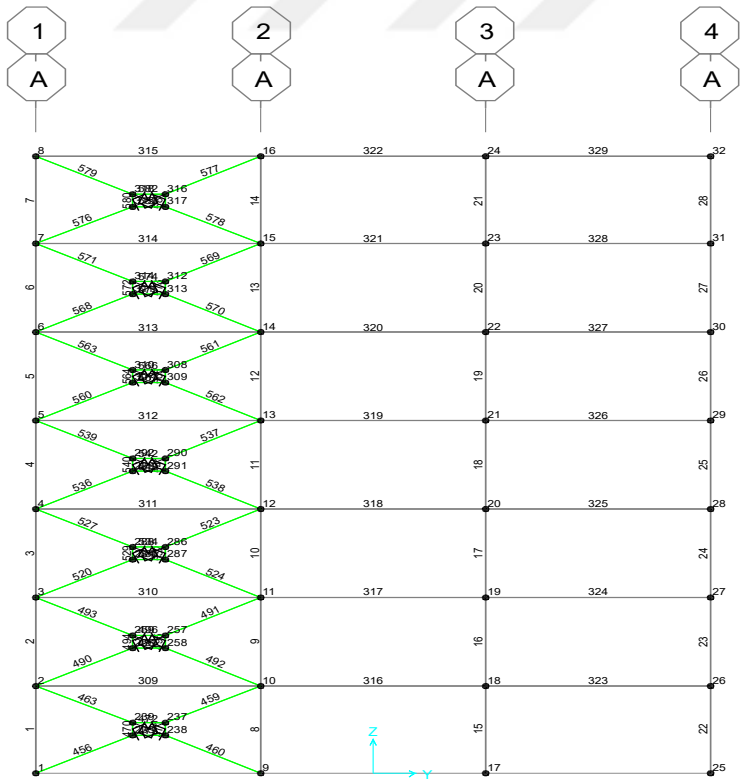


Figure 3.18. Y-Direction Plan View the 7-Story Building with X Friction Bracing (Arr 2)

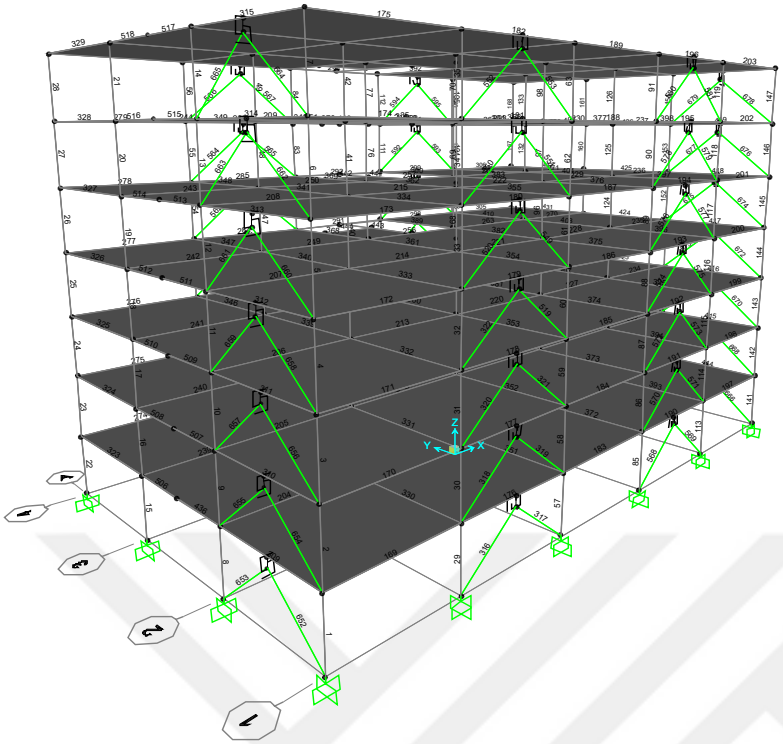


Figure 3.19. Three-Dimensional Model of the 7-Story Building with Inverted V Friction Bracing (Arr 2)

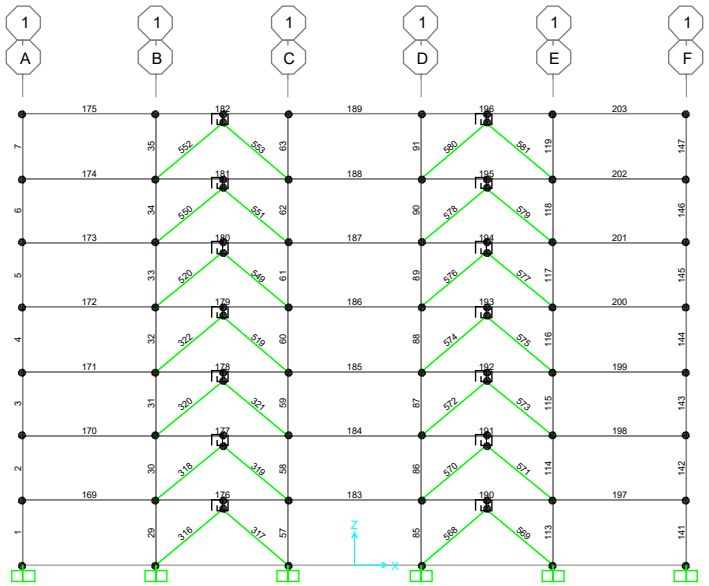


Figure 3.20. X-Direction Plan View of the 7-Story Building with Inverted V Friction Bracing (Arr 2)

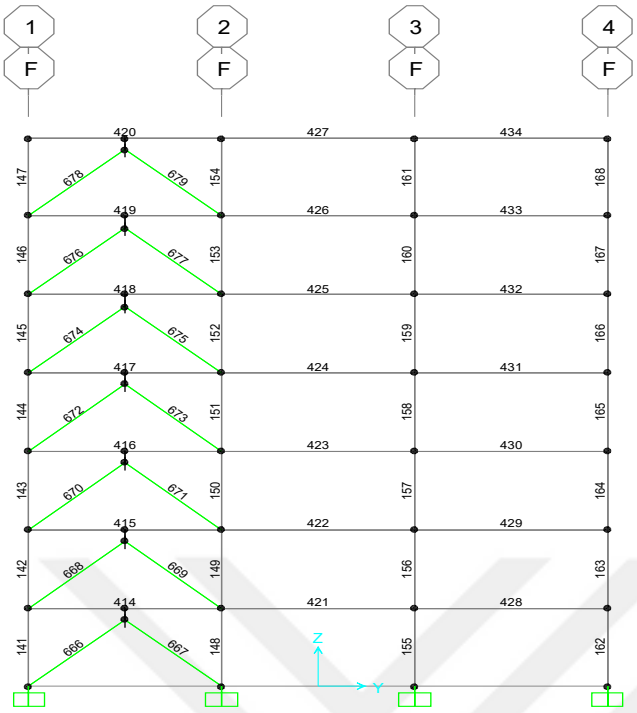


Figure 3.21. Y-Direction Plan View the 7-Story Building with Inverted V Friction Bracing (Arr 2)

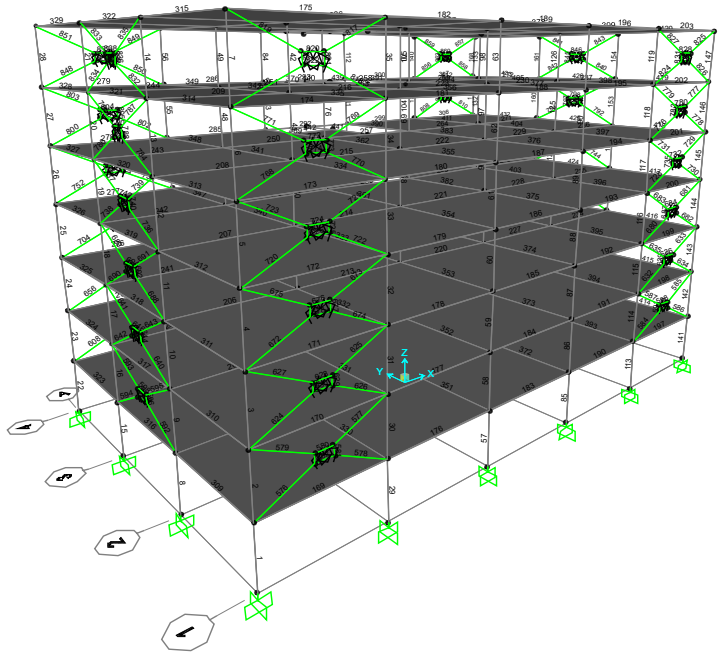


Figure 3.22. Three-Dimensional Model of the 7-Story Building without X Friction Bracing at the 1st Story

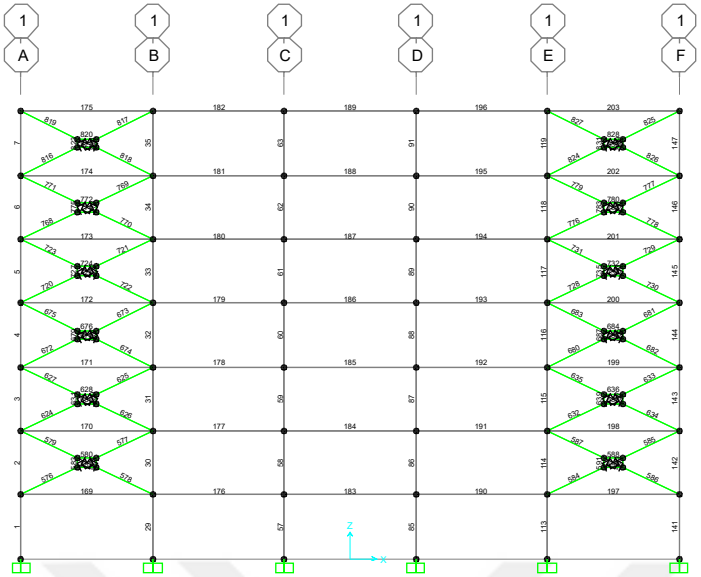


Figure 3.23. X-Direction Plan View of the 7-Story Building without X Friction Bracing at the 1st Story

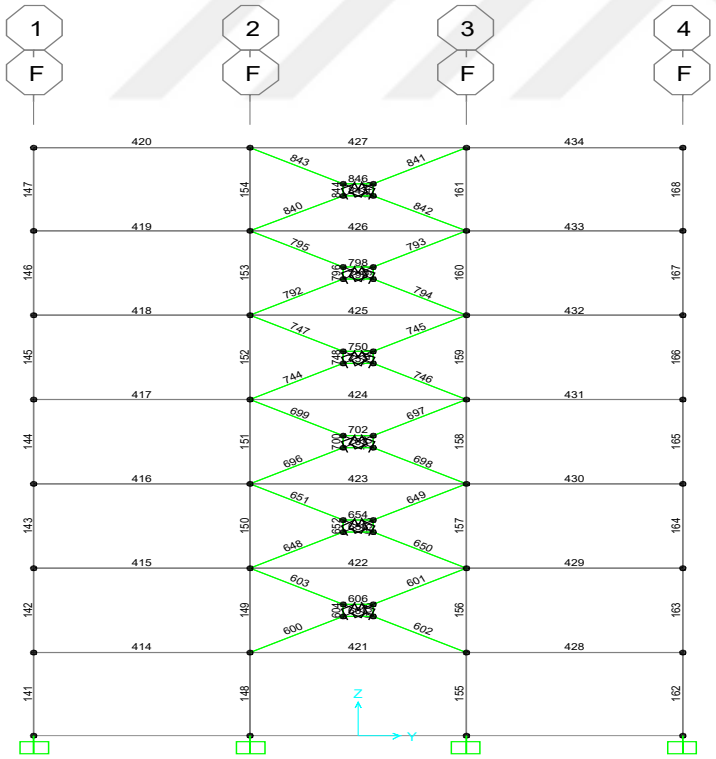


Figure 3.24. Y-Direction Plan View the 7-Story Building without X Friction Bracing at the 1st Story

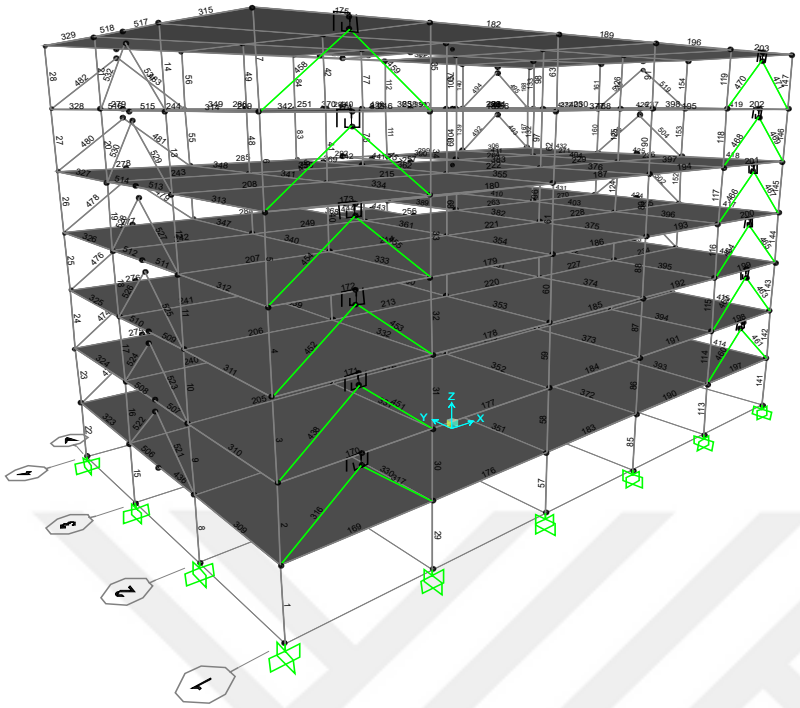


Figure 3.25. Three-Dimensional Model of the 7-Story Building without Inverted V Friction Bracing at the 1st Story

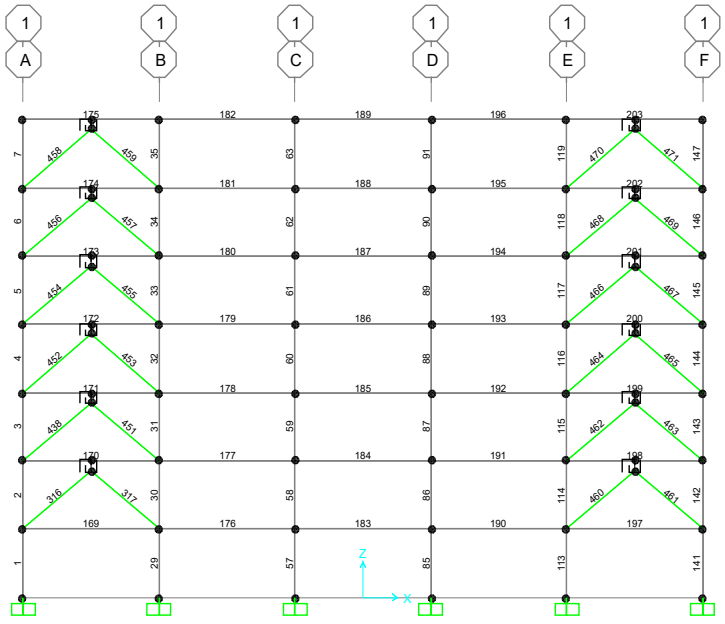


Figure 3.26. X-Direction Plan View of the 7-Story Building without Inverted V Friction Bracing at the 1st story

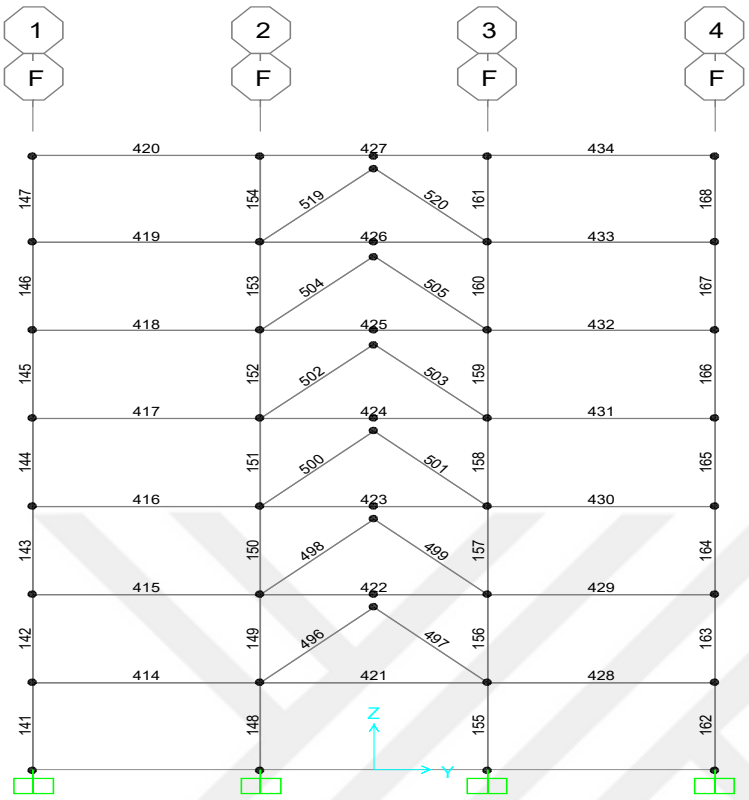


Figure 3.27. Y-Direction Plan View the 7-Story Building without Inverted V Friction Bracing at the 1st Story

3.6 Design Considerations

At this dissertation, the design procedure proposed by Filiatrault and Chery has been used to design the building with friction damper. The stages of the procedures are listed below:

Step 1:

In the case of a new structure, design the unbraced moment-resisting frame to carry safely the usual load combinations but without considering earthquake effects. In the situation of retrofit of an existing building, verify that the unbraced moment-resisting frame can carry safely the usual load combinations but without considering earthquake effects. It is assumed that the friction dampers will fully dissipate the seismic energy. The designer may choose to include earthquake loads in the load combination in order to fall back on

conventional ductility design as an added factor of safety in the event of a catastrophic earthquake.

Step 2:

Calculate the fundamental period of the unbraced structure, T_u. Choose sections for the diagonal cross braces such that $T_b/T_u < 0.40$, if economically possible. Estimate the peak ground acceleration a_g (according to the ground motion) and the predominant ground period T_g for the construction site I is recommended that T_g be approximated by the empirical formulas proposed by Vanmarcke and Lai (Equation 3.10 and Equation 3.11).

$$T_g = \frac{2\pi}{27 - 0.09R} \qquad 10km \leq R \leq 160km \qquad (3.10)$$

$$T_g = \frac{2\pi}{65 - 7.5M_L} \qquad 5 \leq M_L \leq 7 \qquad (3.11)$$

Where; T_g is predominant ground period, R is epicentral distance and M_L is local Richter magnitude.

Step 3:

Verify that the non-dimensional ratios fall within the following limits:

$$0.2 \leq \frac{T_b}{T_u} \leq 0.8 \quad , \quad 0.05 \leq \frac{T_g}{T_u} \leq 20 \quad , \quad 0.05 \leq \frac{a_g}{g} \leq 0.4$$

Where; T_b is natural period of braced structure, T_u is natural period of unbraced structure, a_g is peak ground acceleration and g shows the acceleration of the gravity.

Step 4:

An approximate design equation for the total optimum slip shear V_0 is proposed as below (Equation 3.12):

$$\frac{V_0}{ma_g} = \begin{cases} \left[\frac{[\frac{(-1.24NS-0.31)T_b}{T_u}+1.04NS+0.43]T_g]}{T_u}\right. & 0 \le \frac{T_g}{T_u} < 1 \\ \frac{[\frac{(0.01NS+0.02)T_g}{T_u}-1.25NS-0.32]T_b}{T_u} & \\ +\frac{(0.002-0.002NS)T_g}{T_u} + 1.04NS + 0.42 & \frac{T_g}{T_u} > 1 \end{cases} \quad (3.12)$$

Equation 3.9 can be used directly to estimate the total optimum slip shear V_0. However, a graphical representation of this equation in the form of a design slip-load spectrum provides a more convenient and simplified method for establishing V_0. If a plot of $\frac{V_0}{ma_g}$ versus $\frac{T_g}{T_u}$ is made for particular values of $\frac{T_b}{T_u}$ and NS, using equation 3.9, a bilinear curve will be obtained as shown in Fig 3.28. This curve represents a general design slip-load spectrum for multistory friction damped structures. This spectrum is completely described by specifying the ordinate α, representing the upper bound of the first branch of the bilinear curve and corresponding to $\frac{T_g}{T_u} = 1$ for all NS, and any other ordinate data β, compatible with the second linear branch and taken here as the ordinate values at $\frac{T_g}{T_u} = 15$

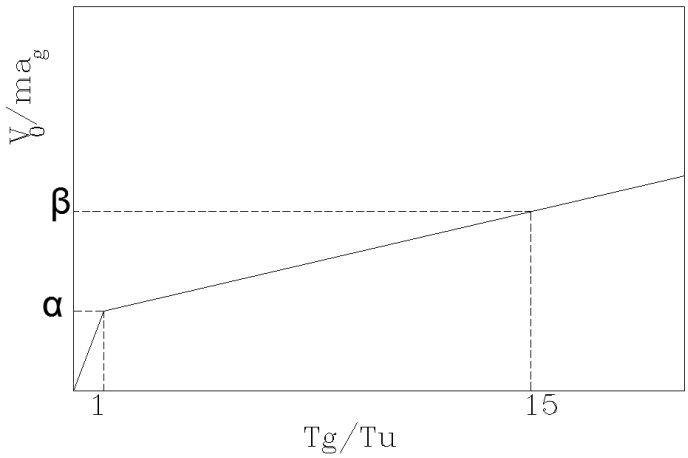


Figure 3.28 Construction of Design Slip-Load Spectrum

The ordinates of α and β of these points can be calculated from the below (Equation 3.13) and (Equation 3.14):

$$\alpha = \frac{(-1.24NS - 0.31)T_b}{T_u} + 1.04NS + 0.43 \qquad (3.13)$$

$$\beta = \frac{(-1.07NS - 0.1)T_b}{T_u} + 1.01NS + 0.45 \qquad (3.14)$$

Where; α and β are ordinates to construct design slip load spectrum, NS is the number of the stories, T_b is natural period of braced structure and T_u is natural period of unbraced structure.

Step 5:

Use the constructed design slip-load spectrum to estimate the total slip shear V_0. Distribute this total slip shear uniformly among the floors of the structure (Equation 3.15).

$$V_{s(i)} = \frac{V_0}{NS} \qquad (3.15)$$

Where;

$V_{s(i)}$ is slip shear in (i) story, V_0 is total optimum slip shear and NS is the number of the stories.

Step 6:

Distribute the slip shear of each floor $V_{s(i)}$ among the number of friction dampers inserted in each floor.

$$\sum_{j=1}^{N_{Di}} 2P_{0ij\ cos\alpha_{ij}} = V_{s(i)} \qquad (3.16)$$

Where, N_{Di} is the number of friction dampers inserted in the rth floor, P_0 is the optimum local slip load, cos α is angle of inclination of diagonal braces from horizontal, (i) the story number, (j) the number of braces, and $V_{s(i)}$ is slip shear in (i) story.

Step 7:

Estimate the tensile-yield load of the cross braces and verify that these cross braces do not yield before slipping occurs using the following expressions.
For slender braces which $P_{0ij} > P_{(cr)ij}$ (Equation 3.17):

$$P_{0ij} \leq \frac{A_{bij}\sigma_{yij} + P_{(cr)ij}}{2} \qquad (3.17)$$

Where;

A_{bij} is cross sectional area for the (j)th tensile brace in the (i)th floor
σ_{yij} is the tensile yield stress for the (j)th tensile brace in the (i)th floor
P_0 is the optimum local slip load
$P_{(cr)}$ is critical Euler buckling load

For stubby braces which $P_{0ij} \leq P_{(cr)ij}$:

$$P_{0ij} \leq A_{bij}\sigma_{yij}$$

If Equation (3.17) is not verified, one of the following alternatives should be chosen (Equation 3.18):

$$P_{cr} = \frac{\pi^2 EI}{L^2} \qquad (3.18)$$

1. Use a value of the slip load satisfying the equality in Equation 3.17 and perform dynamic analyses to examine the response of the structure;
2. Increase the size of the diagonal cross braces and return to Step 3.

3.6.1 Design of Friction Damper

As mentioned in part 3.3.3 the design procedure is clarified in different steps. At this part the design procedure for a friction damper under Northridge earthquake with the maximum PGA of 0.101g, the epicentral distance (R) of 40.768 km and the magnitude of 7.1 is presented with inverted V bracing.

Step 1:

All the members carry safely the usual load combinations but without considering earthquake effects.

Step 2:

The fundamental period of the unbraced structure in Y (Mode 1) and X (Mode 2) direction is, T_{uy} = 1.2304 and T_{ux} = 1.212.

Choosing the section of the diagonal braces such that $T_b/T_u < 0.40$ is not economically. So, the value of T_b with the first assumption of 2UNP80 in SAP2000 for the braces in Y and X directions are 0.9378 and 0.7883 respectively.

$$T_g = \frac{2\pi}{27 - 0.09R} = \frac{2\pi}{27 - 0.09 * 40.768} = 0.269$$

$$T_g = \frac{2\pi}{65 - 7.5M_L} = \frac{2\pi}{65 - 7.5 \times 7.1} = 0.534$$

The equation based on M_L is used for T_g definition as the value is greater than the equation based on R.

Step 3:

Verify that the non-dimensional ratios fall within the following limits:

For the Y Direction:

$$0.2 \leq \left(\frac{T_b}{T_u}\right)_y = \frac{0.9378}{1.2304} = 0.762 \leq 0.8 \qquad OK.$$

$$0.05 \leq \left(\frac{T_g}{T_u}\right)_y = \frac{0.534}{1.2304} = 0.434 \leq 20 \qquad OK.$$

$$0.05 \leq \left(\frac{a_g}{g}\right) = 0.101 \leq 0.4 \qquad OK.$$

For the X Direction:

$$0.2 \leq \left(\frac{T_b}{T_u}\right)_x = \frac{0.7883}{1.212} = 0.651 \leq 0.8 \qquad OK.$$

$$0.05 \leq \left(\frac{T_g}{T_u}\right)_x = \frac{0.534}{1.212} = 0.440 \leq 20 \qquad OK.$$

$$0.05 \leq \left(\frac{a_g}{g}\right) = 0.101 \leq 0.4 \qquad OK.$$

Step 4:

Determine the coefficients α (Equation 3.13) and β (Equation 3.14) and construct the appropriate design slip-load spectrum in Figure 3.29 and Figure 3.30 for Y and X direction respectively.

$$\alpha = (-1.24NS - 0.31)\left(\frac{T_b}{T_u}\right)_y + 1.04NS + 0.43$$

$$\alpha = (-1.24 * 7 - 0.31) * \frac{0.9378}{1.2304} + 1.04 * 7 + 0.43$$

$$\alpha = 0.86$$

$$\beta = (-1.07NS - 0.1)\left(\frac{T_b}{T_u}\right)_y + 1.01NS + 0.45$$

$$\beta = (-1.07 * 7 - 0.1) * \frac{0.9378}{1.2304} + 1.01 * 7 + 0.45$$

$$\beta = 1.73$$

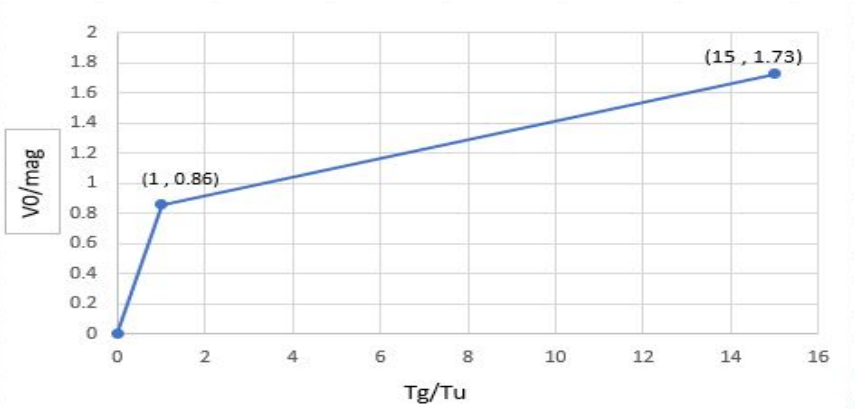


Figure 3.29 Design Slip-Load Spectrum for Y-Direction

$$\alpha = (-1.24NS - 0.31)\left(\frac{T_b}{T_u}\right)_x + 1.04NS + 0.43$$

$$\alpha = (-1.24 * 7 - 0.31) * \frac{0.7883}{1.212} + 1.04 * 7 + 0.43$$

$$\alpha = 1.86$$

$$\beta = (-1.07NS - 0.1)\left(\frac{T_b}{T_u}\right)_x + 1.01NS + 0.45$$

$$\beta = (-1.07 * 7 - 0.1) * \frac{0.7883}{1.212} + 1.01 * 7 + 0.45$$

$$\beta = 2.58$$

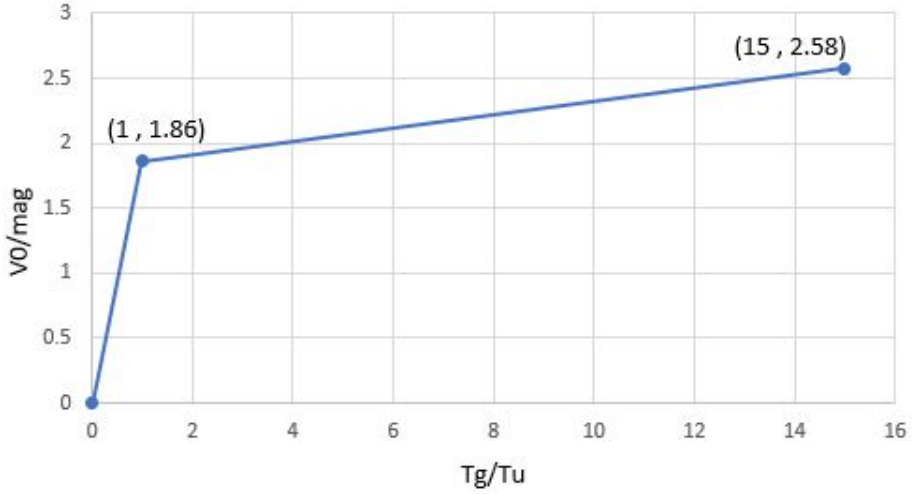


Figure 3.30 Design Slip-Load Spectrum for X-Direction

Step 5:

Use the constructed design slip-load spectrum to estimate the total slip shear V_0. Distribute this total slip shear uniformly among the floors of the structure (Equation 3.15).

For Y direction:

$$\left(\frac{V_0}{m * a_g}\right)_y = 0.86 * \left(\frac{T_g}{T_u}\right)_y$$

$$(V_0)_y = 0.86 * \left(m * a_g\right)_y * \left(\frac{T_g}{T_u}\right)_y \qquad where;\ a_g = 0.101g$$

$$(V_0)_y = 0.86 * 3051\ kN * 0.101 * 9.81 * 0.434$$

$$(V_0)_y = 1128\ kN$$

$$(V_s)_{i,y} = \frac{(V_0)_y}{NS} = \frac{1128\ kN}{7} = 161\ kN$$

For X direction:

$$\left(\frac{V_0}{m * a_g}\right)_x = 1.86 * \left(\frac{T_g}{T_u}\right)_x$$

$$(V_0)_x = 1.86 * \left(m * a_g\right)_x * \left(\frac{T_g}{T_u}\right)_x \qquad where, a_g = 0.101g$$

$$(V_0)_x = 1.86 * 3051\ kN * 0.101 * 9.81 * 0.440$$

$$(V_0)_x = 2474\ kN$$

$$(V_s)_{i,x} = \frac{(V_0)_x}{NS} = \frac{2474\ kN}{7} = 353\ kN$$

Step 6:

Distribute the slip shear of each floor $V_{s(i)}$ among the number of friction dampers inserted in each floor. According to the presence of 4 damper in each direction we have:

For Y direction:

$$\sum_{j=1}^{N_{Di}} 2P_{0ij\ cos\alpha_{ij}} = V_{s(i)}$$

$$\sum_{j=1}^{4} 2P_{0ij} * cos\,\alpha_{ij} = (V_s)_{i,y}$$

$$\text{Cos } \alpha = \frac{length\ of\ braced\ \text{frame}}{\text{length of the opening}} = \frac{629.3\text{cm}}{700\text{cm}} = 0.899$$

$$P_{0,y} = \frac{(V_s)_{i,y}}{4 * 2 * \text{Cos } \alpha}$$

$$P_{0,y} = \frac{161}{8 * 0.899} = 22.40 \text{ kN}$$

For X direction:

$$P_{0,x} = \frac{(V_s)_{i,x}}{4 * 2 * \text{Cos } \alpha}$$

$$P_{0,x} = \frac{353}{4 * 2 * 0.899} = 49 \text{ kN}$$

Step 7:

Estimate the tensile-yield load of the cross braces and verify that these cross braces do not yield before slipping occurs using the following expressions.

$$P_{cr} = \frac{\pi^2 EI}{L^2} = \frac{\pi^2 * 2141404 * 213.6}{(778)^2} = 73.14 \text{ kN}$$

$P_{0,y}$ and $P_{0,x} \leq P_{cr}$

Therefore, for stubby braces $P_{0,ij} \leq A_{b,ij} * \sigma_{y,ij}$ where $A_{b,ij}$ and $\sigma_{y,ij}$ are cross sectional area and tensile-yeild stress fro the j'th tensile brace and ith floor.

$A_{b,ij} * \sigma_{y,ij} = 22 * 27939.10\text{kN} = 620\text{kN}$ Ok.

So, the braces do not yield before the slip load of the friction damper. The properties of the damper for the Y and X direction have been applied in the software (SAP2000), shown in the section 3.7 modelling of friction dampers in software.

3.7 Modelling of Pall Friction Dampers:

Since the hysteretic loop of the friction dampers which is perfectly rectangular, similar to perfectly elasto-plastic material, makes the modelling of the pall friction damper's simpler. These dampers can be modeled as fictional plasticity element having yield force equal to slip load.

3.7.1 Inverted V (Chevron) Pall Friction Damper Modelling:

The data for the modelling of these dampers are as below:
Type: Plastic (wen)
Mass of Damper = 0.225 kN-m
Weight of Damper = 2.22 kN-m
Rotational inertia 1 = Rotational inertia 2 = Rotational inertia 3 = 0
Direction = U1 (Nonlinear – Put check mark in nonlinear box next to U1)
Ke = Effective Stiffness = 1000 * Damper slip load (P0)
Ce = Effective Damping = 0
K = Stiffness = Ke
Yield Strength = Slip load of friction damper (P0)
Post Yield Stiffness Ratio = 0.0001
Yield Exponent = 10

The brace is modeled as frame element shown in Figure 3.31. The beams at the top are from joints C and D and joints D and F, and the braces are from joints A and E and joints B and E. the friction damper is modeled as a nonlinear axial link element between joints D and E. Make sure that the joint E is 6cm away from joint D and disconnected from the diaphragm.

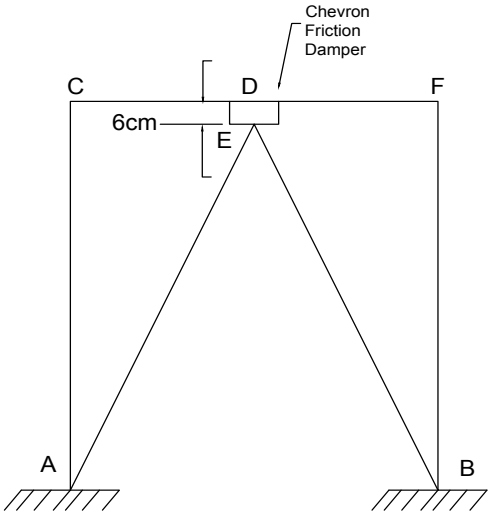


Figure 3.31 Friction Damped Inverted V Brace Frame

3.7.2 Tension Only Cross Brace with Pall Friction Damper (Figure C)

This type of pall friction damper shown in Figure 3.32 is suitable for long tension-only cross bracing, as the SAP2000 have only one value for yielding in tension and compression and the hysteretic loop of each tension brace is equal to hysteretic loop of one single diagonal tension compression brace Shown in Figure 3.33, therefore the model of these dampers is the same as single diagonal dampers explained below:

Type: Plastic (wen)
Mass = Mass of damped brace
Weight = Weight of damped brace
Rotational Inertia 1 = Rotational Inertia 2 = Rotational Inertia 3 = 0
Direction = U1 (Nonlinear – Put check mark in nonlinear box next to U1)
Ke = Effective Stiffness = AE/L (Where A is the area of the brace and L is the length of damper + length of brace)
Ce = Stiffness = Ke
Yield Strength = Slip load of friction damper
Post Yield Stiffness Ratio = 0.0001
Yield Exponent = 10

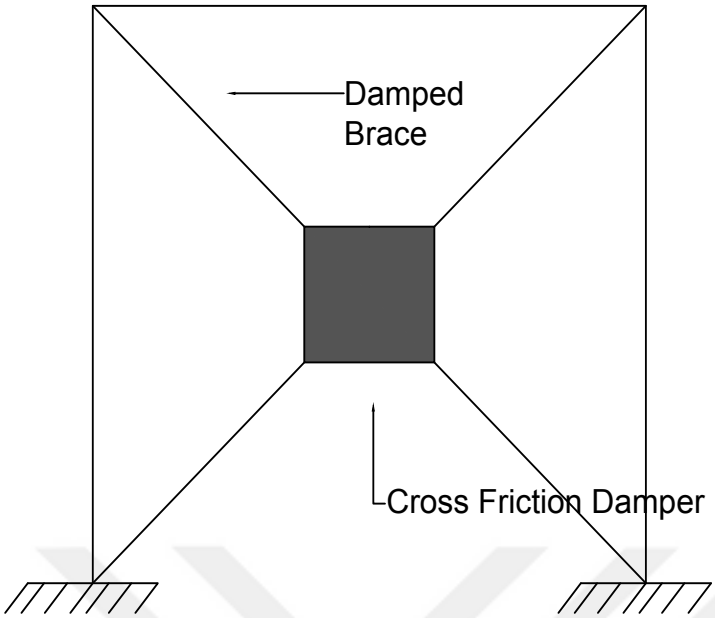


Figure 3.32 Friction Damped X Brace Frame

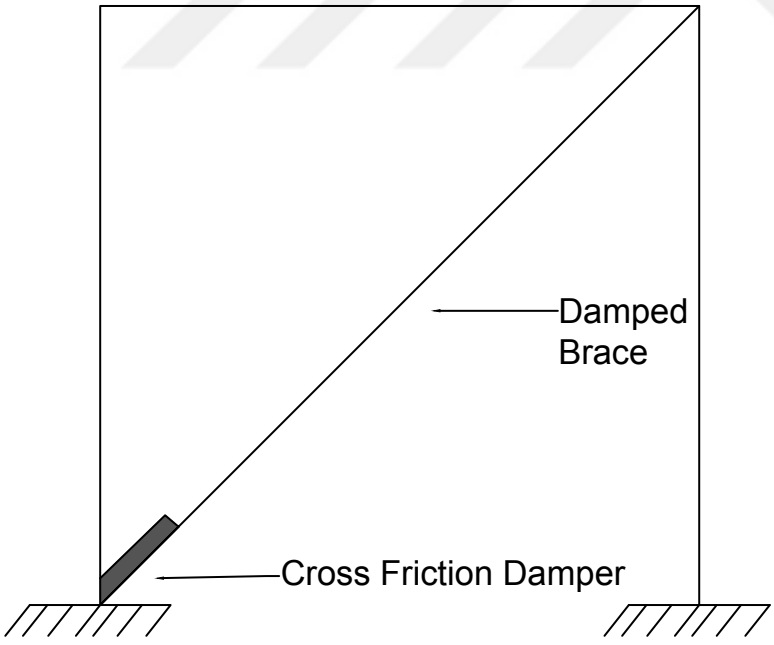


Figure 3.33 Friction Damped Single Diagonal Brace Frame

The calculated data from the section 3.6.1 is used for the below example of adding friction damper characteristics in SAP2000.

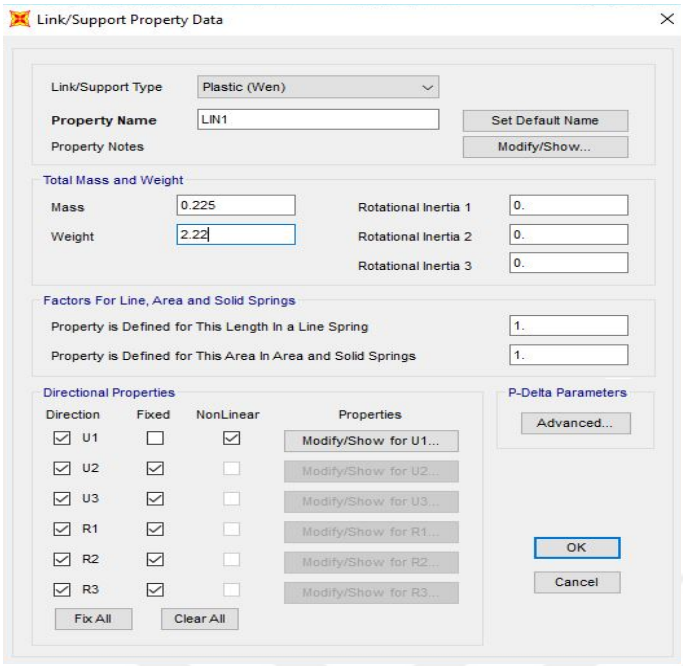


Figure 3.34 Definition of Friction Damper in SAP2000

After entering the above data, click on Modify/show from U1, and the below window appears:

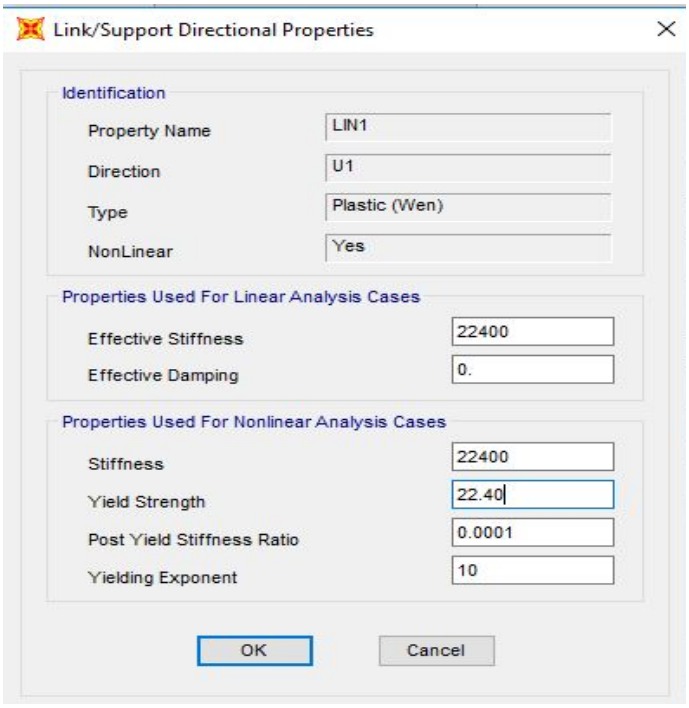


Figure 3.35 Definition of Friction Damper in SAP2000

3.8 Verification Modeling and Design Method

To validating the modeling techniques in SAP2000 and verifying the proposed seismic design procedure proposed by Filiatrault et al, a representative regular low-rise steel industrial building has been utilized from the mentioned study. The structural layout is shown in Fig. 3.36.

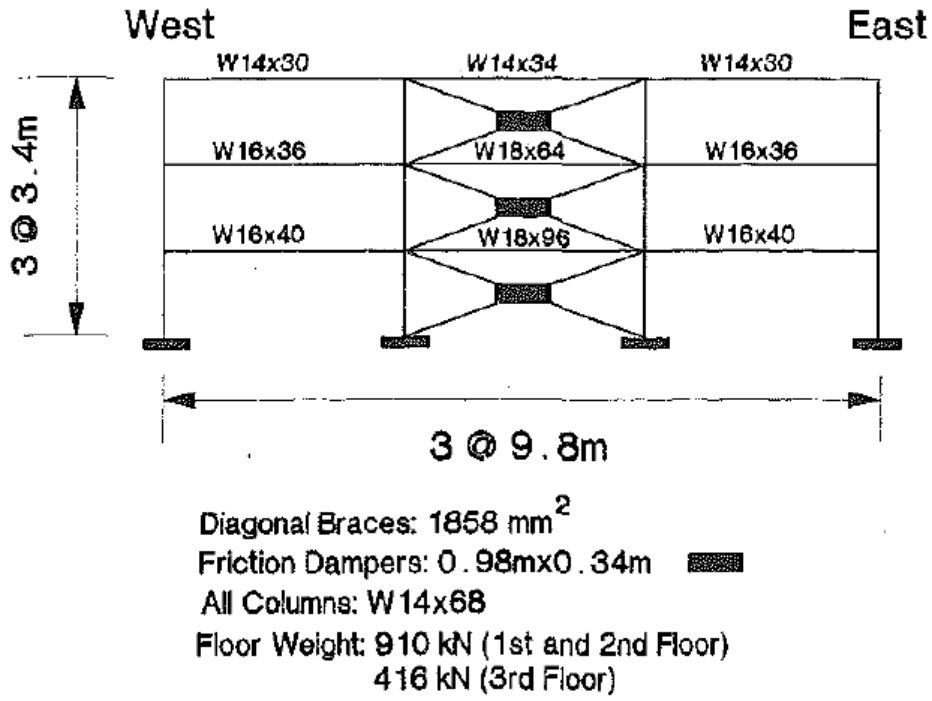


Figure 3.36. Low-Rise Steel Industrial Building

The Newmark-Blume-Kapur artificial earthquake (Newmark et al. 1973) scaled to a peak acceleration of 0.5 g was used in the analyses. This record has duration of 15 sec and is an average of many typical earthquakes. Viscous damping is introduced by specifying 2% critical damping in the first mode of vibration of the unbraced structure. According to the paper, the optimum loading slip has been considered for the damper and the result of top floor displacement has been shown in Figure 3.37.

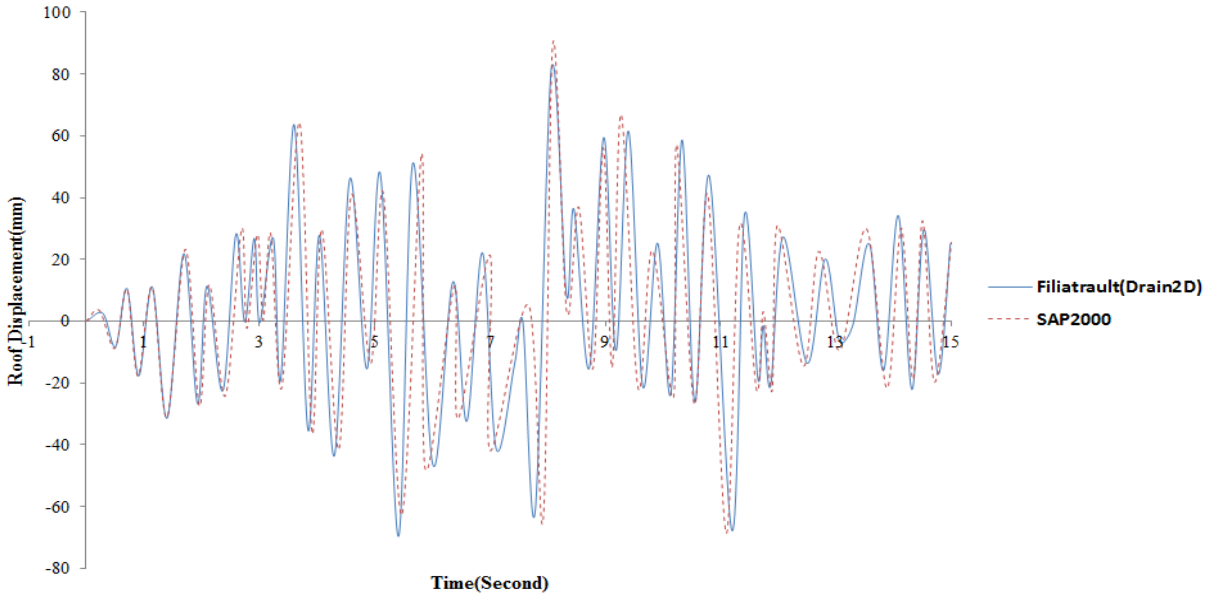


Fig 3.37. The Result of Verification by SAP2000

Fig 3.37. illustrates that the result of SAP2000 for friction damper modeling with wen link element could be trustable.

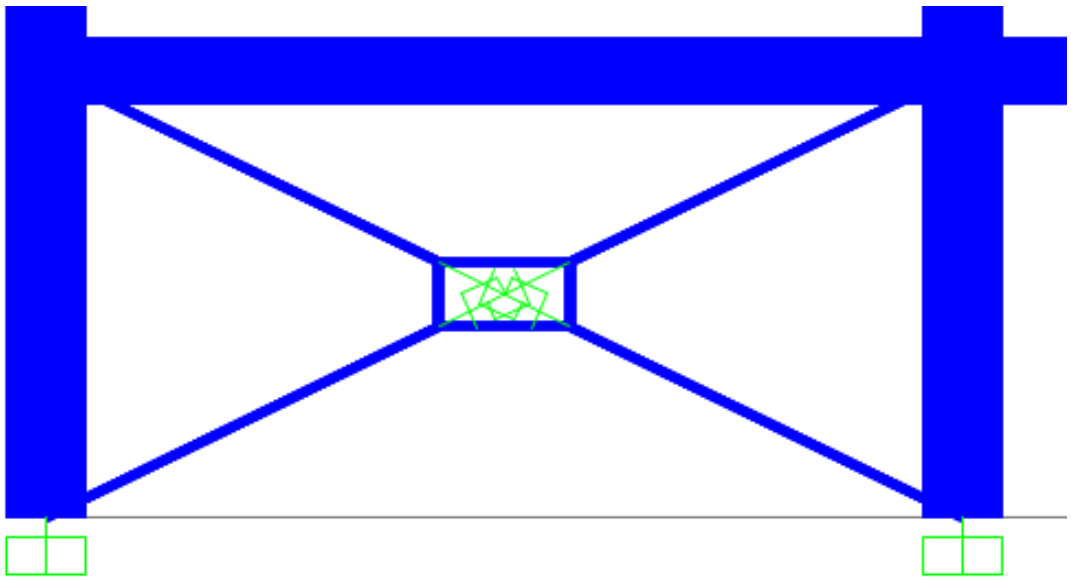


Figure 3.38 Damper Configuration in SAP2000 (X Bracing)

The results of dampers characteristics for each direction have been summarized in Table 3.3 through Table 3.6 for X and inverted V configurations respectively based on the method presented above.

Table 3.3. The Characteristics of Damper with X Configuration for Arrangement (1)

Y-Direction		**X-Direction**	
Earthquake	**Slip Load(kN)**	**Earthquake**	**Slip Load(kN)**
Northridge	2.02	Northridge	4.46
Kobe	1.58	Kobe	3.48
Imperial Valley-06	2.8	Imperial Valley-06	6.13
Bam	2.11	Bam	4.64
Southern Calif	0.7	Southern Calif	1.46
Parkfield	0.72	Parkfield	1.6
Düzce Turkey	0.72	Düzce Turkey	6.7

Table 3.4. The Characteristics of Damper with Inverted V Configuration Arrangement (1)

Y-Direction		**X-Direction**	
Earthquake	**Slip Load(kN)**	**Earthquake**	**Slip Load(kN)**
Northridge	25.7	Northridge	56.4
Kobe	20.2	Kobe	44.1
Imperial Valley-06	35.3	Imperial Valley-06	77.5
Bam	26.8	Bam	58.7
Southern Calif	8.5	Southern Calif	18.5
Parkfield	10	Parkfield	20
Düzce Turkey	38.6	Düzce Turkey	84.6

Table 3.5. The Characteristics of Damper with X Configuration for Arrangement (2)

Y-Direction		X-Direction	
Earthquake	**Slip Load(kN)**	**Earthquake**	**Slip Load(kN)**
Northridge	20.2	Northridge	44.6
Kobe	15.8	Kobe	34.8
Imperial Valley-06	28	Imperial Valley-06	61.3
Bam	21.1	Bam	46.4
Southern Calif	7	Southern Calif	14.6
Parkfield	7.2	Parkfield	16
Düzce Turkey	7.2	Düzce Turkey	67

Table 3.6. The Characteristics of Damper with Inverted V Configuration Arrangement (2)

Y-Direction		X-Direction	
Earthquake	**Slip Load(kN)**	**Earthquake**	**Slip Load(kN)**
Northridge	25.7	Northridge	56.4
Kobe	20.2	Kobe	44.1
Imperial Valley-06	35.3	Imperial Valley-06	77.5
Bam	26.8	Bam	58.7
Southern Calif	8.5	Southern Calif	18.5
Parkfield	10	Parkfield	20
Düzce Turkey	38.6	Düzce Turkey	84.6

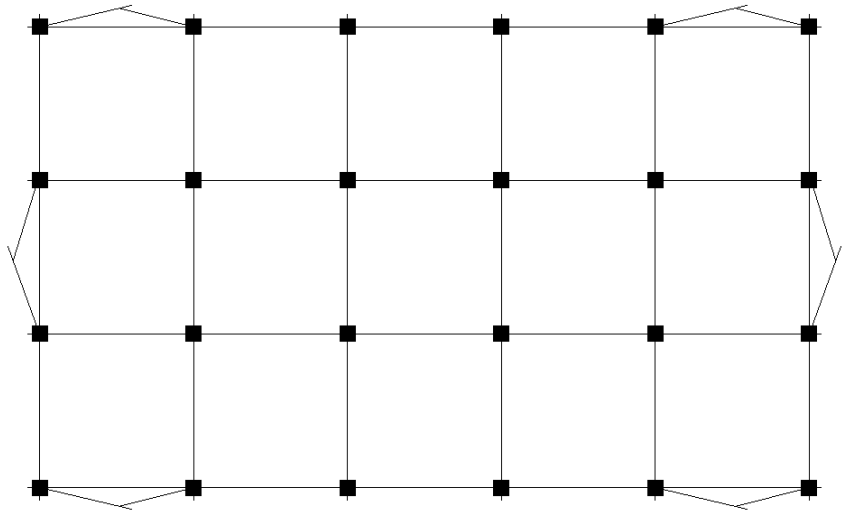


Figure 3.39. The Arrangement (1) for Dampers

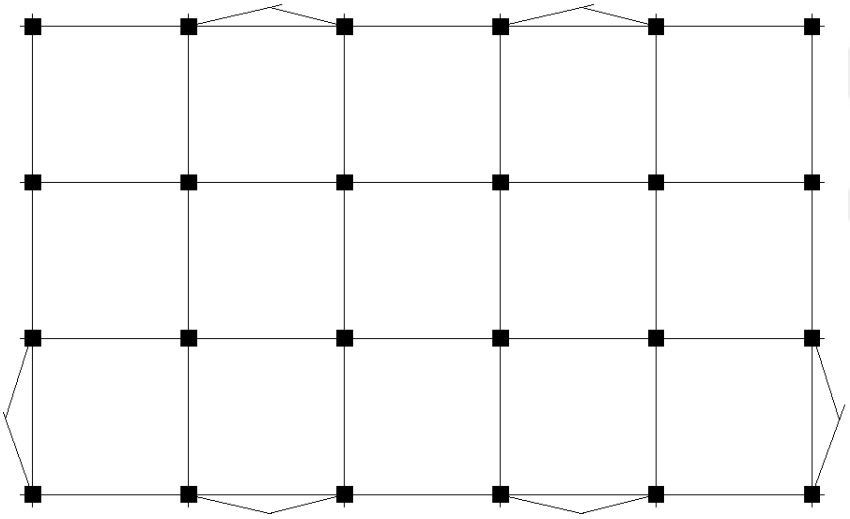


Figure 3.40. The Arrangement (2) for Dampers

According to the range of slip load, a value of 68kN and 85 kN is selected for the design of proposed building at each direction for X and inverted bracing respectively for both of the arrangements.

4. FINDING AND DISCUSSIONS

4.1 Introduction

Nonlinear time history analysis has been done based on the selected ground motion listed in Table 4.1 with their characteristic. All the earthquakes satisfy the site class C (V_s = 1200 to 2500 ft/s), according to the ASCE7-16. Figure 4.1 to 4.7 display the unscaled horizontal acceleration time histories for two components H1 and H2. H1 represents the horizontal ground motion with higher peak ground acceleration (PGA).

Ground motion records scaled to represent a specific intensity. Record scaling involves two steps. First, individual records in each set are "normalized" by their respective peak ground velocities, as described in section 4.1.1. This step is intended to remove unwarranted variability between records due to inherent differences in event magnitude, distance to source, source type and site conditions, without eliminating overall record-to-record variability. The data for the time history analysis is taken from the (peer.berkeley.edu/nga) website and analyzed in SAP2000.

Table 4.1 Ground Motions Properties

No	Name	Station	Vs (m/s)	R (Km)	M_L	PGA (H1)	PGA (H2)	dt
1	Northridge	Alhambra- Fremont School	549.75	35.66	6.7	0.101	0.08	0.02
2	Kobe	OKA	609	86.93	7.3	0.079	0.06	0.02
3	Imperial Valley-06	Cerro Prieto	471.53	15.19	6.53	0.168	0.157	0.01
4	Bam	Mohammad Abade-Madkoon	574.88	46.2	6.6	0.123	0.0702	0.005
5	Southern Calif	San Luis Obispo	493.5	73.35	6	0.05	0.036	0.005
6	Parkfield	Cholame- Shandon Array #12	408.93	17.64	6.19	0.06	0.054	0.01
7	Düzce Turkey	Barcis	481	11.46	7.14	0.131	0.101	0.01

Where;

V_s = Average Shear Wave Velocity

R = epicentral distance

M_L = local Richter magnitude

Second, normalized ground motions are collectively scaled to a specific ground motion intensity such that the median spectral acceleration of the record set matches the spectral acceleration at the fundamental period, T, of the index archetype that is being analyzed.

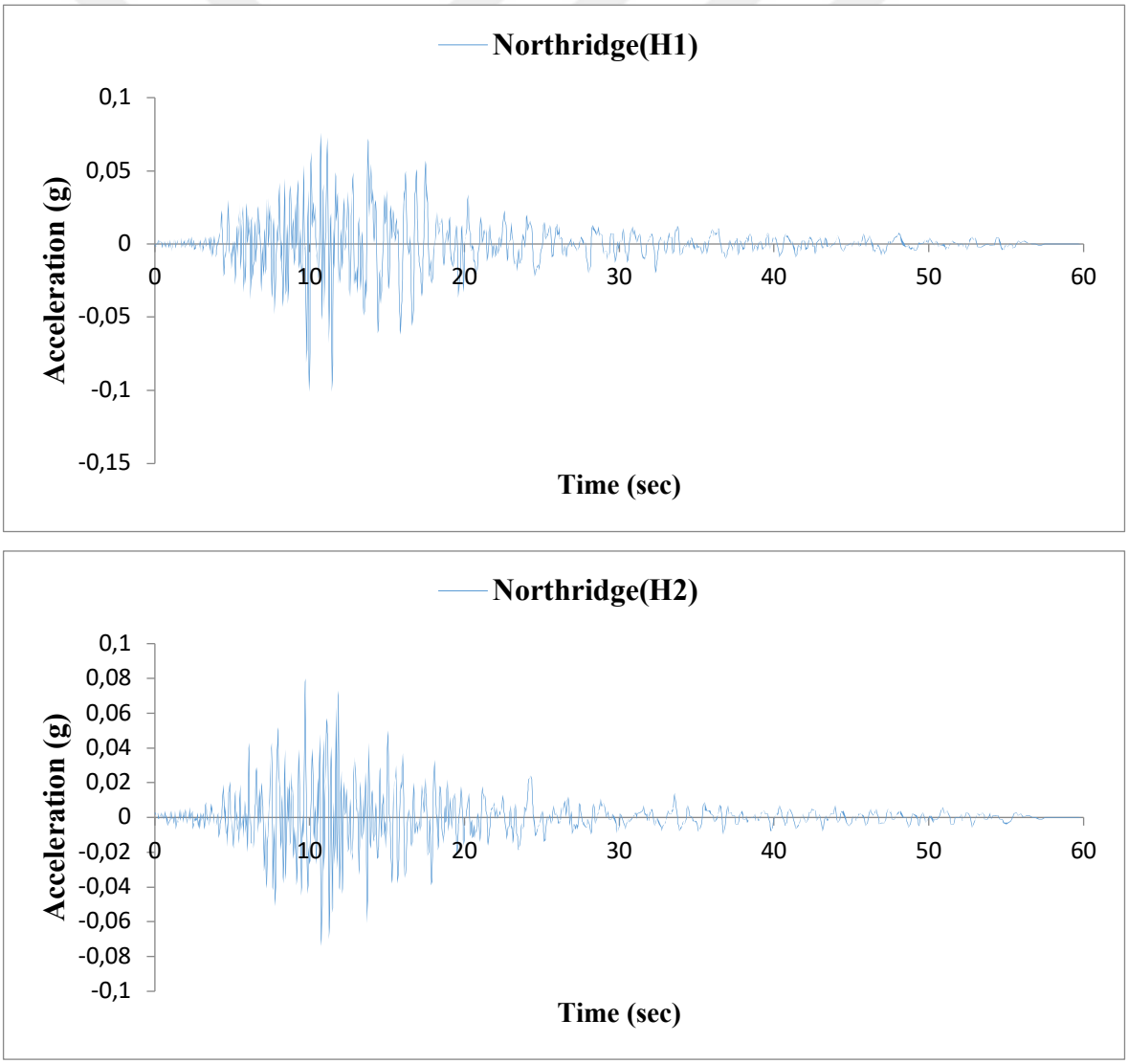


Figure 4.1 Northridge Horizontal Acceleration Time Histories

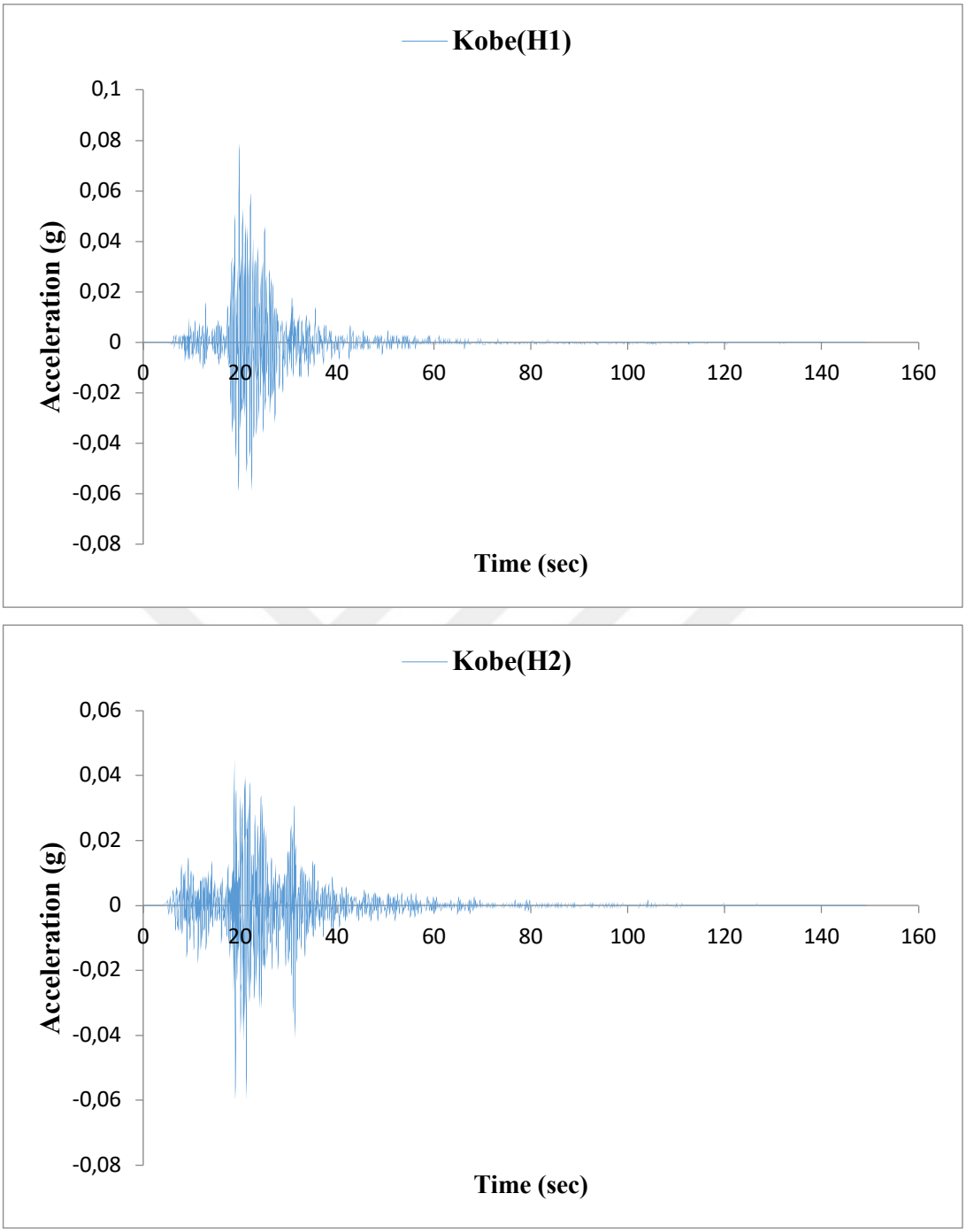


Figure 4.2 Kobe Horizontal Acceleration Time Histories

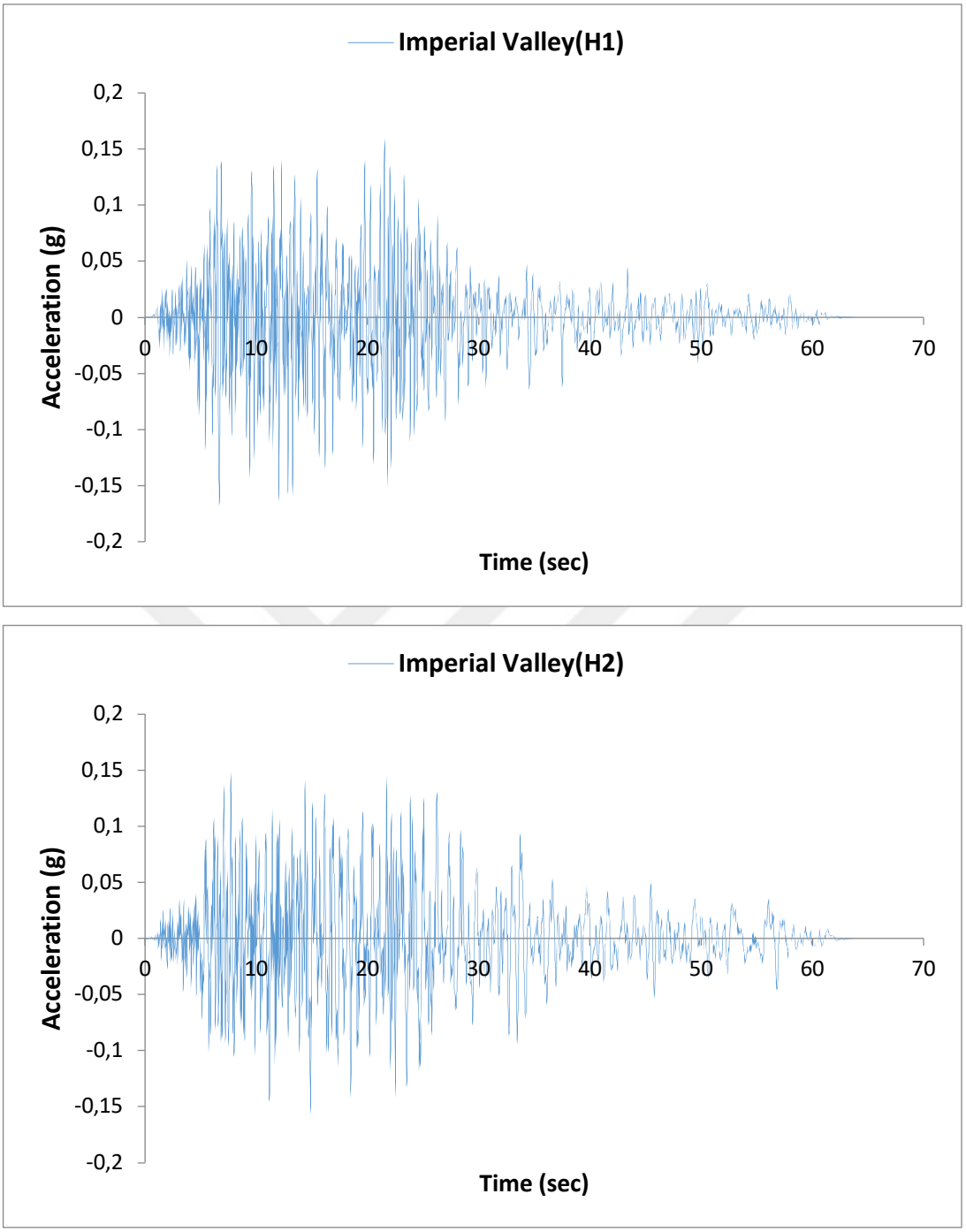


Figure 4.3 Imperial Valley Horizontal Acceleration Time Histories

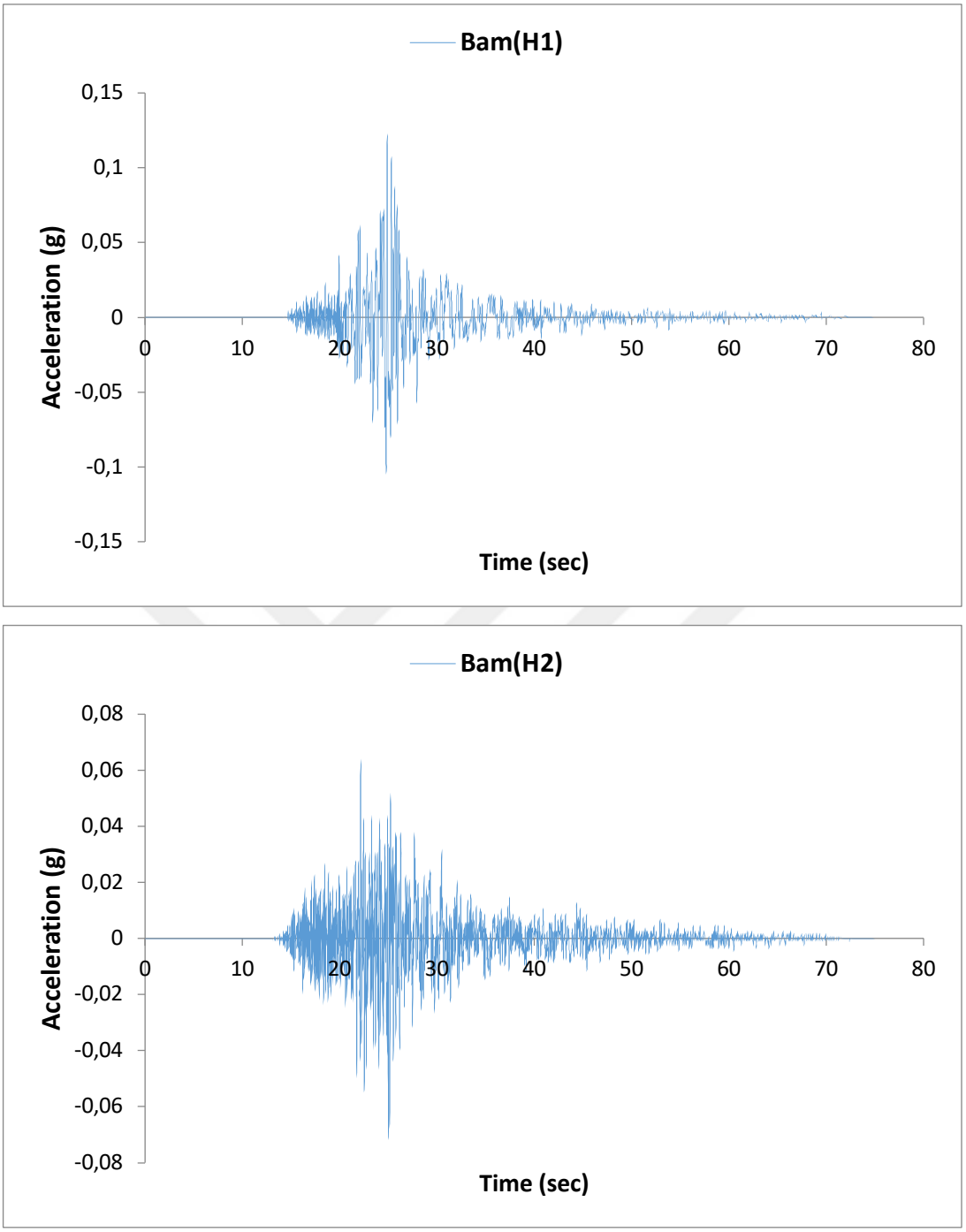


Figure 4.4 Bam Horizontal Acceleration Time Histories

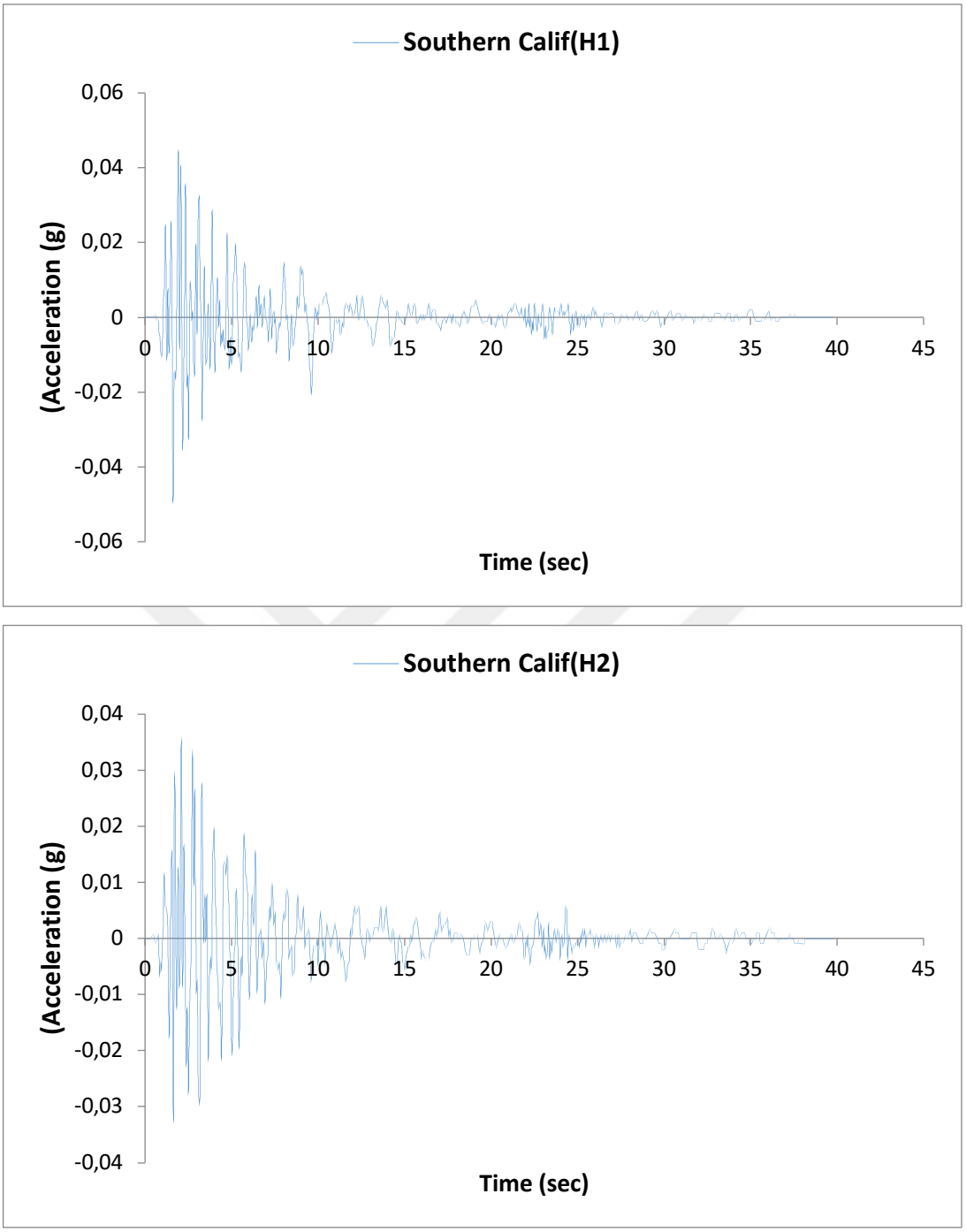


Figure 4.5 Southern Calif Horizontal Acceleration Time Histories

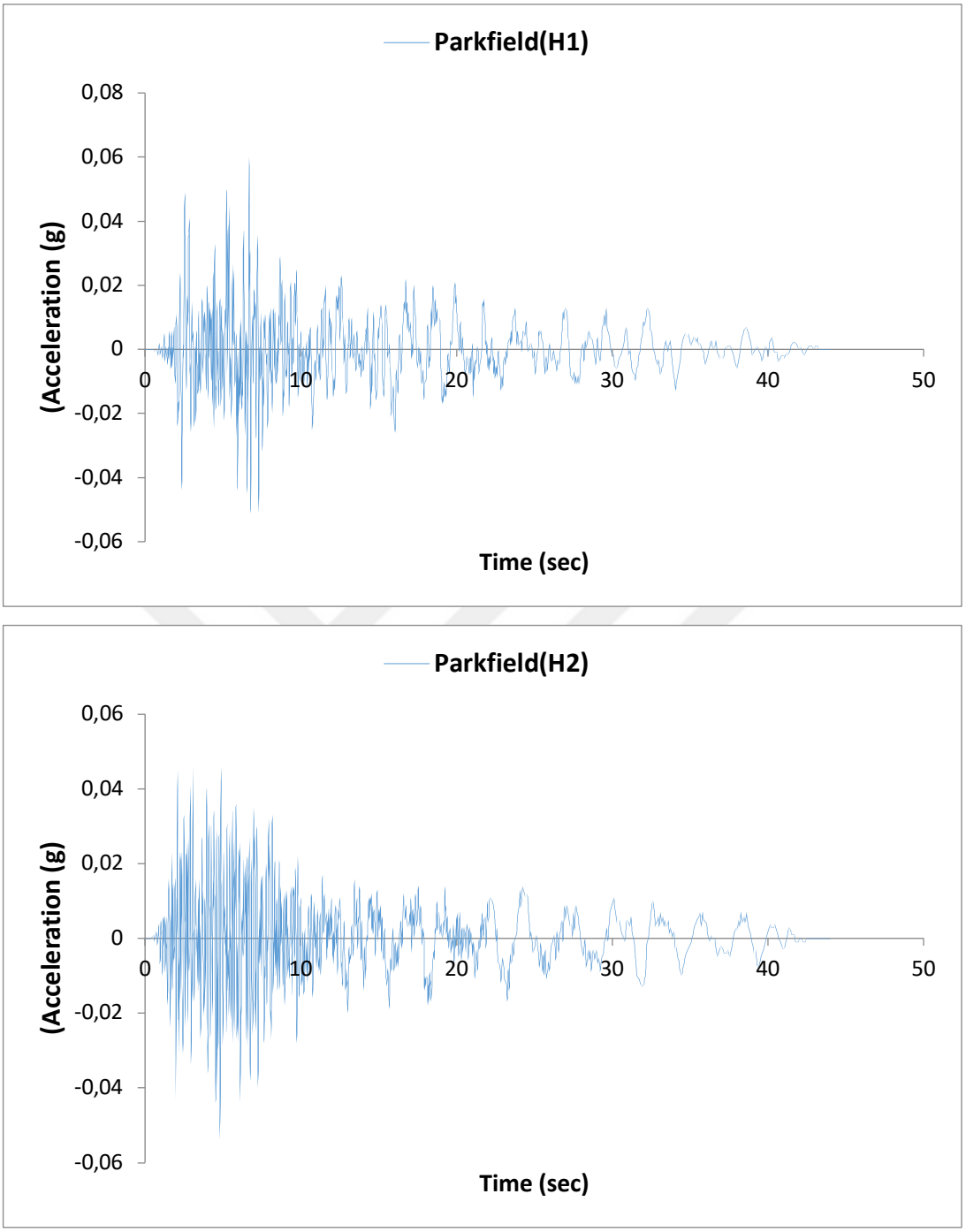


Figure 4.6 Parkfield Horizontal Acceleration Time Histories

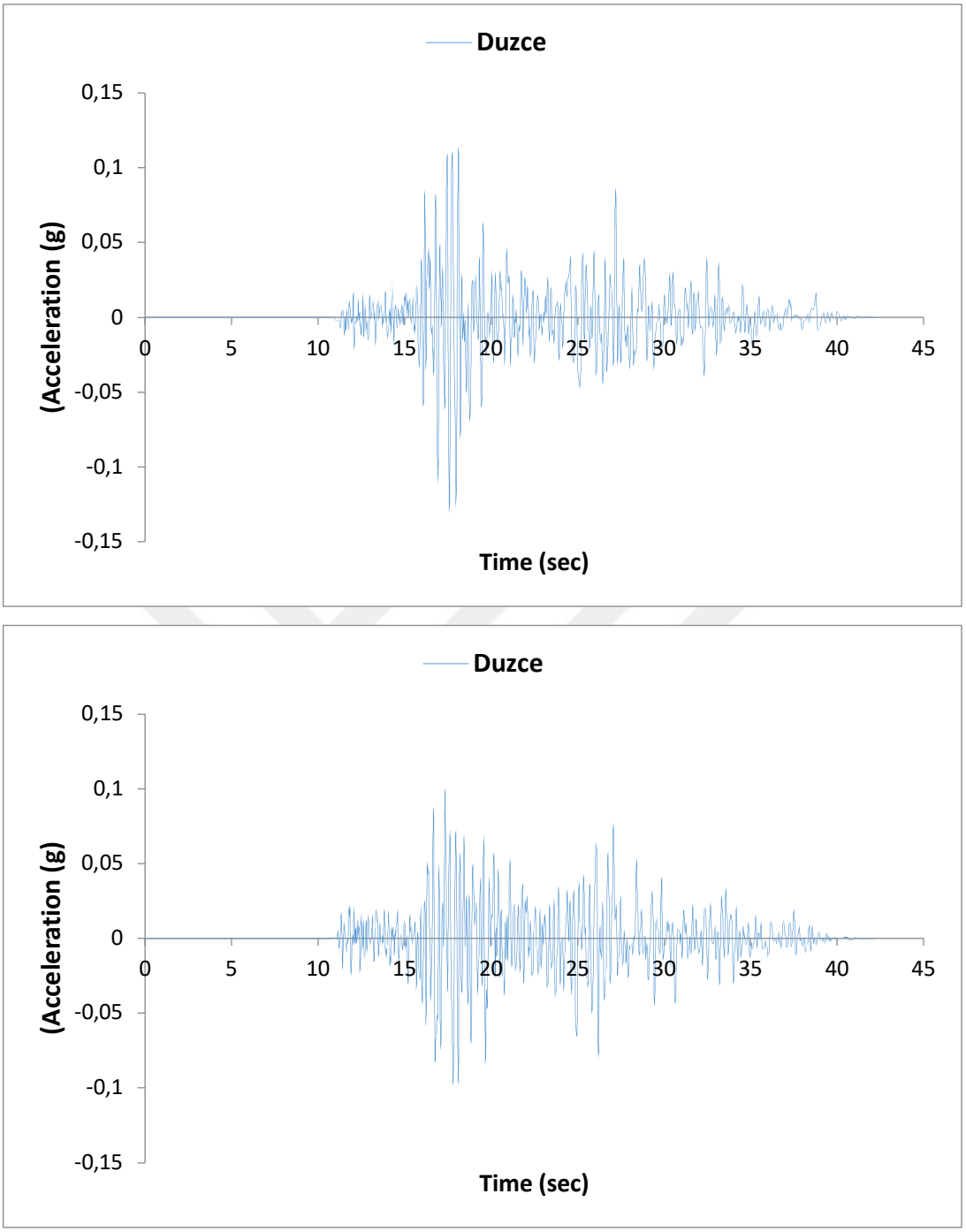


Figure 4.7 Düzce Horizontal Acceleration Time Histories

4.1.1 Scaling Procedure

According to the FEMA P695 [31] the steps are summarized as below:

- Step 1: Normalize the two-horizontal component to the maximum of PGA;
- Step 2: Plot the spectrum of the normalized records at Step 1;
- Step 3: Calculate the Square-Root-of-Sum-of-Squares (SRSS) of Spectrum values at each period;
- Step 4: Calculate the mean of SRSS values for all the records at each time periods.
- Step 5: The scale facture value is calculated in a way that the mean value at the fundamental period of the structure should not be less than design spectrum.

As mentioned before, according to step 1 and step 2, the spectrums of the normalized records are required. These graphs have been illustrated in Figures 4.8 to 4.14 for all the ground motions for 0.05 damping.

For completing the step 5 and extracting the scale factor value, the mean values diagram is compared with the ASE7-16 spectrum (Figure 4.15). As its obvious the mean value is higher than the design spectrum, but for economic design the mean value at T_1 period is taken equal to the design spectrum. So, the scale factor is: $\mathrm{S.F} = 2.51$

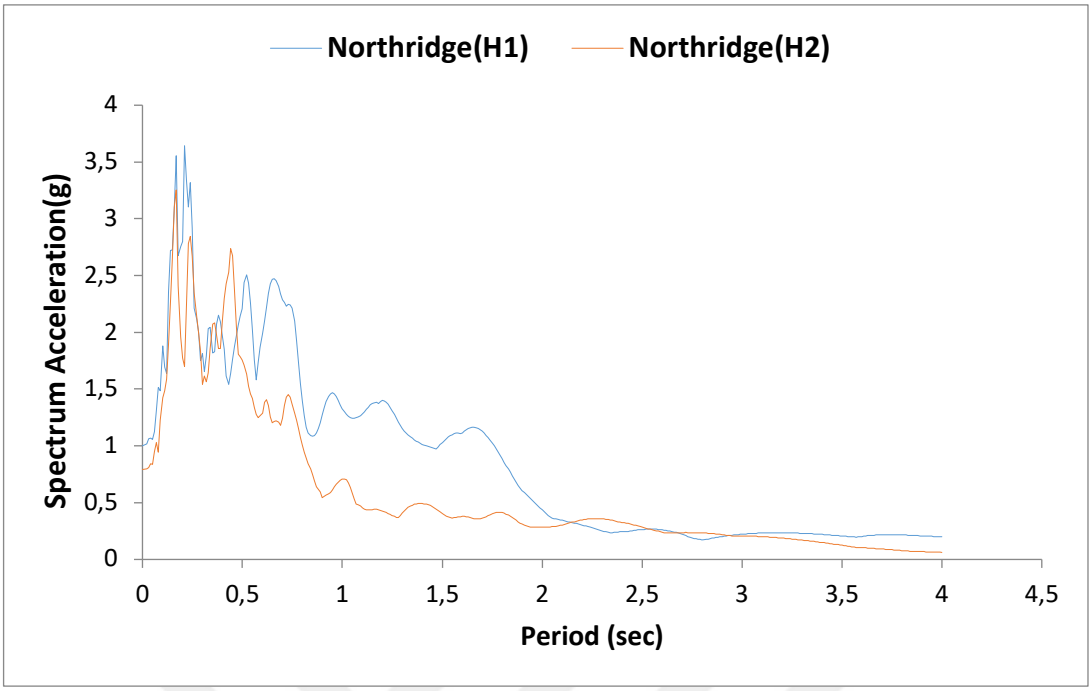


Figure 4.8 Spectrum Accelerations of Northridge Ground Motions for Normalized Records

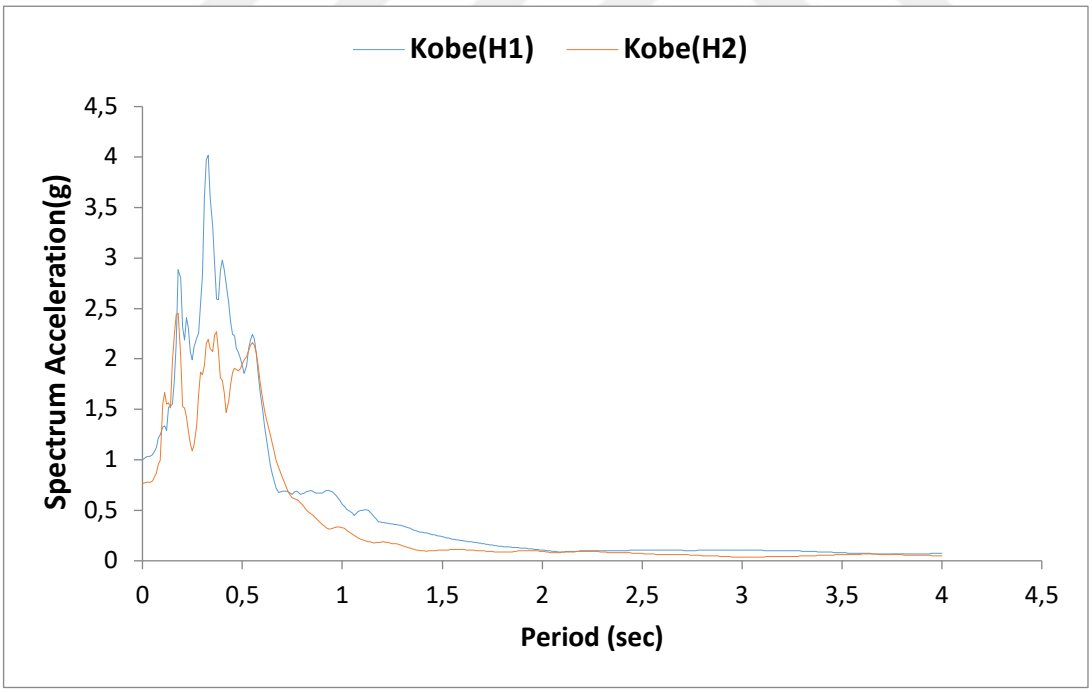


Figure 4.9 Spectrum Accelerations of Kobe Ground Motions for Normalized Records

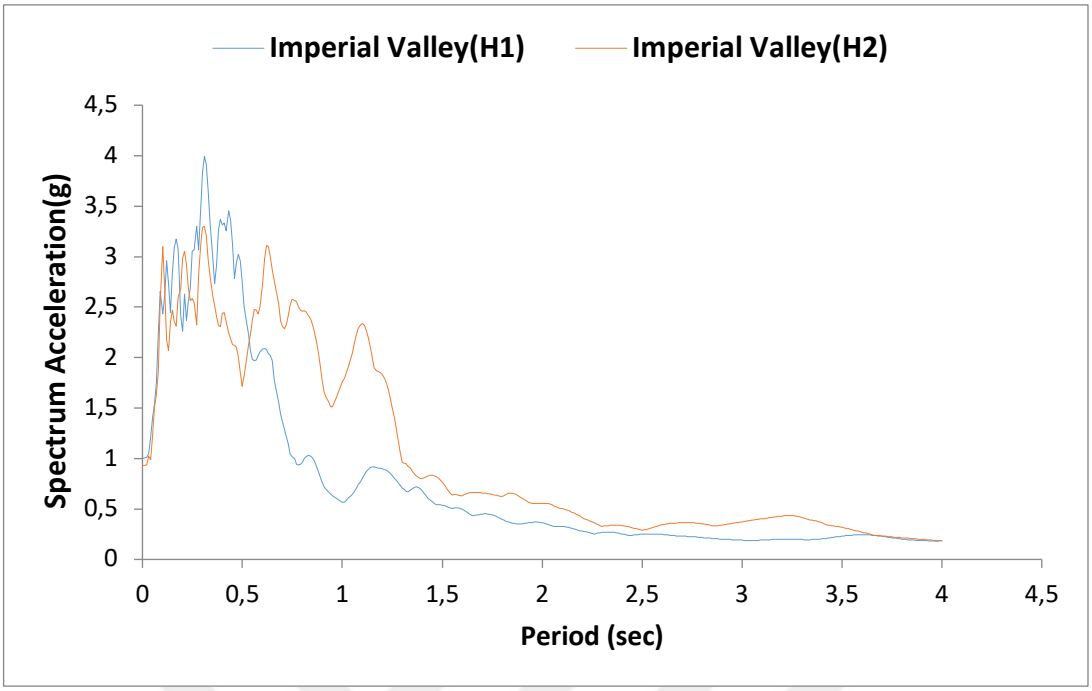


Figure 4.10 Spectrum Accelerations of Imperial Valley Ground Motions for Normalized Records

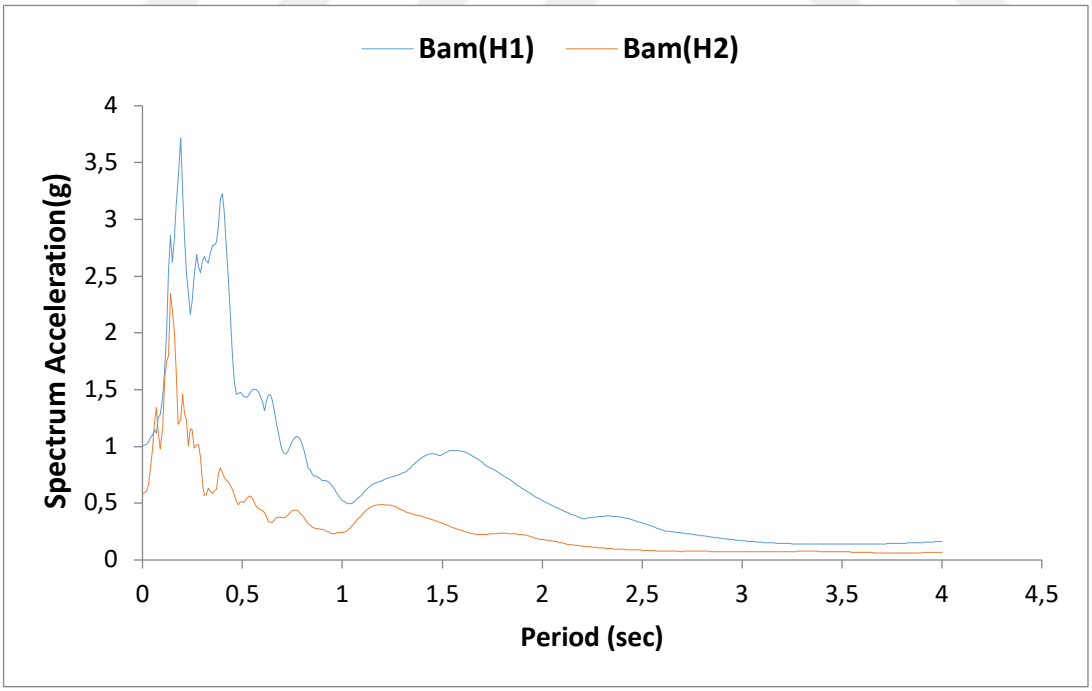


Figure 4.11 Spectrum Accelerations of Bam Ground Motions for Normalized Records

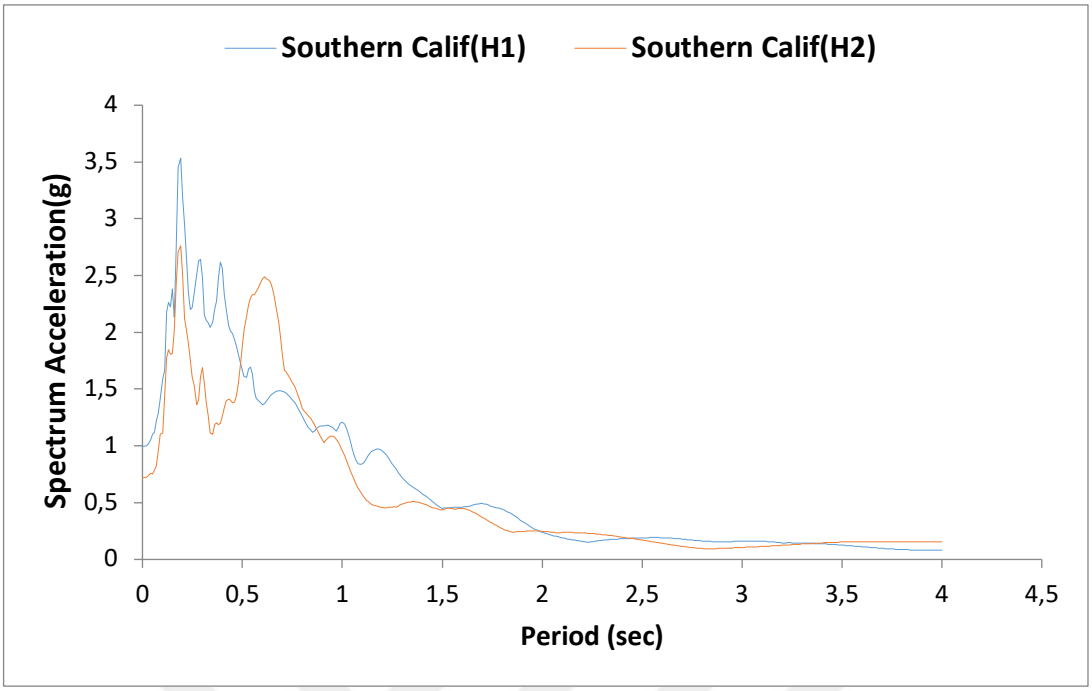


Figure 4.12 Spectrum Accelerations of Southern Calif Ground Motions for Normalized Records

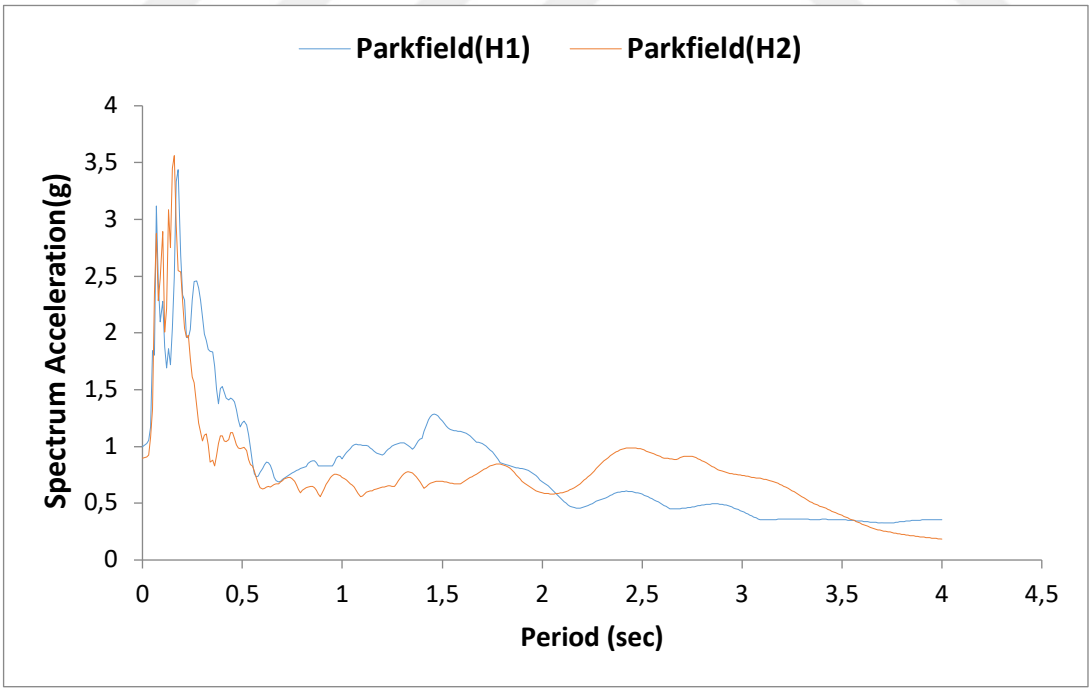


Figure 4.13 Spectrum Accelerations of Parkfield Ground Motions for Normalized Records

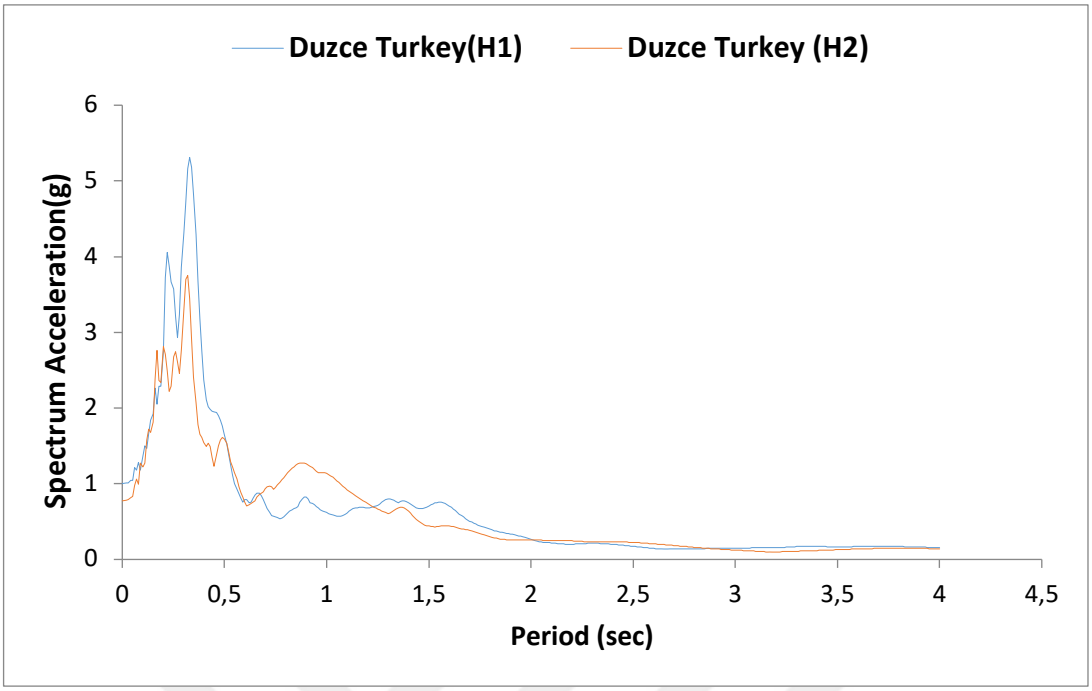


Figure 4.14 Spectrum Accelerations of Düzce Ground Motions for Normalized Records

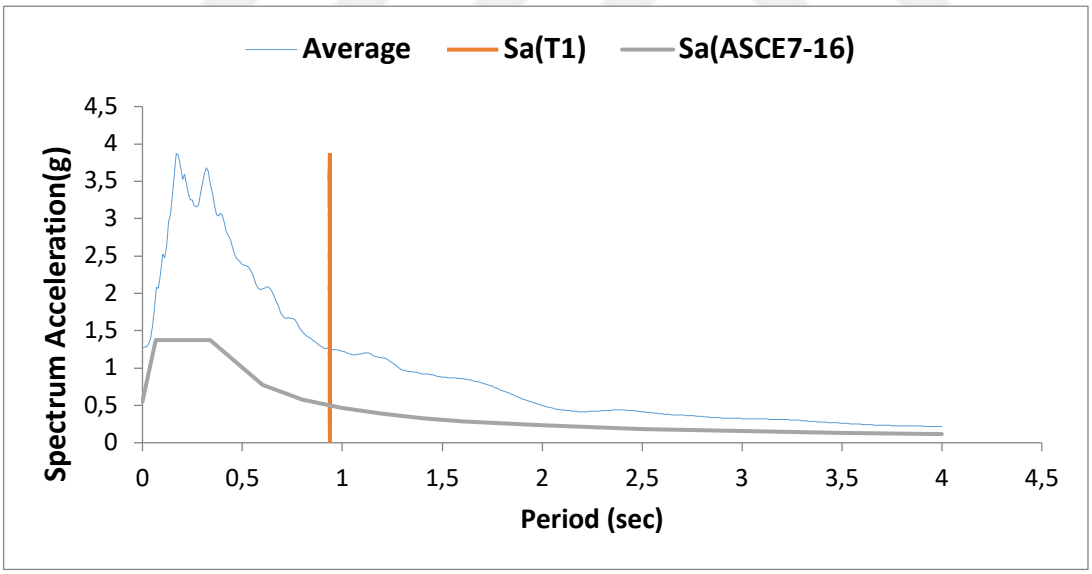


Figure 4.15 The Comparison Between the Mean Value of Calculated Spectrum with ASCE7-16 Design Spectrum at Sa(T1)

4.2 Nonlinear Time History Analyses (NTHA) Results

The results display the maximum story drift ratio at each direction (X and Y) and the maximum base shear values for three types of structure (without damper, with X friction damper and inverted V damper). Both of the ground motions have two horizontal components (H1 and H2). They have been applied simultaneously at 2 conditions as below:

Condition i: The H1 component excites the X direction of the structure and the H2 one excites the Y direction simultaneously (‘’Earthquake name’’ 1, for example Kobe 1);

Condition ii: The H2 component excites the X direction of the structure and the H1 one excites the Y direction simultaneously (“Earthquake name” 2).

It is noted that the H1 component has the bigger value of peak ground acceleration. So, all the drift ratios extracted from the analyses includes four cases:

1) Drift X for Earthquake 1 and three types of buildings;
2) Drift Y for Earthquake 1 and three types of buildings;
3) Drift X for Earthquake 2 and three types of buildings;
4) Drift Y for Earthquake 2 and three types of buildings.

According to the above description, for all the ground motions, we will have 4 graphs with 3 plots at each one stands for the structures without damper, with X damper and with inverted V damper.

4.2.1 Evidence About Northridge Earthquake

January 17, 1994, at 4:31 AM, the Northridge earthquake with a magnitude of 6.7 Mw occurred in the Fernando Valley region of the county of Los Angeles, California and lasted for more than 20 seconds. More than 12,000 homes, schools, hospitals and freeways were damaged in this earthquake. The Los Angeles Memorial Coliseum, home to the 1932 and 1984 Olympics, suffered more than $44 million in damage. Farther south of Downtown, the Watts Towers sustained $2 million damage that required seven years to repair.

The results of the story drift ratios for all the ground motions are displayed at this part. Figures 4.16 to 4.19 show the results of drift ratios for Northridge earthquake. The maximum values of story drift are calculated and analyzed from SAP200.

Table 4.2 The Maximum Values of Story Drift Ratios for Northridge (1) Earthquake

Northridge 1										
Story ID	Without Damper		X Damper				V Damper			
			Arrangement (1)		Arrangement (2)		Arrangement (1)		Arrangement (2)	
	X Drifts	Y Drifts	X Drifts	Y Drifts	X Drifts	Y Drifts	X Drifts	Y Drifts	X Drifts	Y Drifts
Story 7	0.00438	0.00218	0.00220	0.00198	0.00243	0.00230	0.00240	0.00200	0.00260	0.00300
Story 6	0.00450	0.00344	0.00333	0.00275	0.00365	0.00365	0.00350	0.00300	0.00370	0.00400
Story 5	0.00449	0.00480	0.00409	0.00322	0.00410	0.00440	0.00420	0.00500	0.00460	0.00500
Story 4	0.00519	0.00559	0.00464	0.00409	0.00470	0.00510	0.00480	0.00500	0.00510	0.00500
Story 3	0.00519	0.00585	0.00473	0.00382	0.00490	0.00620	0.00490	0.00500	0.00530	0.00600
Story 2	0.004521	0.0063	0.00380	0.00291	0.00391	0.0050	0.00390	0.00500	0.00520	0.00600
Story 1	0.00308	0.00418	0.00270	0.00170	0.00298	0.00290	0.00300	0.00400	0.00320	0.00400

The result of the drift ratio from the above table 4.2 for X-direction is shown in the form of graphs, and it shows the drift of the X damper in arrangement 1 (the light blue color) is less than the other arrangement while in some stories it is the same as the X damper in arrangement 2 and V damper in arrangement 1, for Northridge earthquake.

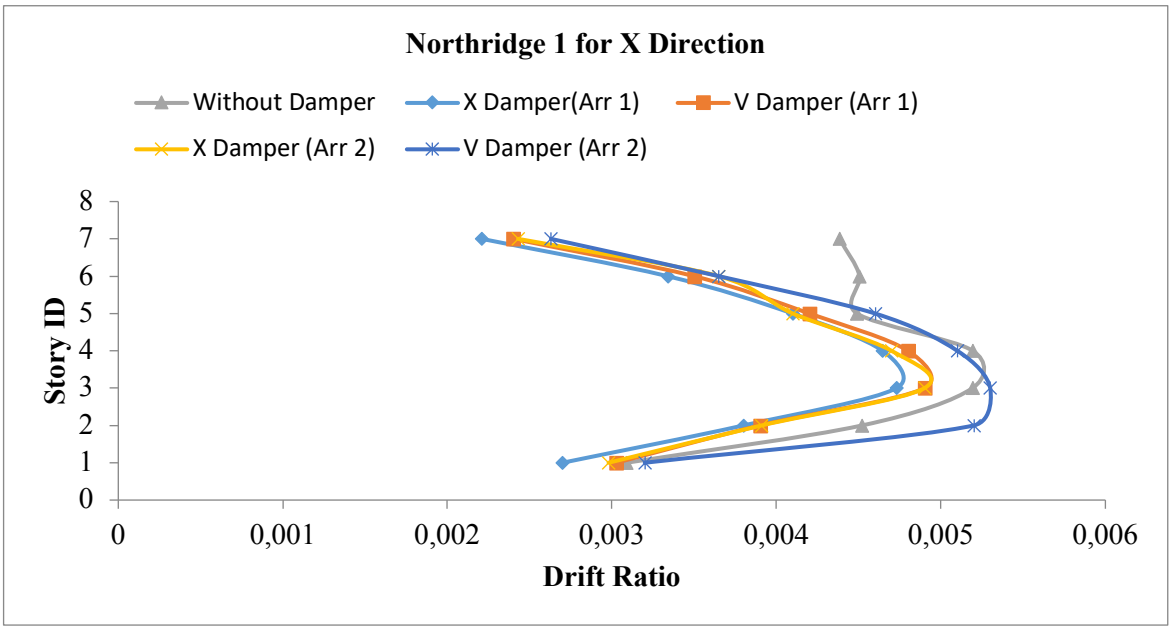


Figure 4.16 The Results of Drift Ratio for Northridge 1 Earthquake at X-Direction

The result of the drift ratio from the above table 4.2 for Y-direction is shown in the form of graphs, and it shows the drift of the X damper in arrangement 1 (the light blue color) is less than the other arrangement and at the 7th-story it is close to the X damper in arrangement 2 for Northridge earthquake.

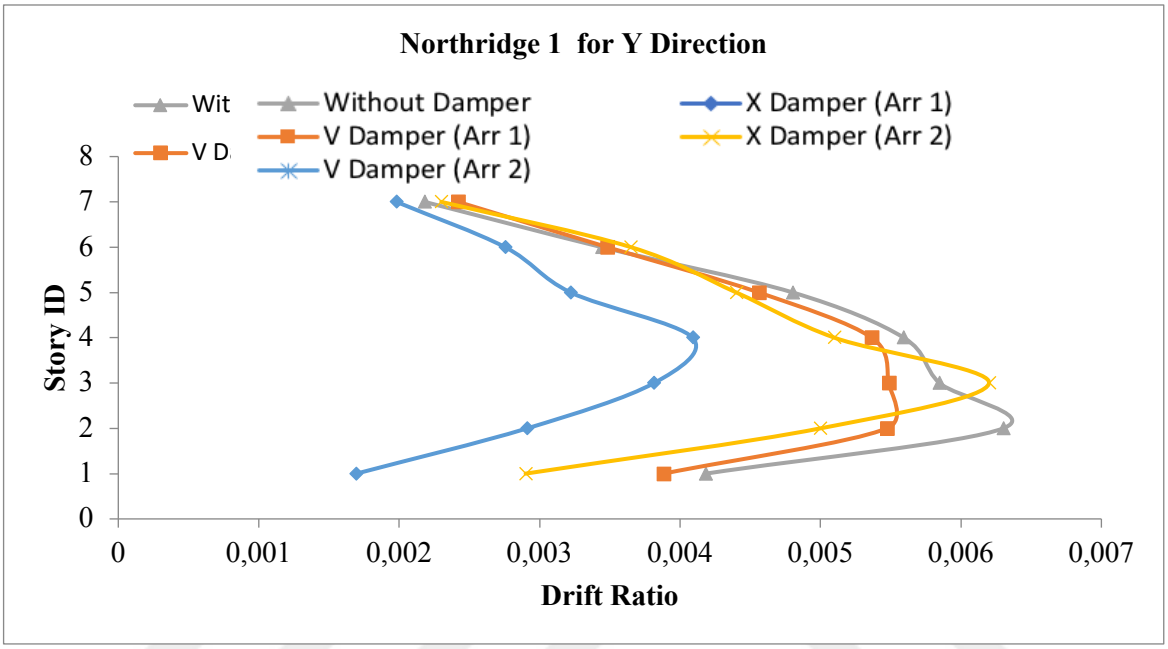


Figure 4.17 The Results of Drift Ratio for Northridge 1 Earthquake at Y-Direction

Table 4.3. The Maximum Values of Story Drift Ratios for Northridge (2) Earthquake

Northridge 2										
Story ID	Without Damper		X Damper				V Damper			
			Arrangement (1)		Arrangement (2)		Arrangement (1)		Arrangement (2)	
	X Drifts	Y Drifts	X Drifts	Y Drifts	X Drifts	Y Drifts	X Drifts	Y Drifts	X Drifts	Y Drifts
Story 7	0.00384	0.00318	0.00147	0.00298	0.00145	0.00220	0.00155	0.00218	0.00190	0.00290
Story 6	0.00580	0.00423	0.00252	0.00398	0.00254	0.00360	0.00261	0.00385	0.00410	0.00430
Story 5	0.00716	0.00465	0.00372	0.00418	0.00389	0.00410	0.00384	0.00430	0.00490	0.00510
Story 4	0.00759	0.00529	0.00463	0.00495	0.00501	0.00470	0.00497	0.00496	0.00550	0.00530
Story 3	0.00884	0.00596	0.00492	0.00511	0.00530	0.00490	0.00569	0.00520	0.00610	0.00532
Story 2	0.00890	0.00576	0.00481	0.00440	0.00520	0.00490	0.00584	0.00520	0.00594	0.00560
Story 1	0.00546	0.00308	0.00322	0.00182	0.00298	0.00290	0.00368	0.00290	0.00512	0.00360

The result of the drift ratio from the above table 4.3 for X-direction is shown in the form of graphs, and it shows the drift of the X damper in arrangement 1 (the light blue color) is less than the other arrangement while in 1st, 5th, 6th and 7th stories the X damper in arrangement 2 is close to the drift ratios as the X damper in arrangement 1, and V damper in arrangement 1 is close to the X-damper in arrangement 2 at 1st story and it is in the same drift ratio at the 5th, 6th and 7th stories, for Northridge 2 earthquake.

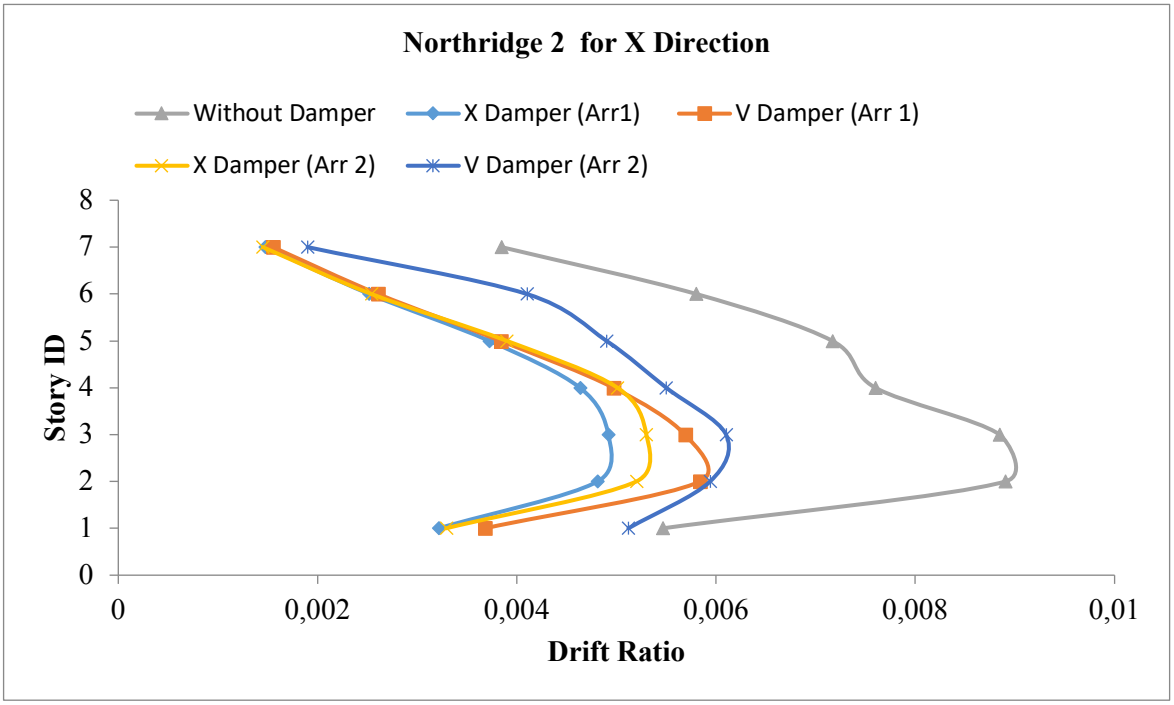


Figure 4.18 The Results of Drift Ratio for Northridge 2 Earthquake at X-Direction

The result of the drift ratio from the table 4.3 for Y-direction is shown in the form of graphs, and it shows the drift of the X damper in arrangement 1 (the light blue color) has the same drift ratios as the X damper in arrangement 2 for the first three stories. And at the 4th, 5th and 6th stories the drift ratio of X damper in arrangement 1 & 2 and V damper in arrangement 1 becomes so close to each other. At the 7th story the V damper in arrangement 1 has the lower drift ratio while it acts so close to the without damper in the 1st story.

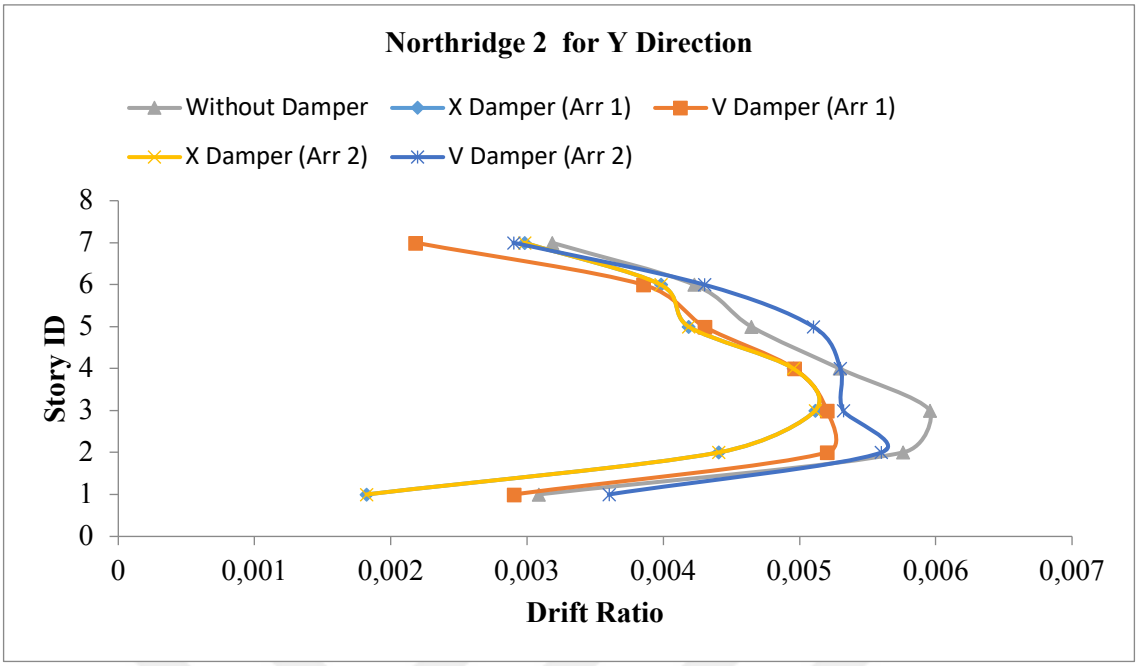


Figure 4.19 The Results of Drift Ratio for Northridge 2 Earthquake at Y-Direction

4.2.2 Evidence About Kobe Earthquake

January 17, 1995, at 5:46 AM, the Kobe earthquake also known as Great Hanshin earthquake hits western Japan with a magnitude of 7.3 Richter, this earthquake is called to be one of the strongest, deadliest and costliest earthquakes that ever happened in Japan which lasted in approximately 20 Seconds. This earthquake left behind 5,000 people died, 300,000 homeless, more than 102,000 buildings damaged and 100 billion Euros estimated to cost to rebuild the basics.

Figures 4.20 to 4.23 show the results of drift ratios for Kobe earthquake and the values of maximum story drifts have been summarized in Table 4.4 and Table 4.5.

Table 4.4 The Values of Maximum Story Drift Ratios for Kobe (1) Earthquake

Kobe 1										
Story ID	Without Damper		X Damper				V Damper			
			Arrangement (1)		Arrangement (2)		Arrangement (1)		Arrangement (2)	
	X Drifts	Y Drifts	X Drifts	Y Drifts	X Drifts	Y Drifts	X Drifts	Y Drifts	X Drifts	Y Drifts
Story 7	0.01238	0.01109	0.00306	0.00300	0.00500	0.00800	0.00630	0.01100	0.00710	0.01200
Story 6	0.01469	0.01372	0.00463	0.00500	0.00900	0.01200	0.01070	0.01500	0.01200	0.01700
Story 5	0.01383	0.01420	0.00553	0.00600	0.00900	0.01000	0.01210	0.01300	0.01420	0.01600
Story 4	0.01590	0.01452	0.00599	0.00600	0.00900	0.01000	0.01380	0.01200	0.01420	0.01500
Story 3	0.01916	0.01500	0.00667	0.00700	0.00900	0.00800	0.01630	0.01000	0.01800	0.01200
Story 2	0.02075	0.01439	0.00689	0.00600	0.00900	0.00700	0.01700	0.01100	0.01900	0.01200
Story 1	0.01468	0.01424	0.00649	0.00500	0.00700	0.00600	0.01280	0.00800	0.01320	0.01000

The result of the drift ratio from the table 4.4 for the X-direction for Kobe 1 is shown in the form of graphs, and it shows the drift of the X damper in arrangement 1 (the light blue color) is less than the other arrangement and after that the drift ration of X damper in arrangement 2 is smaller, where V damper arrangement 2 acts similar to without damper analyze and close to V damper in arrangement 1 at some stories.

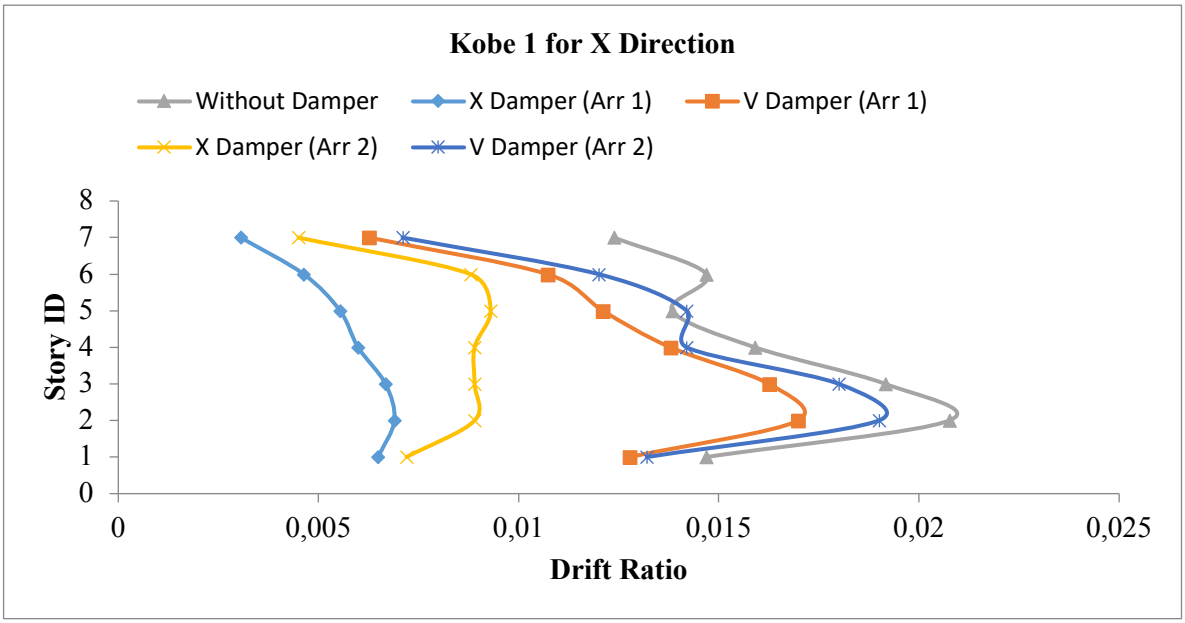


Figure 4.20 The Results of Drift Ratio for Kobe 1 Earthquake at X-Direction

The result of the drift ratio from the table 4.4 for the Y-direction for Kobe 1 is shown in the form of graphs, and it shows the drift of the X damper in arrangement 1 (the light blue color) is less than the other arrangement and the other arrangements are acting so close to the without damper analyze in this case.

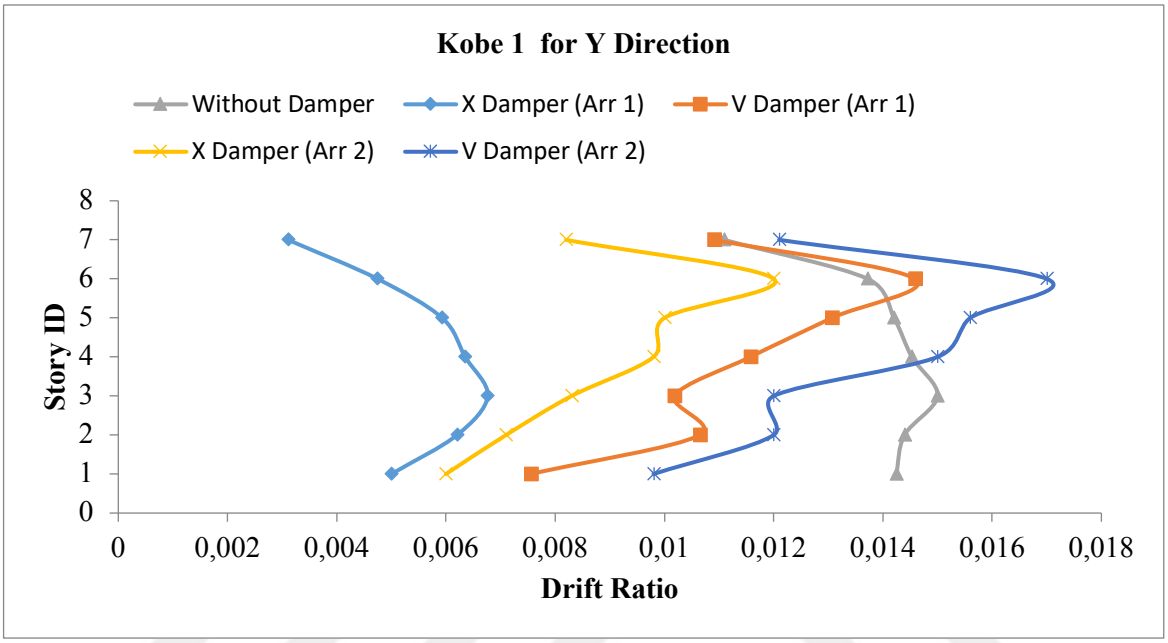


Figure 4.21 The Results of Drift Ratio for Kobe 1 Earthquake at Y-Direction

Table 4.5. The Values of Maximum Story Drift Ratios for Kobe (2) Earthquake

Kobe 2										
Story ID	Without Damper		X Damper				V Damper			
			Arrangement (1)		Arrangement (2)		Arrangement (1)		Arrangement (2)	
	X Drifts	Y Drifts	X Drifts	Y Drifts	X Drifts	Y Drifts	X Drifts	Y Drifts	X Drifts	Y Drifts
Story 7	0.01263	0.01442	0.00250	0.00216	0.00430	0.00880	0.00533	0.01340	0.00540	0.01054
Story 6	0.01558	0.01527	0.00404	0.00299	0.00630	0.00910	0.00815	0.01940	0.00910	0.02200
Story 5	0.01355	0.01370	0.00541	0.00488	0.00980	0.01100	0.01058	0.01991	0.01200	0.02300
Story 4	0.00922	0.01415	0.00622	0.00634	0.00870	0.01250	0.01343	0.01779	0.01360	0.01920
Story 3	0.00968	0.02032	0.00660	0.00711	0.00810	0.01150	0.01525	0.02124	0.01680	0.02100
Story 2	0.01380	0.02131	0.00569	0.00717	0.00710	0.01010	0.01292	0.02786	0.01360	0.02830
Story 1	0.01259	0.01489	0.00285	0.00415	0.00620	0.00550	0.00750	0.02775	0.00760	0.02910

The result of the drift ratio from the table 4.5 for the X-direction for Kobe 2 is shown in the form of graphs, and it shows the drift of the X damper in arrangement 1 (the light blue color) is less than the other arrangement and the other arrangements are acting so close to the without damper analyze in this case while at 3rd and 4th stories the drift ration of without damper analyze is less than the V damper in arrangement 2 and V damper in arrangement 1.

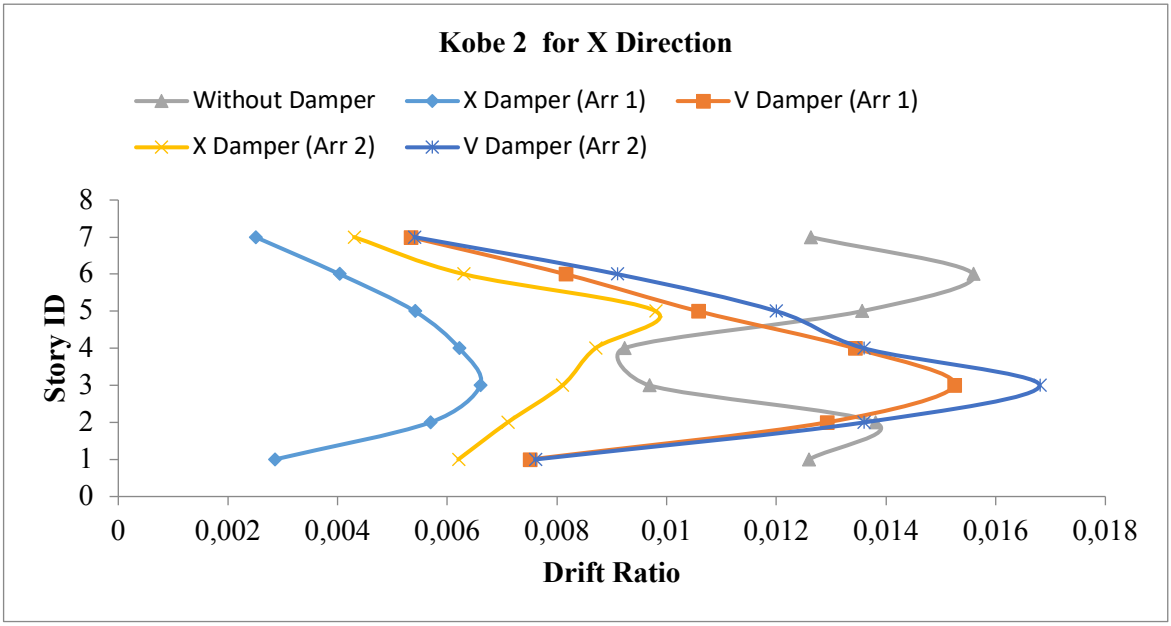


Figure 4.22 The Results of Drift Ratio for Kobe 2 Earthquake at X-Direction

The result of the drift ratio from the table 4.5 for the Y-direction for Kobe 2 is shown in the form of graphs, and it shows the drift of the X damper in arrangement 1 (the light blue color) is less than the other arrangement, while without damper arrangement has got less drift ratio in this case than V damper arrangement 1 and 2. And the drift ration of them are so close at the 7th story.

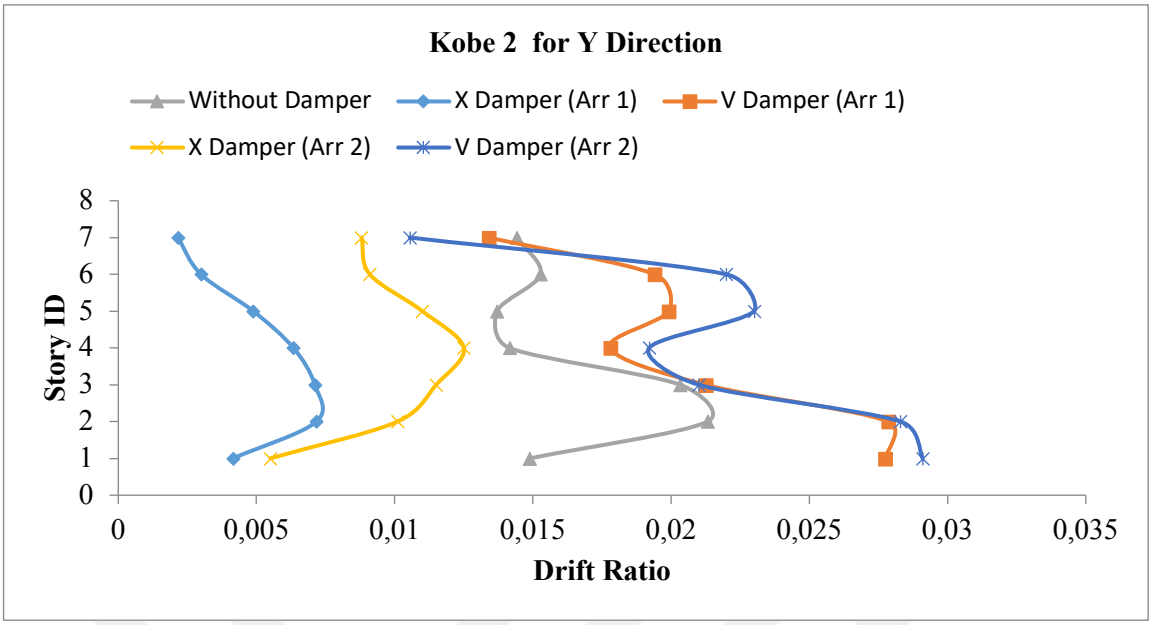


Figure 4.23 The Results of Drift Ratio for Kobe 2 Earthquake at Y-Direction

4.2.3 Evidence About Imperial Valley (El Centro) Earthquake

May 18, 1940, at 21:35 PM, the imperial valley earthquake occurred in the imperial valley in southeastern California with the magnitude of 6.53 and duration of 5-13 Seconds. 80% of the structures were damaged in this earthquake, and it also caused damage to irrigation system.

Figures 4.24 to 4.27 show the results of drift ratios for Imperial Valley earthquake and the values of maximum story drifts have been summarized in Table 4.6 and Table 4.7.

Table 4.6 The Values of Maximum Story Drift Ratios for Imperial Valley (1) Earthquake

Imperial Valley 1										
Story ID	Without Damper		X Damper				V Damper			
			Arrangement (1)		Arrangement (2)		Arrangement (1)		Arrangement (2)	
	X Drifts	Y Drifts	X Drifts	Y Drifts	X Drifts	Y Drifts	X Drifts	Y Drifts	X Drifts	Y Drifts
Story 7	0.01736	0.01917	0.00180	0.00300	0.00800	0.01000	0.01000	0.02300	0.01200	0.02600
Story 6	0.02882	0.03818	0.00270	0.00400	0.01100	0.02000	0.01400	0.04100	0.01500	0.04300
Story 5	0.04919	0.05227	0.00330	0.00500	0.01700	0.02300	0.01880	0.05100	0.01920	0.05400
Story 4	0.09200	0.09347	0.00550	0.00700	0.02100	0.02800	0.02410	0.05600	0.02630	0.05900
Story 3	0.09207	0.10372	0.00790	0.04300	0.01900	0.04600	0.02480	0.05900	0.02560	0.06400
Story 2	0.08220	0.05906	0.00810	0.04100	0.01700	0.04200	0.02580	0.05600	0.02630	0.06600
Story 1	0.07732	0.04268	0.00550	0.03500	0.01200	0.03800	0.01590	0.03300	0.01780	0.06100

The result of the drift ratio from the table 4.6 for the X-direction for Imperial valley 1 is shown in the form of graphs, and it shows the drift of the X damper in arrangement 1 (the light blue color) has much more smaller drift ratio than the other arrangements, the V damper arrangement 1 & 2 are almost at the same level and X damper arrangement 2 is near to the V damper arrangement 1 in 5th story.

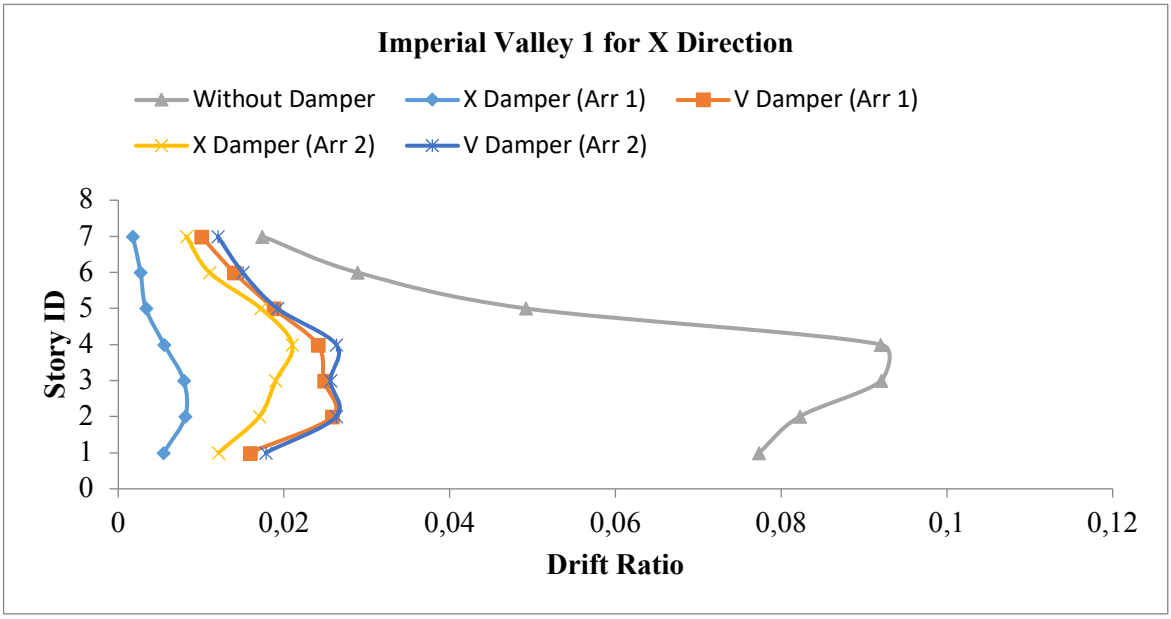


Figure 4.24 The Results of Drift Ratio for Imperial Valley 1 Earthquake at X-Direction

The result of the drift ratio from the table 4.6 for the Y-direction for Imperial valley 1 is shown in the form of graphs, the graph shows that the X damper in arrangement 1 & 2 has almost same drift ratio in the 1st, 2nd and 3rd stories, while V damper arrangement 1 is so close to the X damper arrangement 1 in the 1st story. The without damper graph shows to has less drift ratio than V damper arrangement 1 & 2 in the 6th and 7th story and almost same drift ration at the 2nd and 5th story.

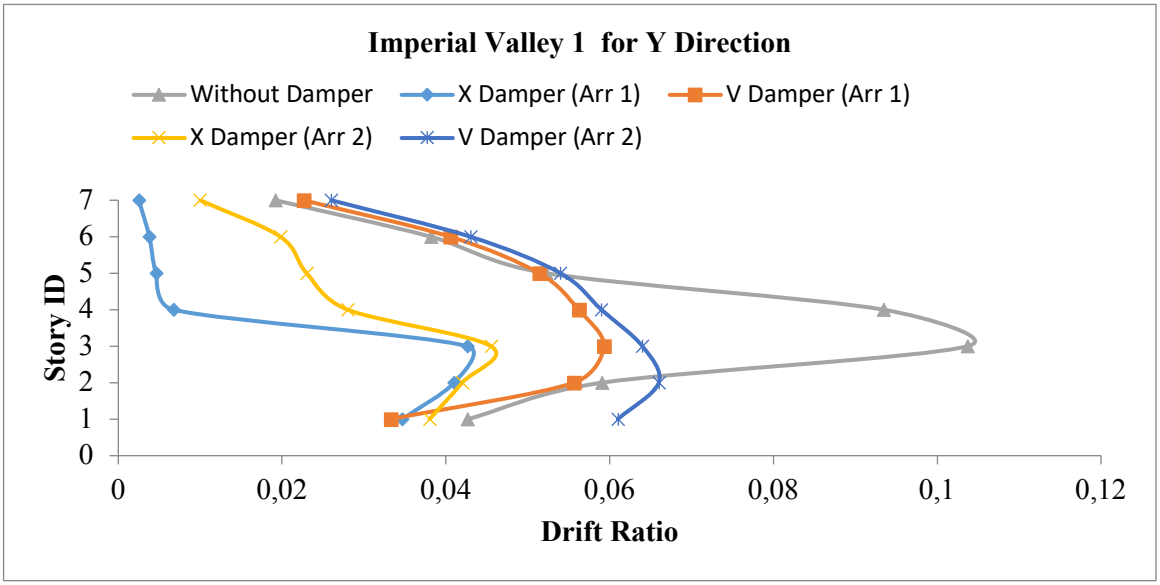


Figure 4.25 The Results of Drift Ratio for Imperial Valley 1 Earthquake at Y-Direction

Table 4.7 The Values of Maximum Story Drift Ratios for Imperial Valley (2) Earthquake

Imperial Valley 2										
Story ID	Without Damper		X Damper				V Damper			
			Arrangement (1)		Arrangement (2)		Arrangement (1)		Arrangement (2)	
	X Drifts	Y Drifts	X Drifts	Y Drifts	X Drifts	Y Drifts	X Drifts	Y Drifts	X Drifts	Y Drifts
Story 7	0.02032	0.01457	0.00197	0.00276	0.0100	0.01310	0.01158	0.01695	0.01540	0.01870
Story 6	0.04362	0.02565	0.00321	0.00378	0.01840	0.01930	0.02623	0.02555	0.02900	0.02890
Story 5	0.06181	0.02689	0.00426	0.00426	0.02200	0.01940	0.04312	0.03201	0.04900	0.03900
Story 4	0.08200	0.03600	0.00593	0.00470	0.02400	0.01740	0.05191	0.03120	0.05500	0.03300
Story 3	0.08403	0.03361	0.02100	0.00758	0.02500	0.01780	0.04879	0.03000	0.05000	0.03200
Story 2	0.06726	0.02566	0.02200	0.00877	0.02400	0.01540	0.04664	0.02300	0.04920	0.02900
Story 1	0.05900	0.02451	0.01980	0.00551	0.02340	0.01100	0.04108	0.02196	0.04200	0.02500

The result of the drift ratio from the table 4.7 for the X-direction for Imperial valley 2 is shown in the form of graphs, the graph shows that the X damper in arrangement 1 has the less drift ratio than the other arrangements. The X damper arrangement 2 got close to the V damper arrangement 2 at the 7th story. V damper arrangement 1 & 2 are almost having the same drift ratio in this case.

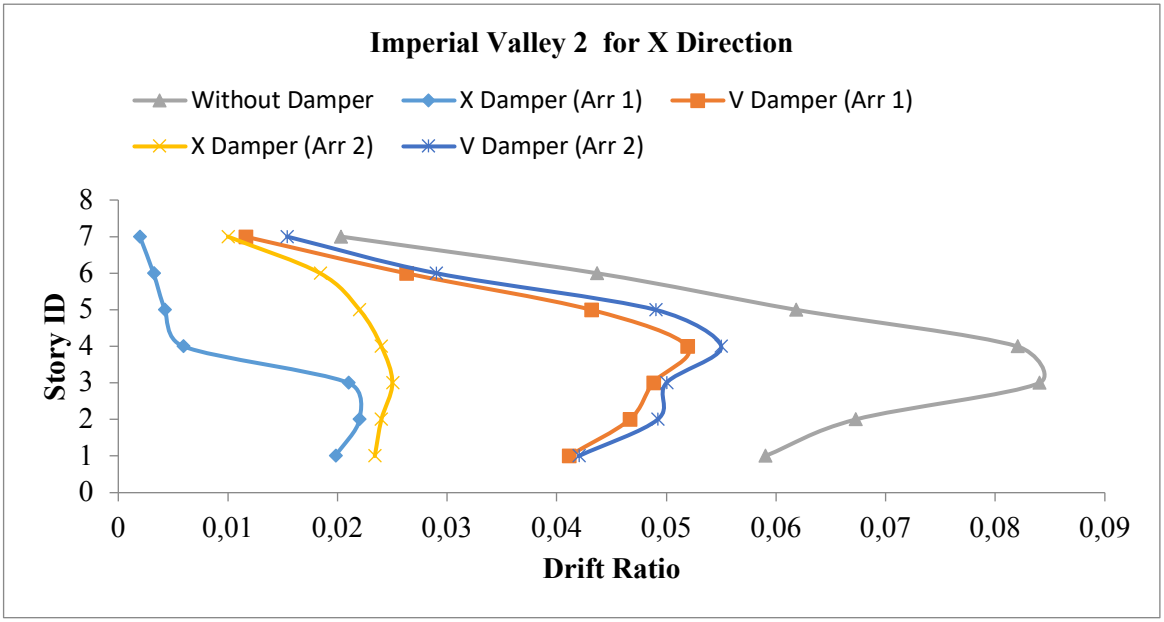


Figure 4.26 The Results of Drift Ratio for Imperial Valley 2 Earthquake at X-Direction

The result of the drift ratio from the table 4.7 for the Y-direction for Imperial valley 2 is shown in the form of graphs, the graph shows that the X damper in arrangement 1 has the less drift ratio than the other arrangements. The X damper arrangement 2 has drift ratio at the 7th story close to without damper analyze. And the without damper analyze has got same drift ration with the V damper arrangement 1 at the 6th story. The V damper arrangement 2 has more drift ration than other ones in this graph.

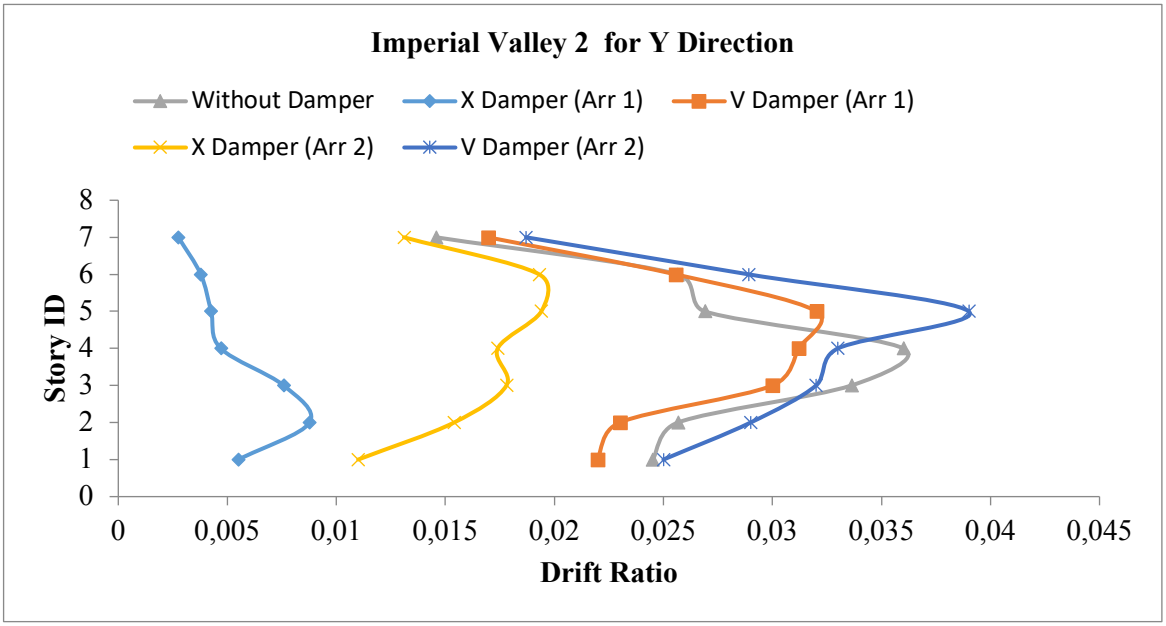


Figure 4.27 The Results of Drift Ratio for Imperial Valley 2 Earthquake at Y-Direction

4.2.4 Evidence About Bam Earthquake

December 26, 2003, at 5:26 Am, the Bam earthquake hit the Kerman province of southeastern Iran. This earthquake had a magnitude of 6.6. at least 26,271 people died and 30,000 injured at this earthquake. 70% of houses were destroyed and the effect of earthquake on the structures was mainly because of poor seismic design and not considering the earthquake regulations. This earthquake left 100,000 people homeless. The united nation estimated that the construction of Bam would cost between 700 million dollars to 1 billion dollars. Figures 4.28 to 4.31 show the results of drift ratios for Bam earthquake and the values of maximum story drifts have been summarized in Table 4.8 and Table 4.9.

Table 4.8 The Values of Maximum Story Drift Ratios for Bam (1) Earthquake

Bam 1										
Story ID	Without Damper		X Damper				V Damper			
			Arrangement (1)		Arrangement (2)		Arrangement (1)		Arrangement (2)	
	X Drifts	Y Drifts	X Drifts	Y Drifts	X Drifts	Y Drifts	X Drifts	Y Drifts	X Drifts	Y Drifts
Story 7	0.01389	0.00879	0.00330	0.00100	0.00800	0.00500	0.00950	0.00900	0.01200	0.01400
Story 6	0.02483	0.01151	0.00510	0.00200	0.01400	0.00600	0.01590	0.01400	0.01780	0.01700
Story 5	0.03952	0.02105	0.00630	0.00300	0.01900	0.00900	0.02570	0.01900	0.02890	0.02100
Story 4	0.05466	0.02147	0.00770	0.00300	0.02500	0.00900	0.03550	0.02100	0.03650	0.02500
Story 3	0.05815	0.02208	0.00840	0.00300	0.02500	0.00800	0.04110	0.02100	0.04150	0.02100
Story 2	0.06405	0.02043	0.00790	0.00400	0.02300	0.00600	0.04660	0.02000	0.04980	0.02100
Story 1	0.04747	0.01443	0.00450	0.00200	0.02000	0.00500	0.04230	0.01300	0.04450	0.01600

The result of the drift ratio from the table 4.8 for the X-direction for Bam 1 earthquake is shown in the form of graphs; the graph shows that the X damper in arrangement 1 has the less drift ratio than the other arrangements. The X damper arrangement 2 has drift ratio at the 7th story close to the V damper arrangement 1 &2 at the 6th and 7th stories.

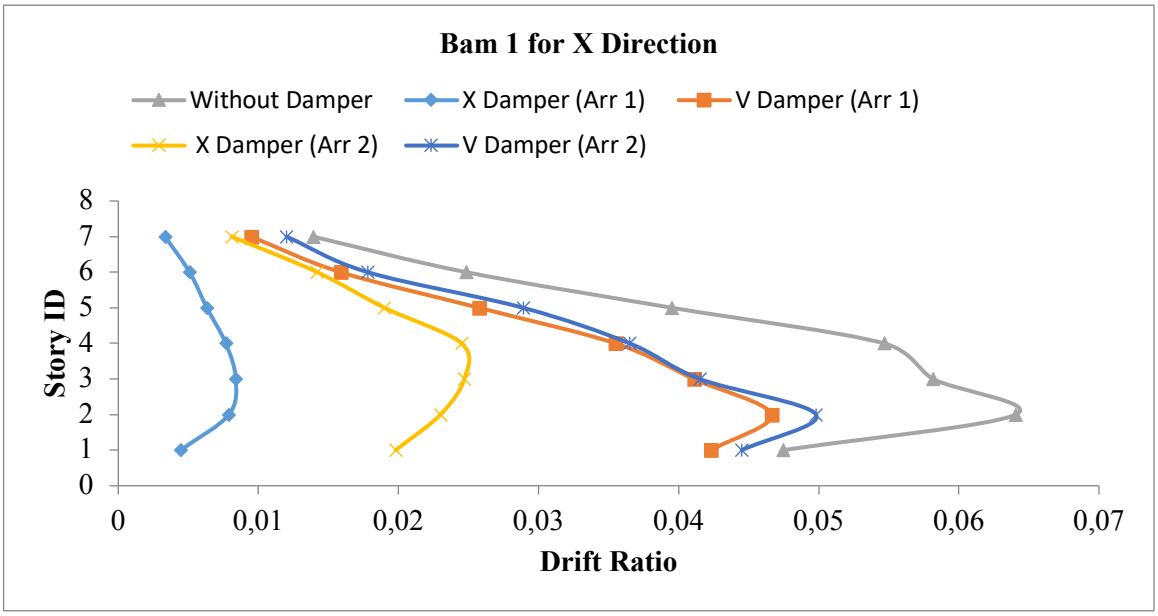


Figure 4.28 The Results of Drift Ratio for Bam 1 Earthquake at X-Direction

The result of the drift ratio from the table 4.8 for the Y-direction for Bam 1 earthquake is shown in the form of graphs, the X damper arrangement 1 & 2 has such a different drift ratio in this analyze, while V damper arrangement 1 & 2 are so close to the without damper analyze.

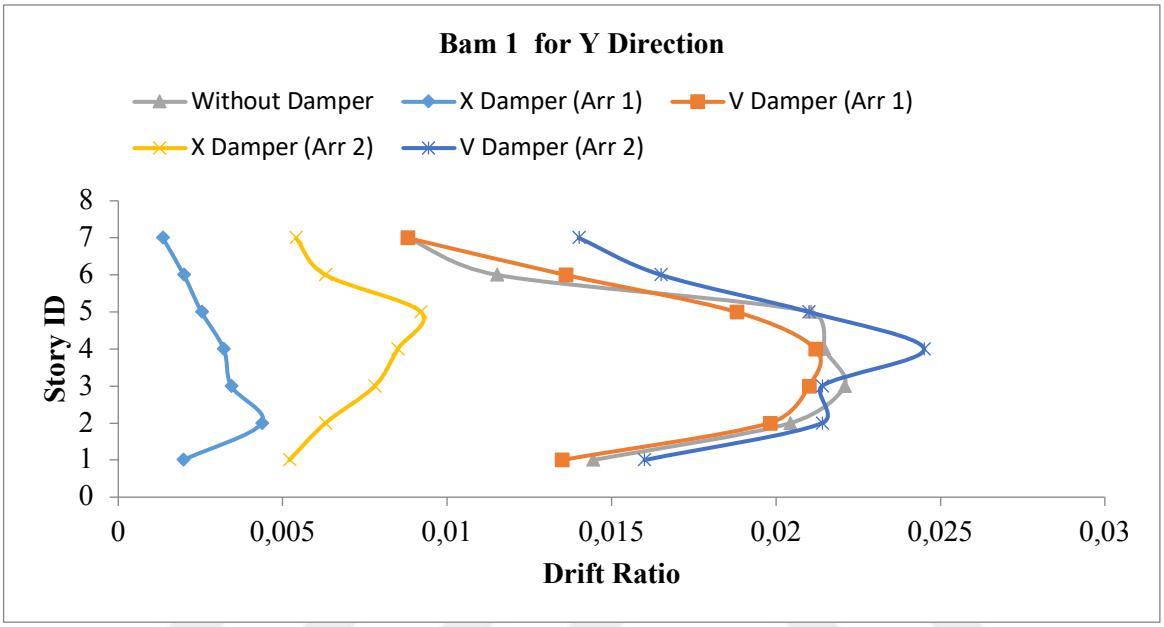


Figure 4.29 The Results of Drift Ratio for Bam 1 Earthquake at Y-Direction

Table 4.9 The Values of Maximum Story Drift Ratios for Bam (2) Earthquake

Bam 2										
Story ID	Without Damper		X Damper				V Damper			
			Arrangement (1)		Arrangement (2)		Arrangement (1)		Arrangement (2)	
	X Drifts	Y Drifts	X Drifts	Y Drifts	X Drifts	Y Drifts	X Drifts	Y Drifts	X Drifts	Y Drifts
Story 7	0.010821	0.01409	0.00075	0.00451	0.00280	0.00870	0.00490	0.01340	0.00620	0.01540
Story 6	0.01614	0.02045	0.00283	0.00704	0.00510	0.01400	0.00777	0.01860	0.00910	0.02100
Story 5	0.02103	0.03937	0.00195	0.00867	0.00870	0.01700	0.01039	0.02200	0.01560	0.02600
Story 4	0.02087	0.03846	0.00725	0.00889	0.01000	0.01500	0.01482	0.02500	0.01620	0.02900
Story 3	0.02175	0.02335	0.00199	0.00818	0.01200	0.01590	0.01777	0.02350	0.01820	0.02560
Story 2	0.02082	0.02016	0.00216	0.00735	0.01100	0.01540	0.01740	0.01900	0.01960	0.02300
Story 1	0.01454	0.01271	0.00132	0.00398	0.00540	0.00740	0.00925	0.01000	0.01500	0.01400

The result of the drift ratio from the table 4.9 for the X-direction for Bam 2 earthquake is shown in the form of graphs, the graph shows that there is so much differences between the drift ration of different arrangement, where X damper arrangement 1 got the smaller drift ration while without damper has got the greater drift ration at the upper stories and close to V damper arrangement 2 in the 1st story.

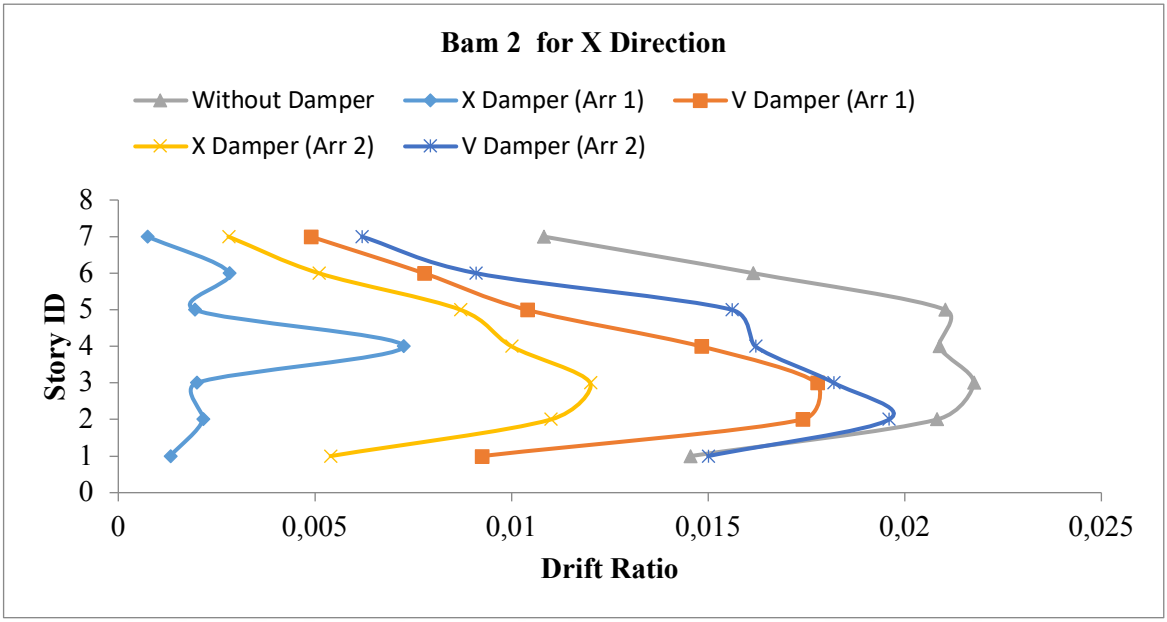


Figure 4.30 The Results of Drift Ratio for Bam 2 Earthquakes at X-Direction

The result of the drift ratio from the table 4.9 for the X-direction for Bam 2 earthquake is shown in the form of graphs, the X damper arrangement 1 got the smaller drift ratio while V damper arrangement 1 & 2 is close to the without damper analyze at the 1st, 2nd, 6th and 7th stories.

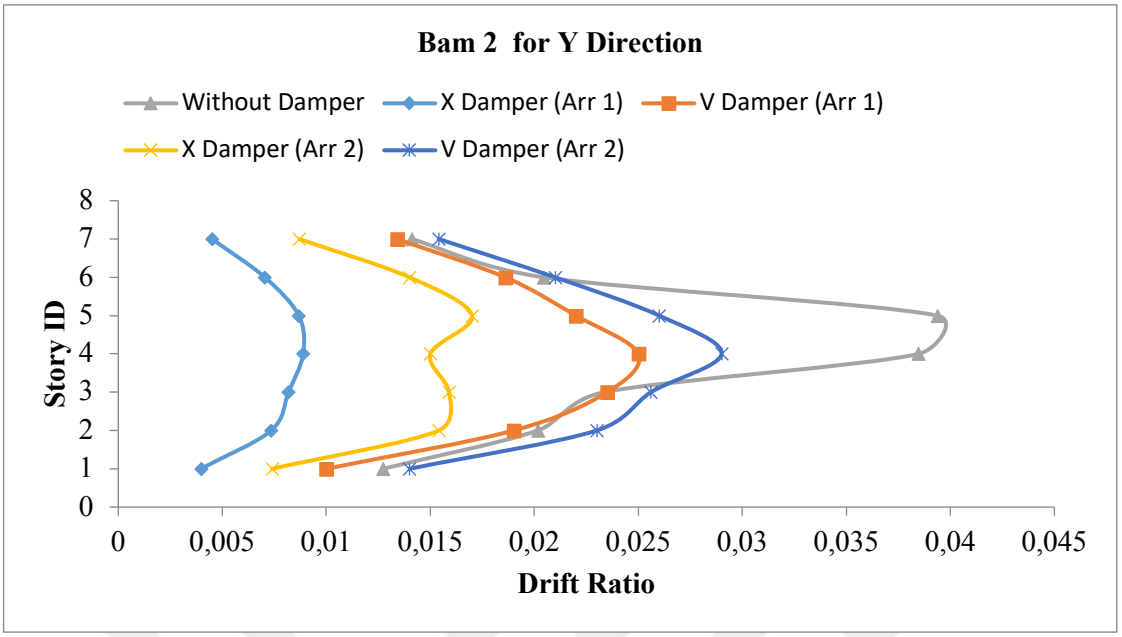


Figure 4.31 The Results of Drift Ratio for Bam 2 Earthquake at Y-Direction

4.2.5 Evidence About Southern California Earthquake

January 9,1857 at 8:20 AM, an earthquake hits San Luis Obispo at the southern California with magnitude of 6 which destroyed a lot of structures and left many people died and injured.

Figures 4.32 to 4.35 show the results of drift ratios for Southern Calif earthquake and the values of maximum story drifts have been summarized in Table 4.10 and Table 4.11.

Table 4.10 The Values of Maximum Story Drift Ratios for Southern Calif (1) Earthquake

Southern Calif 1										
Story ID	Without Damper		X Damper				V Damper			
			Arrangement (1)		Arrangement (2)		Arrangement (1)		Arrangement (2)	
	X Drifts	Y Drifts	X Drifts	Y Drifts	X Drifts	Y Drifts	X Drifts	Y Drifts	X Drifts	Y Drifts
Story 7	0.01463	0.01591	0.00150	0.00100	0.00500	0.01000	0.00720	0.01500	0.01200	0.01800
Story 6	0.02400	0.02373	0.00270	0.00200	0.00700	0.01400	0.01550	0.02100	0.01780	0.02400
Story 5	0.03489	0.02918	0.00450	0.00400	0.00900	0.01600	0.01990	0.02400	0.02100	0.02700
Story 4	0.03727	0.02758	0.00660	0.00500	0.01500	0.01700	0.02540	0.02100	0.02690	0.02500
Story 3	0.03058	0.03013	0.00820	0.00600	0.02100	0.01800	0.03020	0.02200	0.03210	0.02600
Story 2	0.03034	0.03159	0.00900	0.01600	0.01900	0.01900	0.03000	0.02600	0.03410	0.02900
Story 1	0.01512	0.02382	0.00620	0.00400	0.01100	0.01300	0.01390	0.02000	0.01530	0.02300

The result of the drift ratio from the table 4.10 for the X-direction for Southern Calif 1 earthquake is shown in the form of graphs, the X damper arrangement 1 got the lowest drift ration while the V damper in arrangement 1 & 2 are at the same point in 1st, 2nd and 3rd stories with the without friction analysis.

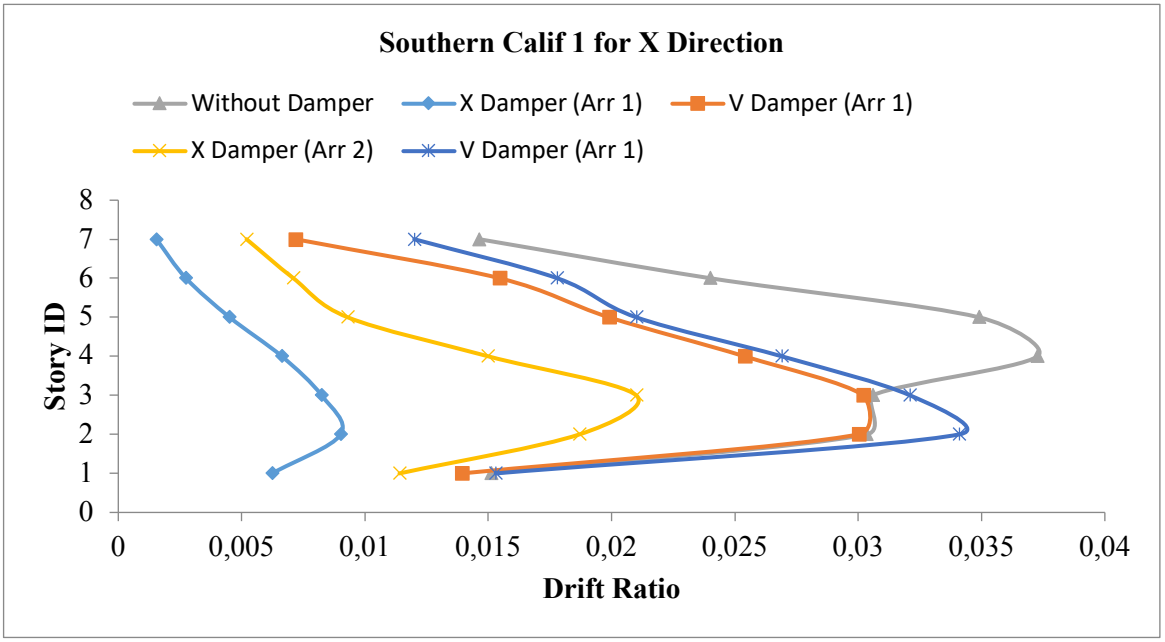


Figure 4.32 The Results of Drift Ratio for Southern Calif 1 Earthquake at X-Direction

The result of the drift ratio from the table 4.10 for the Y-direction Southern Calif 1 earthquake is shown in the form of graphs, the X damper arrangement 1 got the smaller drift ratio than the other analysis, where without friction is close to the V damper arrangement 2 in the 1st and 6th stories.

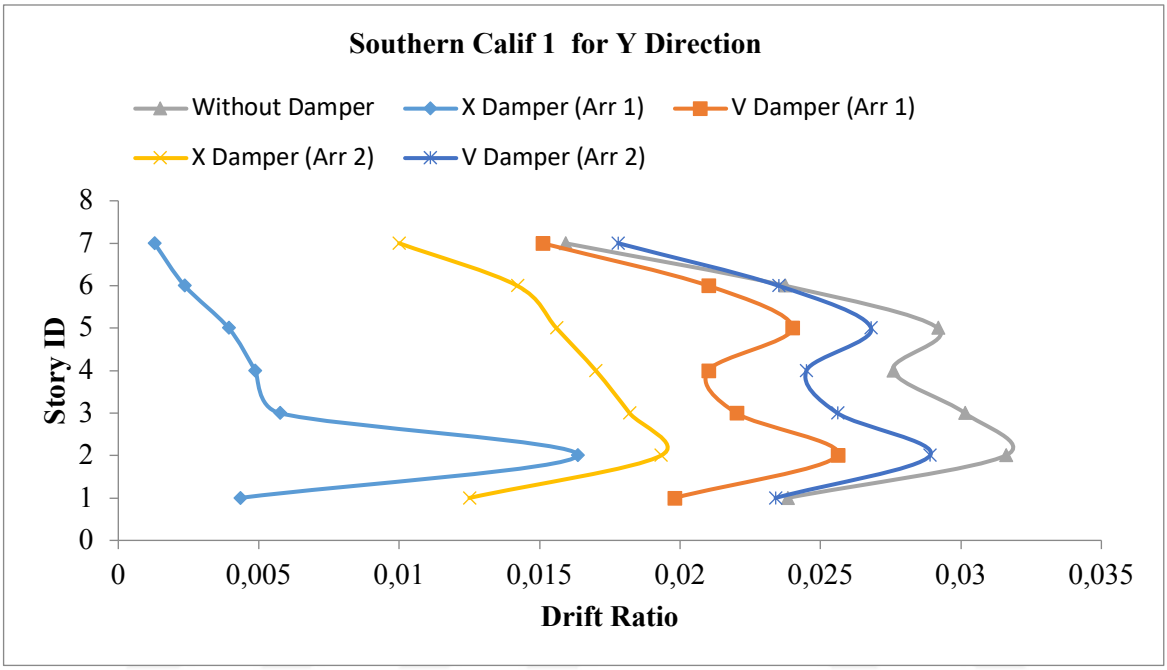


Figure 4.33 The Results of Drift Ratio for Southern Calif 1 Earthquake at Y-Direction

Table 4.11 The Values of Maximum Story Drift Ratios for Southern Calif (2) Earthquake

Southern Calif 2										
Story ID	Without Damper		X Damper				V Damper			
			Arrangement (1)		Arrangement (2)		Arrangement (1)		Arrangement (2)	
	X Drifts	Y Drifts	X Drifts	Y Drifts	X Drifts	Y Drifts	X Drifts	Y Drifts	X Drifts	Y Drifts
Story 7	0.01500	0.01502	0.00136	0.00126	0.00520	0.00680	0.00735	0.01297	0.00923	0.01450
Story 6	0.02316	0.02434	0.00232	0.00236	0.00820	0.00920	0.01498	0.02211	0.01690	0.01630
Story 5	0.03620	0.03495	0.00391	0.00421	0.01300	0.01420	0.02159	0.03057	0.02350	0.02450
Story 4	0.03012	0.03228	0.00422	0.00669	0.01580	0.01510	0.02339	0.02100	0.02480	0.02360
Story 3	0.02949	0.02897	0.014600	0.00857	0.01780	0.01320	0.02271	0.01660	0.02460	0.02450
Story 2	0.03157	0.01902	0.01450	0.00946	0.01740	0.01255	0.02168	0.01620	0.02560	0.02230

The result of the drift ratio from the table 4.11 for the X-direction Southern Calif 2 earthquake is shown in the form of graphs, the X damper arrangement 1 got the smaller drift ratio than the other analysis, and the story drift ratios are so different than each other in this case.

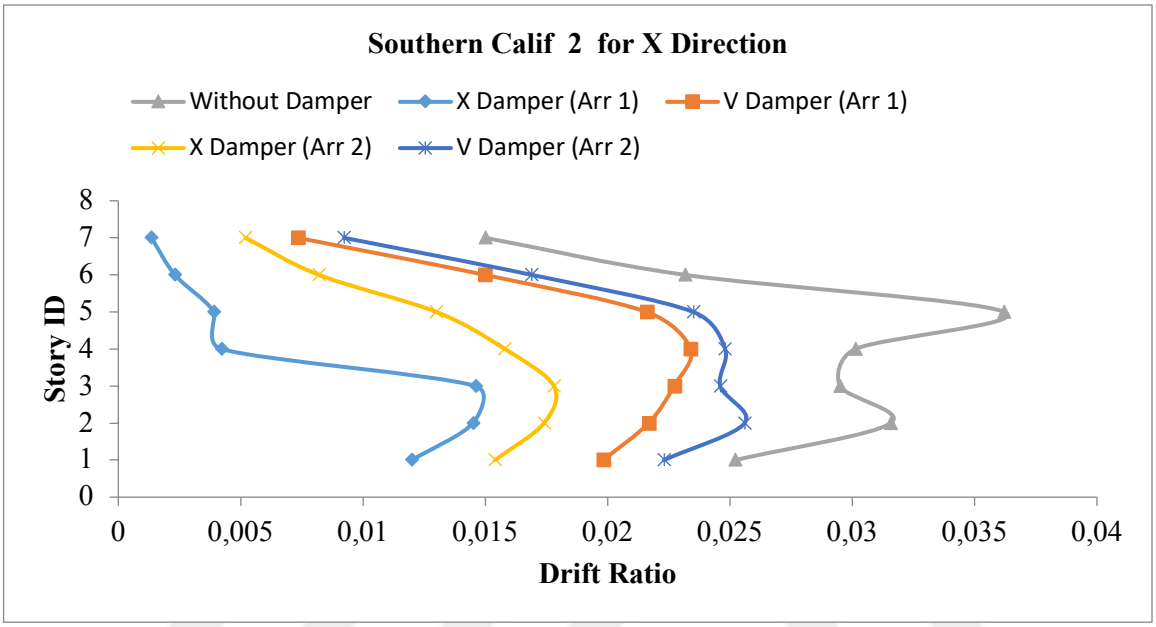


Figure 4.34 The Results of Drift Ratio for Southern Calif 2 Earthquake at X-Direction

The result of the drift ratio from the table 4.11 for the Y-direction Southern Calif 2 earthquake is shown in the form of graphs, the X damper arrangement 1 got the smaller drift ratio than the other analysis, and without friction analysis got smaller drift ratio than V damper arrangement 2 in the 1st and 2nd stories, and V damper arrangement 2 got smaller drift ratio at the 5th, 6th and 7th stories than V damper arrangement 1 and without damper analysis.

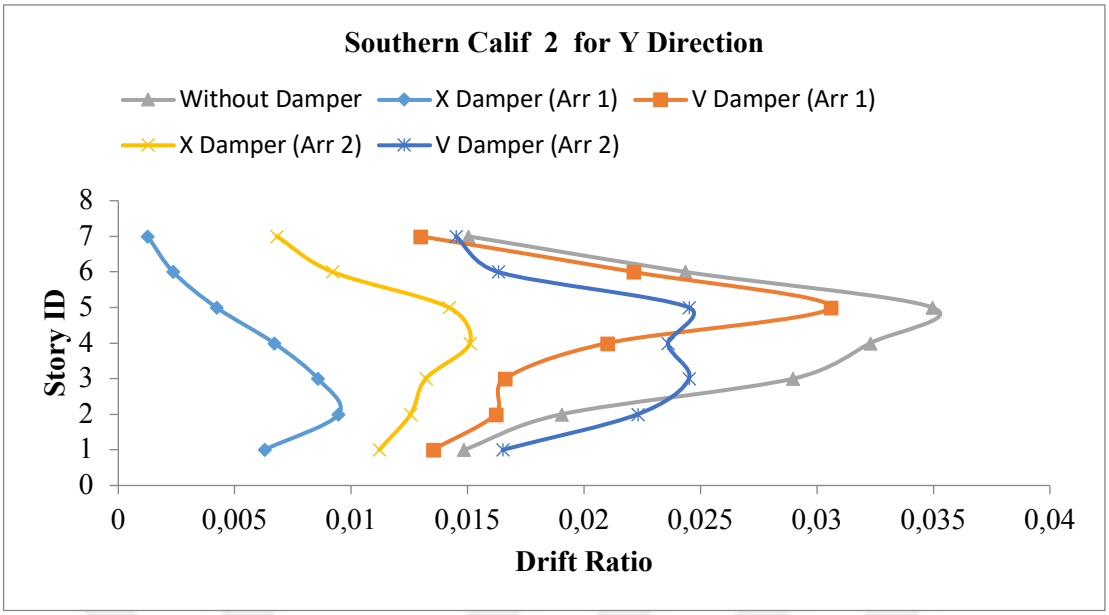


Figure 4.35 The Results of Drift Ratio for Southern Calif 2 Earthquake at Y-Direction

4.2.6 Evidence About Parkfield Earthquake

Parkfield earthquake is a given name to the various large earthquakes which occurred in the Parkfield town of California. Our consideration is the March 3, 1901 earthquake which occurred in parkfield and had magnitude of 6.9.

Figures 4.36 to 4.39 show the results of drift ratios for Parkfield earthquake and the values of maximum story drifts have been summarized in Table 4.12 and Table 4.13.

Table 4.12 The Values of Maximum Story Drift Ratios for Parkfield (1) Earthquake

Parkfield 1										
Story ID	Without Damper		X Damper				V Damper			
			Arrangement (1)		Arrangement (2)		Arrangement (1)		Arrangement (2)	
	X Drifts	Y Drifts	X Drifts	Y Drifts	X Drifts	Y Drifts	X Drifts	Y Drifts	X Drifts	Y Drifts
Story 7	0.01545	0.01886	0.00070	0.00200	0.00500	0.00700	0.00820	0.01200	0.00920	0.01400
Story 6	0.03085	0.02884	0.00100	0.00300	0.00600	0.00900	0.01580	0.02300	0.01690	0.02500
Story 5	0.04715	0.03352	0.00230	0.00300	0.00900	0.01300	0.02560	0.03400	0.02680	0.03600
Story 4	0.04800	0.04447	0.00500	0.00400	0.01200	0.01700	0.03460	0.03900	0.03780	0.04200
Story 3	0.04600	0.05535	0.00810	0.01800	0.01300	0.02100	0.03960	0.04100	0.04210	0.04400
Story 2	0.03800	0.04500	0.00850	0.01300	0.01200	0.02000	0.02400	0.03900	0.02680	0.04400
Story 1	0.02600	0.02541	0.00650	0.01000	0.01000	0.01600	0.02250	0.02600	0.02460	0.02800

The result of the drift ratio from the table 4.12 for the X-direction for the Parkfield 1 earthquake is shown in the form of graphs, the X damper arrangement 1 & 2 got the smaller drift ratios than the other analysis, where V damper arrangement 1 & 2 are close to each other and without damper analysis has greater story drift ration than the other analysis.

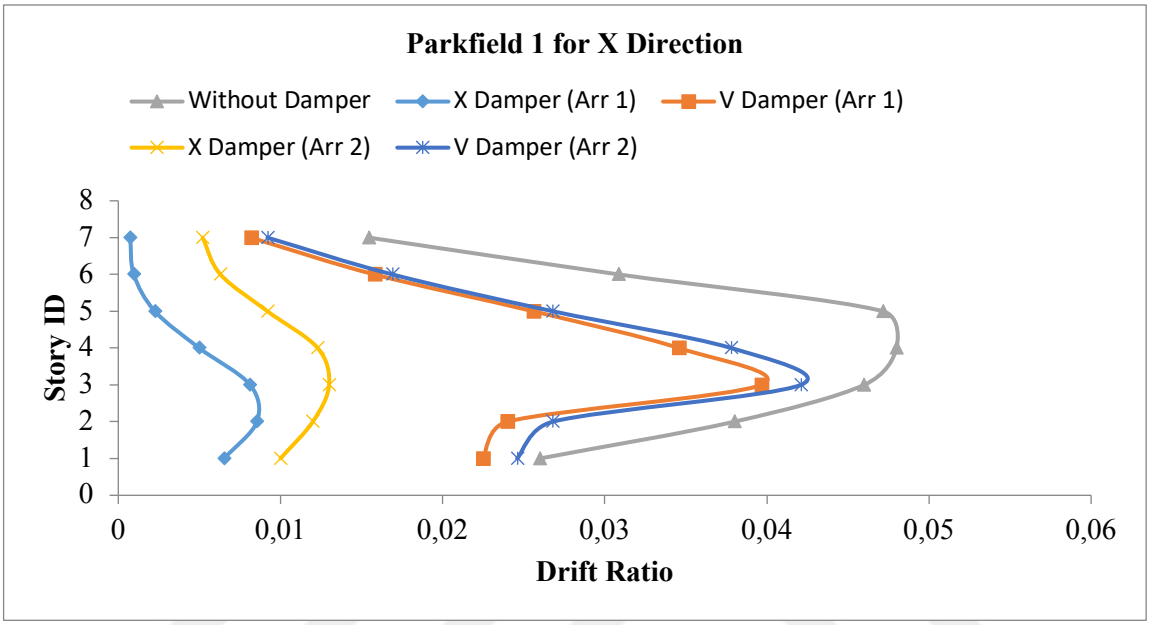


Figure 4.36 The Results of Drift Ratio for Parkfield 1 Earthquake at X-Direction

The result of the drift ratio from the table 4.12 for the Y-direction for the Parkfield 1 earthquake is shown in the form of graphs, the X damper arrangement 1 & 2 got the smaller drift ratios than the other analysis, while X damper arrangement 1 got close to the X damper arrangement 2 at the 3rd story. V damper arrangement 1 & 2 are close to the without damper in the 1st, 2nd and 4th stories.

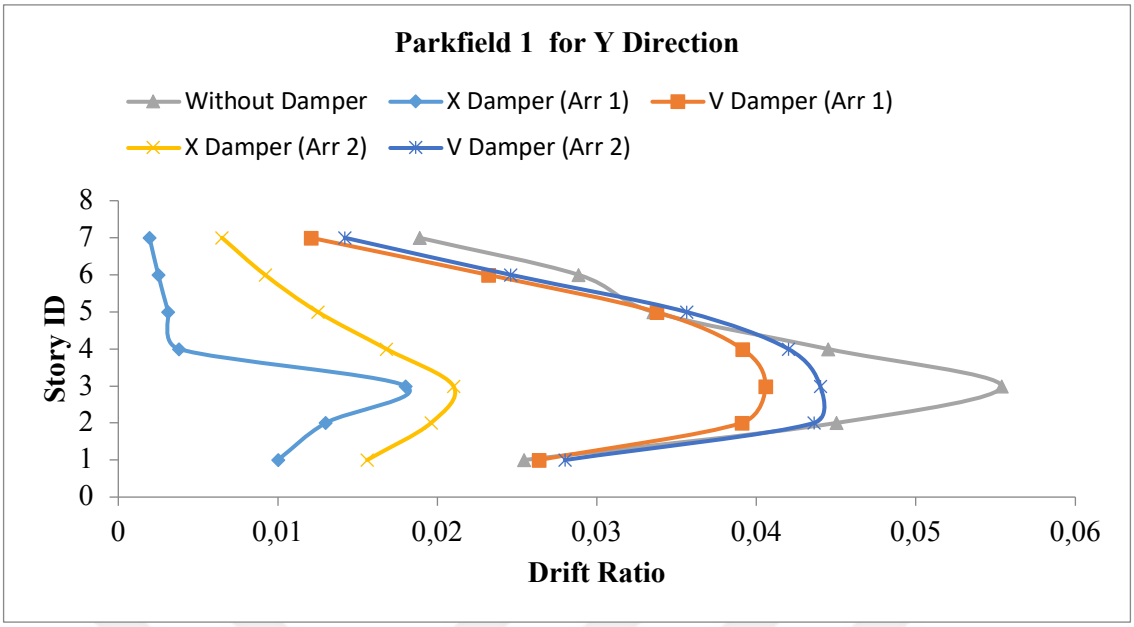


Figure 4.37 The Results of Drift Ratio for Parkfield 1 Earthquake at Y-Direction

Table 4.13 The Values of Maximum Story Drift Ratios for Parkfield (2) Earthquake

Parkfield 2										
Story ID	Without Damper		X Damper				V Damper			
			Arrangement (1)		Arrangement (2)		Arrangement (1)		Arrangement (2)	
	X Drifts	Y Drifts	X Drifts	Y Drifts	X Drifts	Y Drifts	X Drifts	Y Drifts	X Drifts	Y Drifts
Story 7	0.01626	0.00989	0.00134	0.00120	0.00920	0.00630	0.01510	0.00986	0.01750	0.01230
Story 6	0.03572	0.01296	0.00192	0.00470	0.01560	0.00920	0.02580	0.01100	0.02680	0.01450
Story 5	0.04630	0.01957	0.00244	0.00870	0.01840	0.01200	0.02380	0.01500	0.02690	0.01640
Story 4	0.04620	0.02738	0.00295	0.01200	0.02200	0.01560	0.03560	0.01950	0.03680	0.02310
Story 3	0.03680	0.02838	0.00343	0.00980	0.01890	0.01340	0.02650	0.02100	0.02890	0.02450
Story 2	0.03560	0.02867	0.00923	0.00980	0.01780	0.01430	0.02980	0.02630	0.03210	0.02780

The result of the drift ratio from the table 4.13 for the X-direction for the Parkfield 2 earthquake is shown in the form of graphs, the X damper arrangement 1 & 2 got the smaller drift ratios than the other analysis, where V damper arrangement 1 & 2 are close to each other and without damper analysis has greater story drift ration than the other analysis.

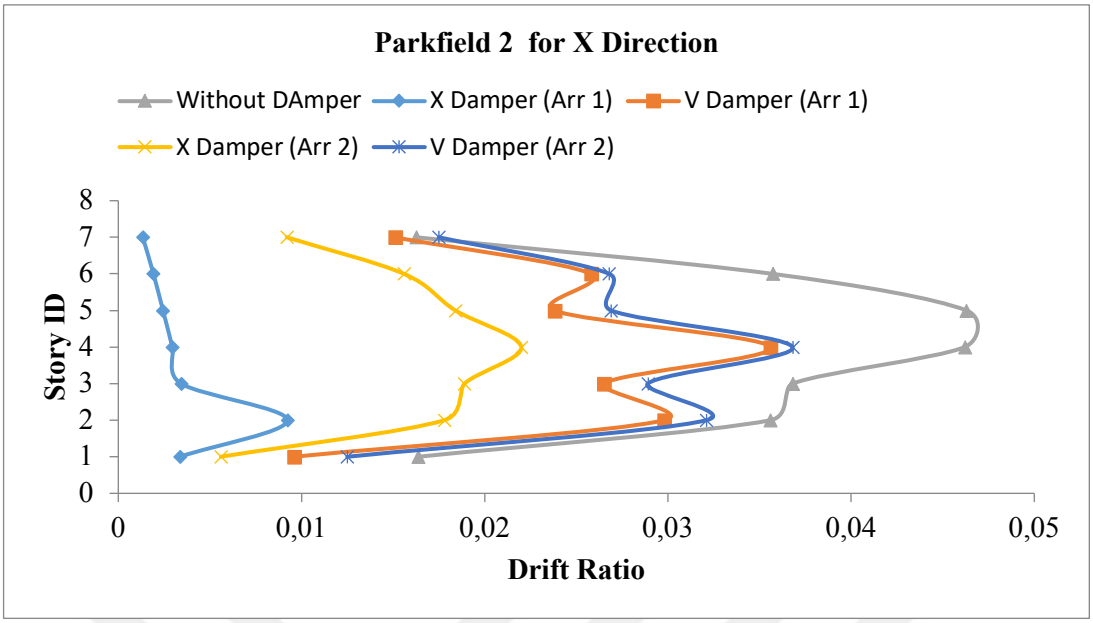


Figure 4.38 The Results of Drift Ratio for Parkfield 2 Earthquake at X-Direction

The result of the drift ratio from the table 4.13 for the Y-direction for the Parkfield 2 earthquake is shown in the form of graphs, the X damper arrangement 1 & 2 got the smaller drift ratios than the other analysis. V damper arrangement 1 & 2 are close to the without damper in the 6th and 7th stories.

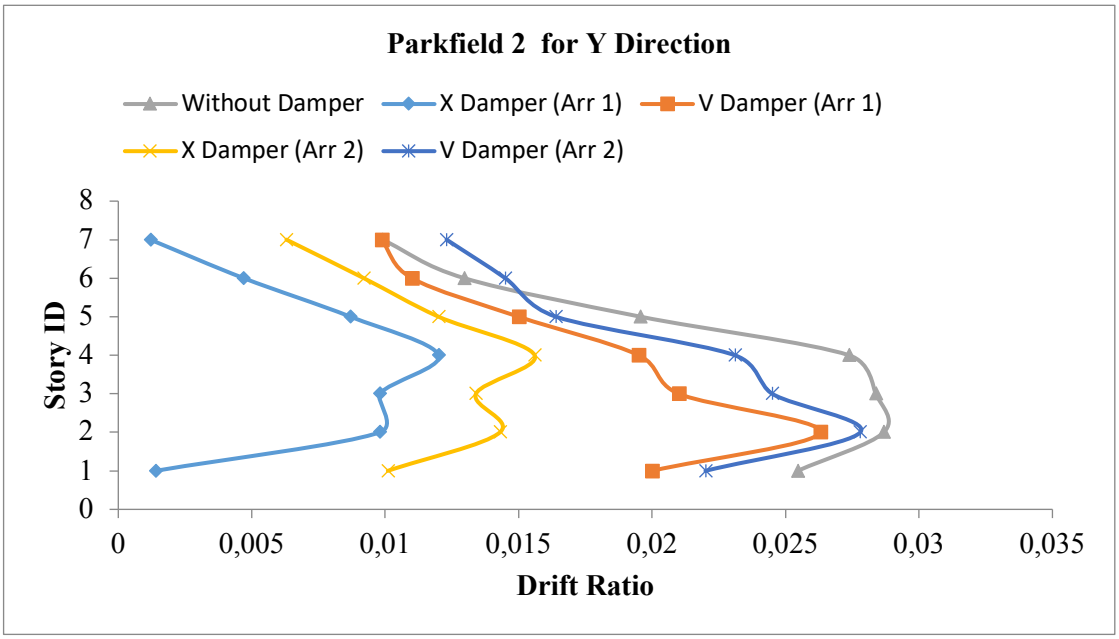


Figure 4.39 The Results of Drift Ratio for Parkfield 2 Earthquake at Y-Direction

4.2.7 Evidence About Düzce Earthquake

November 12, 1999 at 18:57:22 local time, Düzce earthquake with magnitude of 7.14 happened in the south of Düzce, a town with 80,000 population in Bolu province of Turkey. Almost 200 building were damaged at this earthquake, more than 550 people were died and over 3000 people were injured. The financial lost in this earthquake reached 10 million Dollars.

Figures 4.39 to 4-43 show the results of drift ratios for Düzce earthquake and the values of maximum story drifts have been summarized in Table 4.14 and Table 4.15.

Table 4.14 The Values of Maximum Story Drift Ratios for Düzce (1) Earthquake

Düzce 1										
Story ID	Without Damper		X Damper				V Damper			
			Arrangement (1)		Arrangement (2)		Arrangement (1)		Arrangement (2)	
	X Drifts	Y Drifts	X Drifts	Y Drifts	X Drifts	Y Drifts	X Drifts	Y Drifts	X Drifts	Y Drifts
Story 7	0.025457	0.01111	0.00170	0.00060	0.01200	0.00600	0.01980	0.01000	0.02200	0.01600
Story 6	0.03400	0.02553	0.00290	0.00040	0.01400	0.00900	0.02100	0.01900	0.02400	0.02300
Story 5	0.04500	0.04100	0.00480	0.00100	0.01600	0.01200	0.02300	0.02800	0.02630	0.03200
Story 4	0.04600	0.03700	0.00710	0.00200	0.01800	0.01700	0.02940	0.03300	0.03200	0.04100
Story 3	0.04400	0.03600	0.00890	0.00500	0.02000	0.01400	0.03370	0.03400	0.03500	0.03600
Story 2	0.04200	0.04280	0.00930	0.00600	0.01800	0.01800	0.02040	0.03300	0.02200	0.03600
Story 1	0.03900	0.04390	0.00710	0.00800	0.01400	0.01200	0.01910	0.02200	0.02100	0.02200

The result of the drift ratio from the table 4.14 for the X-direction for the Düzce 1 earthquake is shown in the form of graphs, the X damper arrangement 1 & 2 got the smaller drift ratios than the other analysis. V damper arrangement 1 & 2 are close to each other at the 2nd and 3rd stories while without damper got the greater drift ratio.

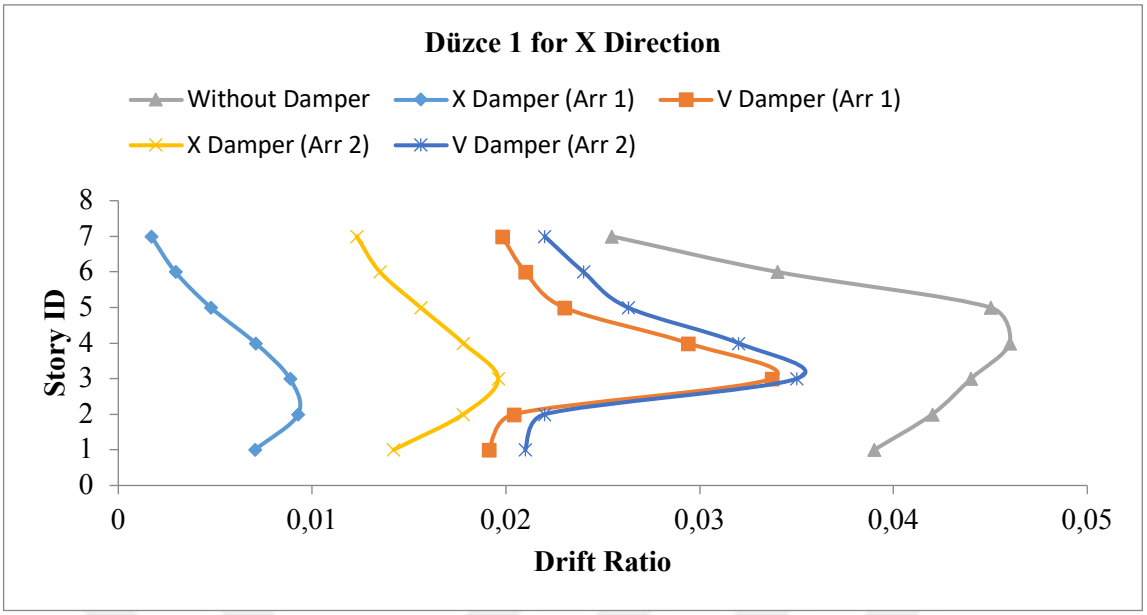


Figure 4.40 The Results of Drift Ratio for Düzce 1 Earthquake at X-Direction

The result of the drift ratio from the table 4.14 for the Y-direction for the Düzce 1 earthquake is shown in the form of graphs, the X damper arrangement 1 got the smallest drift ratio than any other results we got from the other earthquake and at the 6th and 7th stories it is so close to the zero. V damper arrangement 1 & 2 are so close to the without damper at the 3rd, 6th and 7th stories.

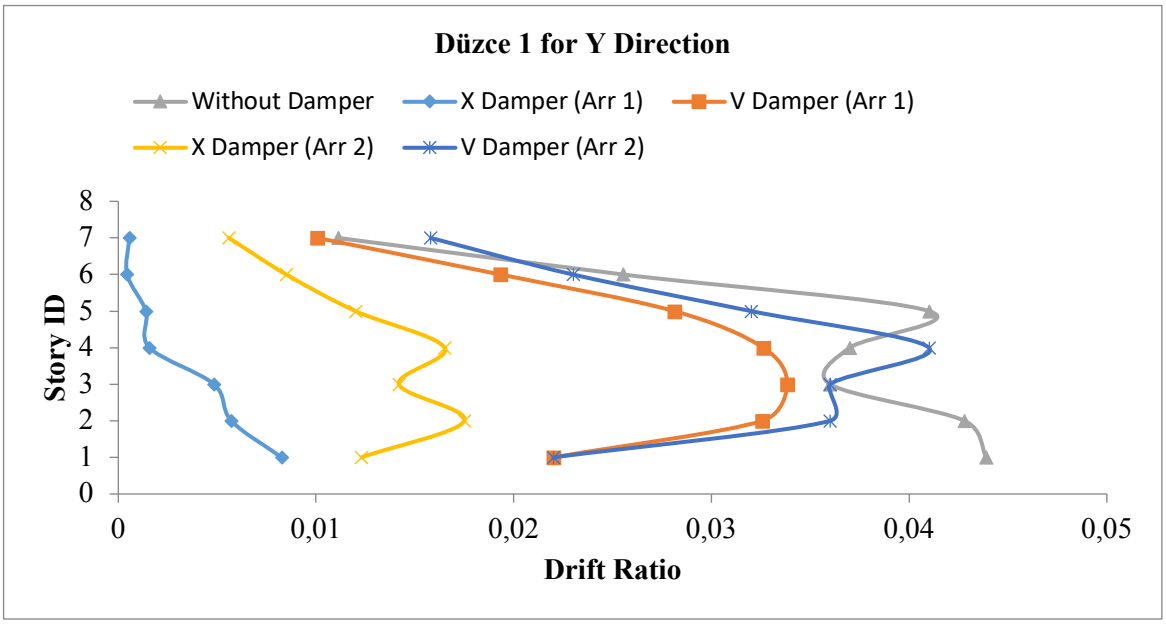


Figure 4.41 The Results of Drift Ratio for Düzce 1 Earthquake at Y-Direction

Table 4.15 The Values of Maximum Story Drift Ratios for Düzce (2) Earthquake

Düzce 2										
Story ID	Without Damper		X Damper				V Damper			
			Arrangement (1)		Arrangement (2)		Arrangement (1)		Arrangement (2)	
	X Drifts	Y Drifts	X Drifts	Y Drifts	X Drifts	Y Drifts	X Drifts	Y Drifts	X Drifts	Y Drifts
Story 7	0.025344	0.02727	0.00035	0.00177	0.00780	0.01460	0.01420	0.01980	0.01620	0.02200
Story 6	0.031829	0.04356	0.00038	0.00293	0.00960	0.01560	0.01520	0.02900	0.01780	0.03200
Story 5	0.05752	0.05321	0.00092	0.00452	0.01450	0.01760	0.01980	0.02300	0.02300	0.02400
Story 4	0.05900	0.03700	0.00125	0.00663	0.01230	0.01970	0.02400	0.02100	0.02630	0.02300
Story 3	0.03390	0.03300	0.00354	0.00879	0.01350	0.01780	0.02100	0.02400	0.02300	0.02600
Story 2	0.04300	0.04600	0.00837	0.00985	0.01400	0.01560	0.02900	0.02900	0.03200	0.03200
Story 1	0.03900	0.04400	0.00717	0.00711	0.01250	0.01230	0.01900	0.01998	0.02100	0.02200

The result of the drift ratio from the table 4.15 for the X-direction for the Düzce 2 earthquake is shown in the form of graphs, the X damper arrangement 1 got the smallest drift ratio than any other results we got from the other earthquake and at the 5th, 6th and 7th stories it is so close to the zero.

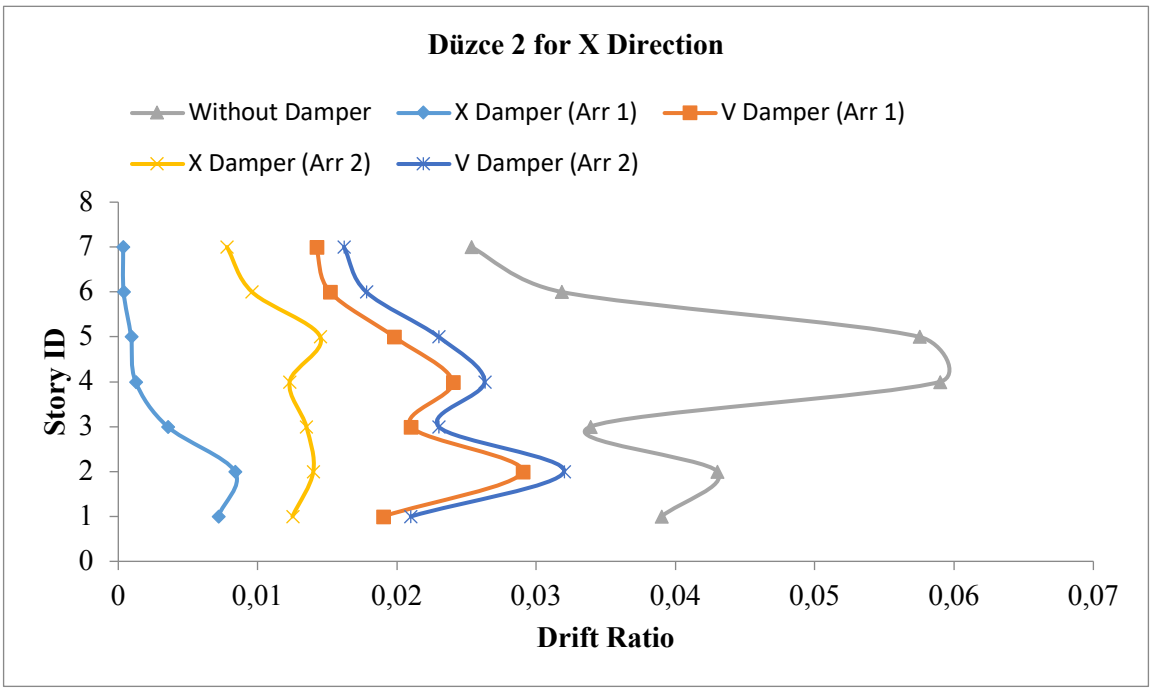


Figure 4.42 The Results of Drift Ratio for Düzce 2 Earthquake at X-Direction

The result of the drift ratio from the table 4.15 for the Y-direction for the Düzce 2 earthquake is shown in the form of graphs, the X damper arrangement 1 got the smallest drift ratio. While X damper arrangement 2 is close to the V damper arrangement 1 at the 3rd story.

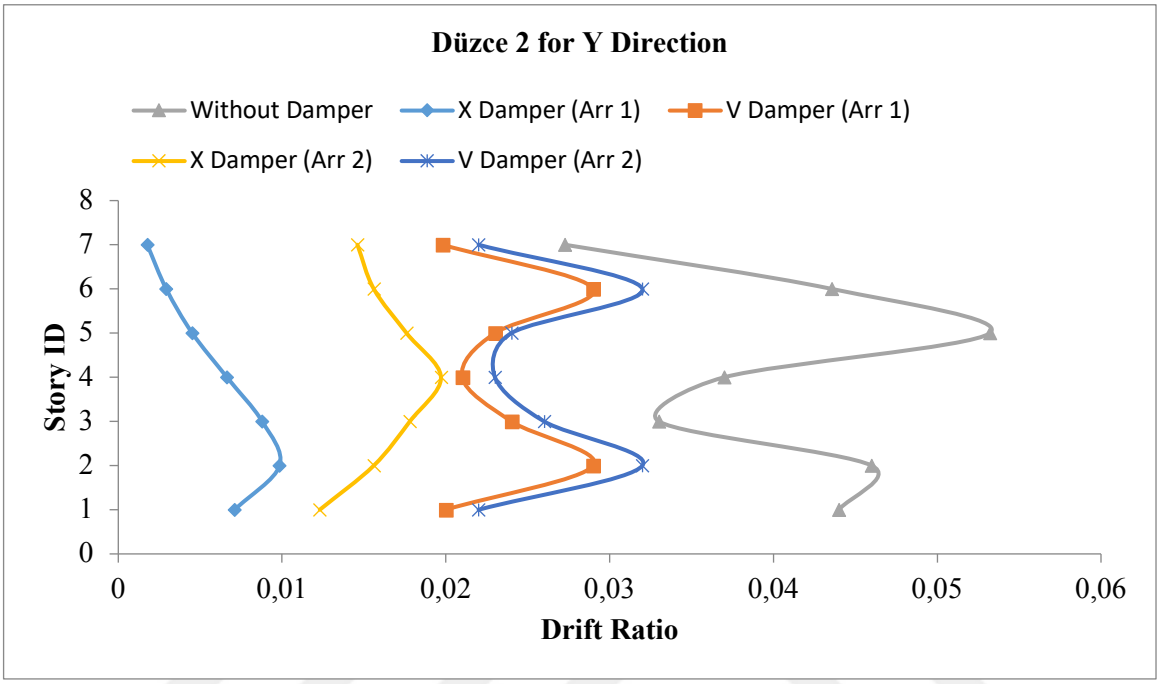


Figure 4.43 The Results of Drift Ratio for Düzce 2 Earthquake at Y-Direction

According to the drift ratios results, it is obvious that using friction damper with X configuration reduces the story drifts significantly in comparison to the inverted V configuration. In some cases, using inverted V configuration exceeds the values of the structure without dampers and at most of the cases the values are in less difference with the bare structure.

Also Figure 4.44 displays the maximum base shear of the structure under different ground motions. The light blue columns show the base share using X damper arrangement 1 in different earthquake records, and it's obvious, using friction damper with X configuration leads to the considerable reduction in base shear.

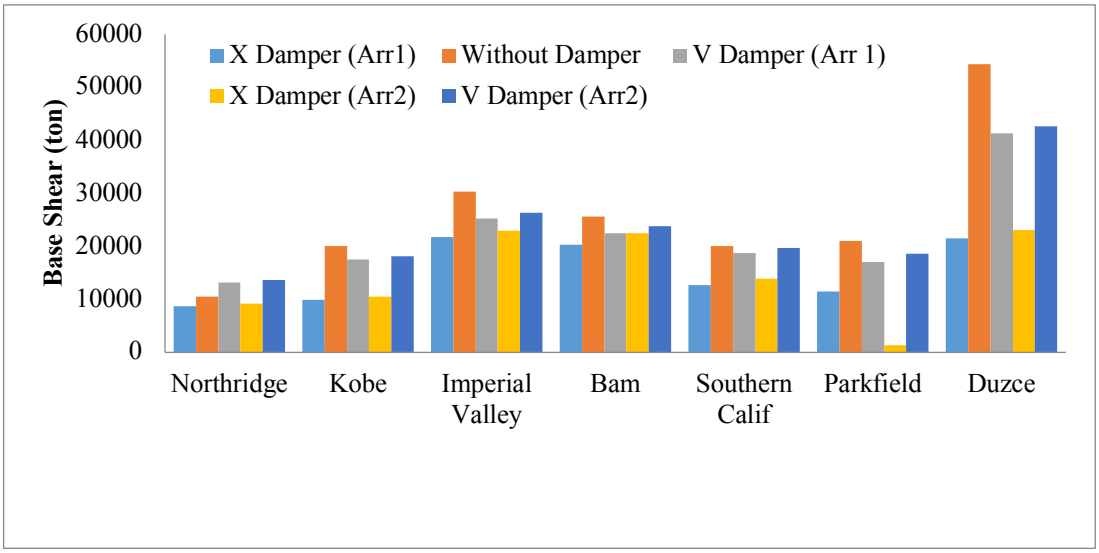


Figure 4.44 The Results of Maximum Base Shear Under Different Ground Motions

The Values of Figure 4.44 also have been summarized in Table 4.16.

Table 4.16 The Values of Maximum Base Shear Under Different Earthquakes

		Arrangement (1)		Arrangement (2)	
Earthquake	**Without Damper**	**With X Damper**	**With V Damper**	**With X Damper**	**With V Damper**
Northridge	10510	8750	13200	9160	13620
Kobe	20090	9860	17500	10540	18100
Imperial Valley	30270	21690	25300	22980	26350
Bam	25670	20320	22530	22450	23780
Southern Calif	20040	12650	18760	13890	19650
Parkfield	20970	11450	17060	1301	18660
Düzce	54320	21500	41250	23050	42650

4.3 Elimination of Dampers

Another option studied, is the elimination of dampers at the first story. The results of maximum story drifts at each story, maximum base shears, internal attempts at the first and last stories and the maximum axial forces of dampers are presented at the below tables. The Drift Ratio of elimination of damper is compared with the drift ratio of without damper, X damper (Arr 1&2) V damper (Arr 1&2) which are shown in figure 4.45 to 4.72.
Table 4.17 to 4.30 displays the maximum values of story drifts with the elimination of dampers at the first stories.

Table 4.17. The Maximum of Story Drifts Values Under Northridge 1 Earthquake with Elimination of Dampers from At The 1st Story

Northridge 1						
Story ID	**Without Damper**		**X Damper**		**V Damper**	
	X Drifts	**Y Drifts**	**X Drifts**	**Y Drifts**	**X Drifts**	**Y Drifts**
Story 7	0.0044	0.0022	0.0022	0.0020	0.0024	0.0024
Story 6	0.0045	0.0034	0.0033	0.0028	0.0035	0.0035
Story 5	0.0045	0.0048	0.0041	0.0032	0.0042	0.0046
Story 4	0.0052	0.0056	0.0046	0.0041	0.0048	0.0054
Story 3	0.0052	0.0058	0.0047	0.0038	0.0049	0.0055
Story 2	0.0045	0.0063	0.0038	0.0029	0.0039	0.0055
Story 1	0.0031	0.0042	0.0027	0.0017	0.0030	0.0039

For the elimination of dampers at the first story, Figure 4.45 shows the comparison of drift ratio with the other arrangements that the X damper elimination has almost same value as the X damper arrangement 1, and also the V damper elimination is at the same graph line as V damper arrangement 1. Therefore, the elimination of dampers under the Northridge earthquake at the first story didn't bring much changes in the drift ratio of the X direction. While in the Y direction as shown in Figure 4.46 the X damper arrangement 1and X damper elimination drift are the exact values and located at the same line.

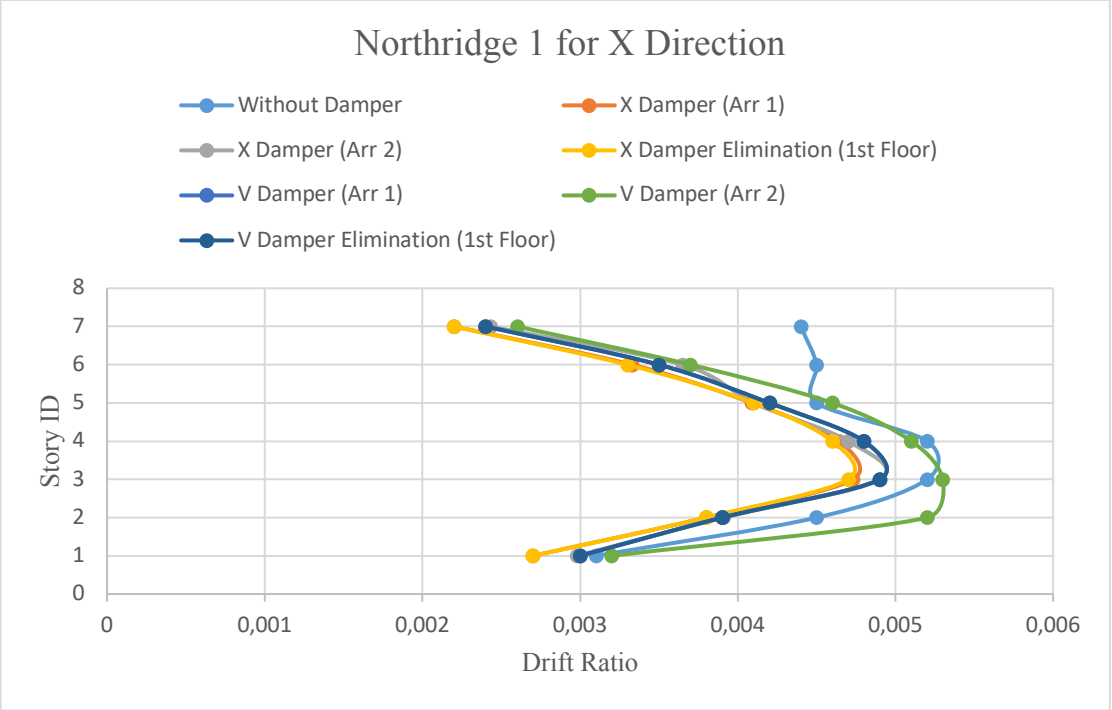


Figure 4.45 The Results of Drift Ratio for Northridge 1 Earthquake at X Direction

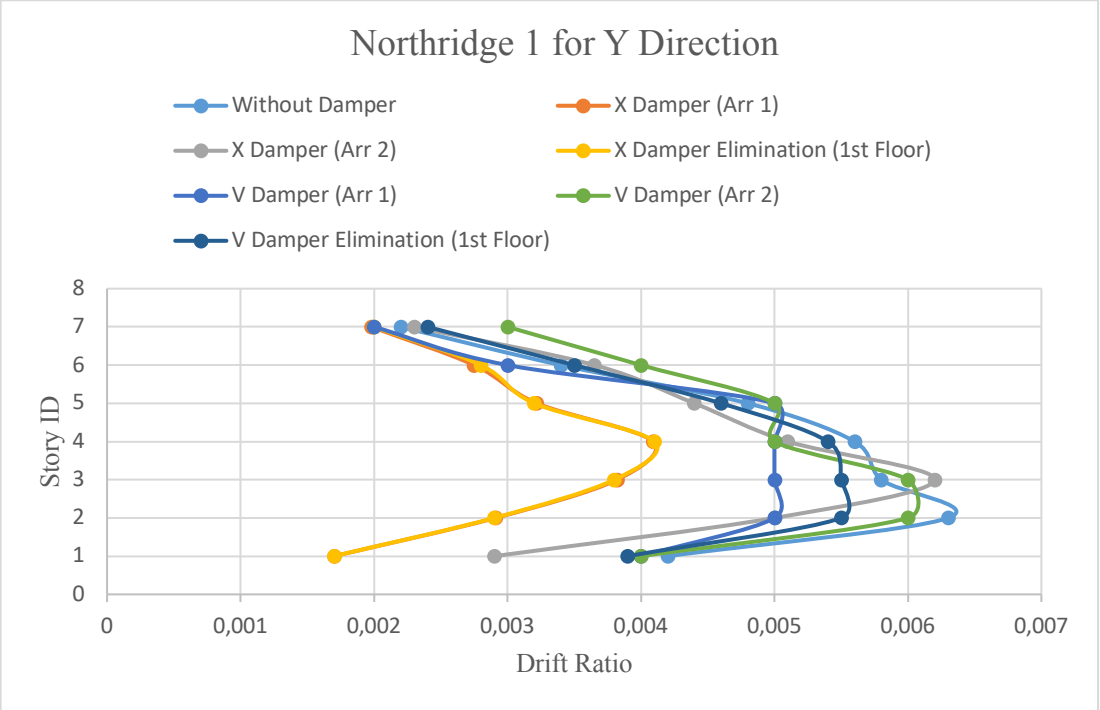


Figure 4.46 The Results of Drift Ratio for Northridge 1 Earthquake at Y Direction

Table 4.18. The Maximum of Story Drifts Values Under Northridge 2 Earthquake with Elimination of Dampers at the 1st Story

Northridge 2						
Story ID	**Without Damper**		**X Damper**		**V Damper**	
	X Drifts	**Y Drifts**	**X Drifts**	**Y Drifts**	**X Drifts**	**Y Drifts**
Story 7	0.0038	0.0032	0.0015	0.0030	0.0016	0.0022
Story 6	0.0058	0.0042	0.0025	0.0040	0.0026	0.0039
Story 5	0.0072	0.0046	0.0037	0.0042	0.0038	0.0043
Story 4	0.0076	0.0053	0.0046	0.0050	0.0050	0.0050
Story 3	0.0088	0.0060	0.0054	0.0056	0.0063	0.0057
Story 2	0.0089	0.0058	0.0058	0.0053	0.0070	0.0062
Story 1	0.0055	0.0031	0.0043	0.0025	0.0050	0.0039

The elimination of dampers at the first story under the Northridge 2 earthquake as shown in Figure 4.47 shows the comparison of drift ratio with the other arrangements that the X damper elimination has almost same value as the X damper arrangement 1 at the 4th, 5th, 6th and 7th stories. And V damper elimination at the first located at the same points as the V damper arrangement 1 at the 4th, 5th, 6th and 7th Stories. But, at the Y direction the elimination of X damper and V dampers are having greater drift ratios than the other arrangements.

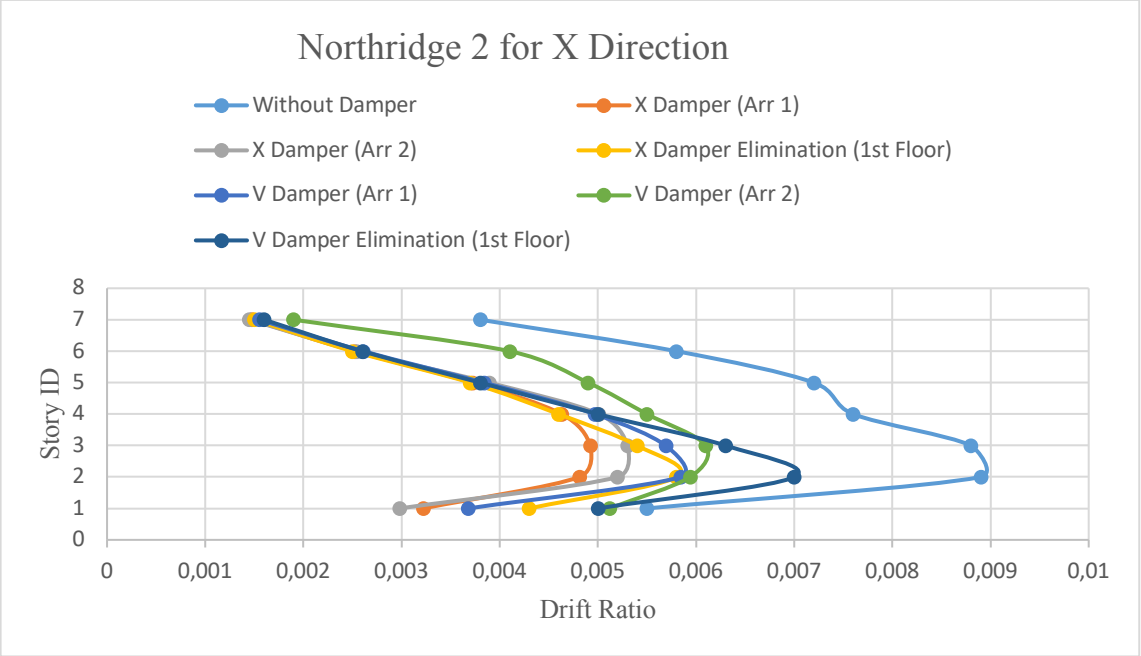


Figure 4.47 The Results of Drift Ratio for Northridge Earthquake 2 at X Direction

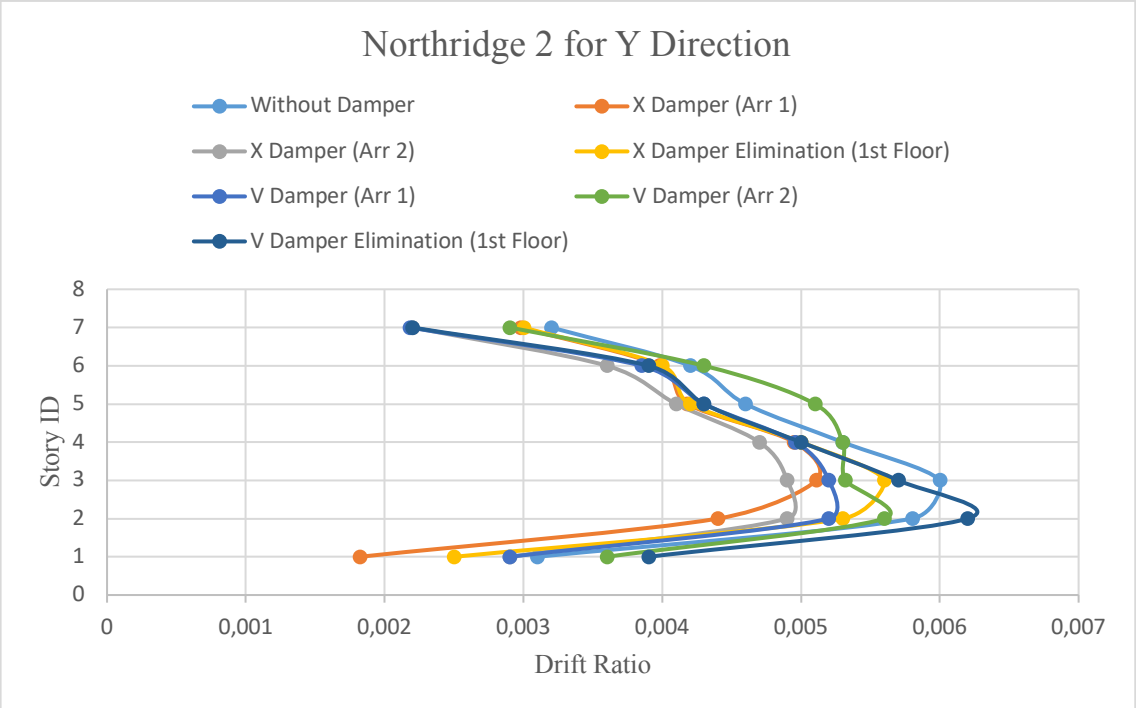


Figure 4.48 The Results of Drift Ratio for Northridge 2 Earthquake at Y Direction

Table 4.19 The Maximum of Story Drifts Values Under Kobe 1 Earthquake with Elimination of Dampers from 1st Story

Kobe 1						
Story ID	**Without Damper**		**X Damper**		**V Damper**	
	X Drifts	**Y Drifts**	**X Drifts**	**Y Drifts**	**X Drifts**	**Y Drifts**
Story 7	0.0124	0.0111	0.0031	0.0031	0.0063	0.0109
Story 6	0.0147	0.0137	0.0046	0.0047	0.0107	0.0146
Story 5	0.0138	0.0142	0.0055	0.0059	0.0121	0.0131
Story 4	0.0159	0.0145	0.0060	0.0064	0.0138	0.0116
Story 3	0.0192	0.0150	0.0067	0.0068	0.0163	0.0102
Story 2	0.0208	0.0144	0.0069	0.0062	0.0170	0.0106
Story 1	0.0147	0.0142	0.0065	0.0050	0.0128	0.0076

The elimination of dampers at the first story under the Kobe 1 earthquake as shown in Figure 4.49 shows that the elimination of X dampers and V dampers at the first story didn't bring any changes to the drift ration at the X direction of the structure as they are placed at the same lines in the below graph. And also, in the Y direction as shown in Figure 4.50 the drift ratios remained same as the X and V dampers arrangement 1.

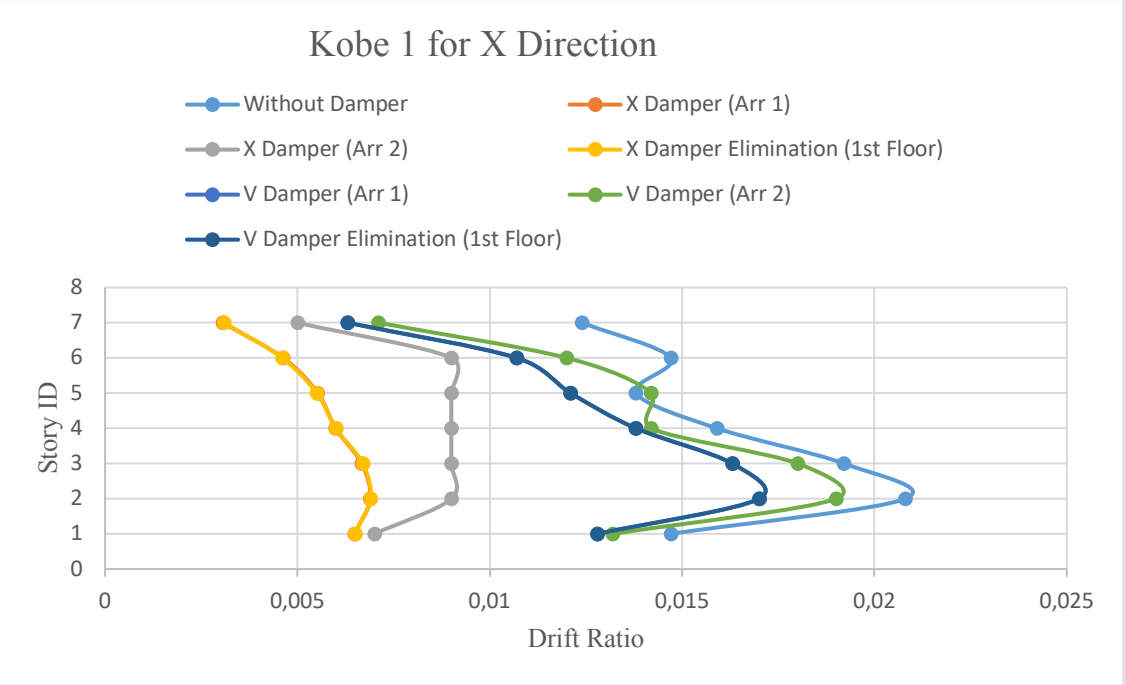


Figure 4.49 The Results of Drift Ratio for Kobe 1 Earthquake at X Direction

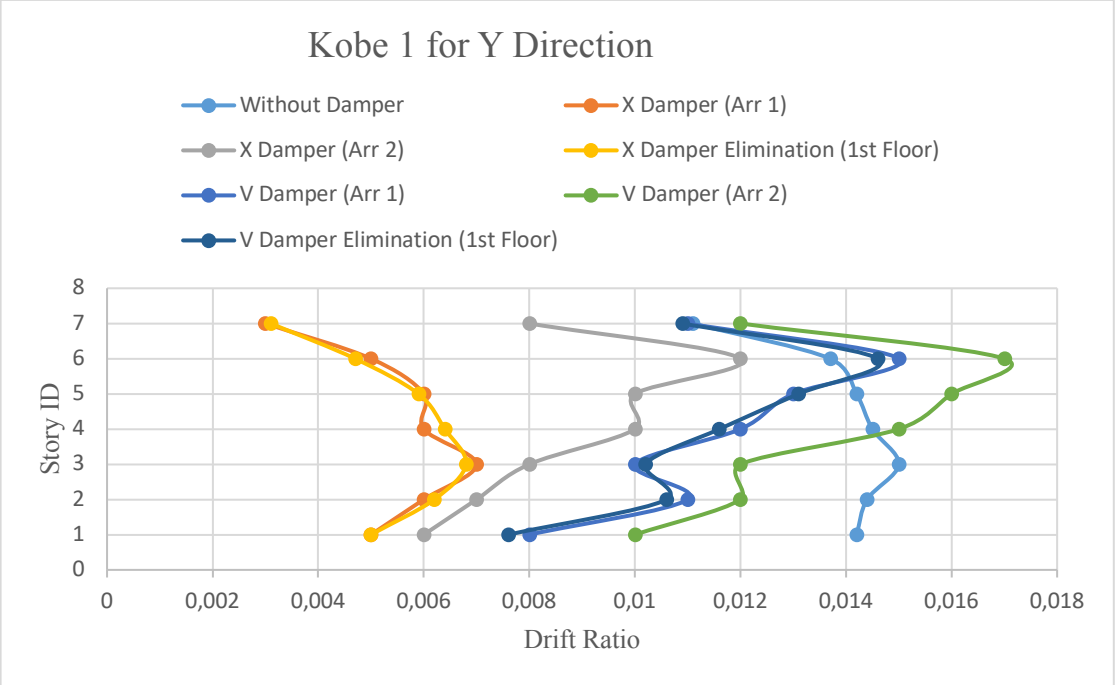


Figure 4.50 The Results of Drift Ratio for Kobe 1 Earthquake at Y Direction

Table 4.20 The Maximum of Story Drifts Values Under Kobe 2 Earthquake with Elimination of Dampers from 1st Story

Kobe 2						
Story ID	**Without Damper**		**X Damper**		**V Damper**	
	X Drifts	**Y Drifts**	**X Drifts**	**Y Drifts**	**X Drifts**	**Y Drifts**
Story 7	0.0126	0.0144	0.0025	0.0022	0.0053	0.0134
Story 6	0.0156	0.0153	0.0040	0.0030	0.0082	0.0194
Story 5	0.0136	0.0137	0.0054	0.0049	0.0106	0.0199
Story 4	0.0092	0.0142	0.0062	0.0063	0.0134	0.0178
Story 3	0.0097	0.0203	0.0078	0.0085	0.0181	0.0253
Story 2	0.0138	0.0213	0.0071	0.0089	0.0161	0.0347
Story 1	0.0126	0.0149	0.0041	0.0060	0.0109	0.0403

The elimination of dampers at the first story under the Kobe 2 earthquake as shown in Figure 4.51 shows the comparison of drift ratio with the other arrangements that the X damper elimination has almost same value as the X damper arrangement 1 at the 4th, 5th, 6th and 7th stories. And V damper elimination at the first located at the same points as the V

damper arrangement. also, at the Y direction shown in Figure 4.52 it acts the same as the X direction.

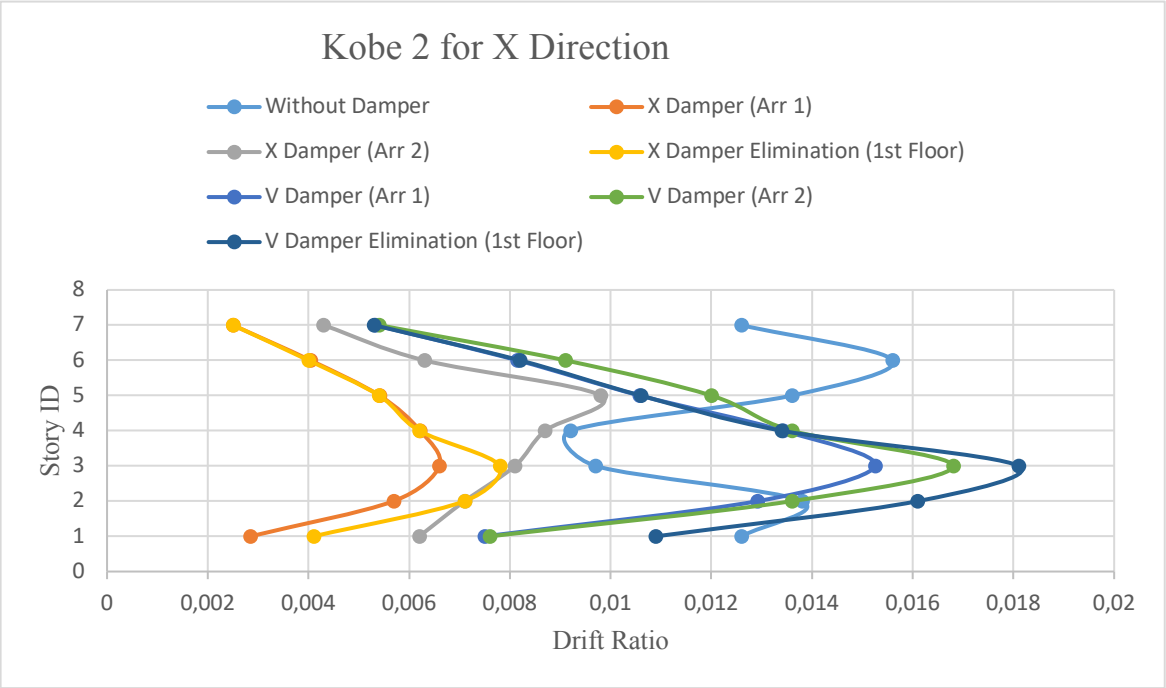


Figure 4.51 The Results of Drift Ratio for Kobe 2 Earthquake at X Direction

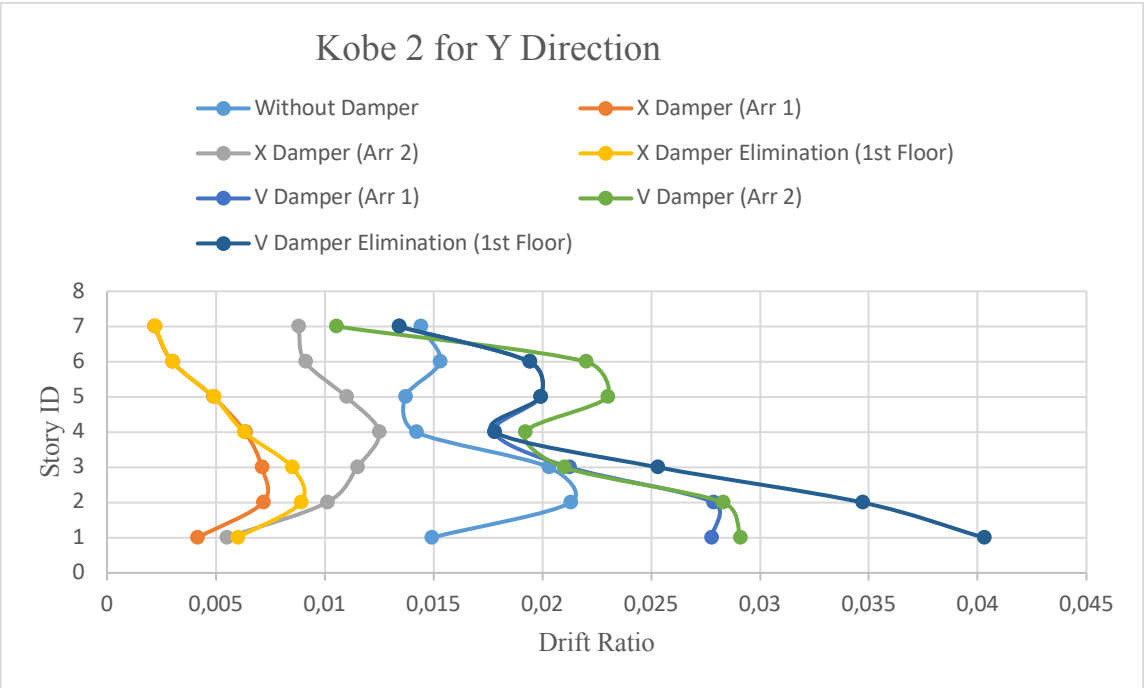


Figure 4.52 The Results of Drift Ratio for Kobe 2 Earthquake at Y Direction

Table 4.21 The Maximum of Story Drifts Values Under Imperial Valley 1 Earthquake with Elimination of Dampers from 1st Story

Imperial Valley 1						
Story ID	**Without Damper**		**X Damper**		**V Damper**	
	X Drifts	**Y Drifts**	**X Drifts**	**Y Drifts**	**X Drifts**	**Y Drifts**
Story 7	0.0174	0.0192	0.0018	0.0025	0.0100	0.0226
Story 6	0.0288	0.0382	0.0027	0.0038	0.0140	0.0405
Story 5	0.0492	0.0523	0.0033	0.0046	0.0188	0.0514
Story 4	0.0920	0.0935	0.0055	0.0067	0.0241	0.0562
Story 3	0.0921	0.1037	0.0079	0.0426	0.0248	0.0593
Story 2	0.0822	0.0591	0.0081	0.0410	0.0258	0.0556
Story 1	0.0773	0.0427	0.0055	0.0347	0.0159	0.0333

Elimination of X damper and V damper under the imperial valley 1 earthquake as shown in Figure 4.53 has the same drift ratio as the X damper arrangement 1 and V damper arrangement 1 as they are located at the same graph line. And same in the Y direction case shown in Figure 4.54.

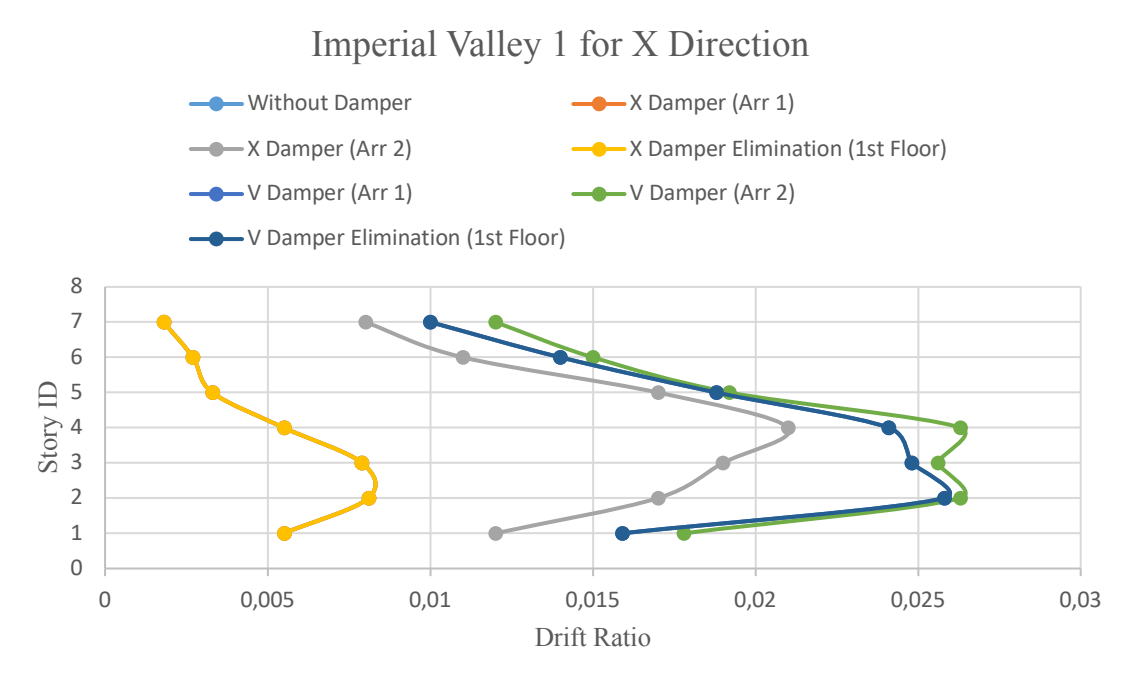


Figure 4.53 The Results of Drift Ratio for Imperial Valley 1 Earthquake at X Direction

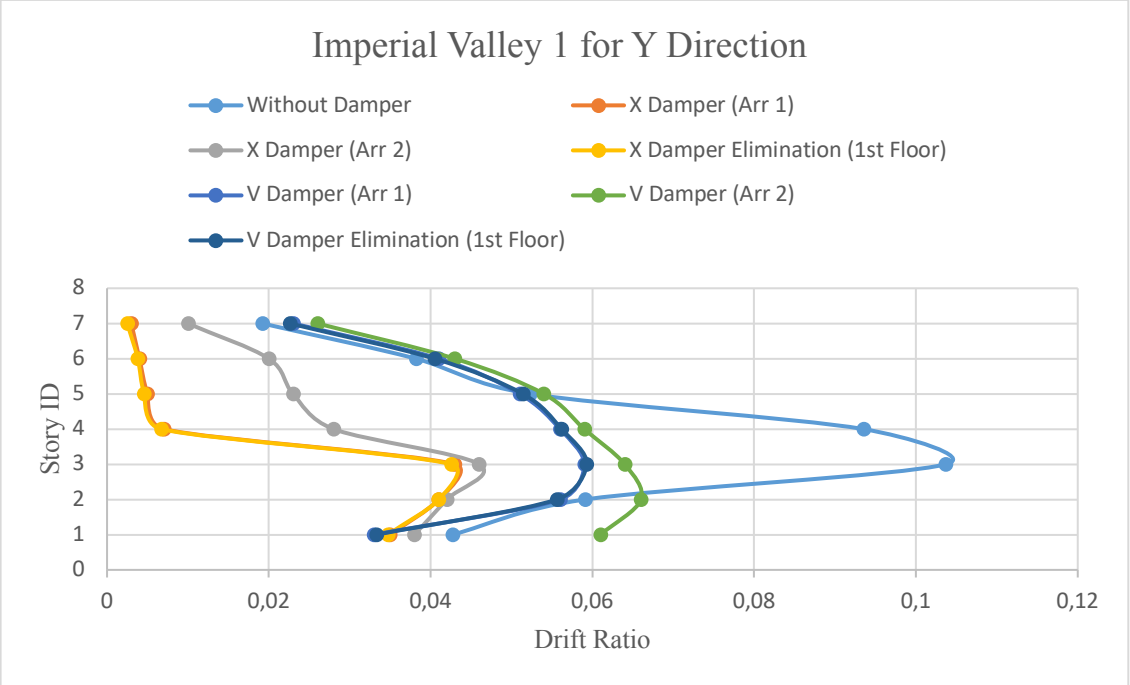


Figure 4.54 The Results of Drift Ratio for Imperial Valley 1 Earthquake at Y Direction

Table 4.22 The Maximum of Story Drifts Values Under Imperial Valley 2 Earthquake with Elimination of Dampers from 1st Story

Imperial Valley 2						
Story ID	**Without Damper**		**X Damper**		**V Damper**	
	X Drifts	**Y Drifts**	**X Drifts**	**Y Drifts**	**X Drifts**	**Y Drifts**
Story 7	0.0203	0.0146	0.0020	0.0028	0.0116	0.0170
Story 6	0.0436	0.0257	0.0032	0.0038	0.0262	0.0256
Story 5	0.0618	0.0269	0.0043	0.0043	0.0431	0.0320
Story 4	0.0820	0.0360	0.0059	0.0047	0.0519	0.0312
Story 3	0.0840	0.0336	0.0229	0.0083	0.0531	0.0327
Story 2	0.0673	0.0257	0.0262	0.0104	0.0555	0.0273
Story 1	0.0590	0.0245	0.0255	0.0071	0.0529	0.0283

Elimination of X damper and V damper under the imperial valley 2 earthquake as shown in Figure 4.55 has the same drift ratio as the X damper arrangement 1 and V damper arrangement 1 as they are located at the same graph line. And same in the Y direction case

shown in Figure 4.56. just in the first story the drift ratio of X damper arrangement 1 is smaller than the elimination of damper.

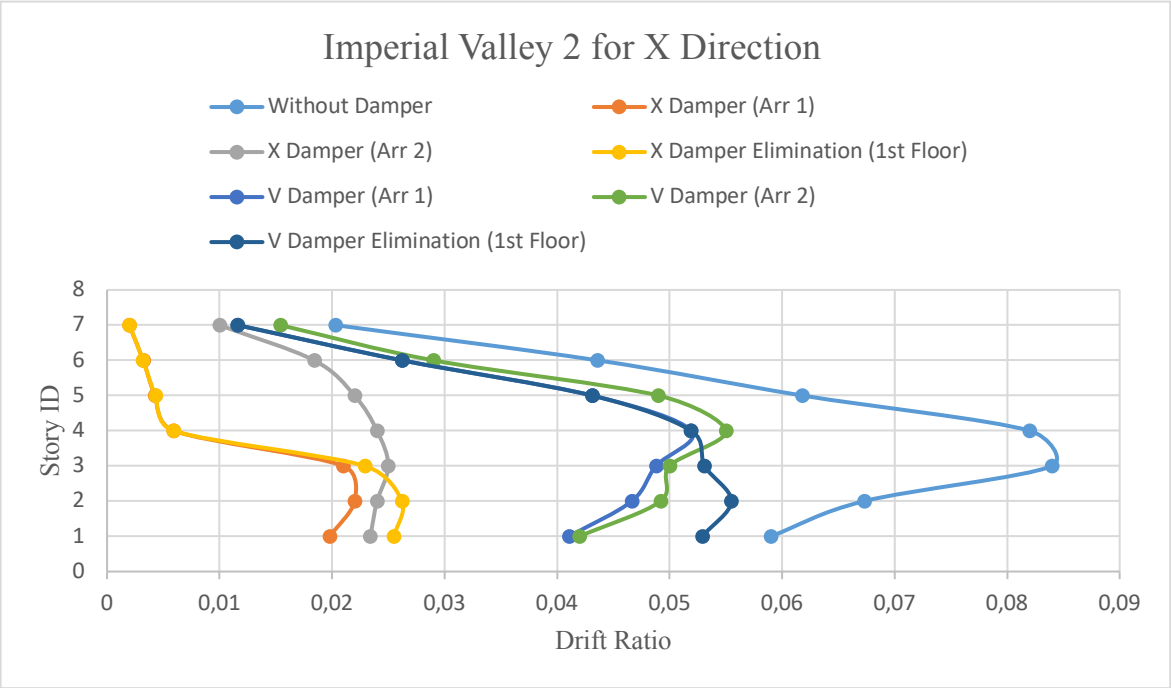


Figure 4.55 The Results of Drift Ratio for Imperial Valley 2 Earthquake at X Direction

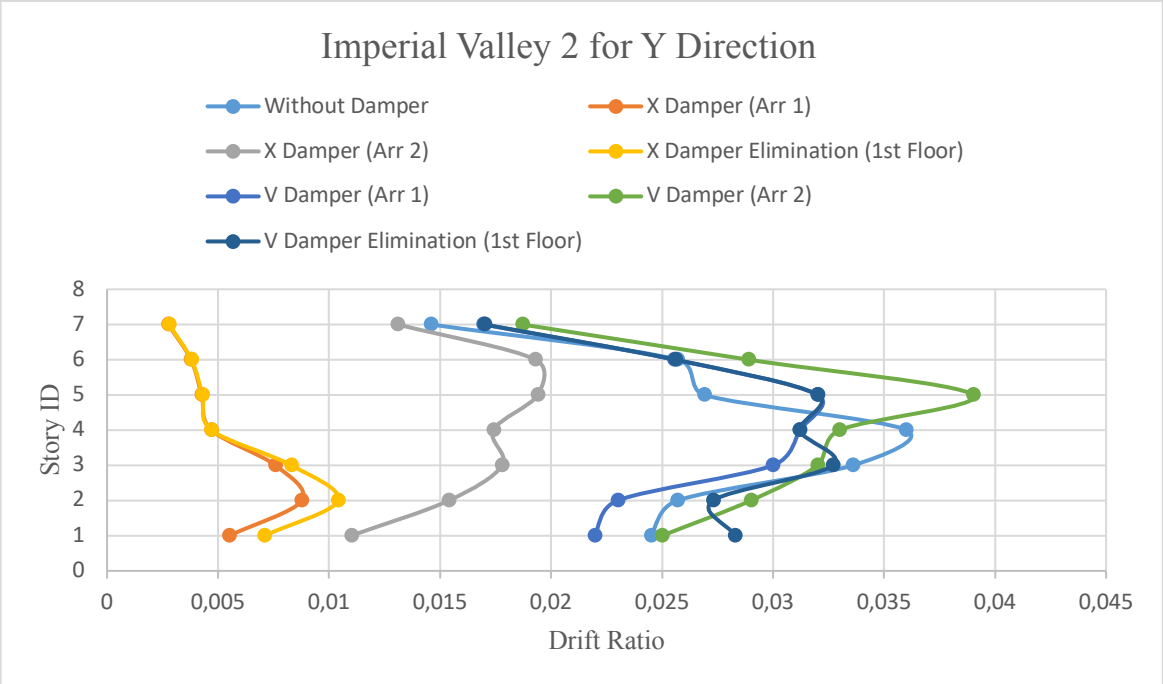


Figure 4.56 The Results of Drift Ratio for Imperial Valley 2 Earthquake at Y Direction

Table 4.23 The Maximum of Story Drifts Values Under Bam 1 Earthquake with Elimination of Dampers from 1st Story

Bam 1						
Story ID	**Without Damper**		**X Damper**		**V Damper**	
	X Drifts	**Y Drifts**	**X Drifts**	**Y Drifts**	**X Drifts**	**Y Drifts**
Story 7	0.0139	0.0088	0.0033	0.0014	0.0095	0.0088
Story 6	0.0248	0.0115	0.0051	0.0020	0.0159	0.0136
Story 5	0.0395	0.0211	0.0063	0.0025	0.0257	0.0188
Story 4	0.0547	0.0215	0.0077	0.0032	0.0355	0.0212
Story 3	0.0582	0.0221	0.0084	0.0034	0.0411	0.0210
Story 2	0.0641	0.0204	0.0079	0.0044	0.0466	0.0198
Story 1	0.0475	0.0144	0.0045	0.0020	0.0423	0.0135

Elimination of X damper and V damper under the Bam 1 earthquake as shown in Figure 4.57 has the same drift ratio as the X damper arrangement 1 and V damper arrangement 1 as they are located at the same graph line. And in the Y direction shown in Figure 4.58 at some stories the X damper drift ration is greater and at some stories the eliminated X damper ratios are smaller. But, for the V dampers they remained at the same drift ratios.

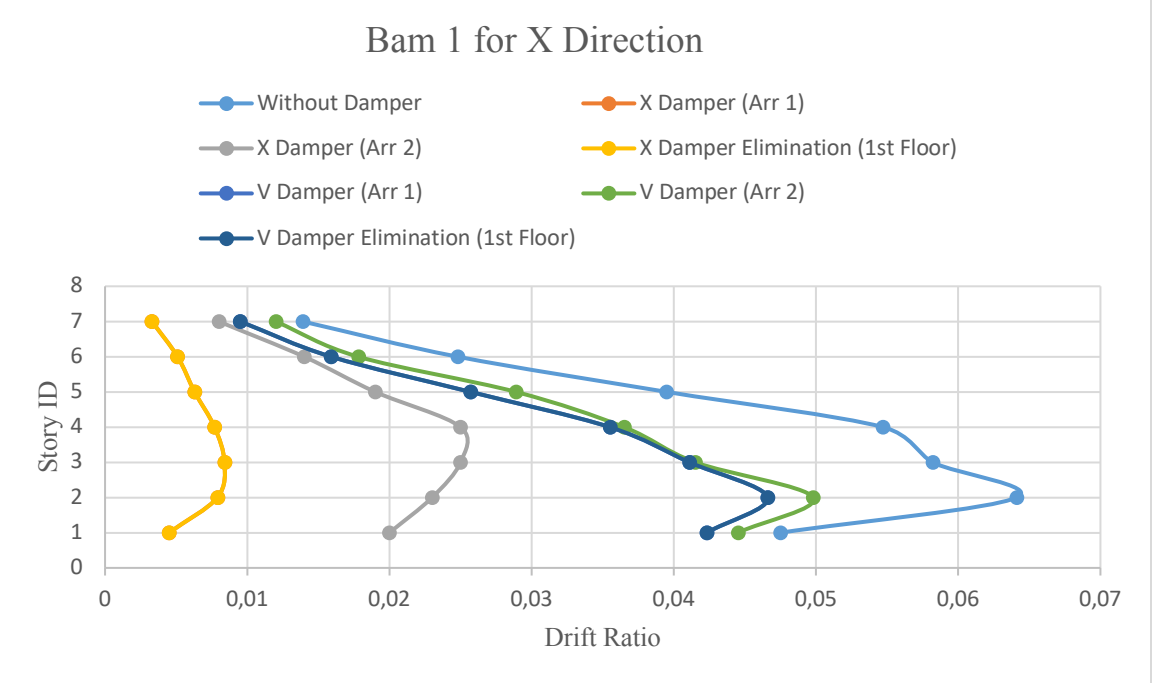


Figure 4.57 The Results of Drift Ratio for Bam 1 Earthquake at X Direction

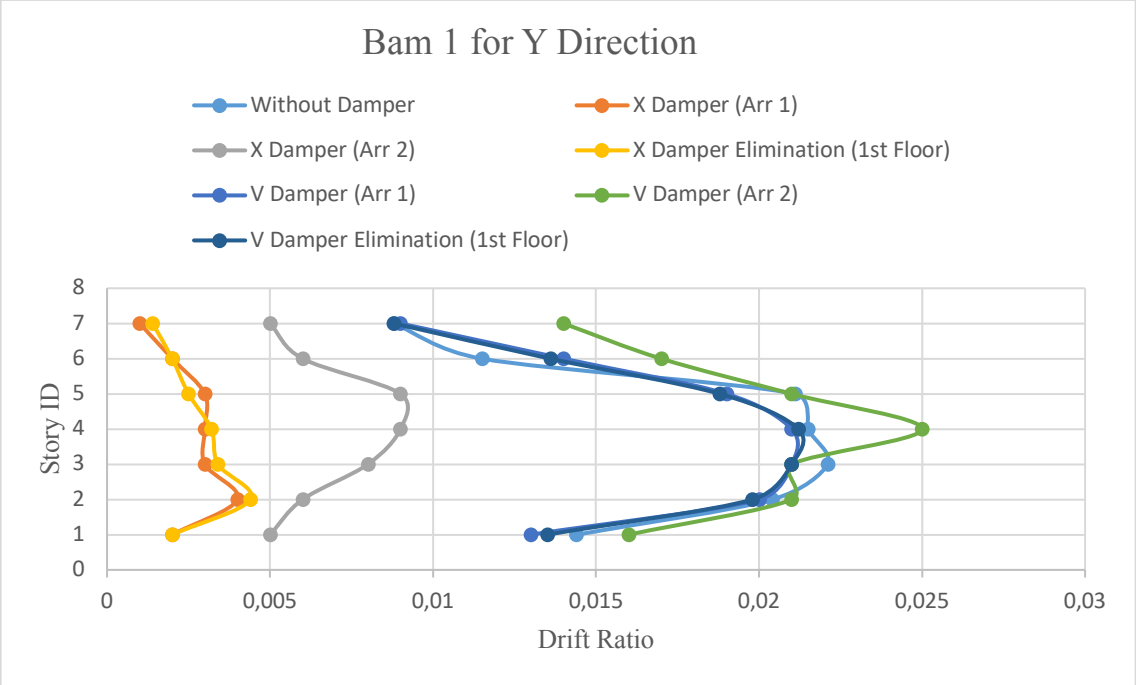


Figure 4.58 The Results of Drift Ratio for Bam 1 Earthquake at Y Direction

Table 4.24 The Maximum of Story Drifts Values Under Bam 2 Earthquake with Elimination of Dampers from 1st Story

Bam 1						
Story ID	**Without Damper**		**X Damper**		**V Damper**	
	X Drifts	**Y Drifts**	**X Drifts**	**Y Drifts**	**X Drifts**	**Y Drifts**
Story 7	0.0139	0.0088	0.0033	0.0014	0.0095	0.0088
Story 6	0.0248	0.0115	0.0051	0.0020	0.0159	0.0136
Story 5	0.0395	0.0211	0.0063	0.0025	0.0257	0.0188
Story 4	0.0547	0.0215	0.0077	0.0032	0.0355	0.0212
Story 3	0.0582	0.0221	0.0084	0.0034	0.0411	0.0210
Story 2	0.0641	0.0204	0.0079	0.0044	0.0466	0.0198
Story 1	0.0475	0.0144	0.0045	0.0020	0.0423	0.0135

Elimination of X damper and V damper under the Bam 2 earthquake as shown in Figure 4.59 has the same drift ratio as the X damper arrangement 1 at the 4thm 5th, 6th and 7th stories and neglectable differences in 1st, 2nd and 3rd stories. There are no drift ration changes for the V damper. And it is the same for the Y direction shown in Figure 4.60.

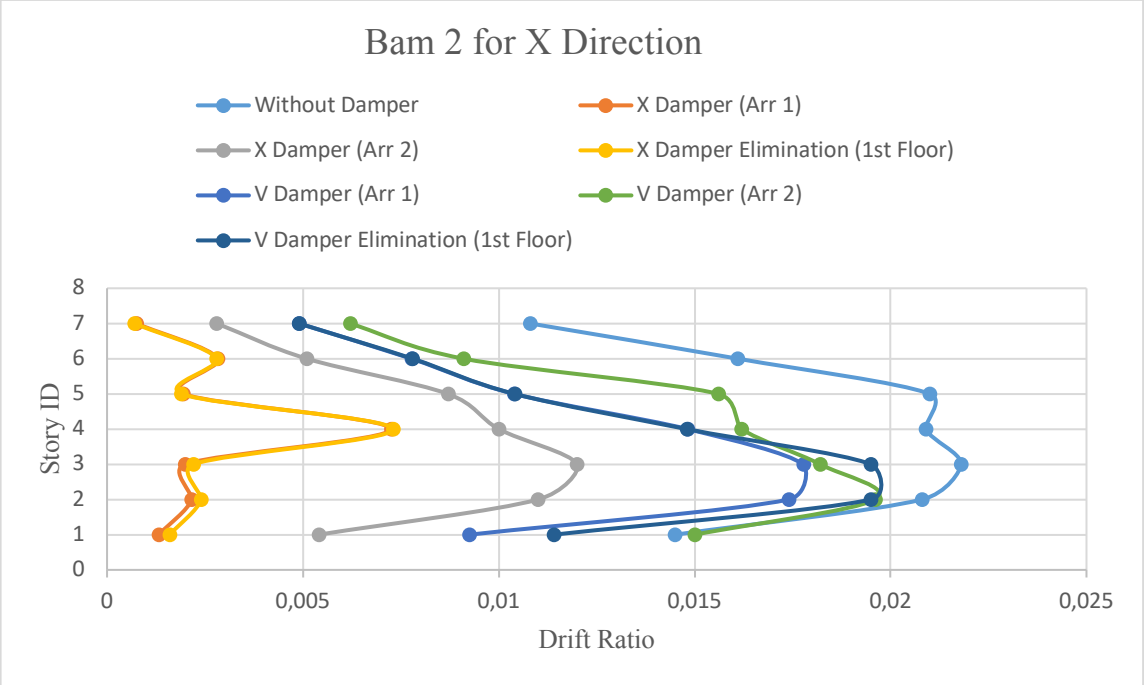


Figure 4.59 The Results of Drift Ratio for Bam 2 Earthquake at X Direction

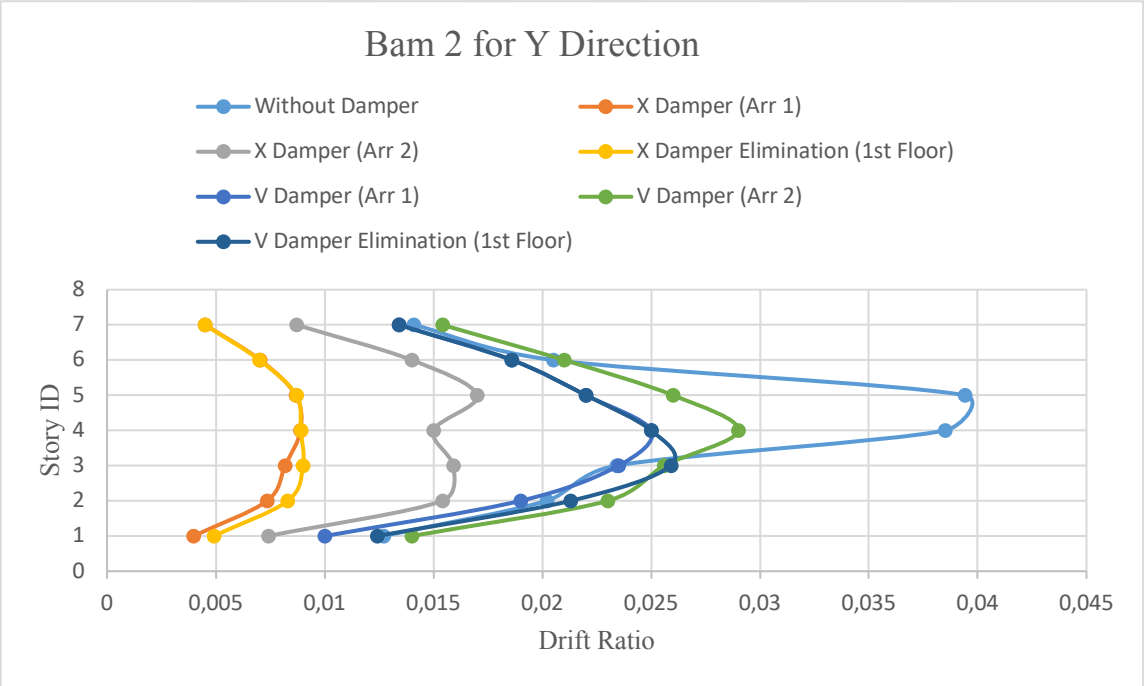


Figure 4.60 The Results of Drift Ratio for Bam 2 Earthquake at Y Direction

Table 4.25 The Maximum of Story Drifts Values Under Southern Calif 1 Earthquake with Elimination of Dampers from 1st Story

Southern Calif 1						
Story ID	Without Damper		X Damper		V Damper	
	X Drifts	Y Drifts	X Drifts	Y Drifts	X Drifts	Y Drifts
Story 7	0.0146	0.0159	0.0015	0.0013	0.0072	0.0151
Story 6	0.0240	0.0237	0.0027	0.0024	0.0155	0.0210
Story 5	0.0349	0.0292	0.0045	0.0039	0.0199	0.0240
Story 4	0.0373	0.0276	0.0066	0.0049	0.0254	0.0210
Story 3	0.0306	0.0301	0.0082	0.0057	0.0302	0.0220
Story 2	0.0303	0.0316	0.0090	0.0164	0.0300	0.0256
Story 1	0.0151	0.0238	0.0062	0.0043	0.0139	0.0198

Elimination of X damper and V damper under the Southern Calif 1 earthquake as shown in Figure 4.61 has the same drift ratio as the X damper arrangement 1 and V damper arrangement 1 as they are located at the same graph line. And in the Y direction shown in Figure 4.62 at some stories the X damper drift ration is greater and at some stories the eliminated X damper ratios are smaller. But, for the V dampers they remained at the same drift ratios.

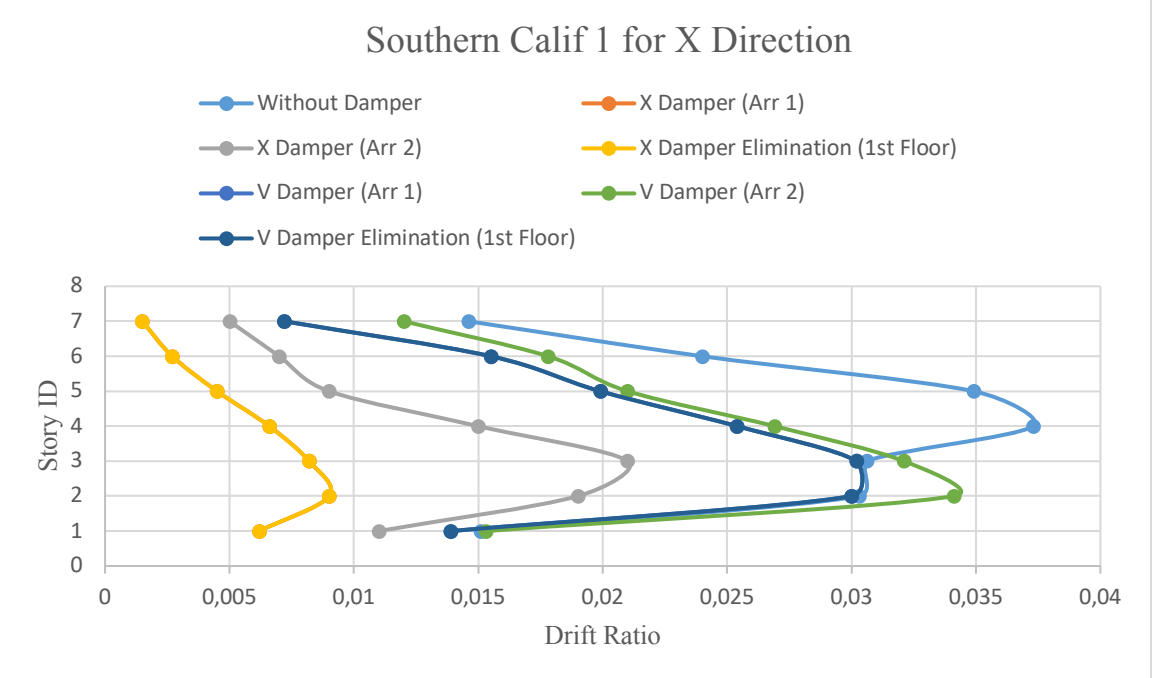


Figure 4.61 The Results of Drift Ratio for Southern Calif 1 Earthquake at X Direction

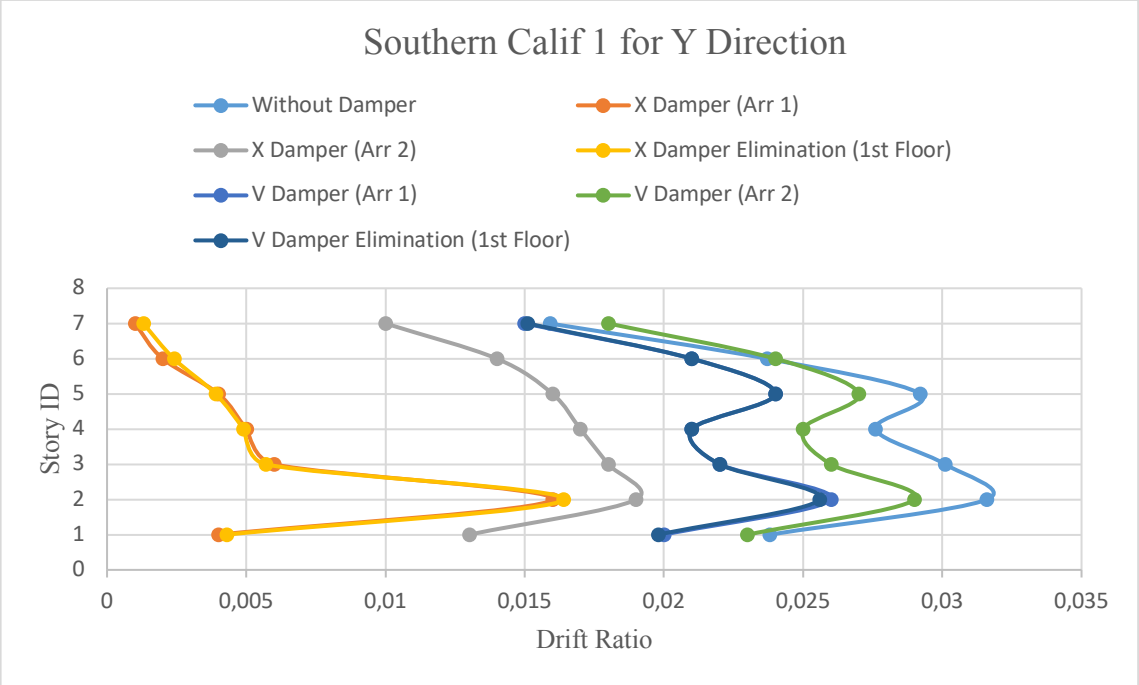


Figure 4.62 The Results of Drift Ratio for Southern Calif 1 Earthquake at Y Direction

Table 4.26 The Maximum of Story Drifts Values Under Southern Calif 2 Earthquake with Elimination of Dampers from 1st Story

Southern Calif 2						
Story ID	**Without Damper**		**X Damper**		**V Damper**	
	X Drifts	**Y Drifts**	**X Drifts**	**Y Drifts**	**X Drifts**	**Y Drifts**
Story 7	0.0150	0.0150	0.0014	0.0013	0.0073	0.0130
Story 6	0.0232	0.0243	0.0023	0.0024	0.0150	0.0221
Story 5	0.0362	0.0350	0.0039	0.0042	0.0216	0.0306
Story 4	0.0301	0.0323	0.0042	0.0067	0.0234	0.0210
Story 3	0.0295	0.0290	0.0167	0.0098	0.0260	0.0190
Story 2	0.0316	0.0190	0.0176	0.0115	0.0263	0.0197
Story 1	0.0252	0.0148	0.0162	0.0085	0.0268	0.0183

Elimination of X damper and V damper under the Southern Calif 2 earthquake as shown in Figure 4.63 has the same drift ratio as the X damper arrangement 1 and V damper arrangement 1 in all stories but 1st and 2nd story. And in the Y direction shown in Figure 4.63 at some stories the X damper drift ratio is changed at the 1st and 2nd stories while it has the same values at the other stories greater and at some stories the eliminated X damper ratios are smaller.

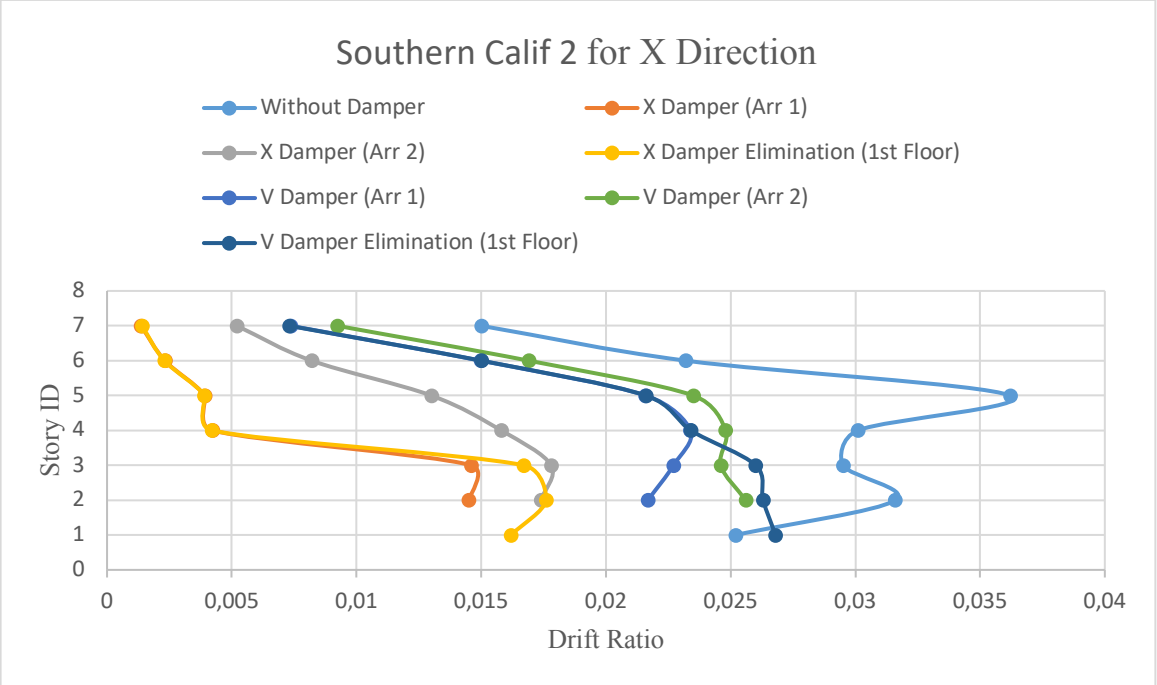


Figure 4.63 The Results of Drift Ratio for Southern Calif 2 Earthquake at X Direction

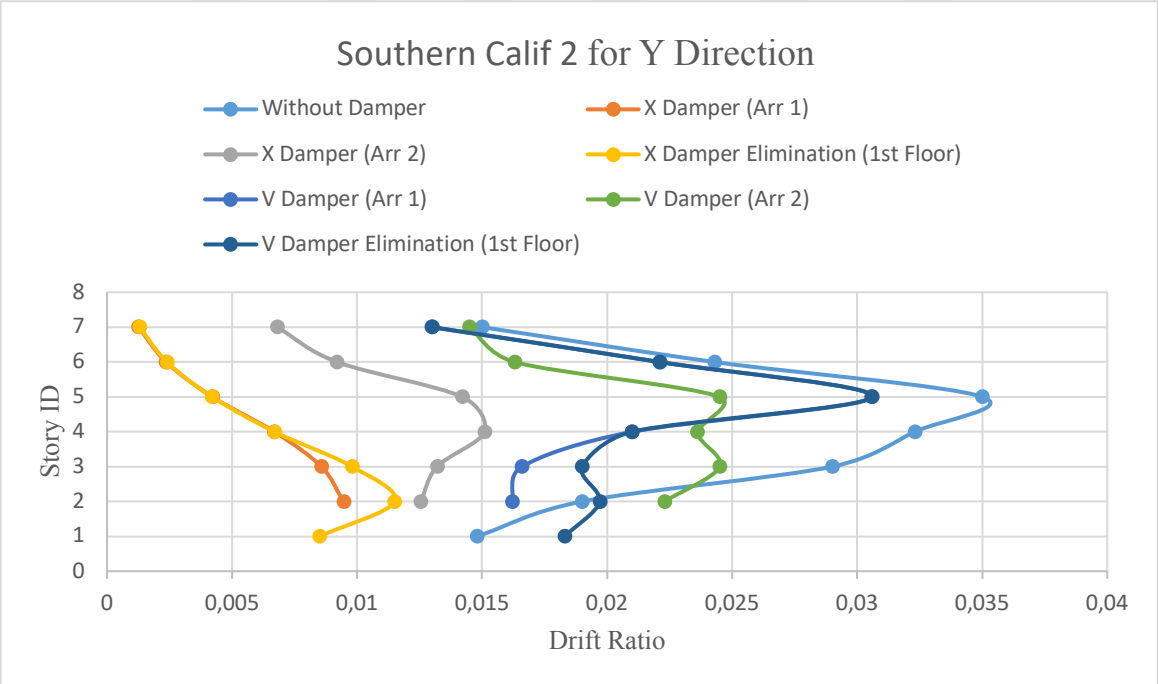


Figure 4.64 The Results of Drift Ratio for Southern Calif 2 Earthquake at Y Direction

Table 4.27 The Maximum of Story Drifts Values Under Parkfield 1 Earthquake with Elimination of Dampers from 1st Story

Parkfield 1						
Story ID	**Without Damper**		**X Damper**		**V Damper**	
	X Drifts	**Y Drifts**	**X Drifts**	**Y Drifts**	**X Drifts**	**Y Drifts**
Story 7	0.0155	0.0189	0.0007	0.0020	0.0082	0.0121
Story 6	0.0309	0.0288	0.0010	0.0025	0.0158	0.0232
Story 5	0.0472	0.0335	0.0023	0.0031	0.0256	0.0337
Story 4	0.0480	0.0445	0.0050	0.0038	0.0346	0.0391
Story 3	0.0460	0.0554	0.0081	0.0180	0.0396	0.0406
Story 2	0.0380	0.0450	0.0085	0.0130	0.0240	0.0391
Story 1	0.0260	0.0254	0.0065	0.0100	0.0225	0.0264

At the X direction for the X damper as shown in Figure 4.65, the X damper arrangement 1 and elimination of X damper at the 1st story is located at the same drift ratio line. but for the V dampers the elimination of V dampers has got greater drift ration than the V damper arrangement 1. And for the Y direction the drift ratios for both V damper elimination and X damper elimination as shown in Figure 4.65 are at the same points.

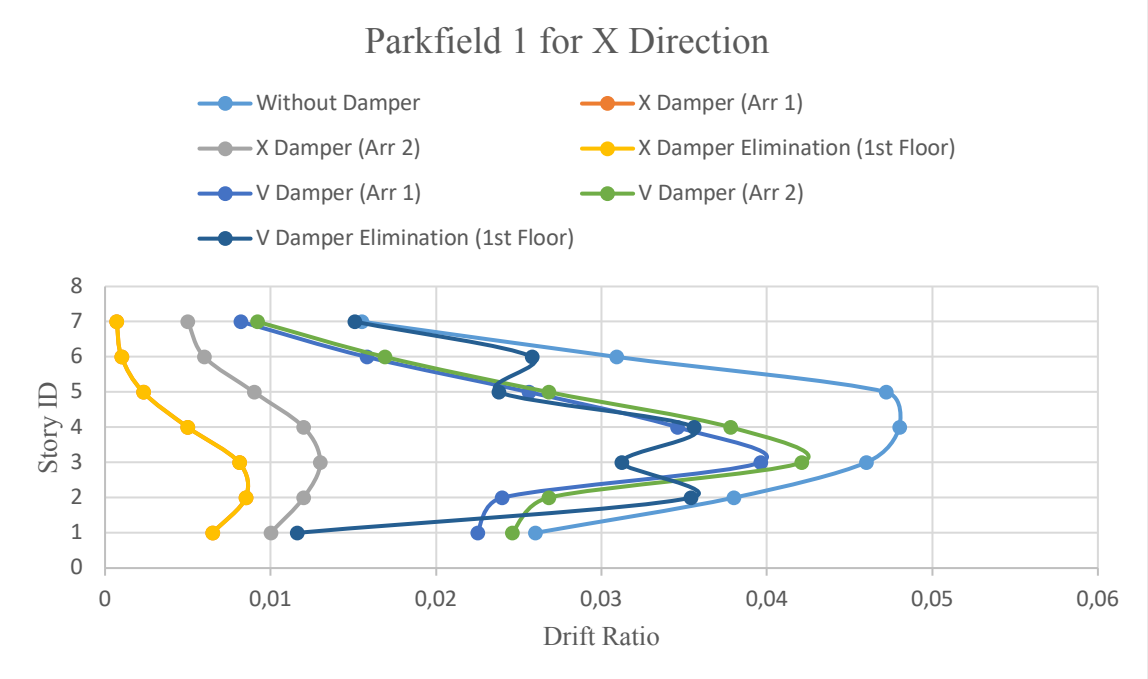


Figure 4.65 The Results of Drift Ratio for Parkfield 1 Earthquake at X Direction

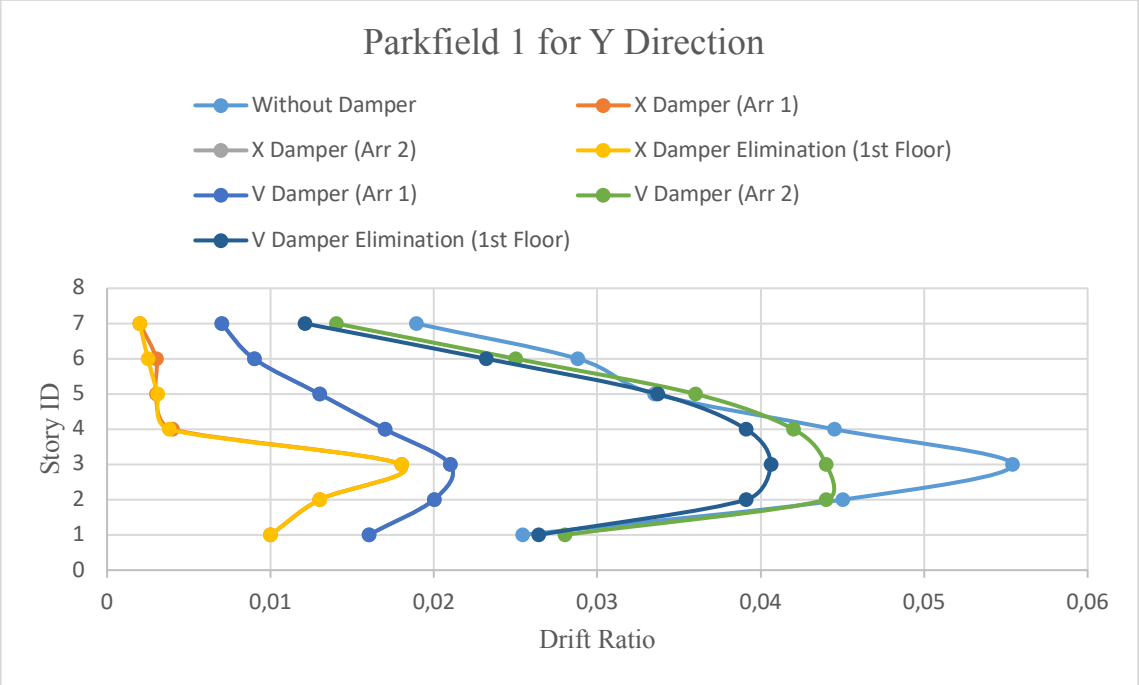


Figure 4.66 The Results of Drift Ratio for Parkfield 1 Earthquake at Y Direction

Table 4.28 The Maximum of Story Drifts Values Under Parkfield 2 Earthquake with Elimination of Dampers from 1st Story

Parkfield 2						
Story ID	**Without Damper**		**X Damper**		**V Damper**	
	X Drifts	**Y Drifts**	**X Drifts**	**Y Drifts**	**X Drifts**	**Y Drifts**
Story 7	0.0163	0.0099	0.0013	0.0012	0.0151	0.0099
Story 6	0.0357	0.0130	0.0019	0.0047	0.0258	0.0110
Story 5	0.0463	0.0196	0.0024	0.0087	0.0238	0.0150
Story 4	0.0462	0.0274	0.0029	0.0120	0.0356	0.0195
Story 3	0.0368	0.0284	0.0040	0.0115	0.0312	0.0247
Story 2	0.0356	0.0287	0.0110	0.0116	0.0354	0.0312
Story 1	0.0164	0.0255	0.0041	0.0017	0.0116	0.0243

At the X direction for the X damper as shown in Figure 4.67, the X damper arrangement 1 and elimination of X damper at the 1st story is located at the same drift ratio line with some differences at the 1st and 2nd stories. And for the V dampers the elimination of V dampers has got greater drift ratio at the 1st to the 4th stories and merged to the V damper

arrangement 1 at the upper stories. And they acted the same at the Y direction shown in Figure 4.68.

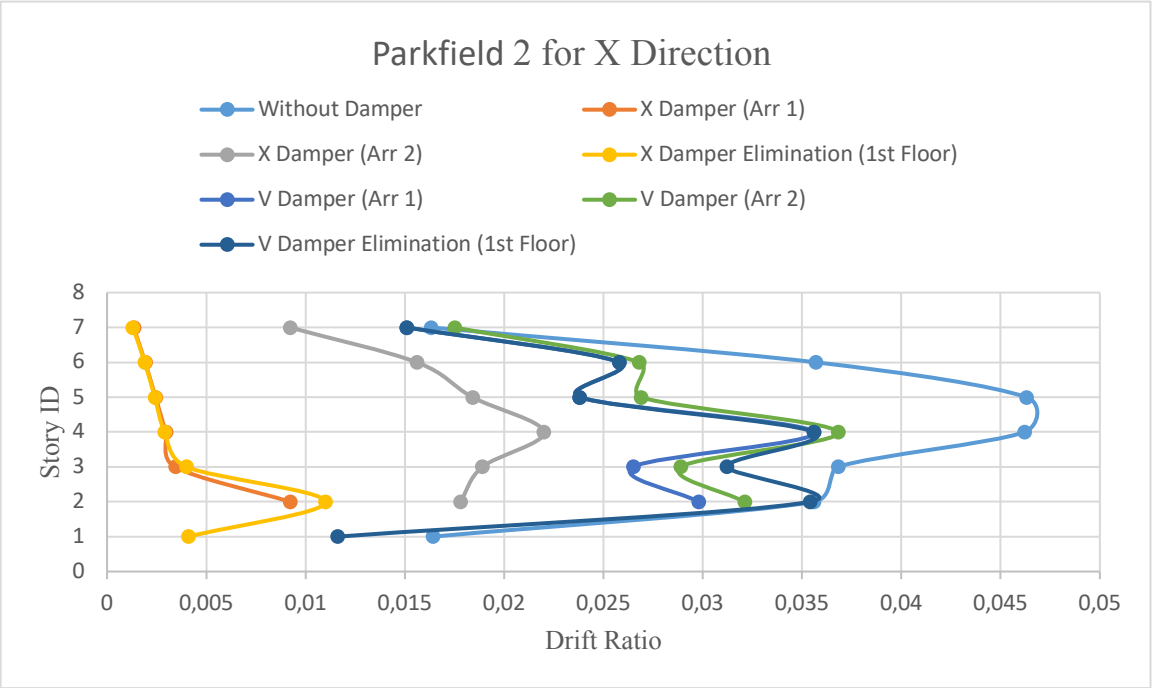


Figure 4.67 The Results of Drift Ratio for Parkfield 2 Earthquake at X Direction

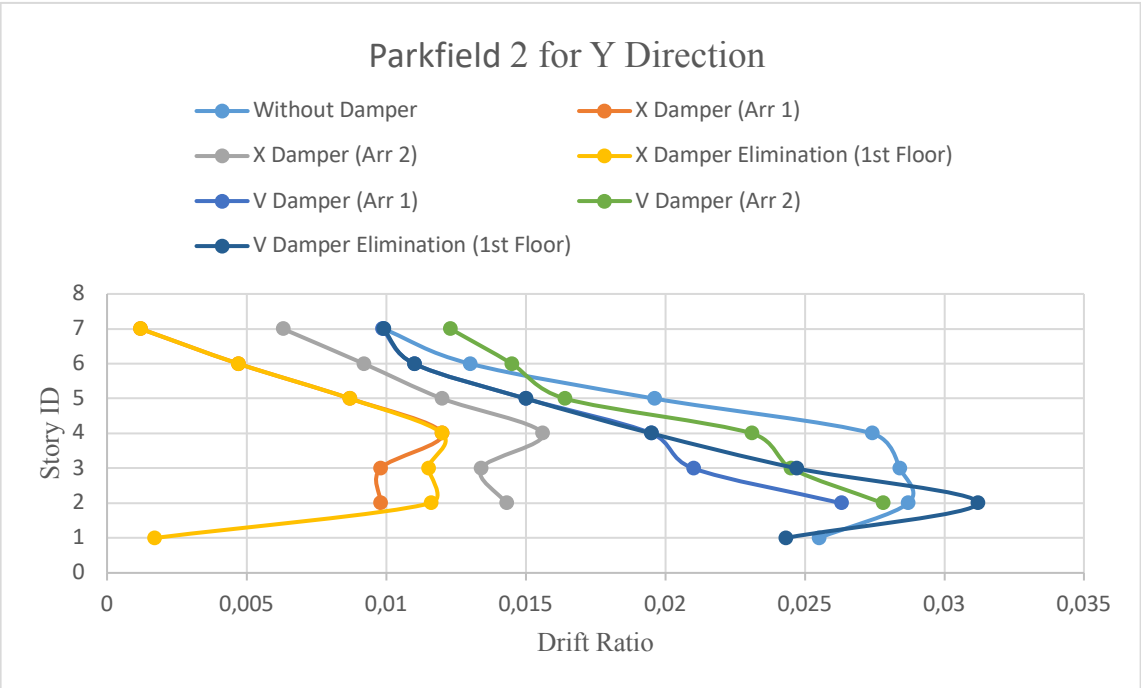


Figure 4.68 The Results of Drift Ratio for Parkfield 2 Earthquake at Y Direction

Table 4.29 The Maximum of Story Drifts Values Under Düzce 1 Earthquake with Elimination of Dampers from 1st Story

Düzce 1						
Story ID	**Without Damper**		**X Damper**		**V Damper**	
	X Drifts	**Y Drifts**	**X Drifts**	**Y Drifts**	**X Drifts**	**Y Drifts**
Story 7	0.0255	0.0111	0.0017	0.0006	0.0198	0.0101
Story 6	0.0340	0.0255	0.0029	0.0004	0.0210	0.0193
Story 5	0.0450	0.0410	0.0048	0.0014	0.0230	0.0281
Story 4	0.0460	0.0370	0.0071	0.0016	0.0294	0.0326
Story 3	0.0440	0.0360	0.0089	0.0048	0.0337	0.0338
Story 2	0.0420	0.0428	0.0093	0.0057	0.0204	0.0326
Story 1	0.0390	0.0439	0.0071	0.0083	0.0191	0.0220

The drift ratio of the elimination of X dampers at the first story of the X direction of the structure under the Düzce 1 earthquake shown if Figure 4.69 remained the same and located at the same line as the X damper arrangement 1. And the V damper elimination has close drift ratio as the V damper arrangement 2 and smaller than the V damper arrangement 1. For the Y direction shown in Figure 4.68 the drift ratios are so close and the same at some stories.

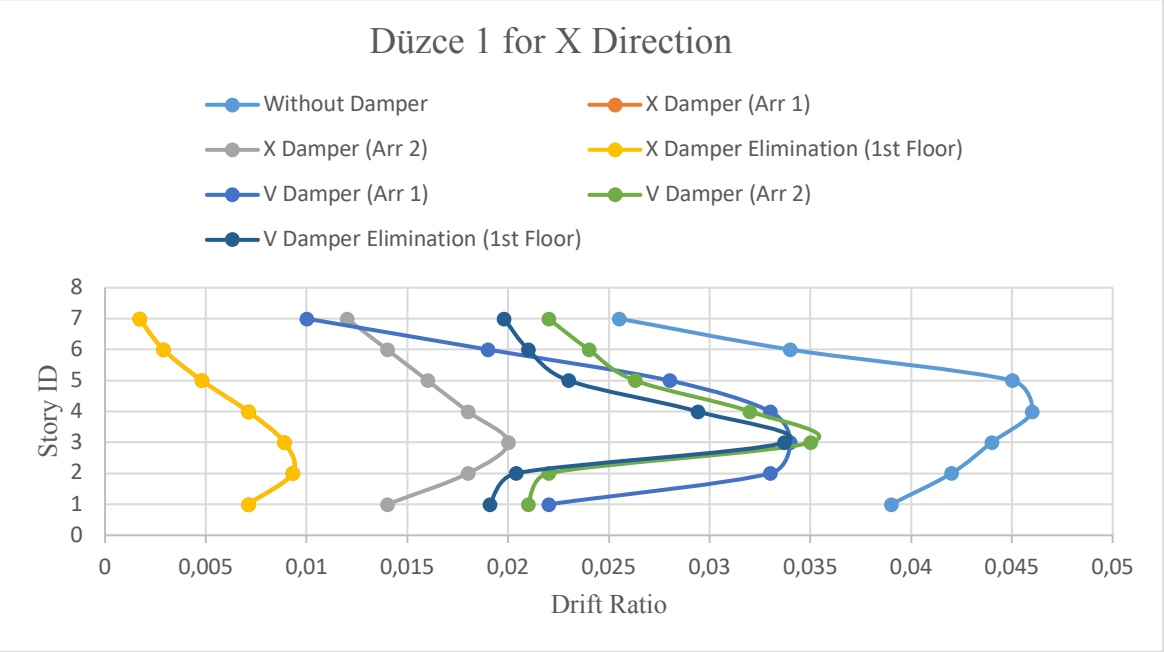


Figure 4.69 The Results of Drift Ratio for Düzce 1 Earthquake at X Direction

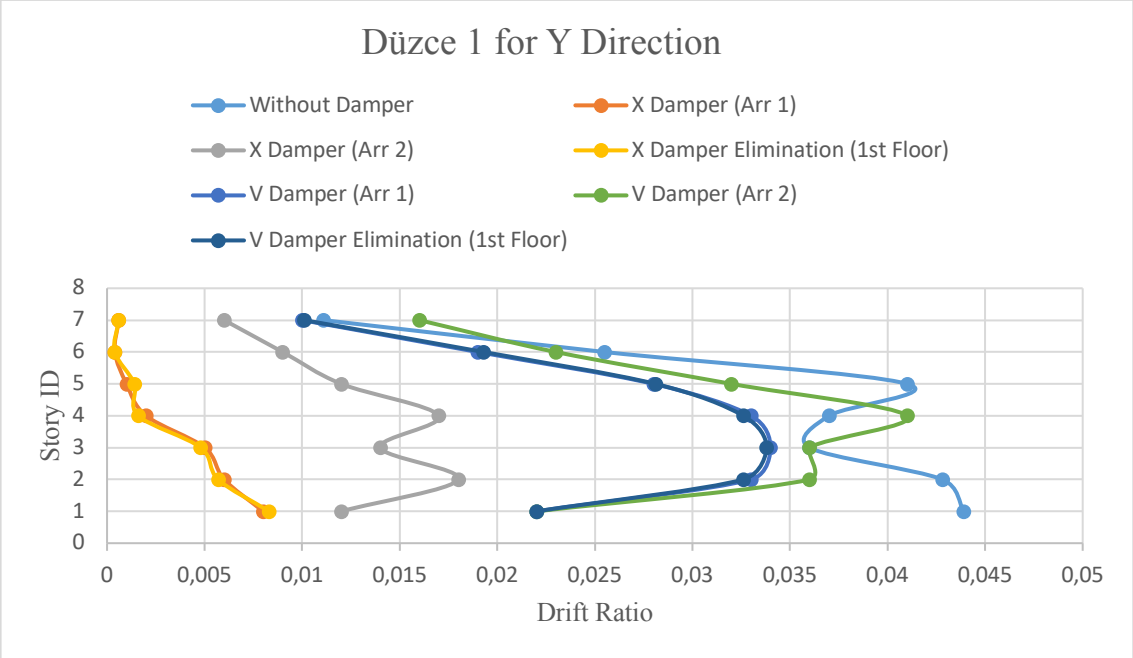


Figure 4.70 The Results of Drift Ratio for Düzce 1 Earthquake at Y Direction

Table 4.30 The Maximum of Story Drifts Values Under Düzce 2 Earthquake with Elimination of Dampers from 1st Story

Düzce 2						
Story ID	**Without Damper**		**X Damper**		**V Damper**	
	X Drifts	**Y Drifts**	**X Drifts**	**Y Drifts**	**X Drifts**	**Y Drifts**
Story 7	0.0253	0.0273	0.0003	0.0018	0.0142	0.0198
Story 6	0.0318	0.0436	0.0004	0.0029	0.0152	0.0290
Story 5	0.0575	0.0532	0.0009	0.0045	0.0198	0.0230
Story 4	0.0590	0.0370	0.0012	0.0066	0.0240	0.0210
Story 3	0.0339	0.0330	0.0042	0.0103	0.0247	0.0282
Story 2	0.0430	0.0460	0.0099	0.0117	0.0344	0.0344
Story 1	0.0390	0.0440	0.0087	0.0086	0.0231	0.0243

The drift ratio of the elimination of X dampers at the first story of the X direction of the structure under the Düzce 1 earthquake shown in Figure 4.71 remained the same and located at the same line as the X damper arrangement 1 with some differences at the 1st and 2nd stories. While the V damper elimination has bigger drift ratios at the 1st, 2nd and 3rd stories than the V damper arrangement 1 & 2 and emerged the V damper arrangement 1 at the 4th,

5th, 6th and 7th stories. At the Y direction the drift ration of X damper and X damper elimination crossed each other at the 4th, 5th, 6th and 7th stories with some differences at the 3 first stories.

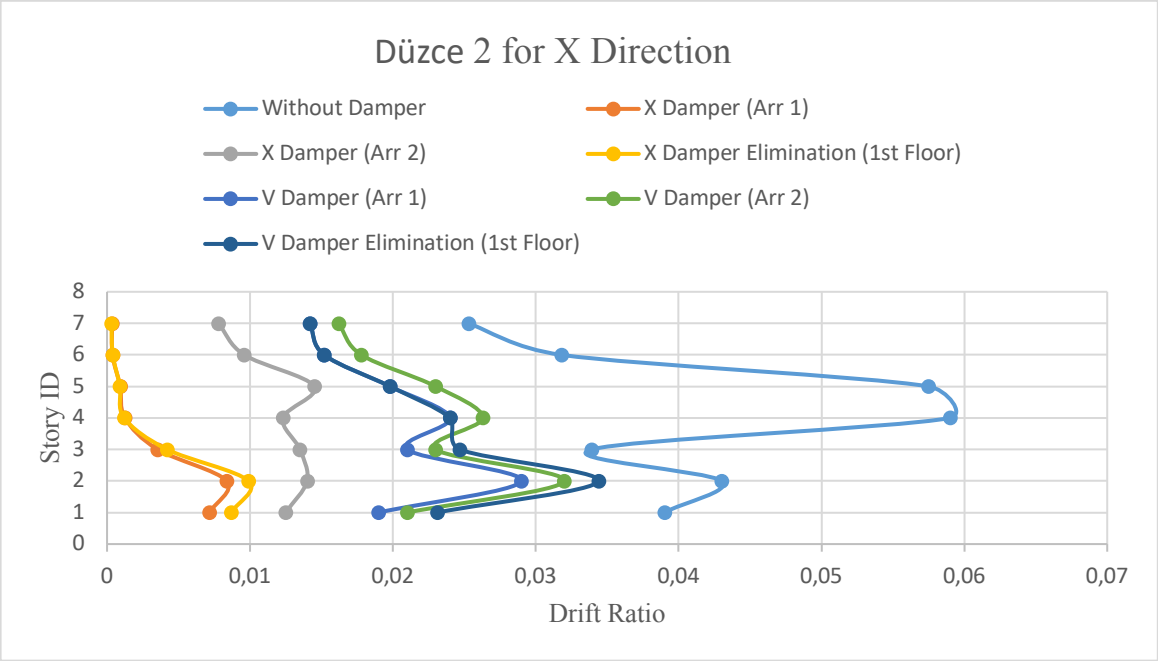


Figure 4.71 The Results of Drift Ratio for Düzce 2 Earthquake at X Direction

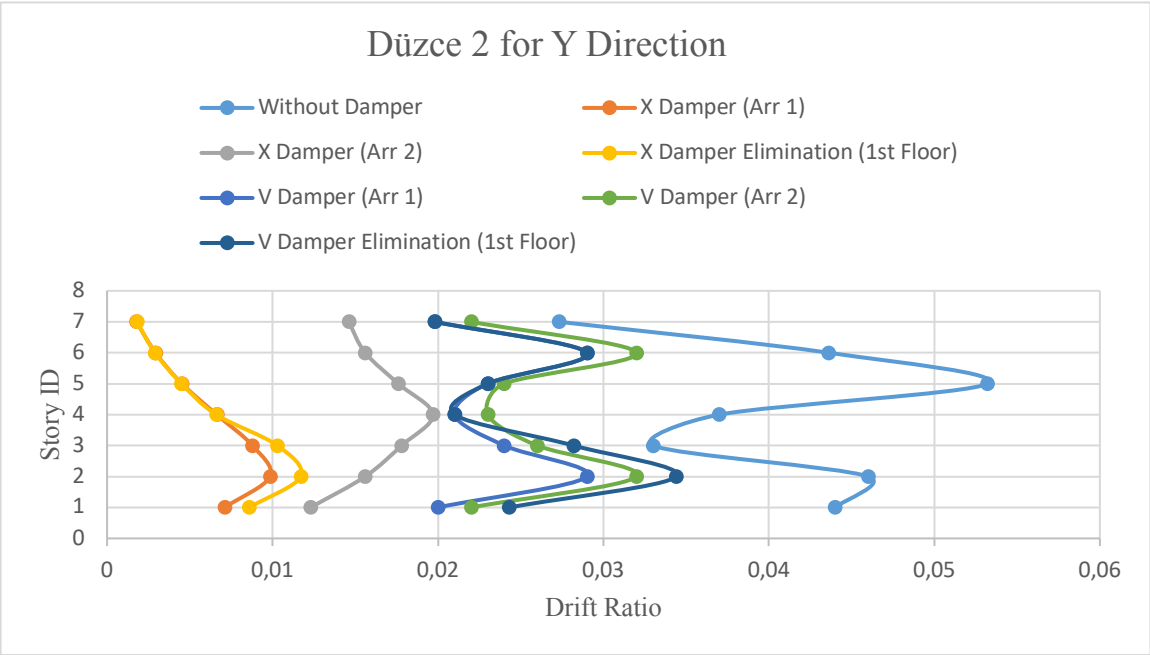


Figure 4.72 The Results of Drift Ratio for Düzce 2 Earthquake at Y Direction

With the comparison to the previous data obtained from NTHA, the values of story drifts increase about 30, 20 and 10 percent at the 1st, 2nd and 3rd stories, respectively with the omitting of dampers from 1st story.

Table 4.31 Displays the Maximum Values of Base Shears with The Elimination of Dampers at The First Stories.

Table 4.31 The Maximum Values of Base Shears with Elimination of Dampers 1st Story

With X Damper		With V Damper	
Normal Condition	**Omitted condition**	**Normal Condition**	**Omitted condition**
8750	9600	13200	15972
9860	13311	17500	21700
21690	26245	25300	29095
20320	22962	22530	26540
12650	17078	18760	21067
11450	16603	17060	18800
21500	30745	41250	46819

As it is obvious in Table 4.31, elimination of the dampers at story 1 affects the base shear values and increases it almost from 10 to 40 percent at different earthquake. The increasing is mainly because of the most portion of dampers story in absorbing the induced energy.

4.4 Further Comparison

To further study the effect of friction damper presence the beams and columns forces brace and dampers and braces maximum axial displacements and periods extracted. The labels of beams are depicted in Figure 4.73 to 4.79 for story 1, 2 and 7 respectively. Table 4.32 lists the fundamental period of the buildings.

Table 4.32. Fundamental Period of the Buildings

Without Damper	Arrangement (1)		Arrangement (2)	
	With X Damper	With V Damper	With X Damper	With V Damper
16.625	14.517	16.372	14.548	16.5

4.4.1 Beams Maximum Bending Moments at 1st , 2nd and 7th Story under 6 Different Earthquakes

The maximum bending moment of beams at the first, second and 7th stories are summarized in below tables for six different earthquakes. The tables show the maximum bending moment on a beam and minimum bending moment on a beam.

The below figures 4.73 – 4.79 shows the beam labels from different views and stories.

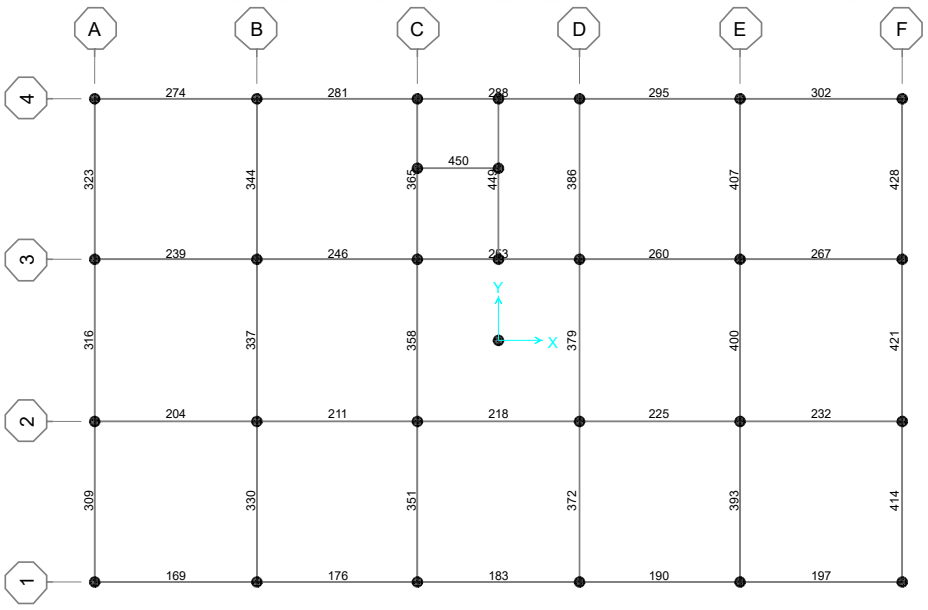


Figure 4.73. Beams Labels at the 1st Story – Top View

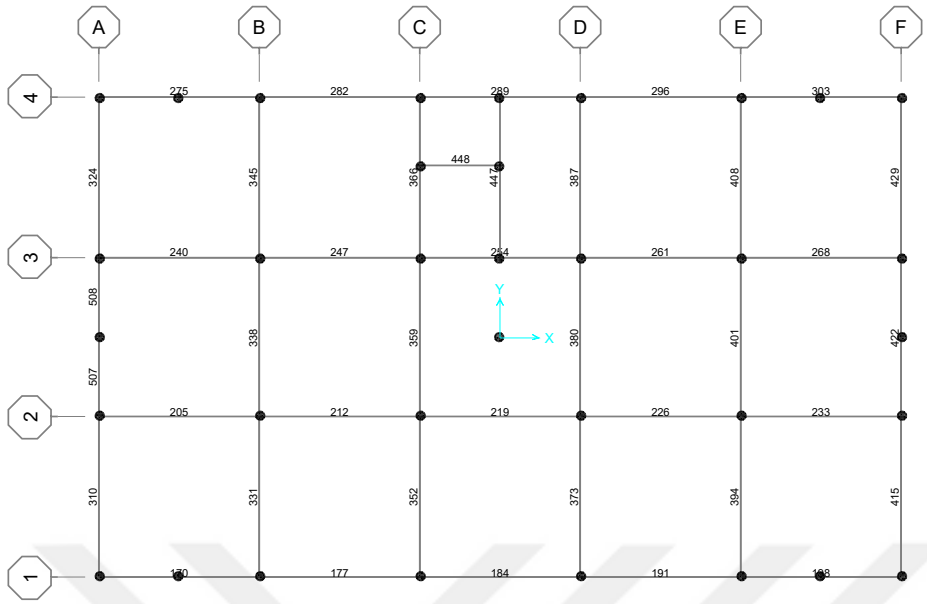


Figure 4.74. Beams Labels at the 2nd Story – Top View

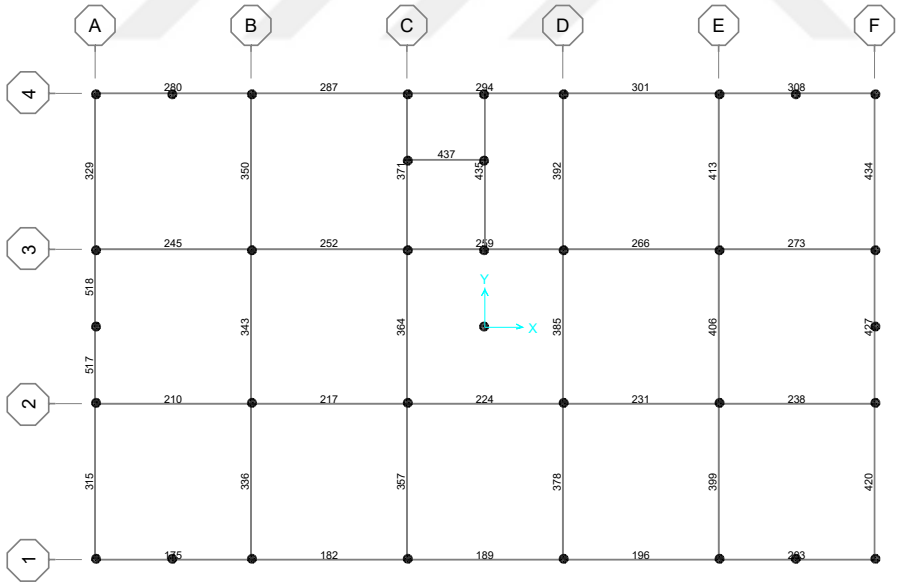


Figure 4.75. Beams Labels at the 7th Story – Top View

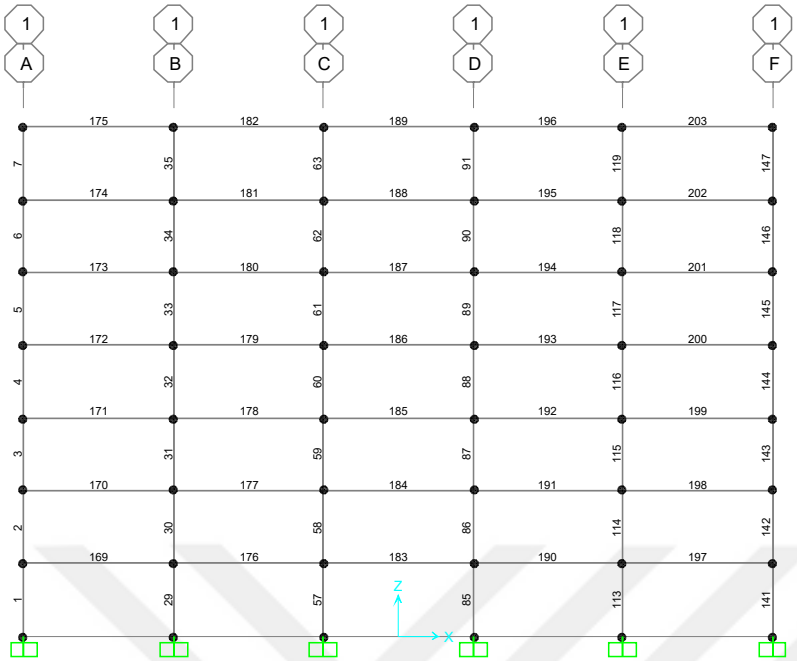


Figure 4.76. Beams and Columns Labels View Section 1-1

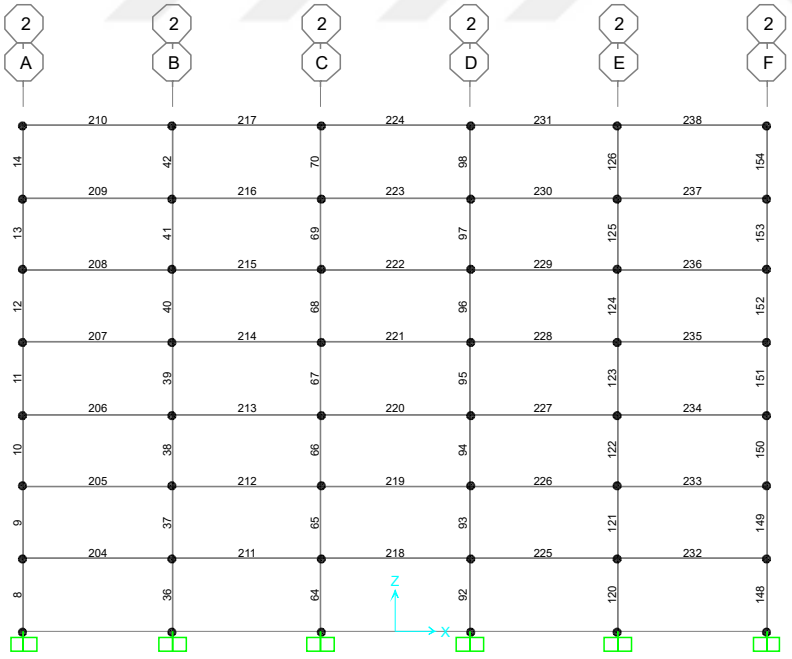


Figure 4.77. Beams and Columns Labels View Section 2-2

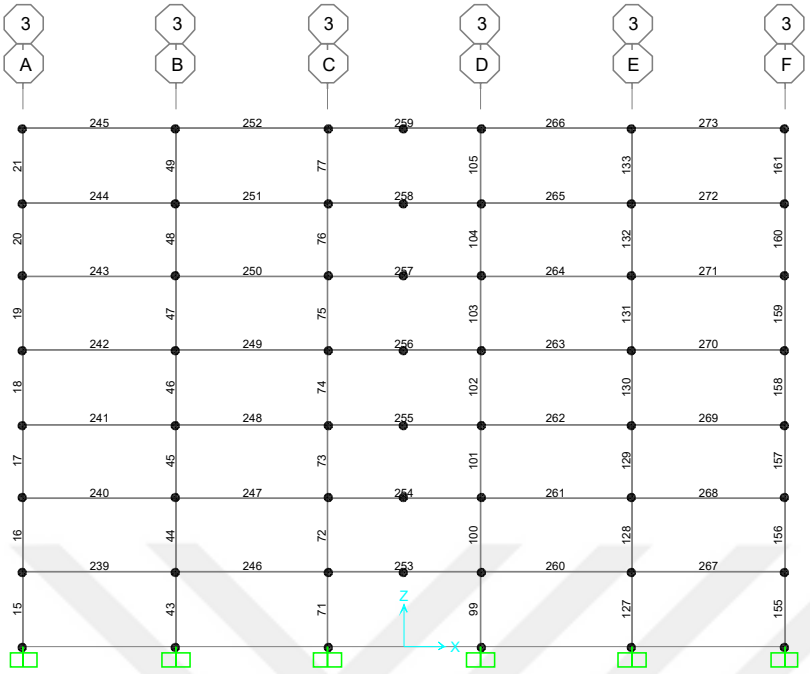


Figure 4.78. Beams and Columns Labels View Section 3-3

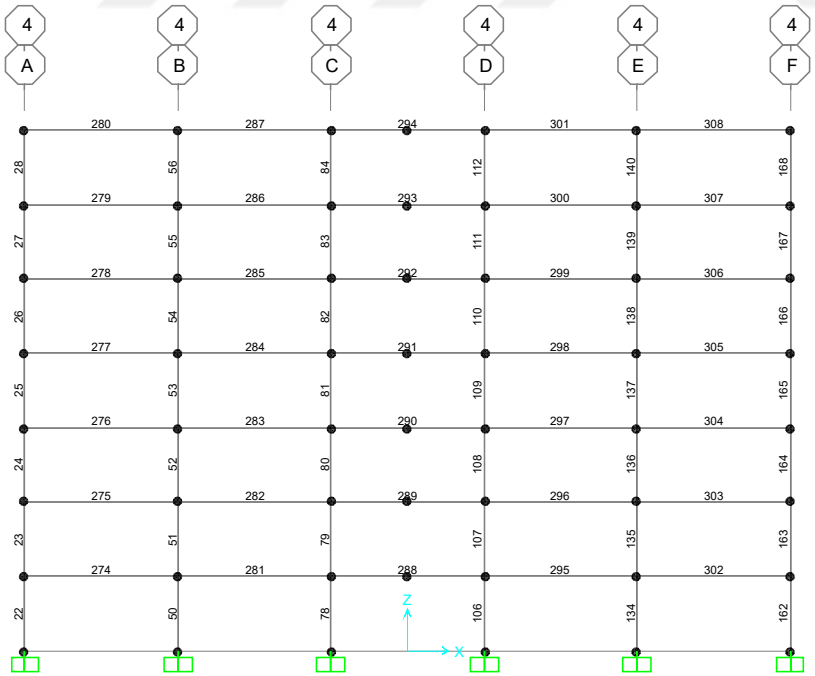


Figure 4.79. Beams and Columns Labels View Section 4-4

Table 4.33. Maximum and Minimum Bending Moment on Beams under Northridge Earthquake

Stories	Earthquake	Beam Label		Arrangements	Bending Moments
1st Story	Northridge	372	Max	Without Damper	122
		414	Min		89
		372	Max	X Damper Arr 1	65
		414	Min		48
		372	Max	V Damper Arr 1	89
		414	Min		66
		372	Max	X Damper Arr 2	73
		414	Min		57
		372	Max	V Damper Arr 2	103
		414	Min		76
2nd Story		366	Max	Without Damper	**123**
		289	Min		62
		366	Max	X Damper Arr 1	65
		289	Min		35
		366	Max	V Damper Arr 1	90
		289	Min		47
		366	Max	X Damper Arr 2	74
		289	Min		43
		366	Max	V Damper Arr 2	104
		289	Min		55
7th Story		252	Max	Without Damper	61
		399	Min		34
		252	Max	X Damper Arr 1	32
		399	Min		**18**
		252	Max	V Damper Arr 1	44
		399	Min		25
		252	Max	X Damper Arr 2	38
		399	Min		20
		252	Max	V Damper Arr 2	52
		399	Min		29

The above table shows the maximum and minimum bending moment on the beams at the 1st, 2nd and 7th stories under the Northridge earthquake. Where at the 1st story the maximum bending moment occurred at the beam number 372 and minimum occurred at the beam number 414 where the beam labels are shown in table 4.31. At the second story the maximum bending moment between all the other beams has affected the beam number 366

and minimum on the beam 289. For the 7th story it is maximum on the beam number 252 and minimum on the beam 399. Comparing the named 3 stories the maximum bending moment has occurred at the second floor on beam number 366 when there is no friction damper installed and minimum has happened at the 7th floor on beam number 399 at the X-damper arrangement 1 condition. The result can be written that the building is on the safer side with the X-damper arrangement 1 under the Northridge earthquake. The maximum bending moment on the beam number 366 at the second story is equal to 123 and the minimum is equal to 18 on the beam number 399 at the 7th story.

- Bending Moment Comparison under the Northridge Earthquake at the 1st Story:

$$\frac{\text{Bending Moment on Beam 372 (No Damper)}}{\text{Bending Moment on Beam 372 (X} - \text{damper Arrangement 1)}} = \frac{122}{65} = 1.87$$

$= 18.7\%$, the comparison gives us approximately 2 stories which is acceptable.

$$\frac{\text{Bending Moment on Beam 372 (No Damper)}}{\text{Bending Moment on Beam 372 (V} - \text{damper Arrangement 1)}} = \frac{122}{89} = 1.37$$

$= 13.7\%$, the comparison shows 1.37 stories which is acceptable.

$$\frac{\text{Bending Moment on Beam 372 (No Damper)}}{\text{Bending Moment on Beam 372 (X} - \text{damper Arrangement 2)}} = \frac{122}{73} = 1.67$$

$= 16.7\%$, the comparison shows 1.67 stories and it is acceptable.

$$\frac{\text{Bending Moment on Beam 372 (No Damper)}}{\text{Bending Moment on Beam 372 (V} - \text{damper Arrangement 2)}} = \frac{122}{103} = 1.18$$

$= 11.8\%$, the comparison shows 1.18 stories and it is acceptable.

- Bending Moment Comparison under the Northridge Earthquake at the 2nd Story:

$$\frac{\text{Bending Moment on Beam 366 (No Damper)}}{\text{Bending Moment on Beam 366 (X} - \text{damper Arrangement 1)}} = \frac{123}{65} = 1.89$$

$= 18.9\%$, the comparison gives us 1.89 stories which is acceptable.

$$\frac{\text{Bending Moment on Beam 366 (No Damper)}}{\text{Bending Moment on Beam 366 (V} - \text{damper Arrangement 1)}} = \frac{123}{90} = 1.36$$

$= 13.6\%$, the comparison shows 1.36 stories which is acceptable.

$$\frac{\text{Bending Moment on Beam 366 (No Damper)}}{\text{Bending Moment on Beam 366 (X} - \text{damper Arrangement 2)}} = \frac{123}{74} = 1.66$$

$= 16.6\%$, the comparison shows 1.66 stories and it is acceptable.

$$\frac{\text{Bending Moment on Beam 366 (No Damper)}}{\text{Bending Moment on Beam 366 (V} - \text{damper Arrangement 2)}} = \frac{123}{104} = 1.17$$

$= 11.7\%$, the comparison shows 1.17 stories and it is acceptable.

- Bending Moment Comparison under the Northridge Earthquake at the 7th Story:

$$\frac{\text{Bending Moment on Beam 252 (No Damper)}}{\text{Bending Moment on Beam 252 (X} - \text{damper Arrangement 1)}} = \frac{61}{32} = 1.90$$

$= 19\%$, the comparison gives us approximatly 2 stories which is acceptable.

$$\frac{\text{Bending Moment on Beam 252 (No Damper)}}{\text{Bending Moment on Beam 252 (V} - \text{damper Arrangement 1)}} = \frac{61}{44} = 1.38$$

$= 13.8\%$, the comparison shows 1.38 stories which is acceptable.

$$\frac{\text{Bending Moment on Beam 252 (No Damper)}}{\text{Bending Moment on Beam 252 (X} - \text{damper Arrangement 2)}} = \frac{61}{38} = 1.60$$

$= 16\%$, the comparison shows 1.60 stories and it is acceptable.

$$\frac{\text{Bending Moment on Beam 252 (No Damper)}}{\text{Bending Moment on Beam 252 (V} - \text{damper Arrangement 2)}} = \frac{61}{52} = 1.17$$

$= 11.7\%$, the comparison shows 1.17 stories and it is acceptable.

The above bending moment comparison for the 1st, 2nd and 7th stories are almost at the same range and acceptable.

Table 4.34. Maximum and Minimum Bending Moment on Beams under Kobe Earthquake

Stories	Earthquake	Beam Label		Arrangements	Bending Moments
1st Story	Kobe	253	Max	Without Damper	163
		288	Min		102
		253	Max	X Damper Arr 1	85
		288	Min		55
		253	Max	V Damper Arr 1	118
		288	Min		75
		253	Max	X Damper Arr 2	94
		288	Min		63
		253	Max	V Damper Arr 2	163
		288	Min		87
2nd Story		254	Max	Without Damper	**170**
		289	Min		84
		254	Max	X Damper Arr 1	89
		289	Min		46
		254	Max	V Damper Arr 1	123
		289	Min		62
		254	Max	X Damper Arr 2	97
		289	Min		54
		254	Max	V Damper Arr 2	141
		289	Min		72
7th Story		250	Max	Without Damper	70
		257	Min		36
		250	Max	X Damper Arr 1	37
		257	Min		**19**
		250	Max	V Damper Arr 1	51
		257	Min		27
		250	Max	X Damper Arr 2	43
		257	Min		22
		250	Max	V Damper Arr 2	59
		257	Min		31

The bending moments under the Kobe earthquake at the 1st, 2nd and 7th stories are shown in the above table 4.34 , At the first story the maximum bending moment in Inverted V damper arrangement 2 and No damper condition are the same at the beam number 253. At the second story the maximum bending moment is on the beam 254 in without damper condition of the structure while at the 7th story the bending moments are at their lowest which is minimum on the beam 257. With comparison of the above 3 stories according to the

analyzed bending moments by SAP2000, we can read that the maximum bending moment under the Kobe earthquake has occurred at the second story in "without damper" situation which is 170 at the beam 254 and the minimum is equal to 19 at the 7th floor on the beam number 257 in X-damper arrangement 1 condition.

- Bending Moment Comparison under the Kobe Earthquake at the 1st Story:

$$\frac{\text{Bending Moment on Beam 253 (No Damper)}}{\text{Bending Moment on Beam 253 (X} - \text{damper Arrangement 1)}} = \frac{163}{85} = 1.9$$

$= 19\%$, the comparison gives us approximately 2 stories which is acceptable.

$$\frac{\text{Bending Moment on Beam 253 (No Damper)}}{\text{Bending Moment on Beam 253 (V} - \text{damper Arrangement 1)}} = \frac{163}{118} = 1.38$$

$= 13.8\%$, the comparison shows 1.38 stories which is acceptable.

$$\frac{\text{Bending Moment on Beam 253 (No Damper)}}{\text{Bending Moment on Beam 253 (X} - \text{damper Arrangement 2)}} = \frac{163}{94} = 1.73$$

$= 17.3\%$, the comparison shows 1.73 stories and it is acceptable.

$$\frac{\text{Bending Moment on Beam 253 (No Damper)}}{\text{Bending Moment on Beam 253 (V} - \text{damper Arrangement 2)}} = \frac{163}{163} = 1$$

$= 10\%$, the comparison shows 1 stories and it is acceptable.

- Bending Moment Comparison under the Kobe Earthquake at the 2nd Story:

$$\frac{\text{Bending Moment on Beam 254 (No Damper)}}{\text{Bending Moment on Beam 254 (X} - \text{damper Arrangement 1)}} = \frac{170}{89} = 1.9$$

$= 19\%$, the comparison gives us 1.9 stories which is acceptable.

$$\frac{\text{Bending Moment on Beam 254 (No Damper)}}{\text{Bending Moment on Beam 254 (V} - \text{damper Arrangement 1)}} = \frac{170}{123} = 1.38$$

$= 13.8\%$, the comparison shows 1.38 stories which is acceptable.

$$\frac{\text{Bending Moment on Beam 254 (No Damper)}}{\text{Bending Moment on Beam 254 (X} - \text{damper Arrangement 2)}} = \frac{170}{97} = 1.75$$

$= 17.5\%$, the comparison shows 1.75 stories and it is acceptable.

$$\frac{\text{Bending Moment on Beam 254 (No Damper)}}{\text{Bending Moment on Beam 254 (V} - \text{damper Arrangement 2)}} = \frac{170}{141} = 1.20$$

$= 12\%$, the comparison shows 1.20 stories and it is acceptable.

- Bending Moment Comparison under the Kobe Earthquake at the 7th Story:

$$\frac{\text{Bending Moment on Beam 250 (No Damper)}}{\text{Bending Moment on Beam 250 (X} - \text{damper Arrangement 1)}} = \frac{70}{37} = 1.89$$

$= 18.9\%$, the comparison gives us 1.89 stories which is acceptable.

$$\frac{\text{Bending Moment on Beam 250 (No Damper)}}{\text{Bending Moment on Beam 250 (V} - \text{damper Arrangement 1)}} = \frac{70}{51} = 1.37$$

$= 13.7\%$, the comparison shows 1.37 stories which is acceptable.

$$\frac{\text{Bending Moment on Beam 250 (No Damper)}}{\text{Bending Moment on Beam 250 (X} - \text{damper Arrangement 2)}} = \frac{70}{43} = 1.62$$

$= 16.2\%$, the comparison shows 1.62 stories and it is acceptable.

$$\frac{\text{Bending Moment on Beam 250 (No Damper)}}{\text{Bending Moment on Beam 250 (V} - \text{damper Arrangement 2)}} = \frac{70}{59} = 1.18$$

$= 11.8\%$, the comparison shows 1.18 stories and it is acceptable.

The above bending moment comparison for the 1st, 2nd and 7th stories are almost at the same range and acceptable. And the results are so close to the Northridge earthquake.

Table 4.35 Maximum and Minimum Bending Moment on Beams under Imperial Valley Earthquake

Stories	Earthquake	Beam Label		Arrangements	Bending Moments
1st Story	Imperial Valley	253	Max	Without Damper	169
		421	Min		102
		253	Max	X Damper Arr 1	131
		421	Min		61
		253	Max	V Damper Arr 1	181
		421	Min		84
		253	Max	X Damper Arr 2	139
		421	Min		70
		253	Max	V Damper Arr 2	209
		421	Min		97
2nd Story		254	Max	Without Damper	**246**
		422	Min		94
		254	Max	X Damper Arr 1	127
		422	Min		51
		254	Max	V Damper Arr 1	176
		422	Min		69
		254	Max	X Damper Arr 2	135
		422	Min		59
		254	Max	V Damper Arr 2	203
		422	Min		80
7th Story		250	Max	Without Damper	77
		257	Min		41
		250	Max	X Damper Arr 1	41
		257	Min		**22**
		250	Max	V Damper Arr 1	56
		257	Min		30
		250	Max	X Damper Arr 2	48
		257	Min		25
		250	Max	V Damper Arr 2	66
		257	Min		34

The table 4.35 Shows the bending moment at the beams under the Imperial Valley earthquake at the 1st, 2nd and 7th stories. Comparing the bending moments at the first story shows that the maximum bending moment at the first story has occurred at the beam 253 at the V damper arrangement 2 condition and the minimum is at the X-damper arrangement 1 on beam 421. For the 2nd story it is maximum at the beam number 254 on without damper condition and it is also minimum at the beam number 422 on X-damper arrangement 1. At

the 7th story the maximum bending moment is at the without damper condition on beam number 250 and minimum is at the X-damper arrangement 1 on beam number 257. Comparing the bending moments in 1st, 2nd and 7th stories the maximum bending moment is equal to 246 at the second floor on beam number 254 under the without damper condition and the minimum is equal to 22 at the 7th floor under the X-damper arrangement 1. Comparing the bending moment of beams under Northridge, Kobe and Imperial Valley earthquake we can state that the maximum bending moment is on the without damper condition while X-damper arrangement 1 had the best performance till this point.

- Bending Moment Comparison under the Imperial Valley Earthquake at the 1st Story:

$$\frac{\text{Bending Moment on Beam 253 (No Damper)}}{\text{Bending Moment on Beam 253 (X} - \text{damper Arrangement 1)}} = \frac{169}{131} = 1.29$$

$$= 12.9\%\text{ , the comparison gives us 1.29 stories which is acceptable.}$$

$$\frac{\text{Bending Moment on Beam 253 (No Damper)}}{\text{Bending Moment on Beam 253 (V} - \text{damper Arrangement 1)}} = \frac{169}{181} = 0.93$$

$$= 9.3\%\text{ , the comparison shows 0.93 stories which is acceptable.}$$

$$\frac{\text{Bending Moment on Beam 253 (No Damper)}}{\text{Bending Moment on Beam 253 (X} - \text{damper Arrangement 2)}} = \frac{169}{139} = 1.21$$

$$= 12.1\%\text{ , the comparison shows 1.21 stories and it is acceptable.}$$

$$\frac{\text{Bending Moment on Beam 253 (No Damper)}}{\text{Bending Moment on Beam 253 (V} - \text{damper Arrangement 2)}} = \frac{169}{209} = 0.80$$

$$= 8\%\text{ , the comparison shows 0.80 stories and it is acceptable.}$$

- Bending Moment Comparison under the Imperial Valley Earthquake at the 2nd Story:

$$\frac{\text{Bending Moment on Beam 254 (No Damper)}}{\text{Bending Moment on Beam 254 (X} - \text{damper Arrangement 1)}} = \frac{246}{127} = 1.93$$

$$= 19.3\%\text{ , the comparison gives us 1.93 stories which is acceptable.}$$

$$\frac{\text{Bending Moment on Beam 254 (No Damper)}}{\text{Bending Moment on Beam 254 (V} - \text{damper Arrangement 1)}} = \frac{246}{176} = 1.39$$

$= 13.9\%$, the comparison shows 1.39 stories which is acceptable.

$$\frac{\text{Bending Moment on Beam 254 (No Damper)}}{\text{Bending Moment on Beam 254 (X} - \text{damper Arrangement 2)}} = \frac{246}{135} = 1.82$$

$= 18.2\%$, the comparison shows 1.82 stories and it is acceptable.

$$\frac{\text{Bending Moment on Beam 254 (No Damper)}}{\text{Bending Moment on Beam 254 (V} - \text{damper Arrangement 2)}} = \frac{246}{203} = 1.21$$

$= 12.1\%$, the comparison shows 1.21 stories and it is acceptable.

- Bending Moment Comparison under the Imperial Valley Earthquake at the 7th Story:

$$\frac{\text{Bending Moment on Beam 250 (No Damper)}}{\text{Bending Moment on Beam 250 (X} - \text{damper Arrangement 1)}} = \frac{77}{41} = 1.87$$

$= 18.7\%$, the comparison gives us 1.87 stories which is acceptable.

$$\frac{\text{Bending Moment on Beam 250 (No Damper)}}{\text{Bending Moment on Beam 250 (V} - \text{damper Arrangement 1)}} = \frac{77}{56} = 1.37$$

$= 13.7\%$, the comparison shows 1.37 stories which is acceptable.

$$\frac{\text{Bending Moment on Beam 250 (No Damper)}}{\text{Bending Moment on Beam 250 (X} - \text{damper Arrangement 2)}} = \frac{77}{48} = 1.60$$

$= 16\%$, the comparison shows 1.60 stories and it is acceptable.

$$\frac{\text{Bending Moment on Beam 250 (No Damper)}}{\text{Bending Moment on Beam 250 (V} - \text{damper Arrangement 2)}} = \frac{77}{66} = 1.16$$

$= 11.6\%$, the comparison shows 1.16 stories and it is acceptable.

The above bending moment comparison for the 1st, 2nd and 7th stories are almost at the same range and acceptable.

Table 4.36 Maximum and Minimum Bending Moment on Beams under Bam Earthquake

Stories	Earthquake	Beam Label		Arrangements	Bending Moments
1st Story	Bam	253	Max	Without Damper	169
		288	Min		102
		253	Max	X Damper Arr 1	88
		288	Min		55
		253	Max	V Damper Arr 1	122
		288	Min		75
		253	Max	X Damper Arr 2	97
		288	Min		63
		253	Max	V Damper Arr 2	141
		288	Min		87
2nd Story		254	Max	Without Damper	**190**
		422	Min		89
		254	Max	X Damper Arr 1	99
		422	Min		48
		254	Max	V Damper Arr 1	137
		422	Min		66
		254	Max	X Damper Arr 2	107
		422	Min		57
		254	Max	V Damper Arr 2	158
		422	Min		76
7th Story		254	Max	Without Damper	77
		422	Min		40
		254	Max	X Damper Arr 1	41
		422	Min		**21**
		254	Max	V Damper Arr 1	56
		422	Min		29
		254	Max	X Damper Arr 2	47
		422	Min		24
		254	Max	V Damper Arr 2	65
		422	Min		34

The above table 4.36 shows the maximum and minimum bending moment on the beams at the 1st, 2nd and 7th stories under the Bam earthquake. Where at the 1st story the maximum bending moment occurred at the beam number 253 at the without damper situation and minimum occurred at the beam number 288 in the X-damper arrangement 1. At the second story the maximum bending moment between all the other beams has affected the beam number 254 at the without damper situation and minimum on the beam 422 under the

X-damper arrangement 1. For the 7th story it is maximum on the beam number 254 and minimum on the beam 422 at the X-damper arrangement 1. Comparing the named 3 stories the maximum bending moment has occurred at the second floor on beam number 254 when there is no friction damper installed and minimum has happened at the 7th floor on beam number 422 at the X-damper arrangement 1 condition. The result can be written that the building is on the safer side with the X-damper arrangement 1 under the Bam earthquake. The maximum bending moment on the beam number 254 at the second story is equal to 190 and the minimum is equal to 21 on the beam number 422 at the 7th story.

- Bending Moment Comparison under the Bam Earthquake at the 1st Story:

$$\frac{\text{Bending Moment on Beam 253 (No Damper)}}{\text{Bending Moment on Beam 253 (X} - \text{damper Arrangement 1)}} = \frac{169}{88} = 1.92$$

$$= 19.2\% \text{, the comparison gives us 1.92 stories which is acceptable.}$$

$$\frac{\text{Bending Moment on Beam 253 (No Damper)}}{\text{Bending Moment on Beam 253 (V} - \text{damper Arrangement 1)}} = \frac{169}{122} = 1.38$$

$$= 13.8\% \text{, the comparison shows 1.38 stories which is acceptable.}$$

$$\frac{\text{Bending Moment on Beam 253 (No Damper)}}{\text{Bending Moment on Beam 253 (X} - \text{damper Arrangement 2)}} = \frac{169}{97} = 1.74$$

$$= 17.4\% \text{, the comparison shows 1.74 stories and it is acceptable.}$$

$$\frac{\text{Bending Moment on Beam 253 (No Damper)}}{\text{Bending Moment on Beam 253 (V} - \text{damper Arrangement 2)}} = \frac{169}{141} = 1.19$$

$$= 11.9\% \text{, the comparison shows 1.19 stories and it is acceptable.}$$

- Bending Moment Comparison under the Bam Earthquake at the 2nd Story:

$$\frac{\text{Bending Moment on Beam 254 (No Damper)}}{\text{Bending Moment on Beam 254 (X} - \text{damper Arrangement 1)}} = \frac{190}{99} = 1.91$$

$$= 19.1\% \text{, the comparison gives us 1.91 stories which is acceptable.}$$

$$\frac{\text{Bending Moment on Beam 254 (No Damper)}}{\text{Bending Moment on Beam 254 (V} - \text{damper Arrangement 1)}} = \frac{190}{137} = 1.38$$

$= 13.8\%$, the comparison shows 1.38 stories which is acceptable.

$$\frac{\text{Bending Moment on Beam 254 (No Damper)}}{\text{Bending Moment on Beam 254 (X} - \text{damper Arrangement 2)}} = \frac{190}{107} = 1.77$$

$= 17.7\%$, the comparison shows 1.77 stories and it is acceptable.

$$\frac{\text{Bending Moment on Beam 254 (No Damper)}}{\text{Bending Moment on Beam 254 (V} - \text{damper Arrangement 2)}} = \frac{190}{158} = 1.20$$

$= 12\%$, the comparison shows 1.20 stories and it is acceptable.

- Bending Moment Comparison under the Bam Earthquake at the 7th Story:

$$\frac{\text{Bending Moment on Beam 254 (No Damper)}}{\text{Bending Moment on Beam 254 (X} - \text{damper Arrangement 1)}} = \frac{77}{41} = 1.87$$

$= 18.7\%$, the comparison gives us 1.87 stories which is acceptable.

$$\frac{\text{Bending Moment on Beam 254 (No Damper)}}{\text{Bending Moment on Beam 254 (V} - \text{damper Arrangement 1)}} = \frac{77}{56} = 1.37$$

$= 13.7\%$, the comparison shows 1.37 stories which is acceptable.

$$\frac{\text{Bending Moment on Beam 254 (No Damper)}}{\text{Bending Moment on Beam 254 (X} - \text{damper Arrangement 2)}} = \frac{77}{47} = 1.63$$

$= 16.3\%$, the comparison shows 1.63 stories and it is acceptable.

$$\frac{\text{Bending Moment on Beam 254 (No Damper)}}{\text{Bending Moment on Beam 254 (V} - \text{damper Arrangement 2)}} = \frac{77}{65} = 1.18$$

$= 11.8\%$, the comparison shows 1.18 stories and it is acceptable.

The above bending moment comparison for the 1st, 2nd and 7th stories are almost at the same range and acceptable.

Table 4.37. Maximum and Minimum Bending Moment on Beams under Parkfield Earthquake

Stories	Earthquake	Beam Label		Arrangements	Bending Moments
1st Story		365	Max	Without Damper	114
		169	Min		62
		365	Max	X Damper Arr 1	60
		169	Min		34
		365	Max	V Damper Arr 1	82
		169	Min		46
		365	Max	X Damper Arr 2	68
		169	Min		43
		365	Max	V Damper Arr 2	95
		169	Min		54
2nd Story	Parkfield	366	Max	Without Damper	**128**
		415	Min		60
		366	Max	X Damper Arr 1	59
		415	Min		34
		366	Max	V Damper Arr 1	81
		415	Min		46
		366	Max	X Damper Arr 2	68
		415	Min		42
		366	Max	V Damper Arr 2	94
		415	Min		53
7th Story		250	Max	Without Damper	84
		257	Min		44
		250	Max	X Damper Arr 1	45
		257	Min		**23**
		250	Max	V Damper Arr 1	61
		257	Min		32
		250	Max	X Damper Arr 2	52
		257	Min		27
		250	Max	V Damper Arr 2	72
		257	Min		37

The analyzed bending moments under the Parkfield earthquake as shown in above table 4.37 is also at the same range and result as the Northridge, Kobe, Bam, Imperial Valley earthquake on different beams. from the above table we can notice that the beams in X-damper arrangement 1has the minimum bending moment in all the 1st, 2nd and 7th stories. While without damper arrangement and V-damper arrangement 2 gave almost the same values for beams bending moments. The maximum bending moment under the Parkfield

earthquake is at the beam number 366 and is equal to 128 in without damper situation, and the minimum is equal 23 in beam number 257 at the 7th floor in the X-damper arrangement 1.

- Bending Moment Comparison under the Parkfield Earthquake at the 1st Story:

$$\frac{\text{Bending Moment on Beam 365 (No Damper)}}{\text{Bending Moment on Beam 365 (X} - \text{damper Arrangement 1)}} = \frac{114}{60} = 1.9$$

$= 19\%$, the comparison gives us 1.9 stories which is acceptable.

$$\frac{\text{Bending Moment on Beam 365 (No Damper)}}{\text{Bending Moment on Beam 365 (V} - \text{damper Arrangement 1)}} = \frac{114}{82} = 1.3$$

$= 13\%$, the comparison shows 1.3 stories which is acceptable.

$$\frac{\text{Bending Moment on Beam 365 (No Damper)}}{\text{Bending Moment on Beam 365 (X} - \text{damper Arrangement 2)}} = \frac{114}{68} = 1.67$$

$= 16.7\%$, the comparison shows 1.67 stories and it is acceptable.

$$\frac{\text{Bending Moment on Beam 365 (No Damper)}}{\text{Bending Moment on Beam 365 (V} - \text{damper Arrangement 2)}} = \frac{114}{95} = 1.2$$

$= 12\%$, the comparison shows 1.2 stories and it is acceptable.

- Bending Moment Comparison under the Parkfield Earthquake at the 2nd Story:

$$\frac{\text{Bending Moment on Beam 366 (No Damper)}}{\text{Bending Moment on Beam 366 (X} - \text{damper Arrangement 1)}} = \frac{128}{59} = 2.1$$

$= 21\%$, the comparison gives us 2.1 stories which is acceptable.

$$\frac{\text{Bending Moment on Beam 366 (No Damper)}}{\text{Bending Moment on Beam 366 (V} - \text{damper Arrangement 1)}} = \frac{128}{81} = 1.58$$

$= 15.8\%$, the comparison shows 1.58 stories which is acceptable.

$$\frac{\text{Bending Moment on Beam 366 (No Damper)}}{\text{Bending Moment on Beam 366 (X} - \text{damper Arrangement 2)}} = \frac{128}{68} = 1.88$$

$= 18.8\%$, the comparison shows 1.88 stories and it is acceptable.

$$\frac{\text{Bending Moment on Beam 366 (No Damper)}}{\text{Bending Moment on Beam 366 (V} - \text{damper Arrangement 2)}} = \frac{128}{94} = 1.36$$

$$= 13.6\% \text{ , the comparison shows 1.36 stories and it is acceptable.}$$

- Bending Moment Comparison under the Parkfield Earthquake at the 7th Story:

$$\frac{\text{Bending Moment on Beam 250 (No Damper)}}{\text{Bending Moment on Beam 250 (X} - \text{damper Arrangement 1)}} = \frac{84}{45} = 1.86$$

$$= 18.6\% \text{ , the comparison gives us 1.86 stories which is acceptable.}$$

$$\frac{\text{Bending Moment on Beam 250 (No Damper)}}{\text{Bending Moment on Beam 250 (V} - \text{damper Arrangement 1)}} = \frac{84}{61} = 1.37$$

$$= 13.7\% \text{ , the comparison shows 1.37 stories which is acceptable.}$$

$$\frac{\text{Bending Moment on Beam 250 (No Damper)}}{\text{Bending Moment on Beam 250 (X} - \text{damper Arrangement 2)}} = \frac{84}{52} = 1.61$$

$$= 16.1\% \text{ , the comparison shows 1.61 stories and it is acceptable.}$$

$$\frac{\text{Bending Moment on Beam 250 (No Damper)}}{\text{Bending Moment on Beam 250 (V} - \text{damper Arrangement 2)}} = \frac{84}{72} = 1.16$$

$$= 11.6\% \text{ , the comparison shows 1.16 stories and it is acceptable.}$$

The above bending moment comparison for the 1st, 2nd and 7th stories are almost at the same range and acceptable.

Table 4.38. Maximum and Minimum Bending Moment on Beams under Düzce Earthquake

Stories	Earthquake	Beam Label		Arrangements	Bending Moments
1st Story	Düzce	253	Max	Without Damper	**461**
		176	Min		117
		253	Max	X Damper Arr 1	234
		176	Min		62
		253	Max	V Damper Arr 1	326
		176	Min		85
		253	Max	X Damper Arr 2	243
		176	Min		71
		253	Max	V Damper Arr 2	376
		176	Min		99
2nd Story		254	Max	Without Damper	296
		422	Min		99
		254	Max	X Damper Arr 1	152
		422	Min		53
		254	Max	V Damper Arr 1	211
		422	Min		73
		254	Max	X Damper Arr 2	160
		422	Min		62
		254	Max	V Damper Arr 2	243
		422	Min		84
7th Story		253	Max	Without Damper	67
		257	Min		36
		253	Max	X Damper Arr 1	35
		257	Min		**19**
		253	Max	V Damper Arr 1	49
		257	Min		26
		253	Max	X Damper Arr 2	46
		257	Min		22
		253	Max	V Damper Arr 2	56
		257	Min		31

Comparing the beams bending moments under the Northridge, Bam, Kobe, Parkfield, Imperial Valley and Düzce shows that the maximum bending moments has occurred under the Düzce earthquake as shown in Table 4.38.

The maximum bending moment at the first floor under the Düzce earthquake has occurred at the beam number 253 which is equal 461 and the minimum at the first floor is

equal 62 at the beam 176 in the X-damper arrangement 1. The maximum bending moment at the second story is on beam number 254 in without damper condition and the minimum is at the beam 422 in X-damper arrangement 1. At the 7th story the maximum bending moment is at the beam number 253 and minimum is at the 257. The maximum bending moment under the Düzce earthquake is on beam 253 at the 1st floor in without damper condition and the minimum is on beam 257 at the 7th story in X-damper arrangement 1 which is shown in table 4.38.

- Bending Moment Comparison under the Düzce Earthquake at the 1st Story:

$$\frac{\text{Bending Moment on Beam 253 (No Damper)}}{\text{Bending Moment on Beam 253 (X} - \text{damper Arrangement 1)}} = \frac{461}{234} = 1.97$$

$$= 19.7\% \text{, the comparison gives us 1.97 stories which is acceptable.}$$

$$\frac{\text{Bending Moment on Beam 253 (No Damper)}}{\text{Bending Moment on Beam 253 (V} - \text{damper Arrangement 1)}} = \frac{461}{326} = 1.41$$

$$= 14.1\% \text{, the comparison shows 1.41 stories which is acceptable.}$$

$$\frac{\text{Bending Moment on Beam 253 (No Damper)}}{\text{Bending Moment on Beam 253 (X} - \text{damper Arrangement 2)}} = \frac{461}{243} = 1.89$$

$$= 18.9\% \text{, the comparison shows 1.89 stories and it is acceptable.}$$

$$\frac{\text{Bending Moment on Beam 253 (No Damper)}}{\text{Bending Moment on Beam 253 (V} - \text{damper Arrangement 2)}} = \frac{461}{376} = 1.22$$

$$= 12.2\% \text{, the comparison shows 1.22 stories and it is acceptable.}$$

- Bending Moment Comparison under the Düzce Earthquake at the 2nd Story:

$$\frac{\text{Bending Moment on Beam 254 (No Damper)}}{\text{Bending Moment on Beam 254 (X} - \text{damper Arrangement 1)}} = \frac{296}{152} = 1.94$$

$$= 19.4\% \text{, the comparison gives us 1.94 stories which is acceptable.}$$

$$\frac{\text{Bending Moment on Beam 254 (No Damper)}}{\text{Bending Moment on Beam 254 (V} - \text{damper Arrangement 1)}} = \frac{296}{211} = 1.4$$

$= 14\%$, the comparison shows 1.4 stories which is acceptable.

$$\frac{\text{Bending Moment on Beam 254 (No Damper)}}{\text{Bending Moment on Beam 254 (X} - \text{damper Arrangement 2)}} = \frac{296}{160} = 1.85$$

$= 18.5\%$, the comparison shows 1.85 stories and it is acceptable.

$$\frac{\text{Bending Moment on Beam 254 (No Damper)}}{\text{Bending Moment on Beam 254 (V} - \text{damper Arrangement 2)}} = \frac{296}{243} = 1.21$$

$= 12.1\%$, the comparison shows 1.21 stories and it is acceptable.

- Bending Moment Comparison under the Düzce Earthquake at the 7th Story:

$$\frac{\text{Bending Moment on Beam 253 (No Damper)}}{\text{Bending Moment on Beam 253 (X} - \text{damper Arrangement 1)}} = \frac{67}{35} = 1.91$$

$= 19.1\%$, the comparison gives us 1.91 stories which is acceptable.

$$\frac{\text{Bending Moment on Beam 253 (No Damper)}}{\text{Bending Moment on Beam 253 (V} - \text{damper Arrangement 1)}} = \frac{67}{49} = 1.36$$

$= 13.6\%$, the comparison shows 1.36 stories which is acceptable.

$$\frac{\text{Bending Moment on Beam 253 (No Damper)}}{\text{Bending Moment on Beam 253 (X} - \text{damper Arrangement 2)}} = \frac{67}{46} = 1.45$$

$= 14.5\%$, the comparison shows 1.45 stories and it is acceptable.

$$\frac{\text{Bending Moment on Beam 253 (No Damper)}}{\text{Bending Moment on Beam 253 (V} - \text{damper Arrangement 2)}} = \frac{67}{56} = 1.19$$

$= 11.9\%$, the comparison shows 1.19 stories and it is acceptable.

The above bending moment comparison for the 1st, 2nd and 7th stories are almost at the same range and acceptable.

The comparison of the above bending moment on beams shows that the maximum bending moment occurs on the beams at the without damper situation under the Düzce earthquake which is equal to 461 at the first floor and after that under the Imperial Valley earthquake which is equal to 246 at the second floor, for the other earthquake they are almost at the same range.

4.4.2 Beams Maximum Shear Forces Bending at 1st , 2nd and 7th Story under 6 Different Earthquakes

The maximum bending moment of beams at the first, second and 7th stories are summarized in below tables for six different earthquakes. The tables show the maximum bending moment on a beam and minimum bending moment on a beam.

The below figures 4.80 – 4.86 shows the beam labels from different views and stories.

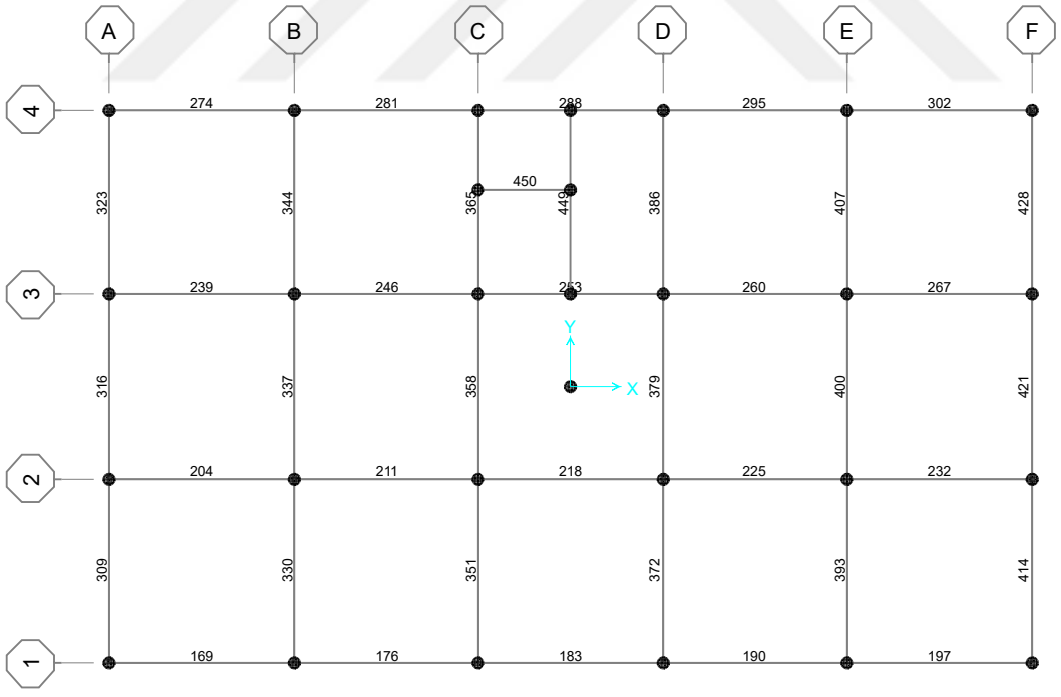


Figure 4.80. Beams Labels at the 1st Story – Top View

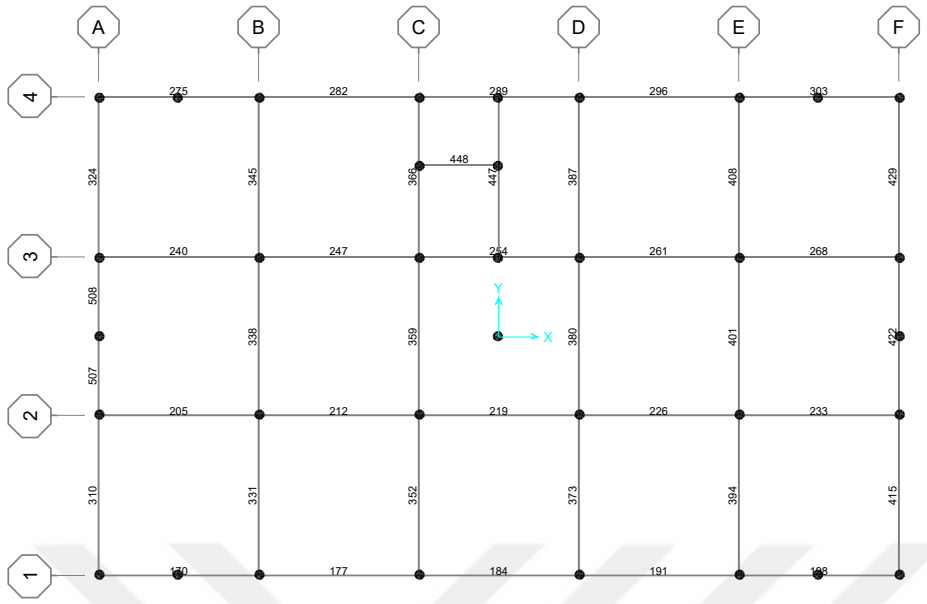


Figure 4.81. Beams Labels at the 2nd Story – Top View

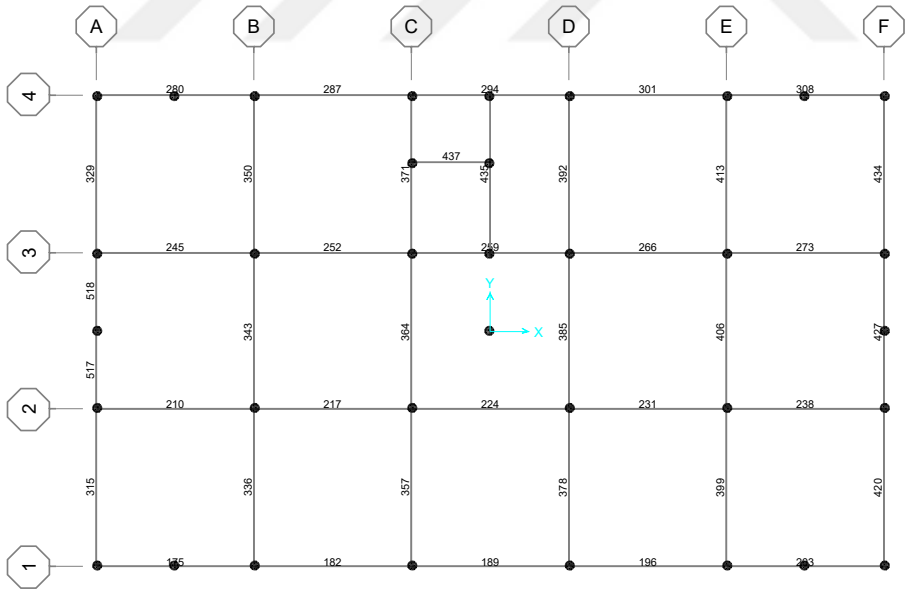


Figure 4.82. Beams Labels at the 7th Story – Top View

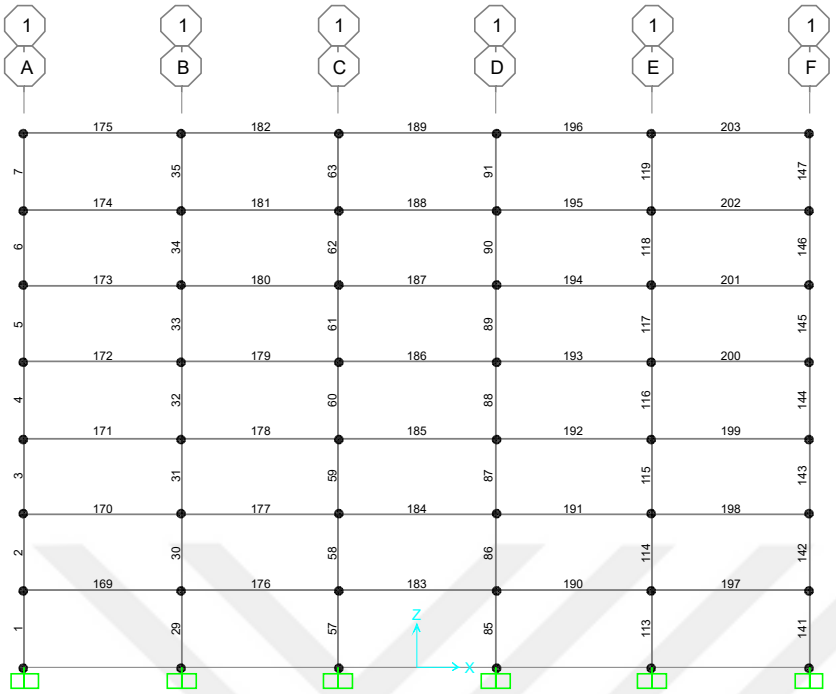


Figure 4.83. Beams and Columns Labels View Section 1-1

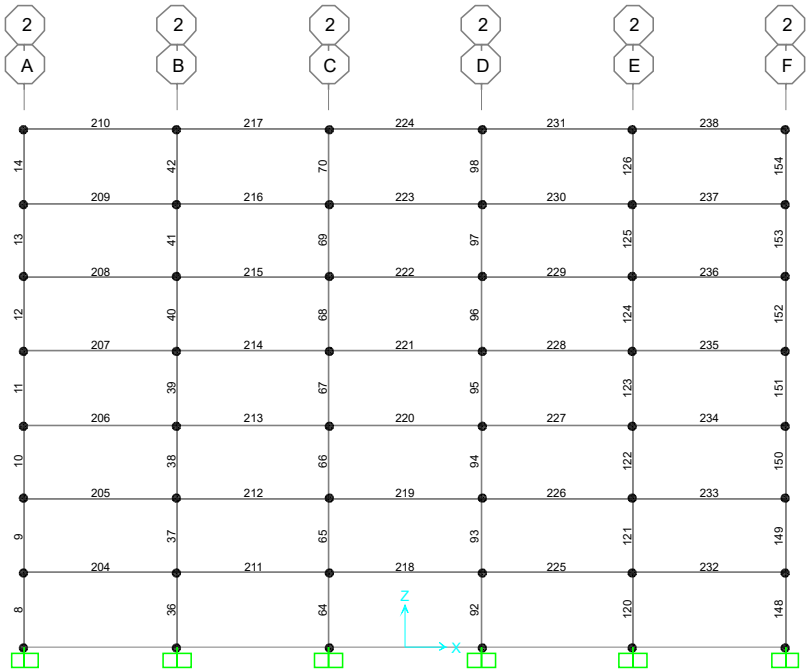


Figure 4.84. Beams and Columns Labels View Section 2-2

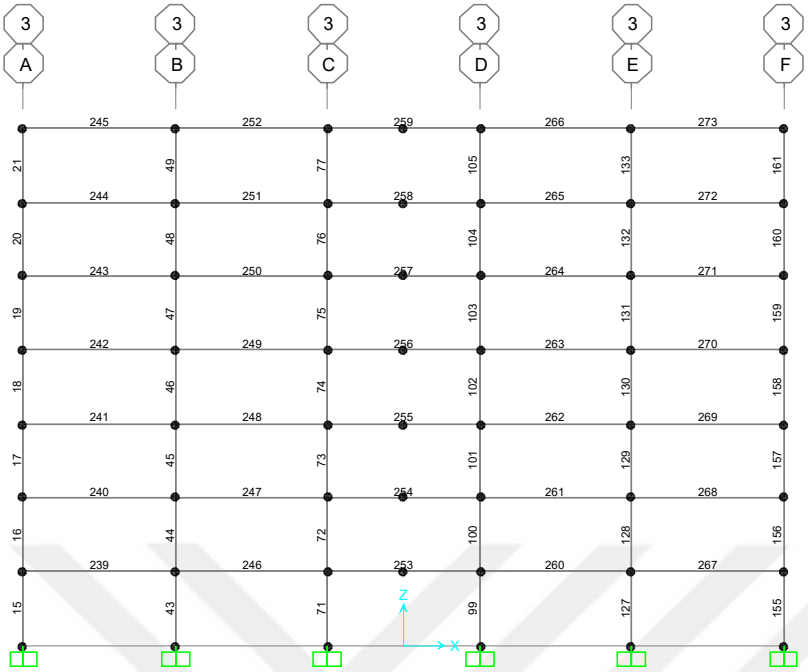


Figure 4.85. Beams and Columns Labels View Section 3-3

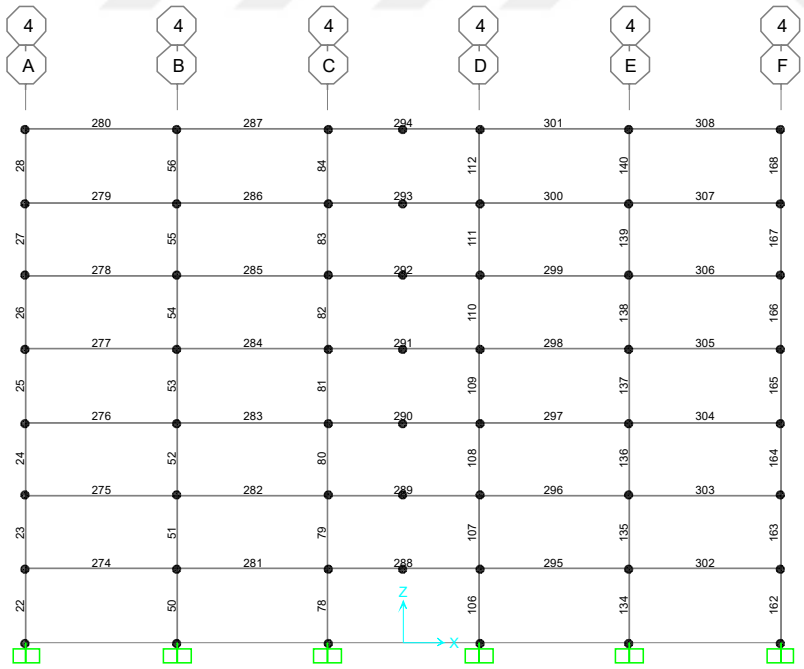


Figure 4.86. Beams and Columns Labels View Section 4-4

Table 4.39. Maximum and Minimum Shear Forces on Beams under Northridge Earthquake.

Stories	Earthquake	Beam Label		Arrangements	Shear Force
1st Story		288	Max	Without Damper	**101**
		414	Min		54
		288	Max	X Damper Arr 1	54
		414	Min		31
		288	Max	V Damper Arr 1	74
		414	Min		41
		288	Max	X Damper Arr 2	63
		414	Min		39
		288	Max	V Damper Arr 2	86
		414	Min		48
2nd Story	Northridge	205	Max	Without Damper	**101**
		415	Min		58
		205	Max	X Damper Arr 1	54
		415	Min		33
		205	Max	V Damper Arr 1	74
		415	Min		44
		205	Max	X Damper Arr 2	63
		415	Min		41
		205	Max	V Damper Arr 2	86
		415	Min		51
7th Story		294	Max	Without Damper	61
		427	Min		35
		294	Max	X Damper Arr 1	33
		427	Min		**19**
		294	Max	V Damper Arr 1	45
		427	Min		26
		294	Max	X Damper Arr 2	37
		427	Min		22
		294	Max	V Damper Arr 2	52
		427	Min		30

As shown in above table 4.39 the maximum shear force at the first story under the Northridge earthquake occurred in beam number 288 in without damper and the minimum is on X-damper arrangement one at the beam number 414, and for the second and 7th stories also the maximum shear force is when no damper has installed, and the minimum is at the X-damper arrangement 1. The result shows that the X-damper arrangement 1 is on the safer side. And the maximum shear force under the Northridge earthquake on the building is equal

to 101 on beam 288 at the first story and the minimum shear force on the building is equal to 19 on beam 427 at the X-damper arrangement 1 situation.

- Shear Force Comparison under the Northridge Earthquake at the 1st Story:

$$\frac{\text{Shear Force on Beam 288 (No Damper)}}{\text{Shear Force on Beam 288 (X} - \text{damper Arrangement 1)}} = \frac{101}{54} = 1.87$$

$= 18.7\%$, the comparison gives us 1.87 stories which is acceptable.

$$\frac{\text{Shear Force on Beam 288 (No Damper)}}{\text{Shear Force on Beam 288 (V} - \text{damper Arrangement 1)}} = \frac{101}{74} = 1.36$$

$= 13.6\%$, the comparison shows 1.36 stories which is acceptable.

$$\frac{\text{Shear Force on Beam 288 (No Damper)}}{\text{Bending Moment on Beam 288 (X} - \text{damper Arrangement 2)}} = \frac{101}{63} = 1.6$$

$= 16\%$, the comparison shows 1.6 stories and it is acceptable.

$$\frac{\text{Shear Force on Beam 288 (No Damper)}}{\text{Shear Force on Beam 288 (V} - \text{damper Arrangement 2)}} = \frac{101}{86} = 1.17$$

$= 11.7\%$, the comparison shows 1.17 stories and it is acceptable.

- Shear Force Comparison under the Northridge Earthquake at the 2nd Story:

$$\frac{\text{Shear Force on Beam 205 (No Damper)}}{\text{Shear Force on Beam 205 (X} - \text{damper Arrangement 1)}} = \frac{101}{54} = 1.87$$

$= 18.7\%$, the comparison gives us 1.87 stories which is acceptable.

$$\frac{\text{Shear Force on Beam 205 (No Damper)}}{\text{Shear Force on Beam 205 (V} - \text{damper Arrangement 1)}} = \frac{101}{74} = 1.36$$

$= 13.6\%$, the comparison shows 1.36 stories which is acceptable.

$$\frac{\text{Shear Force on Beam 205 (No Damper)}}{\text{Shear Force on Beam 205 (X} - \text{damper Arrangement 2)}} = \frac{101}{63} = 1.6$$

$= 16\%$, the comparison shows 1.6 stories and it is acceptable.

$$\frac{\text{Shear Force on Beam 205 (No Damper)}}{\text{Shear Force on Beam 205 (V} - \text{damper Arrangement 2)}} = \frac{101}{86} = 1.17$$

$= 11.7\%$, the comparison shows 1.17 stories and it is acceptable.

- Shear Force Comparison under the Northridge Earthquake at the 7th Story:

$$\frac{\text{Shear Force on Beam 294 (No Damper)}}{\text{Shear Force on Beam 294 (X} - \text{damper Arrangement 1)}} = \frac{61}{33} = 1.84$$

$= 18.4\%$, the comparison gives us 1.84 stories which is acceptable.

$$\frac{\text{Shear Force on Beam 294 (No Damper)}}{\text{Shear Force on Beam 294 (V} - \text{damper Arrangement 1)}} = \frac{61}{45} = 1.35$$

$= 13.5\%$, the comparison shows 1.35 stories which is acceptable.

$$\frac{\text{Shear Force on Beam 294 (No Damper)}}{\text{Shear Force on Beam 294 (X} - \text{damper Arrangement 2)}} = \frac{61}{37} = 1.64$$

$= 16.4\%$, the comparison shows 1.64 stories and it is acceptable.

$$\frac{\text{Shear Force on Beam 294 (No Damper)}}{\text{Shear Force on Beam 294 (V} - \text{damper Arrangement 2)}} = \frac{61}{52} = 1.17$$

$= 11.7\%$, the comparison shows 1.17 stories and it is acceptable.

The result of the shear forces at the 1st, 2nd and 7th stories are the same under the Northridge earthquake.

Table 4.40. Maximum and Minimum Shear Forces on Beams under Kobe Earthquake.

Stories	Earthquake	Beam Label		Arrangements	Shear Force
1st Story	Kobe	253	Max	Without Damper	121
		288	Min		58
		253	Max	X Damper Arr 1	64
		288	Min		33
		253	Max	V Damper Arr 1	88
		288	Min		44
		253	Max	X Damper Arr 2	73
		288	Min		41
		253	Max	V Damper Arr 2	102
		288	Min		51
2nd Story		254	Max	Without Damper	**125**
		289	Min		56
		254	Max	X Damper Arr 1	66
		289	Min		32
		254	Max	V Damper Arr 1	91
		289	Min		43
		254	Max	X Damper Arr 2	75
		289	Min		40
		254	Max	V Damper Arr 2	105
		289	Min		50
7th Story		371	Max	Without Damper	55
		175	Min		28
		371	Max	X Damper Arr 1	29
		175	Min		**15**
		371	Max	V Damper Arr 1	40
		175	Min		21
		371	Max	X Damper Arr 2	34
		175	Min		17
		371	Max	V Damper Arr 2	47
		175	Min		24

The above table 4.40 shows the maximum shear force at the first story under the Kobe earthquake in beam number 253 at the without damper and the minimum on X-damper arrangement one at the beam number 288. The maximum shear force on the building under the Kobe earthquake acted on beam number 254 at the 2nd story in without damper arrangement and the minimum acted on the beam number 175 at the 7th story in X-damper arrangement 1.

- Shear Force Comparison under the Kobe Earthquake at the 1st Story:

$$\frac{\text{Shear Force on Beam 253 (No Damper)}}{\text{Shear Force on Beam 253 (X} - \text{damper Arrangement 1)}} = \frac{121}{64} = 1.89$$

$= 18.9\%$, the comparison gives us 1.89 stories which is acceptable.

$$\frac{\text{Shear Force on Beam 253 (No Damper)}}{\text{Shear Force on Beam 253 (V} - \text{damper Arrangement 1)}} = \frac{121}{88} = 1.37$$

$= 13.7\%$, the comparison shows 1.37 stories which is acceptable.

$$\frac{\text{Shear Force on Beam 253 (No Damper)}}{\text{Bending Moment on Beam 253 (X} - \text{damper Arrangement 2)}} = \frac{121}{73} = 1.6$$

$= 16\%$, the comparison shows 1.6 stories and it is acceptable.

$$\frac{\text{Shear Force on Beam 253 (No Damper)}}{\text{Shear Force on Beam 253 (V} - \text{damper Arrangement 2)}} = \frac{121}{102} = 1.18$$

$= 11.8\%$, the comparison shows 1.18 stories and it is acceptable.

- Shear Force Comparison under the Kobe Earthquake at the 2nd Story:

$$\frac{\text{Shear Force on Beam 254 (No Damper)}}{\text{Shear Force on Beam 254 (X} - \text{damper Arrangement 1)}} = \frac{125}{66} = 1.89$$

$= 18.9\%$, the comparison gives us 1.89 stories which is acceptable.

$$\frac{\text{Shear Force on Beam 254 (No Damper)}}{\text{Shear Force on Beam 254 (V} - \text{damper Arrangement 1)}} = \frac{125}{91} = 1.37$$

$= 13.7\%$, the comparison shows 1.37 stories which is acceptable.

$$\frac{\text{Shear Force on Beam 254 (No Damper)}}{\text{Shear Force on Beam 254 (X} - \text{damper Arrangement 2)}} = \frac{125}{75} = 1.6$$

$= 16\%$, the comparison shows 1.6 stories and it is acceptable.

$$\frac{\text{Shear Force on Beam 254 (No Damper)}}{\text{Shear Force on Beam 254 (V} - \text{damper Arrangement 2)}} = \frac{125}{105} = 1.19$$

$= 11.9\%$, the comparison shows 1.19 stories and it is acceptable.

- Shear Force Comparison under the Kobe Earthquake at the 7th Story:

$$\frac{\text{Shear Force on Beam 371 (No Damper)}}{\text{Shear Force on Beam 371 (X} - \text{damper Arrangement 1)}} = \frac{55}{29} = 1.89$$

$= 18.9\%$, the comparison gives us 1.89 stories which is acceptable.

$$\frac{\text{Shear Force on Beam 371 (No Damper)}}{\text{Shear Force on Beam 371 (V} - \text{damper Arrangement 1)}} = \frac{55}{40} = 1.37$$

$= 13.7\%$, the comparison shows 1.37 stories which is acceptable.

$$\frac{\text{Shear Force on Beam 371 (No Damper)}}{\text{Shear Force on Beam 371 (X} - \text{damper Arrangement 2)}} = \frac{55}{34} = 1.61$$

$= 16.1\%$, the comparison shows 1.61 stories and it is acceptable.

$$\frac{\text{Shear Force on Beam 371 (No Damper)}}{\text{Shear Force on Beam 371 (V} - \text{damper Arrangement 2)}} = \frac{55}{47} = 1.17$$

$= 11.7\%$, the comparison shows 1.17 stories and it is acceptable.

Table 4.41. Maximum and Minimum Shear Forces on Beams under Imperial Valley Earthquake.

Stories	Earthquake	Beam Label		Arrangements	Shear Force
1st Story	Imperial Valley	365	Max	Without Damper	133
		169	Min		62
		365	Max	X Damper Arr 1	106
		169	Min		70
		365	Max	V Damper Arr 1	147
		169	Min		97
		365	Max	X Damper Arr 2	115
		169	Min		79
		365	Max	V Damper Arr 2	170
		169	Min		112
2nd Story		366	Max	Without Damper	129
		170	Min		64
		366	Max	X Damper Arr 1	109
		170	Min		63
		366	Max	V Damper Arr 1	151
		170	Min		88
		366	Max	X Damper Arr 2	117
		170	Min		72
		366	Max	V Damper Arr 2	**174**
		170	Min		101
7th Story		364	Max	Without Damper	91
		175	Min		33
		364	Max	X Damper Arr 1	49
		175	Min		**18**
		364	Max	V Damper Arr 1	66
		175	Min		25
		364	Max	X Damper Arr 2	55
		175	Min		21
		364	Max	V Damper Arr 2	77
		175	Min		28

The shear force on beams under the Imperial Valley earthquake at the first story is on it's maximum at the without damper arrangement on beam 365 and minimum on beam number 169 at the X-damper arrangement 1. At the 2nd story the maximum shear force is on beam number 366 in V-damper arrangement 2 and minimum on X-damper arrangement 1 at the beam number 170. Considering the shear force on the different arrangements on the

building the maximum shear force acted on beam number 366 in V-damper arrangement 2 and the minimum acted on beam number 175 in X-damper arrangement 1.

- Shear Force Comparison under the Imperial Valley Earthquake at the 1st Story:

$$\frac{\text{Shear Force on Beam 365 (No Damper)}}{\text{Shear Force on Beam 365 (X} - \text{damper Arrangement 1)}} = \frac{133}{106} = 1.25$$

$= 12.5\%$, the comparison gives us 1.25 stories which is acceptable.

$$\frac{\text{Shear Force on Beam 365 (No Damper)}}{\text{Shear Force on Beam 365 (V} - \text{damper Arrangement 1)}} = \frac{133}{147} = 0.90$$

$= 9\%$, the comparison shows 0.9 stories which is acceptable.

$$\frac{\text{Shear Force on Beam 365 (No Damper)}}{\text{Bending Moment on Beam 365 (X} - \text{damper Arrangement 2)}} = \frac{133}{115} = 1.15$$

$= 11.5\%$, the comparison shows 1.15 stories and it is acceptable.

$$\frac{\text{Shear Force on Beam 365 (No Damper)}}{\text{Shear Force on Beam 365 (V} - \text{damper Arrangement 2)}} = \frac{133}{170} = 0.78$$

$= 7.8\%$, the comparison shows 0.78 stories and it is acceptable.

- Shear Force Comparison under the Imperial Valley Earthquake at the 2nd Story:

$$\frac{\text{Shear Force on Beam 366 (No Damper)}}{\text{Shear Force on Beam 366 (X} - \text{damper Arrangement 1)}} = \frac{129}{109} = 1.18$$

$= 11.8\%$, the comparison gives us 1.18 stories which is acceptable.

$$\frac{\text{Shear Force on Beam 366 (No Damper)}}{\text{Shear Force on Beam 366 (V} - \text{damper Arrangement 1)}} = \frac{129}{151} = 0.85$$

$= 8.5\%$, the comparison shows 0.85 stories which is acceptable.

$$\frac{\text{Shear Force on Beam 366 (No Damper)}}{\text{Shear Force on Beam 366 (X} - \text{damper Arrangement 2)}} = \frac{129}{117} = 1.10$$

$= 11\%$, the comparison shows 1.10 stories and it is acceptable.

$$\frac{\text{Shear Force on Beam 366 (No Damper)}}{\text{Shear Force on Beam 366 (V} - \text{damper Arrangement 2)}} = \frac{129}{174} = 0.74$$

$= 7.4\%$, the comparison shows 0.74 stories and it is acceptable.

- Shear Force Comparison under the Imperial Valley Earthquake at the 7th Story:

$$\frac{\text{Shear Force on Beam 364 (No Damper)}}{\text{Shear Force on Beam 364 (X} - \text{damper Arrangement 1)}} = \frac{91}{49} = 1.85$$

$= 18.5\%$, the comparison gives us 1.85 stories which is acceptable.

$$\frac{\text{Shear Force on Beam 364 (No Damper)}}{\text{Shear Force on Beam 364 (V} - \text{damper Arrangement 1)}} = \frac{91}{66} = 1.37$$

$= 13.7\%$, the comparison shows 1.37 stories which is acceptable.

$$\frac{\text{Shear Force on Beam 364 (No Damper)}}{\text{Shear Force on Beam 364 (X} - \text{damper Arrangement 2)}} = \frac{91}{55} = 1.65$$

$= 16.5\%$, the comparisonshows 1.65 stories and it is acceptable.

$$\frac{\text{Shear Force on Beam 364 (No Damper)}}{\text{Shear Force on Beam 364 (V} - \text{damper Arrangement 2)}} = \frac{91}{77} = 1.18$$

$= 11.8\%$, the comparison shows 1.18 stories and it is acceptable.

The comparison of shear forces shows that the maximum shear force percentage has occurred on 2nd story.

Table 4.42. Maximum and Minimum Shear Forces on Beams under Bam Earthquake.

Stories	Earthquake	Beam Label		Arrangements	Shear Force
1st Story	Bam	253	Max	Without Damper	120
		288	Min		60
		253	Max	X Damper Arr 1	64
		288	Min		34
		253	Max	V Damper Arr 1	88
		288	Min		46
		253	Max	X Damper Arr 2	72
		288	Min		42
		253	Max	V Damper Arr 2	101
		288	Min		53
2nd Story		254	Max	Without Damper	**132**
		415	Min		60
		254	Max	X Damper Arr 1	70
		415	Min		34
		254	Max	V Damper Arr 1	96
		415	Min		46
		254	Max	X Damper Arr 2	78
		415	Min		42
		254	Max	V Damper Arr 2	111
		415	Min		53
7th Story		371	Max	Without Damper	82
		434	Min		36
		371	Max	X Damper Arr 1	43
		434	Min		**19**
		371	Max	V Damper Arr 1	60
		434	Min		27
		371	Max	X Damper Arr 2	50
		434	Min		22
		371	Max	V Damper Arr 2	69
		434	Min		31

The maximum shear force under the Bam earthquake at the first story same as the other comparisons has happened on without damper condition on beam number 253. At the 2nd story the maximum shear force acted on beam number 254 at the without damper condition and the minimum is on beam 415 on X-damper arrangement 1. For the entire building comparison, the minimum shear force has acted on beam number 434 , 7th story at

the X-damper arrangement 1 and the maximum is on beam 254, 2nd story at the without damper condition.

- Shear Force Comparison under the Bam Earthquake at the 1st Story:

$$\frac{\text{Shear Force on Beam 253 (No Damper)}}{\text{Shear Force on Beam 253 (X} - \text{damper Arrangement 1)}} = \frac{120}{64} = 1.87$$

$= 18.7\%$, the comparison gives us 1.87 stories which is acceptable.

$$\frac{\text{Shear Force on Beam 253 (No Damper)}}{\text{Shear Force on Beam 253 (V} - \text{damper Arrangement 1)}} = \frac{120}{88} = 1.36$$

$= 13.6\%$, the comparison shows 1.36 stories which is acceptable.

$$\frac{\text{Shear Force on Beam 253 (No Damper)}}{\text{Bending Moment on Beam 253 (X} - \text{damper Arrangement 2)}} = \frac{120}{72} = 1.6$$

$= 16\%$, the comparison shows 1.6 stories and it is acceptable.

$$\frac{\text{Shear Force on Beam 253 (No Damper)}}{\text{Shear Force on Beam 253 (V} - \text{damper Arrangement 2)}} = \frac{120}{101} = 1.18$$

$= 11.8\%$, the comparison shows 1.18 stories and it is acceptable.

- Shear Force Comparison under the Bam Earthquake at the 2nd Story:

$$\frac{\text{Shear Force on Beam 254 (No Damper)}}{\text{Shear Force on Beam 254 (X} - \text{damper Arrangement 1)}} = \frac{132}{70} = 1.88$$

$= 18.8\%$, the comparison gives us 1.88 stories which is acceptable.

$$\frac{\text{Shear Force on Beam 254 (No Damper)}}{\text{Shear Force on Beam 254 (V} - \text{damper Arrangement 1)}} = \frac{132}{96} = 1.37$$

$= 13.7\%$, the comparison shows 1.37 stories which is acceptable.

$$\frac{\text{Shear Force on Beam 254 (No Damper)}}{\text{Shear Force on Beam 254 (X} - \text{damper Arrangement 2)}} = \frac{132}{78} = 1.69$$

$= 16.9\%$, the comparison shows 1.69 stories and it is acceptable.

$$\frac{\text{Shear Force on Beam 254 (No Damper)}}{\text{Shear Force on Beam 254 (V} - \text{damper Arrangement 2)}} = \frac{132}{111} = 1.18$$

$= 11.8\%$, the comparison shows 1.18 stories and it is acceptable.

- Shear Force Comparison under the Bam Earthquake at the 7th Story:

$$\frac{\text{Shear Force on Beam 371 (No Damper)}}{\text{Shear Force on Beam 371 (X} - \text{damper Arrangement 1)}} = \frac{82}{43} = 1.9$$

$= 19\%$, the comparison gives us 1.9 stories which is acceptable.

$$\frac{\text{Shear Force on Beam 371 (No Damper)}}{\text{Shear Force on Beam 371 (V} - \text{damper Arrangement 1)}} = \frac{82}{60} = 1.36$$

$= 13.6\%$, the comparison shows 1.36 stories which is acceptable.

$$\frac{\text{Shear Force on Beam 371 (No Damper)}}{\text{Shear Force on Beam 371 (X} - \text{damper Arrangement 2)}} = \frac{82}{50} = 1.64$$

$= 16.4\%$, the comparison shows 1.64 stories and it is acceptable.

$$\frac{\text{Shear Force on Beam 371 (No Damper)}}{\text{Shear Force on Beam 371 (V} - \text{damper Arrangement 2)}} = \frac{82}{69} = 1.18$$

$= 11.8\%$, the comparison shows 1.18 stories and it is acceptable.

Table 4.43. Maximum and Minimum Shear Forces on Beams under Parkfield Earthquake.

Stories	Earthquake	Beam Label		Arrangements	Shear Force
1st Story	Parkfield	253	Max	Without Damper	214
		183	Min		114
		253	Max	X Damper Arr 1	111
		183	Min		61
		253	Max	V Damper Arr 1	153
		183	Min		83
		253	Max	X Damper Arr 2	119
		183	Min		69
		253	Max	V Damper Arr 2	177
		183	Min		96
2nd Story		254	Max	Without Damper	**232**
		422	Min		91
		254	Max	X Damper Arr 1	120
		422	Min		49
		254	Max	V Damper Arr 1	166
		422	Min		67
		254	Max	X Damper Arr 2	128
		422	Min		58
		254	Max	V Damper Arr 2	191
		422	Min		78
7th Story		371	Max	Without Damper	122
		217	Min		59
		371	Max	X Damper Arr 1	65
		217	Min		**32**
		371	Max	V Damper Arr 1	89
		217	Min		43
		371	Max	X Damper Arr 2	74
		217	Min		36
		371	Max	V Damper Arr 2	103
		217	Min		50

The maximum shear force at the first story under the Parkfield earthquake acted in beam number 253 at the without damper and the minimum on X-damper arrangement one at the beam number 183. At the second story the maximum shear force is on the beam number 254 and the minimum is on beam number 422 in X-damper arrangement 1. The minimum shear force is on the 7th story beam number 217 on X-damper arrangement 1.

- Shear Force Comparison under the Parkfield Earthquake at the 1st Story:

$$\frac{\text{Shear Force on Beam 253 (No Damper)}}{\text{Shear Force on Beam 253 (X} - \text{damper Arrangement 1)}} = \frac{214}{111} = 1.9$$

$= 19\%$, the comparison gives us 1.9 stories which is acceptable.

$$\frac{\text{Shear Force on Beam 253 (No Damper)}}{\text{Shear Force on Beam 253 (V} - \text{damper Arrangement 1)}} = \frac{214}{153} = 1.39$$

$= 13.9\%$, the comparison shows 1.39 stories which is acceptable.

$$\frac{\text{Shear Force on Beam 253 (No Damper)}}{\text{Bending Moment on Beam 253 (X} - \text{damper Arrangement 2)}} = \frac{214}{119} = 1.79$$

$= 17.9\%$, the comparison shows 1.79 stories and it is acceptable.

$$\frac{\text{Shear Force on Beam 253 (No Damper)}}{\text{Shear Force on Beam 253 (V} - \text{damper Arrangement 2)}} = \frac{214}{177} = 1.20$$

$= 12\%$, the comparison shows 1.20 stories and it is acceptable.

- Shear Force Comparison under the Parkfield Earthquake at the 2nd Story:

$$\frac{\text{Shear Force on Beam 254 (No Damper)}}{\text{Shear Force on Beam 254 (X} - \text{damper Arrangement 1)}} = \frac{232}{120} = 1.93$$

$= 19.3\%$, the comparison gives us 1.93 stories which is acceptable.

$$\frac{\text{Shear Force on Beam 254 (No Damper)}}{\text{Shear Force on Beam 254 (V} - \text{damper Arrangement 1)}} = \frac{232}{166} = 1.39$$

$= 13.9\%$, the comparison shows 1.39 stories which is acceptable.

$$\frac{\text{Shear Force on Beam 254 (No Damper)}}{\text{Shear Force on Beam 254 (X} - \text{damper Arrangement 2)}} = \frac{232}{128} = 1.81$$

$= 18.1\%$, the comparison shows 1.81 stories and it is acceptable.

$$\frac{\text{Shear Force on Beam 254 (No Damper)}}{\text{Shear Force on Beam 254 (V} - \text{damper Arrangement 2)}} = \frac{232}{191} = 1.21$$

$= 12.1\%$, the comparison shows 1.21 stories and it is acceptable.

- Shear Force Comparison under the Parkfield Earthquake at the 7th Story:

$$\frac{\text{Shear Force on Beam 371 (No Damper)}}{\text{Shear Force on Beam 371 (X} - \text{damper Arrangement 1)}} = \frac{122}{65} = 1.87$$

$= 18.7\%$, the comparison gives us 1.87 stories which is acceptable.

$$\frac{\text{Shear Force on Beam 371 (No Damper)}}{\text{Shear Force on Beam 371 (V} - \text{damper Arrangement 1)}} = \frac{122}{89} = 1.37$$

$= 13.7\%$, the comparison shows 1.37 stories which is acceptable.

$$\frac{\text{Shear Force on Beam 371 (No Damper)}}{\text{Shear Force on Beam 371 (X} - \text{damper Arrangement 2)}} = \frac{122}{74} = 1.64$$

$= 16.4\%$, the comparison shows 1.64 stories and it is acceptable.

$$\frac{\text{Shear Force on Beam 371 (No Damper)}}{\text{Shear Force on Beam 371 (V} - \text{damper Arrangement 2)}} = \frac{122}{103} = 1.18$$

$= 11.8\%$, the comparison shows 1.18 stories and it is acceptable.

Table 4.44. Maximum and Minimum Shear Forces on Beams under Düzce Earthquake

Stories	Earthquake	Beam Label		Arrangements	Shear Force
1st Story	Düzce	253	Max	Without Damper	**257**
		197	Min		61
		253	Max	X Damper Arr 1	132
		197	Min		34
		253	Max	V Damper Arr 1	183
		197	Min		46
		253	Max	X Damper Arr 2	141
		197	Min		43
		253	Max	V Damper Arr 2	211
		197	Min		54
2nd Story		254	Max	Without Damper	196
		415	Min		60
		254	Max	X Damper Arr 1	102
		415	Min		34
		254	Max	V Damper Arr 1	141
		415	Min		46
		254	Max	X Damper Arr 2	110
		415	Min		42
		254	Max	V Damper Arr 2	162
		415	Min		53
7th Story		364	Max	Without Damper	147
		175	Min		34
		364	Max	X Damper Arr 1	79
		175	Min		**18**
		364	Max	V Damper Arr 1	108
		175	Min		25
		364	Max	X Damper Arr 2	90
		175	Min		21
		364	Max	V Damper Arr 2	125
		175	Min		29

As shown in table 4.44, the maximum shear force at the first floor acted on beam 253 on without damper arrangement and the minimum acted on beam number 197 on X-damper arrangement 1. And it has acted the same according to the arrangements on 2nd and 7th stories. The maximum shear force on building under the Düzce earthquake acted on beam 253 at the first floor on without damper arrangement which is equal to 257, and the minimum has acted on beam 175 on 7th floor at the X-damper arrangement 1.

- Shear Force Comparison under the Düzce Earthquake at the 1st Story:

$$\frac{\text{Shear Force on Beam 253 (No Damper)}}{\text{Shear Force on Beam 253 (X} - \text{damper Arrangement 1)}} = \frac{257}{132} = 1.9$$

$= 19\%$, the comparison gives us 1.9 stories which is acceptable.

$$\frac{\text{Shear Force on Beam 253 (No Damper)}}{\text{Shear Force on Beam 253 (V} - \text{damper Arrangement 1)}} = \frac{257}{183} = 1.4$$

$= 14\%$, the comparison shows 1.4 stories which is acceptable.

$$\frac{\text{Shear Force on Beam 253 (No Damper)}}{\text{Bending Moment on Beam 253 (X} - \text{damper Arrangement 2)}} = \frac{257}{141} = 1.82$$

$= 18.2\%$, the comparisonshows 1.82 stories and it is acceptable.

$$\frac{\text{Shear Force on Beam 253 (No Damper)}}{\text{Shear Force on Beam 253 (V} - \text{damper Arrangement 2)}} = \frac{257}{211} = 1.2$$

$= 12\%$, the comparison shows 1.2 stories and it is acceptable.

- Shear Force Comparison under the Düzce Earthquake at the 2nd Story:

$$\frac{\text{Shear Force on Beam 254 (No Damper)}}{\text{Shear Force on Beam 254 (X} - \text{damper Arrangement 1)}} = \frac{196}{102} = 1.9$$

$= 19\%$, the comparison gives us 1.9 stories which is acceptable.

$$\frac{\text{Shear Force on Beam 254 (No Damper)}}{\text{Shear Force on Beam 254 (V} - \text{damper Arrangement 1)}} = \frac{196}{141} = 1.39$$

$= 13.9\%$, the comparison shows 1.39 stories which is acceptable.

$$\frac{\text{Shear Force on Beam 254 (No Damper)}}{\text{Shear Force on Beam 254 (X} - \text{damper Arrangement 2)}} = \frac{196}{110} = 1.78$$

$= 17.8\%$, the comparison shows 1.78 stories and it is acceptable.

$$\frac{\text{Shear Force on Beam 254 (No Damper)}}{\text{Shear Force on Beam 254 (V} - \text{damper Arrangement 2)}} = \frac{196}{162} = 1.2$$

$= 12\%$, the comparison shows 1.2 stories and it is acceptable.

- Shear Force Comparison under the Düzce Earthquake at the 7th Story:

$$\frac{\text{Shear Force on Beam 364 (No Damper)}}{\text{Shear Force on Beam 364 (X} - \text{damper Arrangement 1)}} = \frac{147}{79} = 1.86$$

$= 18.6\%$, the comparison gives us 1.86 stories which is acceptable.

$$\frac{\text{Shear Force on Beam 364 (No Damper)}}{\text{Shear Force on Beam 364 (V} - \text{damper Arrangement 1)}} = \frac{147}{108} = 1.36$$

$= 13.6\%$, the comparison shows 1.36 stories which is acceptable.

$$\frac{\text{Shear Force on Beam 364 (No Damper)}}{\text{Shear Force on Beam 364 (X} - \text{damper Arrangement 2)}} = \frac{147}{90} = 1.63$$

$= 16.3\%$, the comparison shows 1.63 stories and it is acceptable.

$$\frac{\text{Shear Force on Beam 364 (No Damper)}}{\text{Shear Force on Beam 364 (V} - \text{damper Arrangement 2)}} = \frac{147}{125} = 1.17$$

$= 11.7\%$, the comparison shows 1.17 stories and it is acceptable.

4.4.3 Columns Labels Characterizations

For the columns, the labels are shown in table 4.45 and also shown in below Figure 4.87 – 4.90.

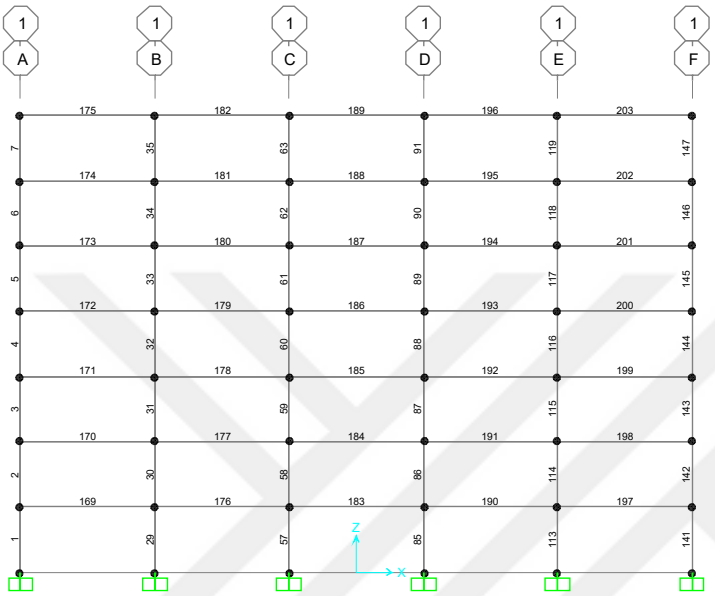


Figure 4.87. Beams and Columns Labels View Section 1-1.

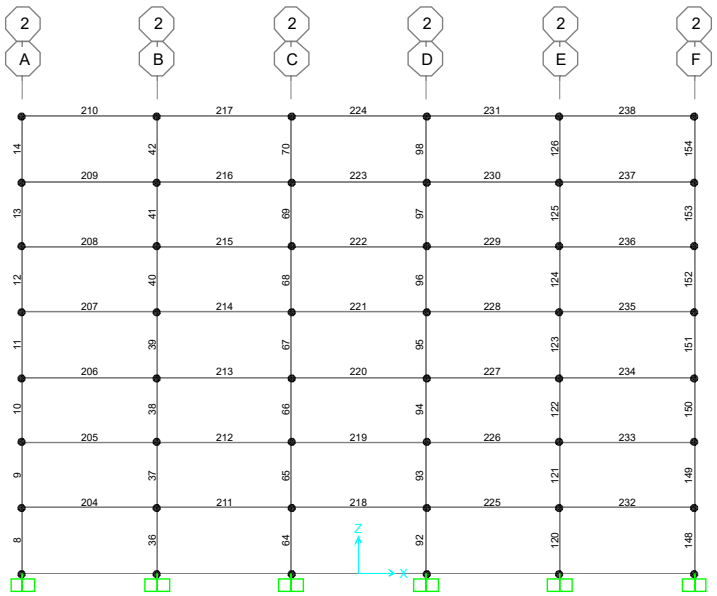


Figure 4.88. Beams and Columns Labels View Section 2-2.

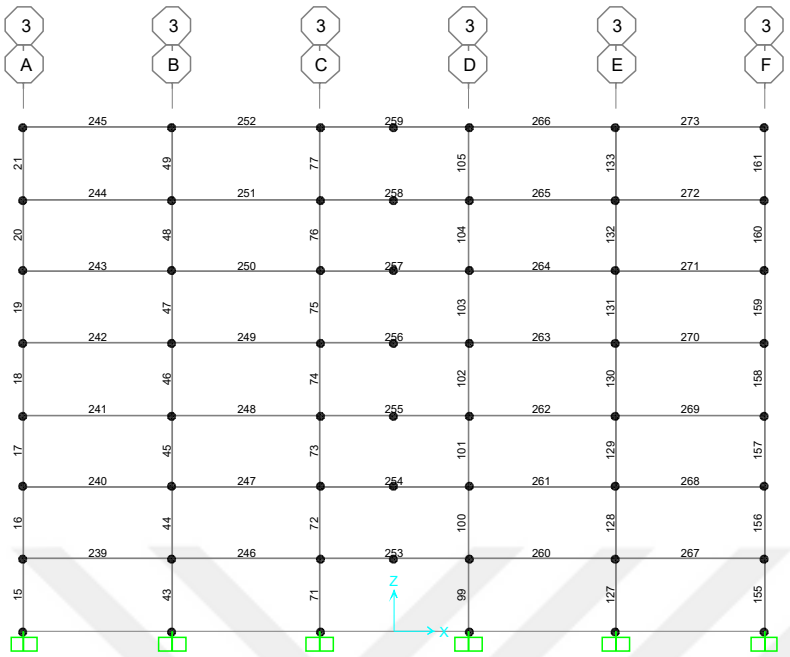


Figure 4.89. Beams and Columns Labels View Section 3-3

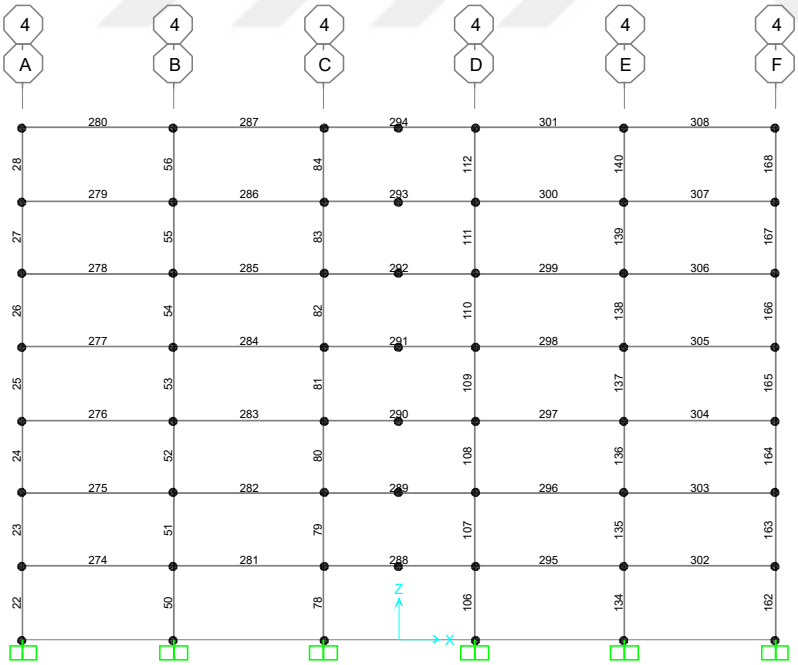


Figure 4.90. Beams and Columns Labels View Section 4-4

Table 4.45. Column Labels Characterization

Label at Story 1	Axis	Label at Story 2	Axis	Label at Story 7	Axis
1	A/1	2	A/1	7	A/1
29	B/1	30	B/1	35	B/1
57	C/1	58	C/1	63	C/1
85	D/1	86	D/1	91	D/1
113	E/1	114	E/1	119	E/1
141	F/1	142	F/1	147	F/1
8	A/2	9	A/2	14	A/2
36	B/2	37	B/2	42	B/2
64	C/2	65	C/2	70	C/2
92	D/2	93	D/2	98	D/2
120	E/2	121	E/2	126	E/2
148	F/2	149	F/2	154	F/2
15	A/3	16	A/3	21	A/3
43	B/3	44	B/3	49	B/3
71	C/3	72	C/3	77	C/3
99	D/3	100	D/3	105	D/3
127	E/3	128	E/3	133	E/3
155	F/3	156	F/3	161	F/3
22	A/4	23	A/4	28	A/4
50	B/4	51	B/4	56	B/4
78	C/4	79	C/4	84	C/4
106	D/4	107	D/4	112	D/4
134	E/4	135	E/4	140	E/4
162	F/4	163	F/4	168	F/4

4.4.4 Columns Maximum Axial Force

The columns maximum axial forces are shown in below tables and also in graphs. Comparing the considered earthquakes, the Kobe and Düzce earthquakes are the strongest, therefore the graphs are shown for these two earthquakes in without damper, X and V damper arrangement 1, X and V damper arrangement 2.

4.4.5 The maximum Axial Forces Under Kobe Earthquake at the 1st, 2nd and 7th Stories

The below graph in figure 4.91 shows the maximum axial forces under the Kobe earthquake when there is no damper installed on the building. The axial forces are at their maximum on the first floor and minimum at the 7th story.

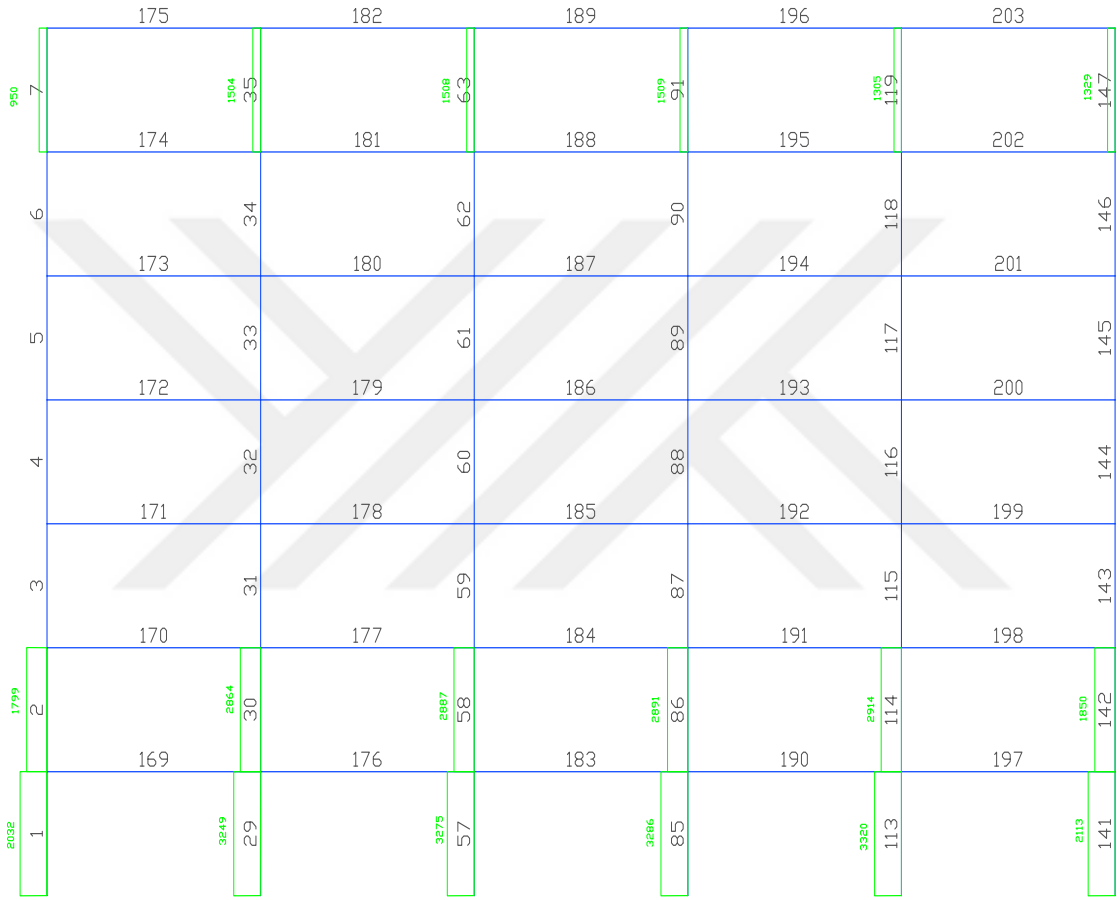


Figure 4.91 Maximum Columns Axial Forces on 1st, 2nd, and 7th Stories under Kobe Earthquake Without Damper X-Z Axis.

Table 4.46. Columns Maximum Axial Forces Under Kobe Earthquake 1st, 2nd and 7th Story, X-Z Axis.

Without Damper		
Story	Column Label	Axial Forces
1st Story X-Z Axis	1	2032
	29	3249
	57	3275
	85	**3286**
	113	3320
	141	2113
2nd Story X-Z Axis	2	1799
	30	2864
	58	2887
	86	2891
	114	2914
	142	1850
7th Story X-Z Axis	7	**950**
	35	1504
	63	1508
	91	1509
	119	1305
	147	1329

The axial forces from the above table are shown in the figure 4.91 in graph form. The maximum is at the 1st floor and the minimum is at the 7th floor. The maximum axial force is at the column number 113 at the first story.

The graph below in figure 4.92 shows the maximum axial forces on the Y-Z axis of the building under the Kobe earthquake at the 1st, 2nd and 7th stories.

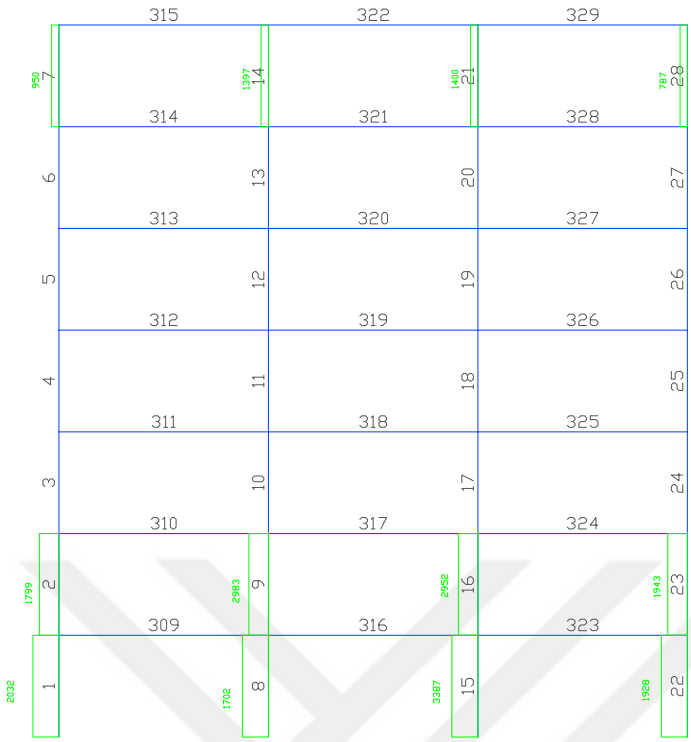


Figure 4.92 Maximum Columns Axial Forces on 1st, 2nd, and 7th Stories under Kobe Earthquake Without Damper Y -Z Axis.

Table 4.47. Columns Maximum Axial Forces Under Kobe Earthquake 1st, 2nd and 7th Story, Y-Z Axis.

Without Damper		
Story	Column Label	Axial Forces
1st Story Y-Z Axis	1	2032
	8	1702
	15	**3387**
	22	1928
2nd Story Y-Z Axis	2	1799
	9	2983
	16	2952
	23	1943
7th Story Y-Z Axis	7	950
	14	1397
	21	1400
	28	**787**

The axial force values from the above table is shown in form of graph in figure 4.92 where the maximum axial force acted on column number 15 at the first floor and the minimum is on beam number 28 at the 7th floor under the Kobe earthquake without damper.

The below graph in figure 4.93 shows the maximum axial forces on columns under the Kobe earthquake in the 1st, 2nd and 7th stories of the X-damped structure.

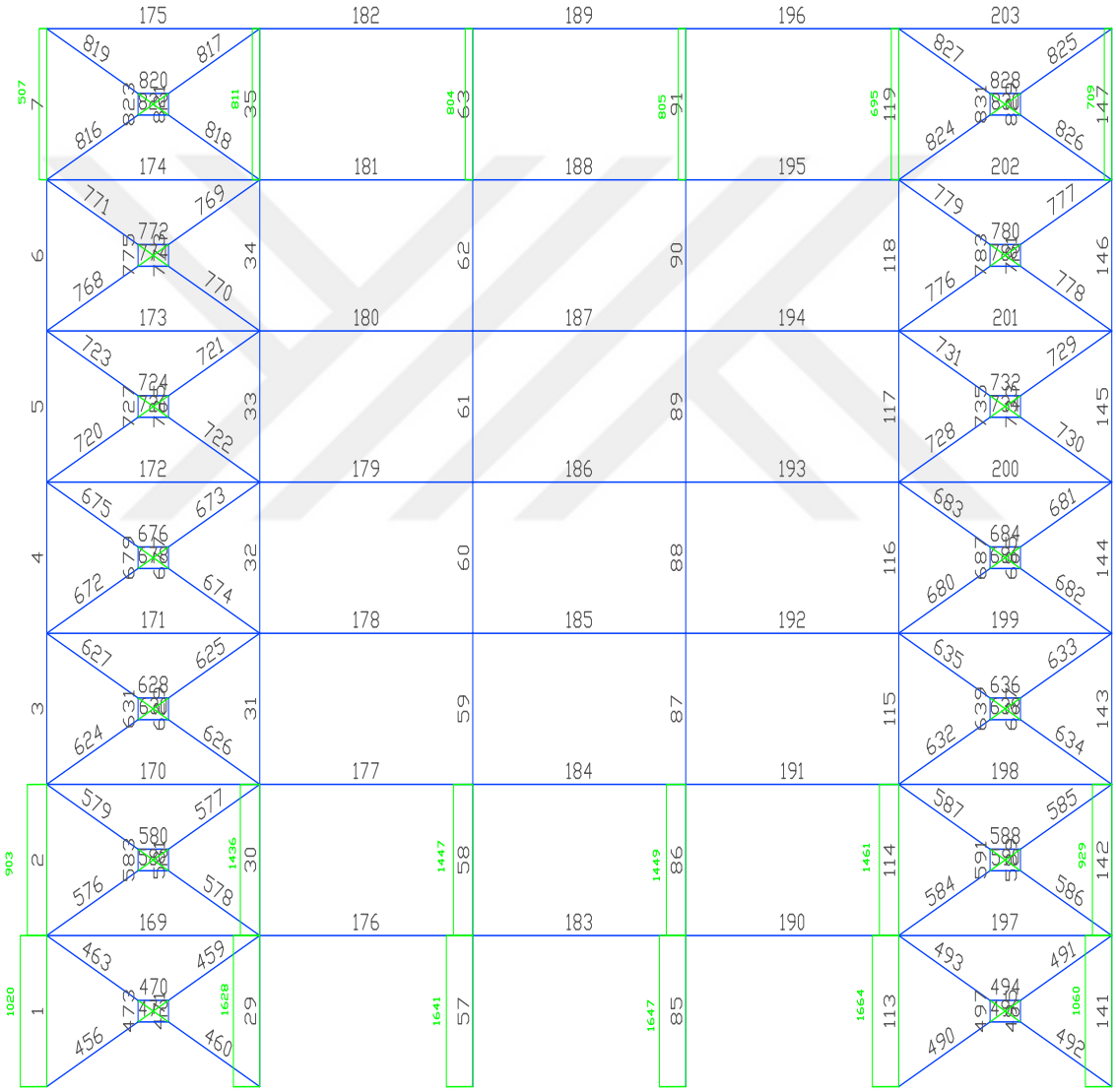


Figure 4.93 Maximum Columns Axial Forces on 1st, 2nd, and 7th Stories under Kobe Earthquake X-Damper Arrangement 1 X -Z Axis.

Table 4.48. Columns Maximum Axial Forces Under Kobe Earthquake 1st, 2nd and 7th Story, X-Z Axis.

X-Damper Arrangement 1		
Story	Column Label	Axial Forces
1st Story X-Z Axis	1	1020
	29	1628
	57	1641
	85	1647
	113	**1664**
	141	1060
2nd Story X-Z Axis	2	903
	30	1436
	58	1447
	86	1449
	114	1461
	142	929
7th Story X-Z Axis	7	**507**
	35	811
	63	804
	91	805
	119	695
	147	709

Table 4.48 shows the column's axial forces under the Kobe earthquake, where the maximum axial force acted on column number 1664 at the first story and the minimum is on column number 7 at the 7th story.

The figure 4.94 shows the maximum axial forces in the graph form for the Y-Z axis of the structure at the 1st, 2nd and 7th stories under the Kobe earthquake.

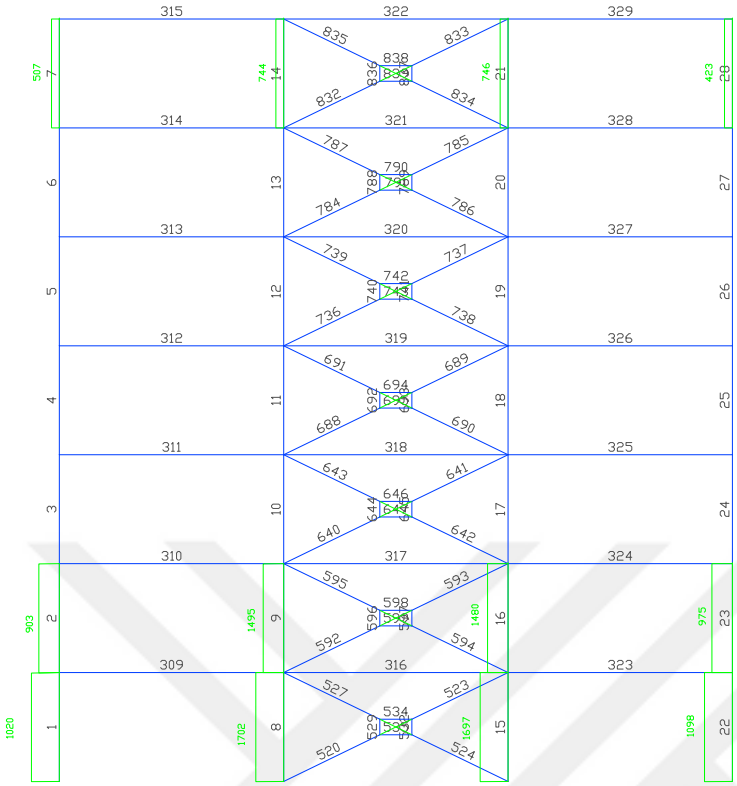


Figure 4.94 Maximum Columns Axial Forces on 1st, 2nd, and 7th Stories under Kobe Earthquake X-Damper Arrangement 1 Y -Z Axis.

Table 4.49. Columns Maximum Axial Forces Under Kobe Earthquake 1st, 2nd and 7th Story, Y-Z Axis.

X-Damper Arrangement 1		
Story	Column Label	Axial Forces
1st Story Y-Z Axis	1	1020
	8	**1702**
	15	1697
	22	1098
2nd Story Y-Z Axis	2	903
	9	1495
	16	1480
	23	975
7th Story Y-Z Axis	7	507
	14	744
	21	746
	28	**423**

Table 4.49 states the maximum axial forces of columns under the Kobe earthquake at the Y-Z axis, where the maximum axial force has acted on beam number 8 at the first floor and minimum is on the beam number 28 at the 7th floor.

Figure 4.95 shows the maximum axial forces of columns in the Inverted-V damped structure form in X-Z axis.

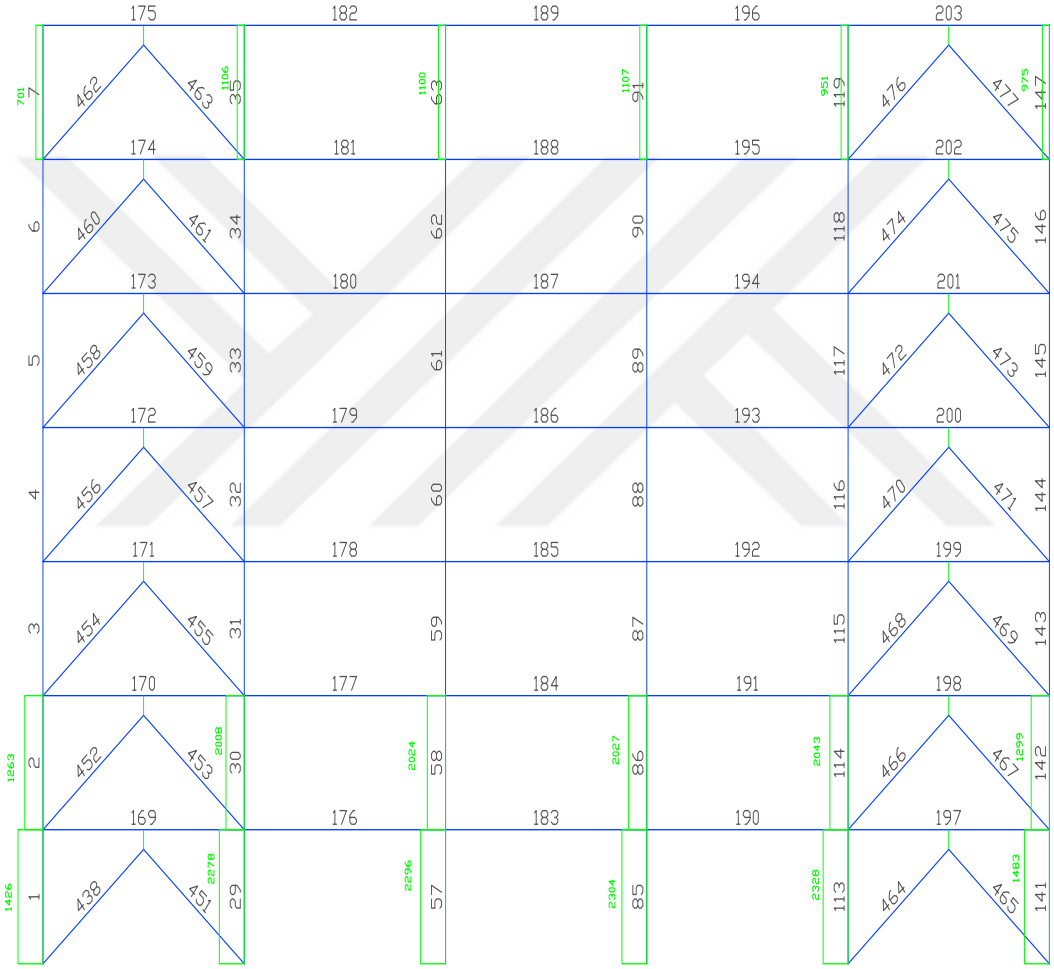


Figure 4.95 Maximum Columns Axial Forces on 1st, 2nd, and 7th Stories under Kobe Earthquake V-Damper Arrangement 1 X -Z Axis.

Table 4.50. Columns Maximum Axial Forces Under Kobe Earthquake 1st, 2nd and 7th Story, X-Z Axis

V-Damper Arrangement 1		
Story	Column Label	Axial Forces
1st Story X-Z Axis	1	1426
	29	2278
	57	2296
	85	2304
	113	**2328**
	141	1483
2nd Story X-Z Axis	2	1263
	30	2008
	58	2024
	86	2027
	114	2043
	142	1299
7th Story X-Z Axis	7	**701**
	35	1106
	63	1100
	91	1107
	119	951
	147	975

The axial forces are shown in the table 4.50 for the Inverted-V damped structure in X-Z axis and the maximum axial force shows to be acted on beam number 113 at the first floor and the minimum is on beam number 7 at the 7th story.

The axial forces are shown in figure 4.96 for the Inverted-V damped structure in Y-Z axis.

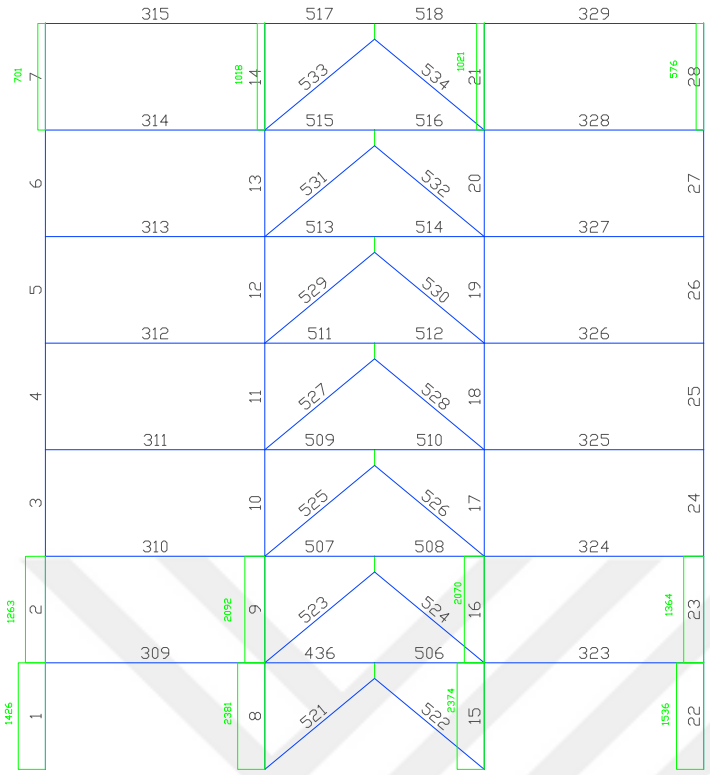


Figure 4.96 Maximum Columns Axial Forces on 1st, 2nd, and 7th Stories under Kobe Earthquake V-Damper Arrangement 1 Y -Z Axis.

Table 4.51 Columns Maximum Axial Forces Under Kobe Earthquake 1st, 2nd and 7th Story, Y-Z Axis.

V-Damper Arrangement 1		
Story	Column Label	Axial Forces
1st Story Y-Z Axis	1	1426
	8	**2381**
	15	2374
	22	1536
2nd Story Y-Z Axis	2	1263
	9	2092
	16	2070
	23	1364
7th Story Y-Z Axis	7	701
	14	1018
	21	1021
	28	**576**

The maximum axial force as shown in above table 4.51 has occurred on beam number 8 at the 1st story and the minimum is on beam number 28 at the 7th story under the Kobe earthquake in Y-Z axis.

The figure 4.97 shows the axial force diagram for the X-damped arrangement 2 structure under the Kobe earthquake.

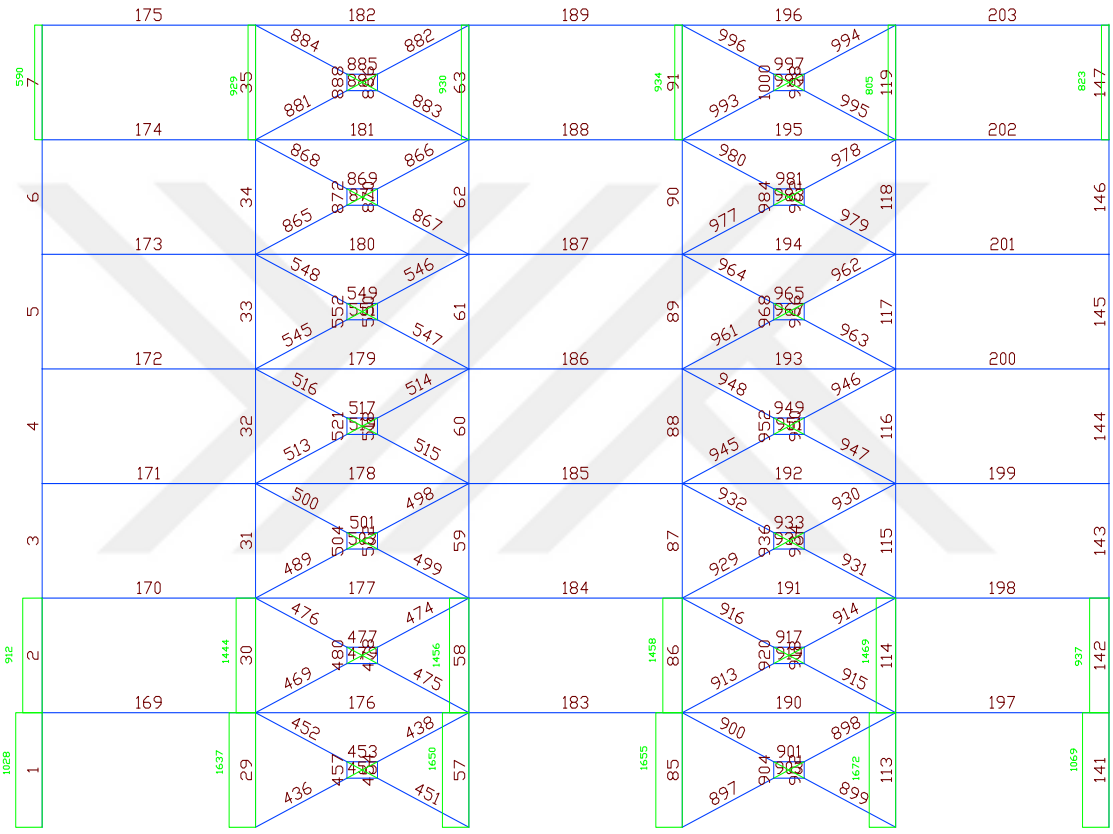


Figure 4.97 Maximum Columns Axial Forces on 1st, 2nd, and 7th Stories under Kobe Earthquake X-Damper Arrangement 2 X-Z Axis.

Table 4.52. Columns Maximum Axial Forces Under Kobe Earthquake 1st, 2nd and 7th Story, X-Z Axis

X-Damper Arrangement 2		
Story	Column Label	Axial Forces
1st Story X-Z Axis	1	1028
	29	1637
	57	1650
	85	1655
	113	**1672**
	141	1069
2nd Story X-Z Axis	2	912
	30	1444
	58	1456
	86	1458
	114	1469
	142	937
7th Story X-Z Axis	7	**590**
	35	929
	63	930
	91	934
	119	805
	147	823

From the above table 4.52, it is clear that the maximum axial force is on column 113 at the 1st story and the minimum is on beam number 7 at the 7th story.

Figure 4.98 shows the maximum axial forces on columns under the Kobe earthquake at the 1st, 2nd and 7th stories in X-damped arrangement 2.

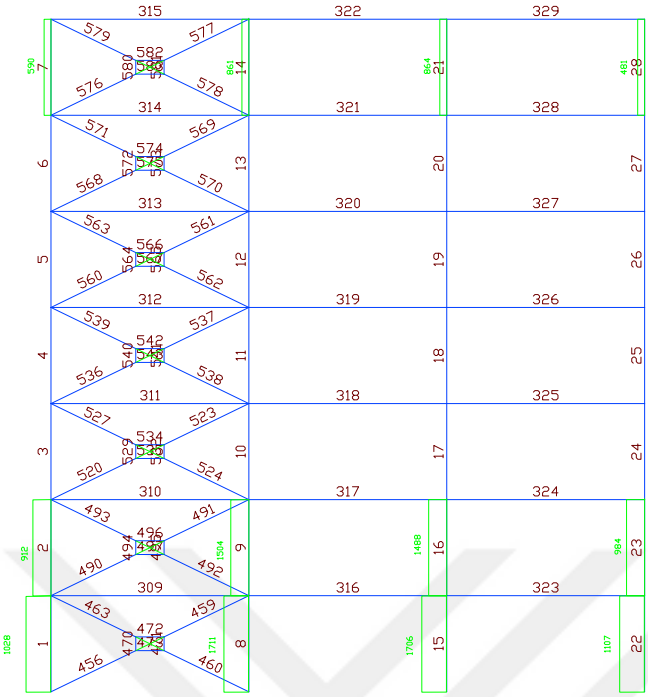


Figure 4.98 Maximum Columns Axial Forces on 1st, 2nd, and 7th Stories under Kobe Earthquake X-Damper Arrangement 2Y-Z Axis.

Table 4.53 Columns Maximum Axial Forces Under Kobe Earthquake 1st, 2nd and 7th Story, Y-Z Axis.

X-Damper Arrangement 2		
Story	Column Label	Axial Forces
1st Story Y-Z Axis	1	1028
	8	1711
	15	**1706**
	22	1107
2nd Story Y-Z Axis	2	912
	9	1504
	16	1488
	23	984
7th Story Y-Z Axis	7	590
	14	861
	21	864
	28	**481**

The above table 4.53 shows the maximum axial forces on columns at the Y-Z axis under the Kobe earthquake. The maximum shear force has acted on column number 8 at the 1st story and the minimum is on column number 28 at the 7th story.

Figure 4.99 shows the maximum axial forces on columns at the 1st, 2nd and 7th stories in Inverted-V arrangement 2.

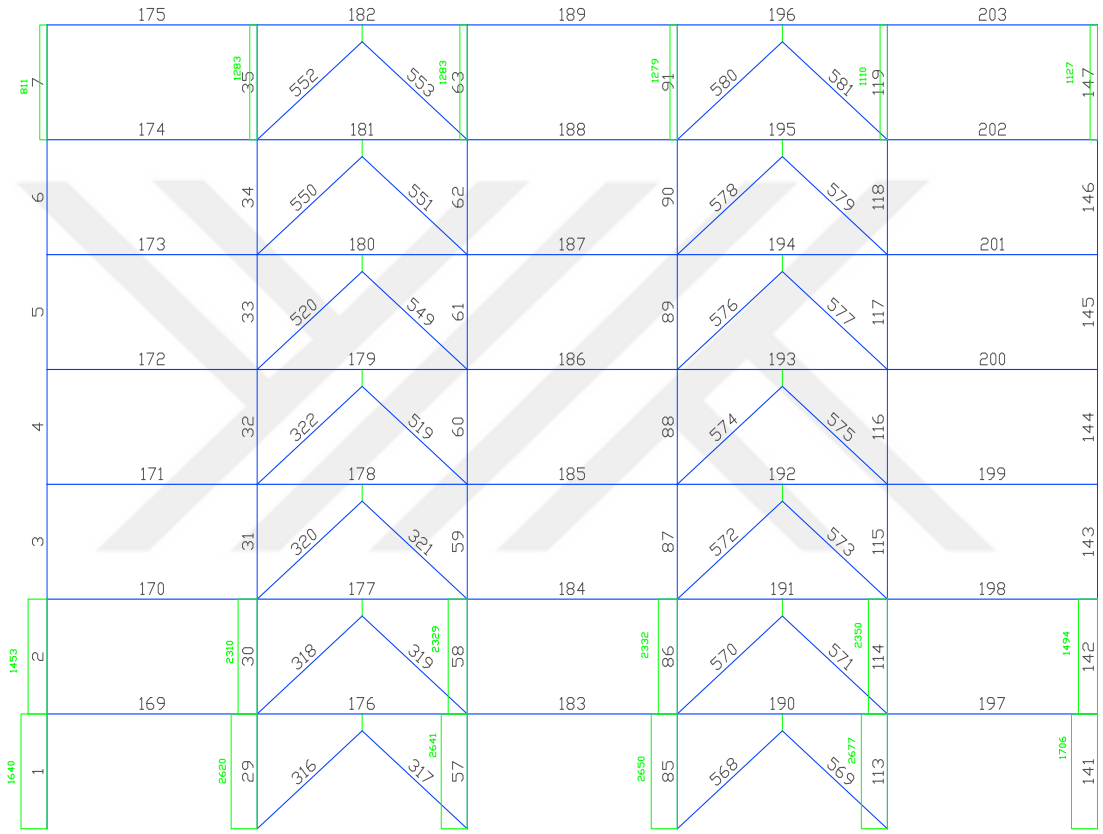


Figure 4.99 Maximum Columns Axial Forces on 1st, 2nd, and 7th Stories under Kobe Earthquake V-Damper Arrangement 2X-Z Axis.

Table 4.54. Columns Maximum Axial Forces Under Kobe Earthquake 1st, 2nd and 7th Story, X-Z Axis.

V-Damper Arrangement 2		
Story	Column Label	Axial Forces
1st Story X-Z Axis	1	1604
	29	2620
	57	2641
	85	2650
	113	**2677**
	141	1706
2nd Story X-Z Axis	2	1453
	30	2310
	58	2329
	86	2332
	114	2350
	142	1494
7th Story X-Z Axis	7	**811**
	35	1203
	63	1283
	91	1279
	119	1110
	147	1127

Figure 4.100 stated the maximum axial forces on columns at the Y-Z axis of the Inverted-V damped arrangement 2.

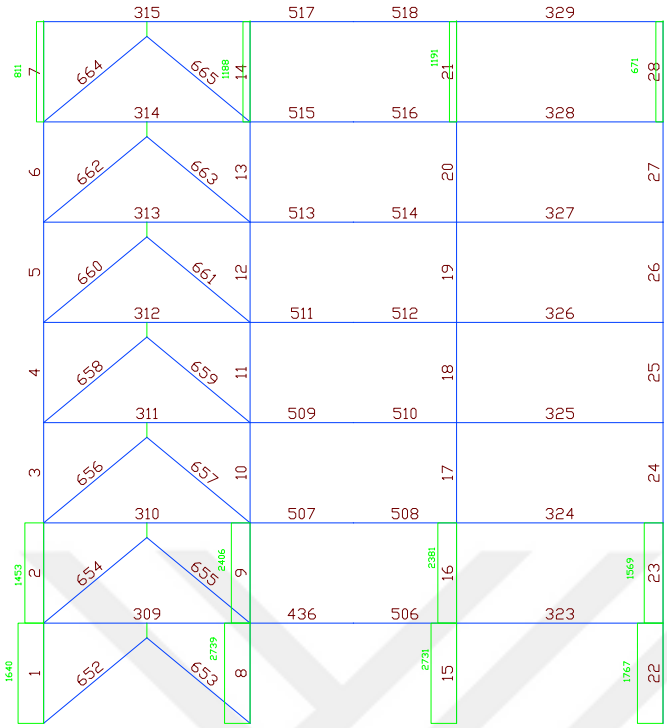


Figure 4.100 Maximum Columns Axial Forces on 1st, 2nd, and 7th Stories under Kobe Earthquake V-Damper Arrangement 2 Y-Z Axis.

Table 4.55. Columns Maximum Axial Forces Under Kobe Earthquake 1st, 2nd and 7th Story, Y-Z Axis.

V-Damper Arrangement 2		
Story	Column Label	Axial Forces
1st Story Y-Z Axis	1	1604
	8	**2739**
	15	2731
	22	1767
2nd Story Y-Z Axis	2	1453
	9	2406
	16	2381
	23	1569
7th Story Y-Z Axis	7	811
	14	1188
	21	1191
	28	**671**

The table 4.55 shows that the maximum axial force is on beam number 8 at the 1st floor and the minimum is on beam number 28 at the 7th story.

Comparing the without damper, X-damper arrangement 1 & 2, Inverted-V damper arrangement 1 & 2 shows that the axial forces are at their maximum in the without damper form and minimum in the X-damper arrangement 1 form. Looking backward to the result of the shear forces and bending moments we can realize that the building can be on the safest side with the X-damper arrangement 1.

4.4.6 The maximum Axial Forces Under Düzce Earthquake at the 1st, 2nd and 7th Stories

The below graph in figure 4.101 shows the column's maximum axial forces under the Düzce earthquake when there is no damper installed on the building. The axial forces are at their maximum on the first floor and minimum at the 7th story.

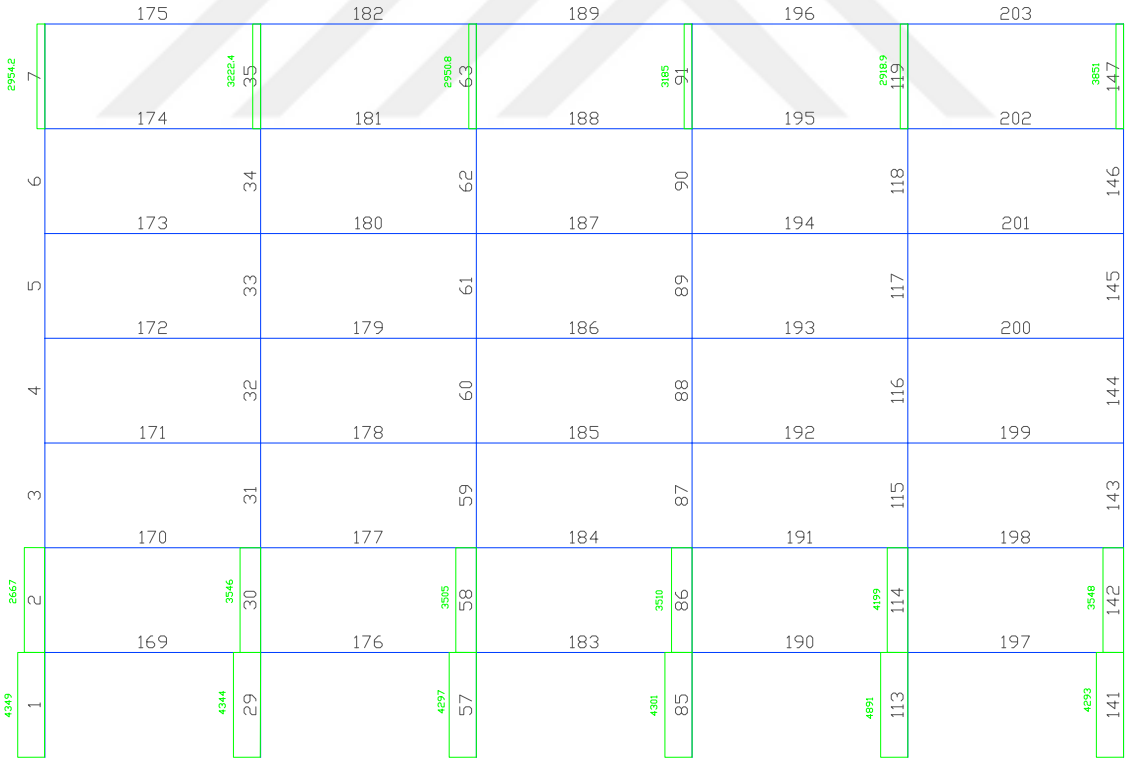


Figure 4.101 Maximum Columns Axial Forces on 1st, 2nd, and 7th Stories under Düzce Earthquake Without Damper X-Z Axis.

Table 4.56. Columns Maximum Axial Forces Under Düzce Earthquake 1st, 2nd and 7th Story, X-Z Axis

Without Damper		
Story	Column Label	Axial Forces
1st Story X-Z Axis	1	4349
	29	4344
	57	4297
	85	4301
	113	**4891**
	141	4293
2nd Story X-Z Axis	2	2667
	30	3546
	58	3505
	86	3510
	114	4199
	142	3548
7th Story X-Z Axis	7	2954.2
	35	3222.4
	63	2950.8
	91	**3185**
	119	2918.9
	147	3851

The maximum axial forces are shown in the above table for the without damper condition on the X-Z axis of the structure where the maximum is on column 113 and the minimum is on column number 147.

Figure 4.102 shows the maximum axial forces on columns in the graph form for the 1st, 2nd and 7th stories.

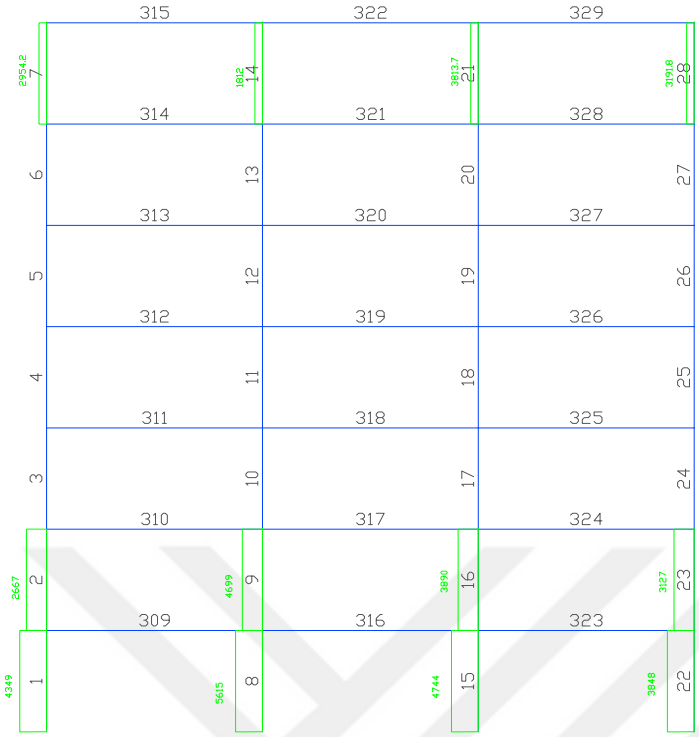


Figure 4.102 Maximum Columns Axial Forces on 1st, 2nd, and 7th Stories under Düzce Earthquake Without Damper Y-Z Axis.

Table 4.57. Columns Maximum Axial Forces Under Düzce Earthquake 1st, 2nd and 7th Story, Y-Z Axis.

Without Damper		
Story	Column Label	Axial Forces
1st Story Y-Z Axis	1	4349
	8	**5615**
	15	4744
	22	3848
2nd Story Y-Z Axis	2	2667
	9	4699
	16	3890
	23	3127
7th Story Y-Z Axis	7	2954.2
	14	**1812**
	21	3813.7
	28	3191.8

The above table 4.57 shows that the maximum axial force is on column number 8 at the first floor and the minimum acted on columns 14 at the 7th floor.

Figure 4.103 shows the maximum axial forces on columns in the form of diagram for the x-damper arrangement 1 installation.

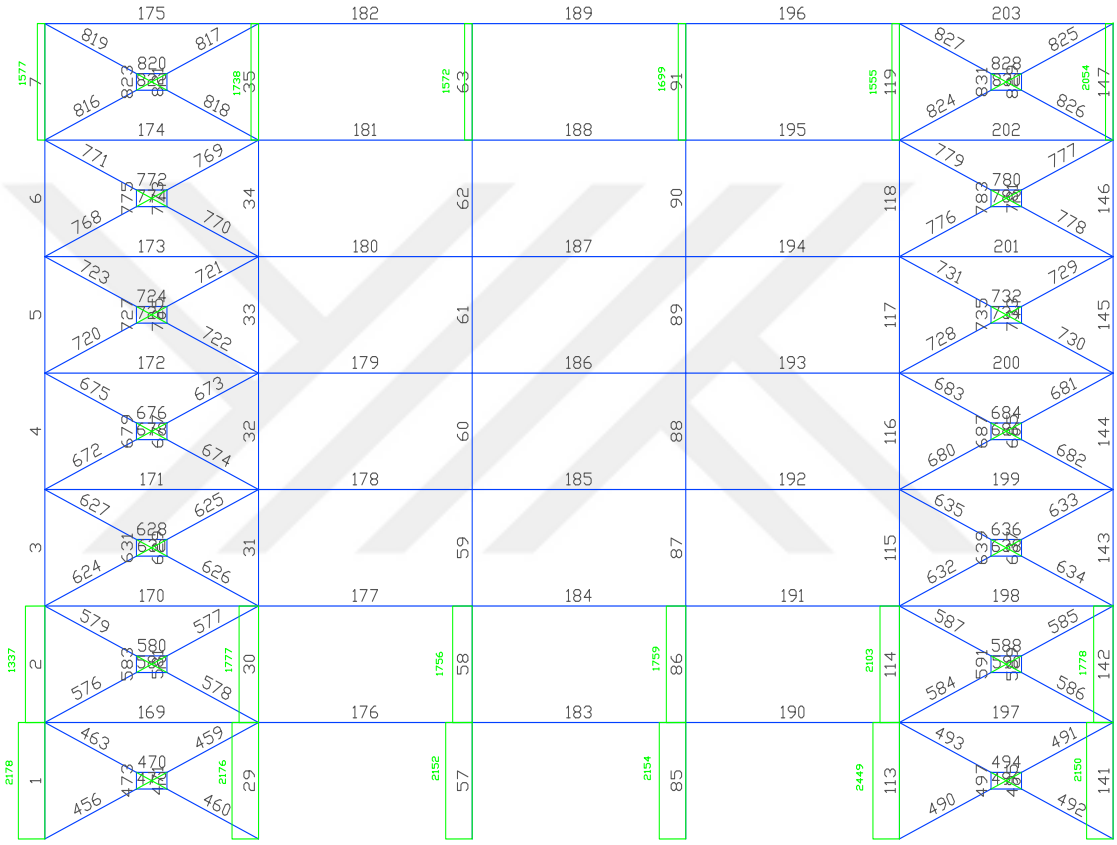


Figure 4.103 Maximum Columns Axial Forces on 1st, 2nd, and 7th Stories under Düzce Earthquake X-Damper Arrangement X-Z Axis.

Table 4.58. Columns Maximum Axial Forces Under Düzce Earthquake 1st, 2nd and 7th Story, X-Z Axis.

X-Damper Arrangement 1		
Story	Column Label	Axial Forces
1st Story X-Z Axis	1	2178
	29	2176
	57	2152
	85	2154
	113	**2449**
	141	2150
2nd Story X-Z Axis	2	**1337**
	30	1777
	58	1756
	86	1759
	114	2103
	142	1778
7th Story X-Z Axis	7	1577
	35	1738
	63	1572
	91	1699
	119	1555
	147	2054

From the above table 4.58, can read that the maximum axial force acted on column 113 at the first floor and the minimum is on column number 119 at the 7th floor.

Figure 4.104 shows the axial forces in the Y-Z axis of the building under the Düzce earthquake.

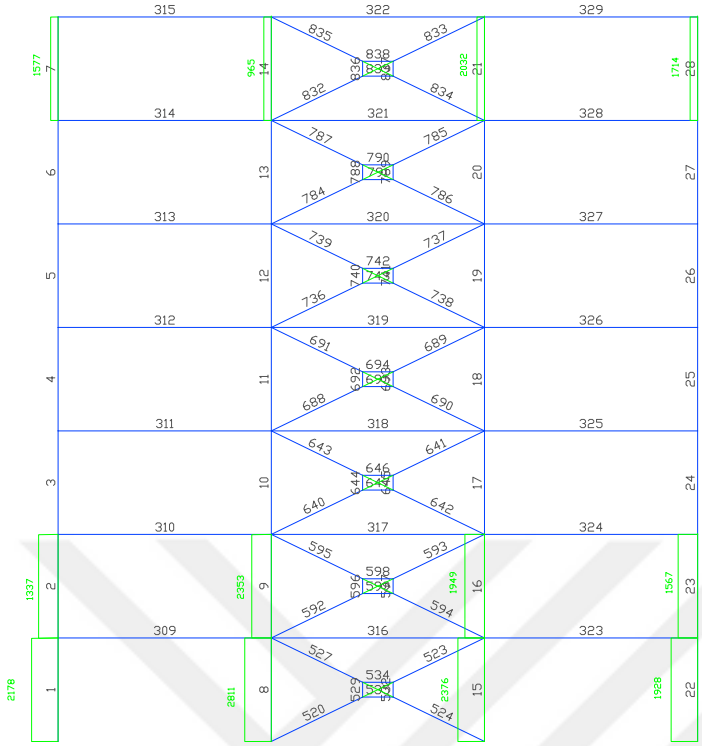


Figure 4.104 Maximum Columns Axial Forces on 1st, 2nd, and 7th Stories under Düzce Earthquake X-Damper Arrangement 1 Y-Z Axis.

Table 4.59. Columns Maximum Axial Forces Under Düzce Earthquake 1st, 2nd and 7th Story, Y-Z Axis.

X-Damper Arrangement 1		
Story	Column Label	Axial Forces
1st Story Y-Z Axis	1	2178
	8	**2811**
	15	2376
	22	1928
2nd Story Y-Z Axis	2	1337
	9	2353
	16	1949
	23	1567
7th Story Y-Z Axis	7	1577
	14	**965**
	21	2032
	28	1714

Table 4.59 shows the maximum axial force on column number 8 at the 1st floor on the X-damper arrangement 1 at the Y-Z axis of the building and the minimum on the column number 14 at the 7th floor.

The values of axial forces of columns are shown in the form of diagram in Figure 4.105 in the X-Z axis of the building at the V-damper arrangement 1.

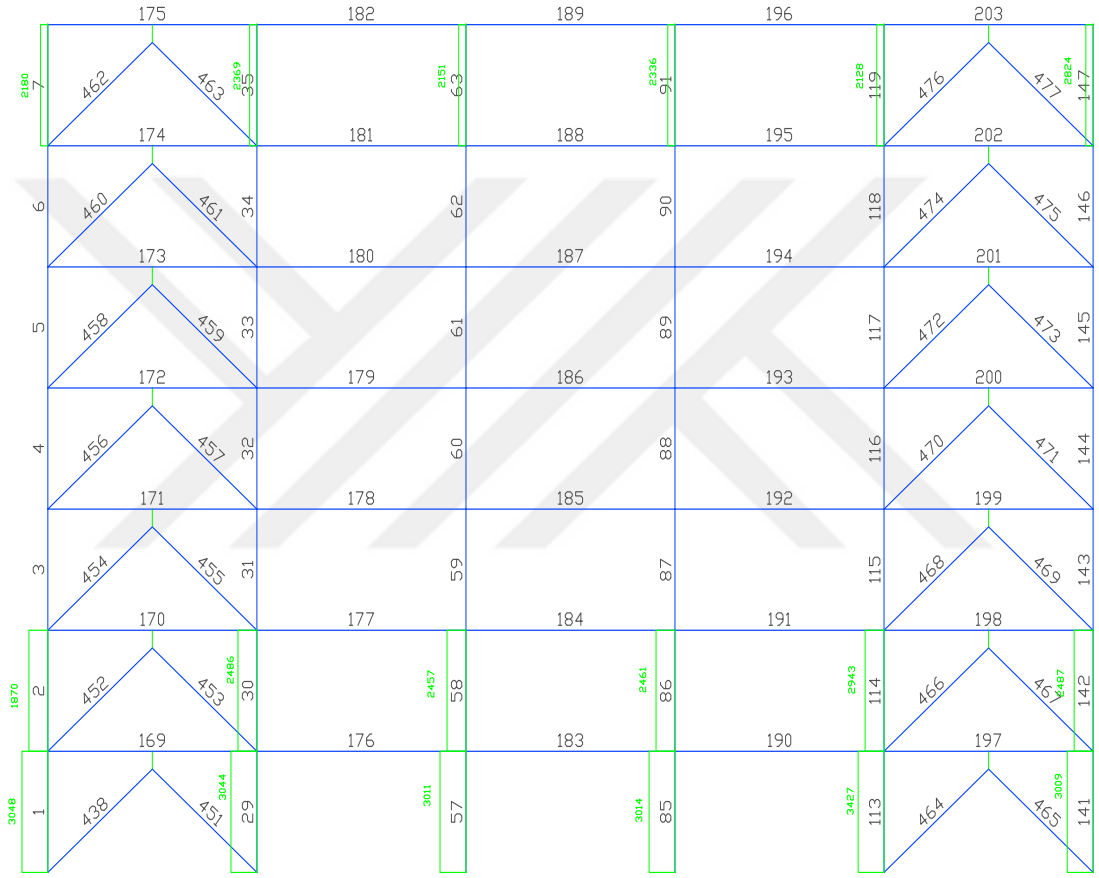


Figure 4.105 Maximum Columns Axial Forces on 1st, 2nd, and 7th Stories under Düzce Earthquake V-Damper Arrangement 1 X-Z Axis.

Table 4.60. Columns Maximum Axial Forces Under Düzce Earthquake 1st, 2nd and 7th Story, X-Z Axis

V-Damper Arrangement 1		
Story	Column Label	Axial Forces
1st Story X-Z Axis	1	3048
	29	3044
	57	3011
	85	3014
	113	**3427**
	141	3009
2nd Story X-Z Axis	2	**1870**
	30	2486
	58	2457
	86	2461
	114	2943
	142	2487
7th Story X-Z Axis	7	2180
	35	2369
	63	2151
	91	2336
	119	2128
	147	2824

Table 4.60 shows the axial forces on the columns of the 1st, 2nd and 7th stories under the Düzce earthquake in the X-Z axis of the structure. Where the maximum axial force is on column 113 at the 1st story and the minimum is at the column number 63 at the 7th story.

Maximum axial forces on columns in the Y-Z axis of the building in V-damper arrangement 1 is shown in the form of diagram in the below figure 4.106.

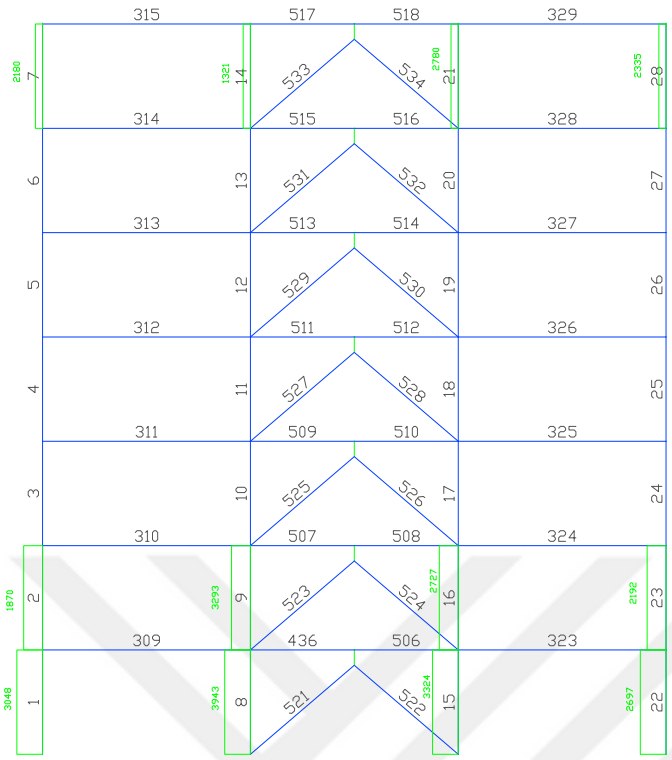


Figure 4.106 Maximum Columns Axial Forces on 1st, 2nd, and 7th Stories under Düzce Earthquake V-Damper Arrangement 1 Y-Z Axis.

Table 4.61. Columns Maximum Axial Forces Under Düzce Earthquake 1st, 2nd and 7th Story, Y-Z Axis.

V-Damper Arrangement 1		
Story	Column Label	Axial Forces
1st Story Y-Z Axis	1	3048
	8	**3943**
	15	3324
	22	2697
2nd Story Y-Z Axis	2	1870
	9	3293
	16	2727
	23	2192
7th Story Y-Z Axis	7	2180
	14	**1321**
	21	2780
	28	2335

The maximum axial force on the V-damper arrangement 1 at the Y-Z axis of the building seems to be on the column number 8 at the first floor and the minimum is on the beam number 14 at the 7th floor.

Figure 4.107 shows the maximum column axial force at the 1st, 2nd and 7th stories under the Düzce earthquake in the X-damper arrangement 2 at the X-Z axis of the structure.

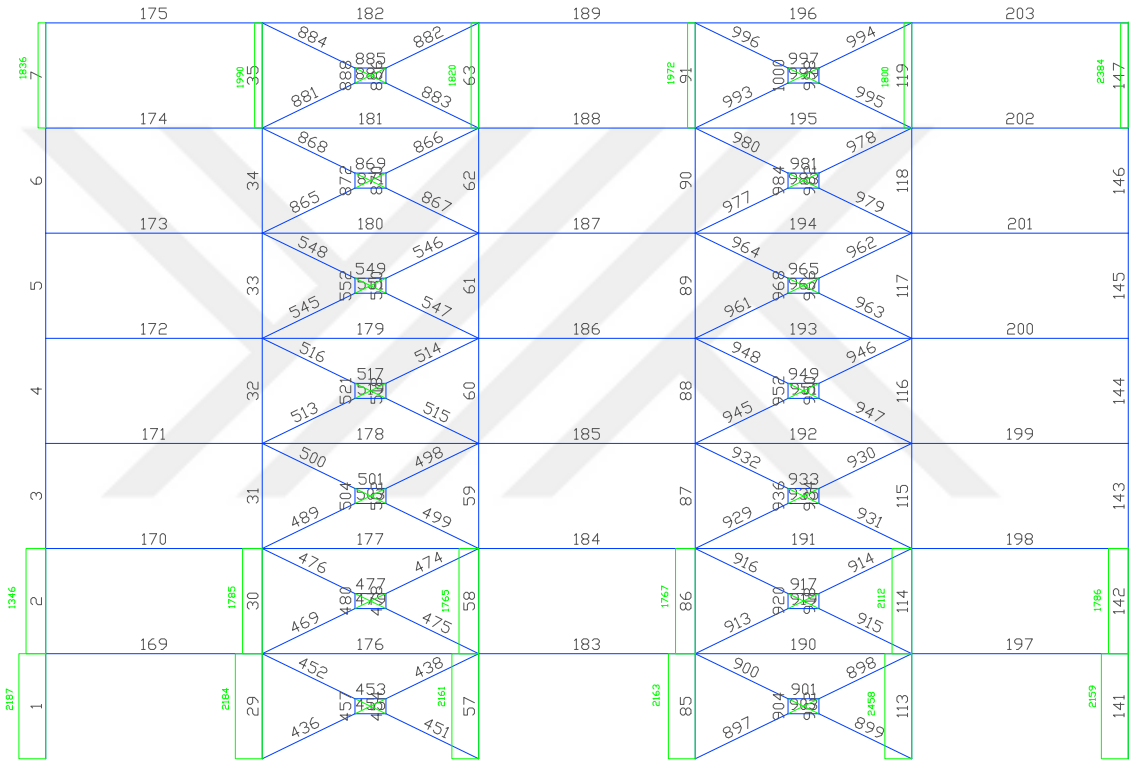


Figure 4.107 Maximum Columns Axial Forces on 1st, 2nd, and 7th Stories under Düzce Earthquake X-Damper Arrangement 2 X-Z Axis.

Table 4.62. Columns Maximum Axial Forces Under Düzce Earthquake 1st, 2nd and 7th Story, X-Z Axis.

X-Damper Arrangement 2		
Story	Column Label	Axial Forces
1st Story X-Z Axis	1	2187
	29	2184
	57	2161
	85	2163
	113	**2458**
	141	2159
2nd Story X-Z Axis	2	**1346**
	30	1785
	58	1765
	86	1767
	114	2112
	142	1786
7th Story X-Z Axis	7	1836
	35	1990
	63	1820
	91	1972
	119	1800
	147	2384

Table 4.62 shows the maximum and minimum axial forces on the X-Z axis of the building in the X-damper arrangement 2 form. Where the maximum is on the column 113 at the 1st story and the minimum is on column 119 at the 7th story. Figure 4.108 shows the diagram of axial forces for the X-damper arrangement 2.

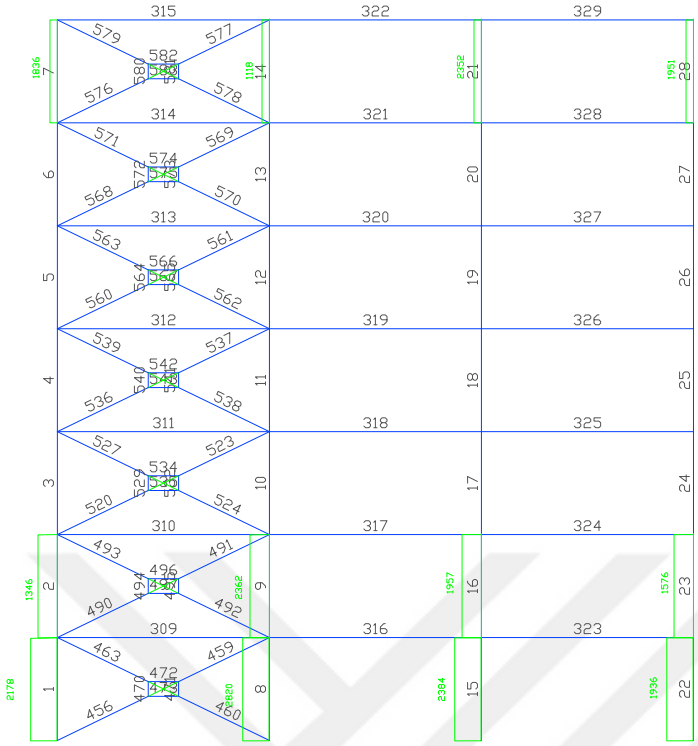


Figure 4.108 Maximum Columns Axial Forces on 1st, 2nd, and 7th Stories under Düzce Earthquake X-Damper Arrangement 2 Y-Z Axis.

Table 4.63. Columns Maximum Axial Forces Under Düzce Earthquake 1st, 2nd and 7th Story, Y-Z Axis.

X-Damper Arrangement 2		
Story	Column Label	Axial Forces
1st Story Y-Z Axis	1	2178
	8	**2820**
	15	2384
	22	1936
2nd Story Y-Z Axis	2	1346
	9	2362
	16	1957
	23	1576
7th Story Y-Z Axis	7	1836
	14	**1118**
	21	2352
	28	1951

Maximum and minimum column axial forces are shown in the above table 4.63 in the X-damper arrangement 2. Where the maximum is on the column number 8 at the 1st floor and the minimum is on the column number 14 at the 7th floor.

Figure 4.109 is the diagram for the maximum column axial forces under the Düzce earthquake at the X-Z axis of the building in the form of V-damper arrangement 2.

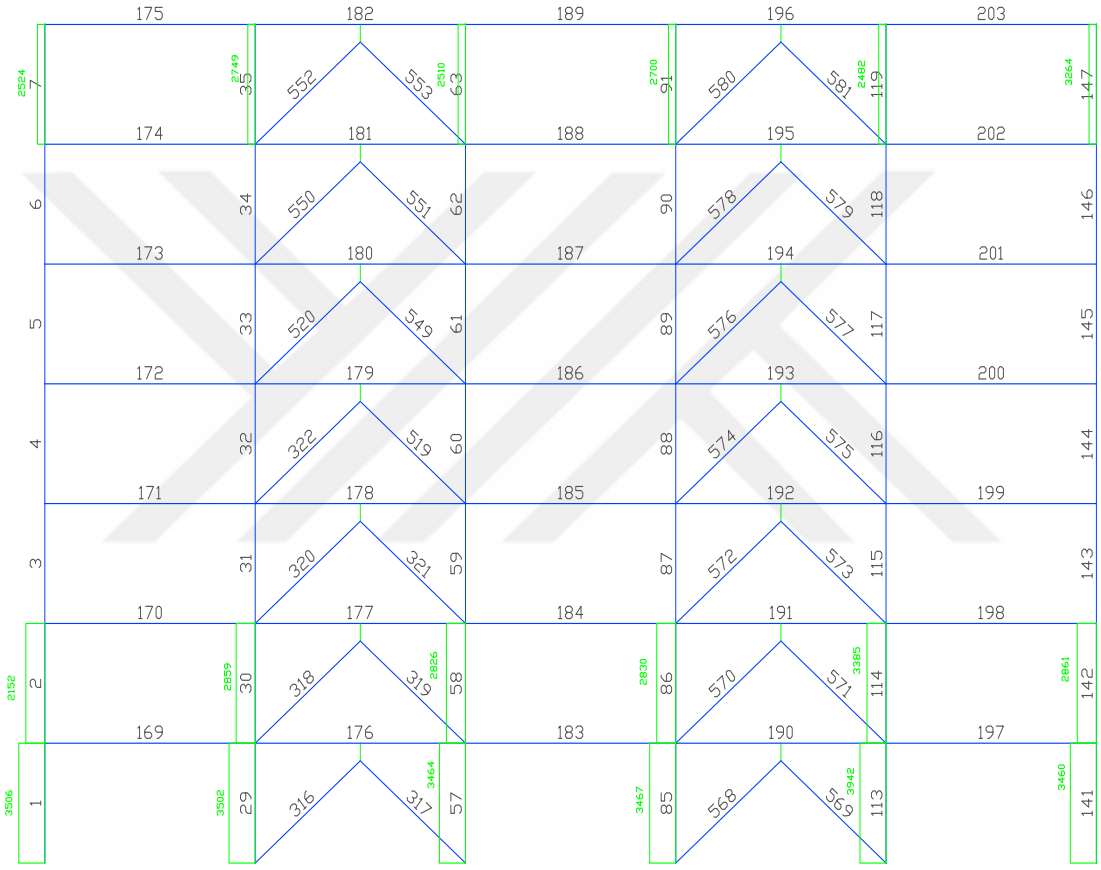


Figure 4.109 Maximum Columns Axial Forces on 1st, 2nd, and 7th Stories under Düzce Earthquake V-Damper Arrangement 2 X-Z Axis.

Table 4.64. Columns Maximum Axial Forces Under Düzce Earthquake 1st, 2nd and 7th Story, X-Z Axis.

V-Damper Arrangement 2		
Story	Column Label	Axial Forces
1st Story X-Z Axis	1	3506
	29	3502
	57	3464
	85	3467
	113	**3942**
	141	3460
2nd Story X-Z Axis	2	**2152**
	30	2859
	58	2826
	86	2830
	114	3385
	142	2861
7th Story X-Z Axis	7	2524
	35	2749
	63	2510
	91	2700
	119	2482
	147	3264

Table 4.64 shows that the maximum axial force is on column number 113 at the first floor and the minimum is on the column 119 at the 7th floor.

Figure 4.110 shows the maximum and minimum axial forces in the diagram form where the values are written in the table 4.63.

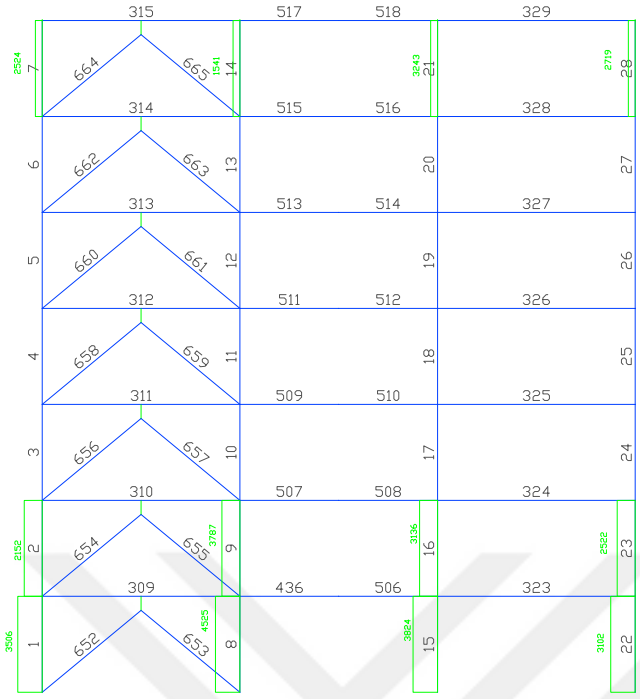


Figure 4.110 Maximum Columns Axial Forces on 1st, 2nd, and 7th Stories under Düzce Earthquake V-Damper Arrangement 2 Y-Z Axis.

Table 4.65 Columns Maximum Axial Forces Under Düzce Earthquake 1st, 2nd and 7th Story, Y-Z Axis.

V-Damper Arrangement 2		
Story	Column Label	Axial Forces
1st Story Y-Z Axis	1	3506
	8	**4525**
	15	3824
	22	3102
2nd Story Y-Z Axis	2	2152
	9	3787
	16	3136
	23	2522
7th Story Y-Z Axis	7	2524
	14	**1541**
	21	3243
	28	2719

Table 4.65 shows that the maximum axial force is on the column number 8 at the 1st floor and the minimum is on the column number 14 at the 7th floor.

The above tables and figures states that the maximum axial forces acted on columns under the without damper form of the structure while it is less than any other forms in the case of X-damper arrangement 1 installation. At the second comparison the V damper arrangement 1 is in safer side comparing to the x-damper arrangement 2 and v-damper arrangement 2.

In the X-Z axis it is mostly column number 113 under the maximum axial forces and at the Y-Z axis it is on the column number 8. The comparison of the axial forces results that the X-damper arrangement 1 is the finest option for the structure.

5. RESULTS AND SUGGESTIONS

At this dissertation, a 7-story-building with concrete moment resisting frames was evaluated under different ground motions by using two conventional friction damper configurations including X and inverted V through nonlinear time history analyses. The X and inverted V friction damper are analyzed in two different arrangements on the structure, and one analyze is done by omitting the friction damper at the first story for the both X and inverted V configurations.

There are total of 7 different analysis for the 7^{th} story building and the differences are on the arrangement of the friction dampers. For this dissertation, the friction damper which is taken in consideration is Pall friction damper which has a good history in the market and mostly had been used in USA and Canada for different huge structures. The structure is designed and analyzed in SAP2000 with the Turkish Building Standards. The results of this analysis were extracted in the term of story drifts and base shear.

The friction dampers are designed according to the Pall friction damper instructions and applied on the SAP2000. The structure is analyzed for the 7 different ground motions, two analysis for each of them regarding their peak values.

The obtained figures from the analyses lead to the below results:

Using friction damper with X configuration reduces the story drift significantly in comparison to V configuration. The result comparison between the different arrangements shows that the X configuration in arrangement 1 & 2 has the minimum story drift than the inverted V configuration 1 & 2.

There are little changes in the story drift between the X and inverted V configuration and X and V friction dampers omitted from the first story. And, salient difference in the story drift of the structure in comparison of the without damper structure's story drift with the X and V configurations.

Using friction damper with X configuration reduces the base shear value considerably in comparison to V configuration. The minimum base share, which is shown in chapter 4, Table 4.15 is under the Düzce ground motion for the without damper configuration.

While the minimum base share is on the X damper configuration 1 and 2 respectively but still the base share is on its maximum under the Düzce ground motion. Considering the base shear, the X damper configuration 1 and 2 are suitable as the base shear is on its minimum in these two configurations.

The decreasing of drift ratio in friction damper with inverted V configuration is not notable in comparison to X one and it exceeds the values of bare structure at some cases. At some points inverted configuration has acted the same as the without damper configuration in case of drift ratios which means there is no effective affect from inverted V configuration on the structure for the drift ratio.

Using friction damper with X and V configuration leads to lesser values of base shear in comparison to the bare structure and the portion of X configuration is significant. The structure is on its best situation in case of the base shear with the X and inverted V dampers arrangement 1 and 2, at some points X damper arrangement 2 has better performance than the inverted V formation.

The significant reduction in story drift and base shear reduced the remarkable damages to the structures and makes it safer. The X damper configuration 1 and 2 shows to be the superior selection for the structure to reduce the applied earthquake forces.

A remarkable reduction was observed in the internal attempts of beams and columns of the structure by using friction damper.

Elimination the dampers from the story 1, effects on the attempts of story 2 and 3 and the other stories remains constant. The dampers act the same as the arrangement 1 and 2 for the both X and inverted V configurations at the other stories.

The comparison of the beams bending moments leads to lesser values with the X damper arrangement 1 and 2 than the inverted V configuration. bending moments are at their highest under the Düzce ground motion. The bending moment comparison between the

without damper, X damper arrangement 1 and 2, V damper arrangement 1 and 2 gives us approximately 2 stories which is acceptable, and the percentages are less than 50%.

The building is on the safest side in the case of shear forces with the usage of X and V dampers in the arrangement 1, While X damper in arrangement 2 acts better than the V dampers arrangement 1 and 2. The maximum shear forces acted on beams are on the without damper configuration and the minimum is for the X damper arrangement 1.

The axial forces on the columns are at their minimums in the X and V damped form of the structure. As the two strongest earthquakes at this study is Kobe earthquake and Düzce earthquake, to make it shorter the axial forces are analyzed under the Kobe and Düzce earthquakes and the axial forces of the columns are at their maximum under the Düzce earthquake in without damper configuration. X damper arrangement 1 and 2, has the best performance on the columns in analyze of axial forces.

Comparing the above results, we can certainly say that the X damper arrangement 1 has the better performance than the other configurations and X damper arrangement 2 keeps the structure on the safer side than the without damper and inverted V configurations. While inverted V configuration 1 acts approximately the same as the X damper arrangement 2. And inverted V damper arrangement 2 is almost the same as the without damper configuration at most of the analysis.

5.1 Suggestions

Based on the literature review and the results of this dissertation, the following suggestions are presented:

- The similar study could be done on other regular an irregular structure in plan or height with different number of stories,
- A comprehensive study could be conducted on the different arrangement of friction damper in plan and height of different building.
- The effect of soil types on the seismic behavior of the structures with friction damper could be studies.
- The response of the structures with different passive control systems compare with friction damper.
- All of the above suggestion could be verified with experimental tests.

REFERENCES

Soong, T. T., and Dargush, G. F. (1997). Passive energy dissipation systems in structural engineering. John Wiley & Sons, Inc., New York.

Skinner, R. I., Robinson, W. H., and McCrery, G. H. (1993), An Introduction to Seismic Isolation, Wiley, Chi Chester and New York.

Soong, T. T. (1990), Active Structural Control: Theory and Practice, Longman, London and Wiley, New York.

Soong. T. T. and Constantinou, M. C., eds. (1994), Passive and Active Vibration Control in Civil Engineering, Springer-Verlag, Wien and New York.

Pre-standard and Commentary for the Seismic Rehabilitation of Buildings, FEMA 356/ November 2000.

Pall, A.S., Marsh, C., Fazio, P., "Friction Joints for Seismic Control of Large Panel Structures", Journal of Prestressed Concrete Institute, 1980, No. 6, 25:38-61. 7.

Pall, A.S., Verganelakis, V., Marsh, C., "Friction-Dampers for Seismic Control of Concordia University Library Building", Fifth Canadian Conference on Earthquake Engineering, Ottawa, 1987, 191-200. 8.

Pall, A.S., Ghorayeb, F., Pall, R., "Friction-Dampers for Rehabilitation of Ecole Polyvalente at Sorel, Quebec", Sixth Canadian Conference on Earthquake Engineering, Toronto, 1991, 389-396.

Vezina, S., Proulx, P., Pall, R., Pall, A., 'Friction-Dampers for Aseismic Design of Canadian Space Agency", Tenth World Conference on Earthquake Engg., Madrid, Spain, 1992, 4123-4128.

REFERENCES (continued)

Pall, A.S., Pall, R., “Friction-Dampers Used for Seismic Control of New and Existing Buildings in Canada”, ATC 17-1 Seminar on Base Isolation, Passive Energy Dissipation and Active Control, San Francisco, USA, 1993a, 2:675-686. 11.

Pall, A., Vezina, S., Proulx, Pall, R., “Friction-Dampers for Seismic Control of Canadian Space Agency Headquarters”, Journal Earthquake Spectra, 1993b, Number 3, 9:547-557.

Pall, Avtar and Pall, R., T, “Performance-based Design Using PALL Friction Dampers - an Economical Design Solution, 13th World Conference on Earthquake Engineering Vancouver, B.C., Canada August 1-6, 2004, Paper No. 1955.

Pall, A. S., and Marsh, C. "Response of friction damped braced frames."J. Struct. Div., 108(6), 1313-1323, (1982).

Filiatrault, A. and Chery, S. Seismic design spectra for friction-damped structures. Journal of Structural Engineering, ASCE, 116(5), 1334-1355, (1990).

Pall. A. S., and Pall. R. “Friction Dampers for Seismic Control of Buildings”. 11th World Conference on Earthquake Engineering., Montreal, Quebec, Canada, (1996).

Mualla. I. H., and Belev. B., “Performance of Steel Frames with a New Friction Damper Device under Earthquake Excitation”, Journal of Engineering Structures, Vol. 112, P 354-362 (2002).

Habib Saeed Monir, Keyvan Zeynali, “A modified friction damper for diagonal bracing of structures”, Journal of Constructional Steel Research, Volume 87, August 2013, Pages 17–30

Papadopoulos. P. K., Salonikios. T. N., Dimitrakis. S. A. and Papadopoulos. A. P., “Experimental investigation of a new steel friction device with link element for seismic.

REFERENCES (continued)

strengthening of structures", Journal of Structural Engineering and Mechanics, Vol. 46, No. 4 (2013).

Gholizad A, Kamrani Moghaddam P., "Friction Damper Dynamic Performance in Seismically Excited Knee Braced Steel Frames", International Journal of Civil Engineering Vol. 12, No. 1, Transaction A: Civil Engineering, March 2014.

S. Mirzabagheri, M. Sanati, A.A. Aghakouchak, S.E. Khadem, "Experimental and numerical investigation of rotational friction dampers with multi units in steel frames subjected to lateral excitation", Archives of Civil and Mechanical Engineering, Volume 15, Issue 2, February 2015, Pages 479–491.

Hamid Rahmani Samani, Masoud Mirtaheri, Amir Peyman Zandi, "Experimental and numerical study of a new adjustable frictional damper", Journal of Constructional Steel Research, Volume 112, September 2015, Pages 354–362.

Newmark, N.M. and Rosenblueth, E. (1971), Fundamentals of Earthquake Engineering, Prentice Hall, Englewood Cliffs, New Jersey.

Hanson, R. D. (1993), Supplemental Damping for Improved Seismic Performance, Earthquake Spectra, 9(3), 319-334.

Tabor, D. (1981), Friction - The Present State of Our Understanding, J. Lubr. Tech., ASME, 103, 169-179.

Larsen-Basse, J. (1992), Basic Theory of Solid Friction, in Friction, Lubrication and Wear Technology, ASM International Handbook Committee, American Society for Metals, Materials Park, Ohio.

REFERENCES (continued)

Bowden, F. P. and Tabor, D. (1950), The Friction and Lubrication of Solids, Part I, Clarendon Press, Oxford.

Bowden, F. P. and Tabor, D. (1964), The Friction and Lubrication of Solids, Part II, Clarendon Press, Oxford.

Johnson, K. L. (1987), Contact Mechanics, Cambridge University Press, Cambridge, UK

Vanmarcke, E. H. (1977). "Structural response to earthquakes." Seismic risk and engineering decisions, C. Lomnitz and E. Rosenblueth, eds., Elsevier Publishing Co., New York, N.Y.

American Society of Civil Engineers, Structural Engineering Institute (2016): Minimum Design Loads for Buildings and Other Structures, ASCE/SEI 7-16.

Fema (2009) Fema P695: Quantification of Building Seismic Performance Factors. Federal Emergency Management Agency, Washington, DC, USA.

CSI (Computers and Structures Inc.). SAP2000 v20.2 Integrated Finite Element Analysis and Design of Structures.CSI, Berkeley.

ASCE/SEI 41-13. Seismic evaluation and retrofit of existing buildings. Virginia, USA: American Society of Civil Engineers.

CSI (Computers and Structures Inc.), SAP2000 knowledge base, CSI, Berkeley.

TS 500. Requirements for Design and Construction of Reinforced Concrete Structures (TS 500-2000), Turkish Standard Institute, Necatibey Street No. 112, Bakanliklar, Ankara.

Turkish 498, 1997. Design Loads for Buildings. Turkish Standard Institute, Necatibet Street No. 112 Ministries, Ankara.

REFERENCES (continued)

TSC 2007, Turkish Seismic Code, Specification for Structures to be Built in Seismic Areas, Official Gazette No. 26454 and 26511, Ministry of Public Works and Settlement, Government of Republic of Turkey.

Eurocode 2, Design of concrete structures: Part 1.2: general rules— structural fire design, European Committee for Standardization, Brussels, BS EN 1992-1-2, 2004.

ACI318-14 (2014), Building Code Requirements for Structural Concrete and Commentary, American Concrete Institute, Farmington Hills, MI, USA.

ASTM A615/A615M-14—Standard Specification for Deformed and Plain Carbon-Steel Bars for Concrete Reinforcement.